THE GENERAL MILLS ELECTRONICS GROUP

IDENTIFICATION OF REPORT SUBMITTED FOR CLEARANCE AND RELEASE
TO DEPARTMENT OF COMMERCE FOR PUBLIC DISTRIBUTION

1. Title: "Fundamental Studies of the Dispersibility of Powdered Materials"

2. Authors: J. H. Nash, G. G. Leiter, A. P. Johnson, D. Stender and H. W. Zeller

3. Originating Agency: Aerospace Research
General Mills Electronics Division
2295 Walnut Street
St. Paul 13, Minnesota

4. This report has no restrictions from either a security or legal standpoint and may be distributed in accordance with existing security regulations.

5. This report has not appeared in any proper, scientific, technical or professional journal. It is not scheduled to be published.

6. [illegible]

"In my opinion, this disclosure does not set forth matter that should be patented, and its publication will not be inimical to the national interest of the United States."

J. H. Nash
G. G. Leiter
[illegible]
Harold W. Stender
[illegible]

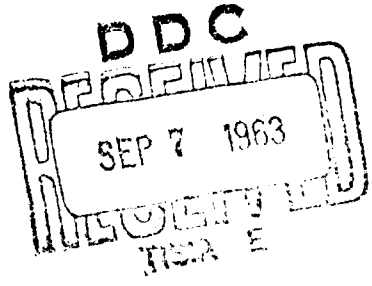

Leonard Cohen

LaMONTE A. TUCKER
Colonel, CmlC
Weapons Systems

Aerospace Research
General Mills Electronics Division
2295 Walnut Street
St. Paul 13, Minnesota

Contract No. DA-18-108-405-CML-824

FINAL REPORT

FUNDAMENTAL STUDIES OF THE DISPERSIBILITY OF POWDERED MATERIALS

Covering the Period
3 June 1960 through 31 January 1963

Prepared by: J. H. Nash
G. G. Leiter
A. P. Johnson
D. Stender
H. W. Zeller

Submitted by: A. A. Anderson
A. A. Anderson
Assistant Director
Aerospace Research

Approved by: S. P. Jones
S. P. Jones
Director
Aerospace Research

Report No: 2381
Project No: 81524
Date: March 15, 1963

Copy 4 of 30 copies

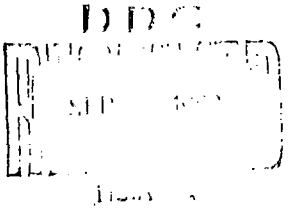

ABSTRACT

This is a fundamental study of factors affecting the flow and dispersibility of finely divided organic powders. Most of the investigations pertain to three base powders: saccharin, Carbowax 6000, and Span 60. These powders were chosen to represent crystalline, waxy, and gummy types of powders, respectively. Late in the program, a fourth powder (egg albumin) was added to the list of powders to be investigated.

The preparation of powders including grinding, deagglomeration, blending, coating with surface active agents, etc. is discussed.

The various tests for measuring physical properties of powders including particle size distribution, shear strength, bulk tensile strength, bulk density, dynamic angle of repose, dispersibility, and electrostatic charge are described.

Each of the major studies is discussed, and experimental data are presented in tabular and graphical forms. The major studies are: 1) bulk tensile strength tests, 2) effects of humidity on powder properties, 3) effects of antiagglomerant agents on powder properties, 4) mechanism by which Cab-O-Sil functions, 5) effects of surface active agents on powder properties, 6) effects of adsorbed foreign vapors on powder properties, 7) effects of removal of adsorbed gases and vapors, 8) energy required to disperse a powder sample, 9) properties of compacted powders, and 10) egg albumin studies.

TABLE OF CONTENTS

TABLE OF CONTENTS (Continued)

TABLE OF CONTENTS (Continued)

LIST OF ILLUSTRATIONS

LIST OF ILLUSTRATIONS (Continued)

LIST OF ILLUSTRATIONS (Continued)

LIST OF ILLUSTRATIONS (Continued)

LIST OF ILLUSTRATIONS (Continued)

LIST OF ILLUSTRATIONS (Continued)

LIST OF TABLES

LIST OF TABLES (Continued)

LIST OF TABLES (Continued)

LIST OF TABLES (Continued)

FINAL REPORT
ON
FUNDAMENTAL STUDIES OF THE DISPERSIBILITY OF POWDERED MATERIALS

I. INTRODUCTION

This report covers research conducted by General Mills, Inc. Electronics Group for the U. S. Army Chemical Center under Contract DA-18-108-405-CML-824 for the period 3 June 1960 through 3 January 1963.

The objectives of this investigation are stated explicitly in the contract and are repeated here.

1) The Contractor will furnish the necessary personnel, materials and equipment (with the exception of any Government furnished property) and will exert its best efforts to perform both theoretical and experimental studies of the deagglomeration and flow of solid particles and their dispersibility in aerosol form. These studies will lead to fundamental correlations between the basic characteristics of powders and their dispersibility in aerosol form for eventual application to the dissemination of solid agents.

2) The materials to be employed experimentally will be selected by mutual agreement between the Contractor and the Project Officer. A study of powders in the particle size range of 2 to 5 microns will be of primary importance. The information available in the literature on related theoretical and experimental studies will be integrated with the results to be obtained.

3) In order to establish the required fundamental correlations, it is suggested that the Contractor perform studies that may include, but not be limited, to the following:

   a) Theoretical Considerations

      (1) Forces between particles

      (2) Deagglomeration of particles

b) Experimental Studies

(1) Forces between particles

(a) Effect of humidity
(b) Effect of absorbed vapors
(c) Effect of compression
(d) Effect of removal of adsorbed gases and vapors at low pressure
(e) Effect of temperature
(f) Effect of chemical composition and intermolecular forces
(g) Effect of electrostatic charging in relation to (a) to (f) above

(2) Dispersibility of particles

(a) Shearing studies
(b) Energy requirement studies
(c) Other studies as devised by the Contractor

(3) Bulk tensile strength of powders

(4) Action of antiagglomerants

(5) Action of antistatic agents

Three powders were chosen for intensive investigation. These are saccharin (benzosulfimide), Carbowax 6000 (polyethylene glycol), and Span 60 (sorbitan monostearate). These specific powders were chosen to represent crystalline, waxy, and gummy powders, respectively, and are referred to as the three base powders in this report. Toward the end of the program, a fourth powder (egg albumin) was added to the list of powders to be investigated. Since the work on egg albumin represents a relatively small part of the overall effort, it was decided to include most of the data pertaining to this powder in a single section rather than to disperse them throughout other sections in the report.

II. PREPARATION OF POWDERS

A. Initial Grinding of Three Base Powders

1. Saccharin, Carbowax 6000, and Span 60

General Mills, Inc. was not equipped with the proper facilities at the beginning of the program to grind powders to the 2 to 5-micron size range; therefore, twenty-pound quantities of each of the three base materials (saccharin, Carbowax 6000, and Span 60) were sent to the Fluid Energy Processing and Equipment Co., Philadelphia, Pennsylvania to be ground. Instructions were given to grind the materials so that the MMD was in the 2 to 5-micron size range. The materials were ground in a No. 0202-2 Jet-O-Miser fluid energy mill using compressed air at a pressure of 91 to 99 psig and at room temperature. Feed rate was 3.92 lb/hr.

The ground samples were returned to us in several different bags along with microscopic size analyses corresponding to each bag. These analyses are given in Table 1.

Since we needed only one particle size distribution for each base powder, we mixed all samples of each powder together. These were the three base powders on which we conducted our investigations during the first 18 months of the program.

Particle size analyses were made on samples of each powder using the microscope technique described in Section III-A. Results of the analyses are given in Table 2.

It is seen that our analyses compare favorably with those furnished by the Fluid Energy Processing and Equipment Co. for saccharin and Span 60, but for Carbowax 6000 our analysis indicates a smaller particle size.

When this first batch of finely ground powders began running low, we sent three more 20-pound quantities of saccharin, Carbowax 6000, and Span 60 to the Fluid Energy Processing and Equipment Co. to be ground in

Table 1. Microscopic Size Analyses Furnished with Custom-Ground Powders

Material	Item	Percent in Size Range		
Span 60	1	10 - 5μ 1 - 2%	5 - 2μ 15 - 20%	<2μ 78 - 84%
Span 60	2	10 - 5μ 10 - 15%	<5μ 85 - 90%	
Span 60	3, 4	10 - 5μ 8 - 10%	5 - 2μ 25 - 30%	<2μ 60 - 70%
Saccharin	5	5 - 2μ 12 - 15%	<2μ 85 - 88%	
Saccharin	6, 7, 8	5 - 2μ 15 - 20%	<2μ 80 - 85%	
Carbowax 6000	9	15 - 10μ 2 - 3%	10 - 5μ 40 - 50%	<5μ 46 - 58%
Carbowax 6000	10	20 - 10μ 3 - 5%	10 - 5μ 30 - 40%	<5μ 55 - 67%

Table 2. Results of Our Microscopic Size Analyses on Three Base Powders

Powder	CMD	Percent in Size Range		
Saccharin	0.58	<5μ 96.7%	2 - 5μ 14.2%	<2μ 82.5%
Carbowax 6000	0.98	<5μ 89.5%	2 - 5μ 18.5%	<2μ 71%
Span 60	0.77	<5μ 94.7%	2 - 5μ 19.7%	<2μ 70.0%

the same manner as was the first batch. When we received the second batch of ground powders, we decided to see how particle size distributions of samples from both batches compare. The Whitby centrifuge sedimentation method was used in these analyses rather than the microscope method because it is less time consuming. Difficulties were encountered with the Span 60 samples because no suitable settling liquid could be found. For this reason, no particle size analyses were made on these samples. No difficulties were encountered with the saccharin samples or the Carbowax 6000 samples, however. The time schedules and other pertinent information regarding the analyses of these powders are given in Tables 6 and 7 in Section III-A. Results of the analyses are given in Tables 3 and 4 and are plotted on logarithmic normal graph paper in Figures 1 and 2. It is seen that the particle size distributions of the two saccharin samples are, for all practical purposes, identical, the MMD being about 6.9 microns in both cases. The particle size distributions of the two Carbowax 6000 samples are slightly different, however. The MMD of the original batch is 11.8 microns, and that of the second batch is 13.8 microns.

2. Egg Albumin

Since the work on egg albumin did not begin until late in the program, there was insufficient time remaining to have the material custom ground. We had acquired a small fluid energy mill at this time and, therefore, decided to grind the material ourselves. This work is reported in Section IV-J.

B. Technique for Deagglomerating Powders

Most fine powders exhibit a tendency to agglomerate. An agglomerate is an assembly of many particles that are in contact with one another and are held together by interparticle forces. The interparticle forces mainly responsible for holding agglomerates together are van der Waals forces.

Table 3. Particle Size Analysis Data for Two Batches of Ground Saccharin

Particle Size Microns	Column Height	Percent Finer than Size
Original Batch		
20	0	100
15	0	100
10	4.5	65.9
8	5.9	55.3
6	7.1	46.2
5	8.9	32.6
4	9.3	29.5
3	9.4	28.8
2	11.5	13.0
1	12.1	8.3
0.5	12.9	2.3
0	13.2	0
New Batch		
20	0	100
15	trace	<100
10	4.5	63.4
8	5.6	54.5
6	6.5	47.2
5	7.6	38.3
4	8.1	34.1
3	8.5	30.9
2	10.6	13.8
1	10.9	11.5
0.5	11.4	7.3
0	12.3	0

Table 4. Particle Size Analysis Data for Two Batches of Ground Carbowax 6000

Particle Size (microns)	Column Height (projector scale units)	Percent Finer than Size
Original Batch		
20	8.0	74.8
15	12.0	62.3
10	18.5	41.8
8	22.0	30.8
6	25.9	21.1
5	27.1	14.8
4	29.1	8.5
3	29.8	6.3
2	31.2	1.9
1	31.5	1.0
0.5	31.7	0.4
0	31.8	0
New Batch		
20	7.5	71.2
15	11.5	55.8
10	16.5	36.5
8	19.5	25.0
6	21.8	16.1
5	23.0	11.5
4	23.8	8.5
3	24.5	5.9
2	25.7	1.2
1	25.8	0.7
0.5	26.0	0
0	26.0	0

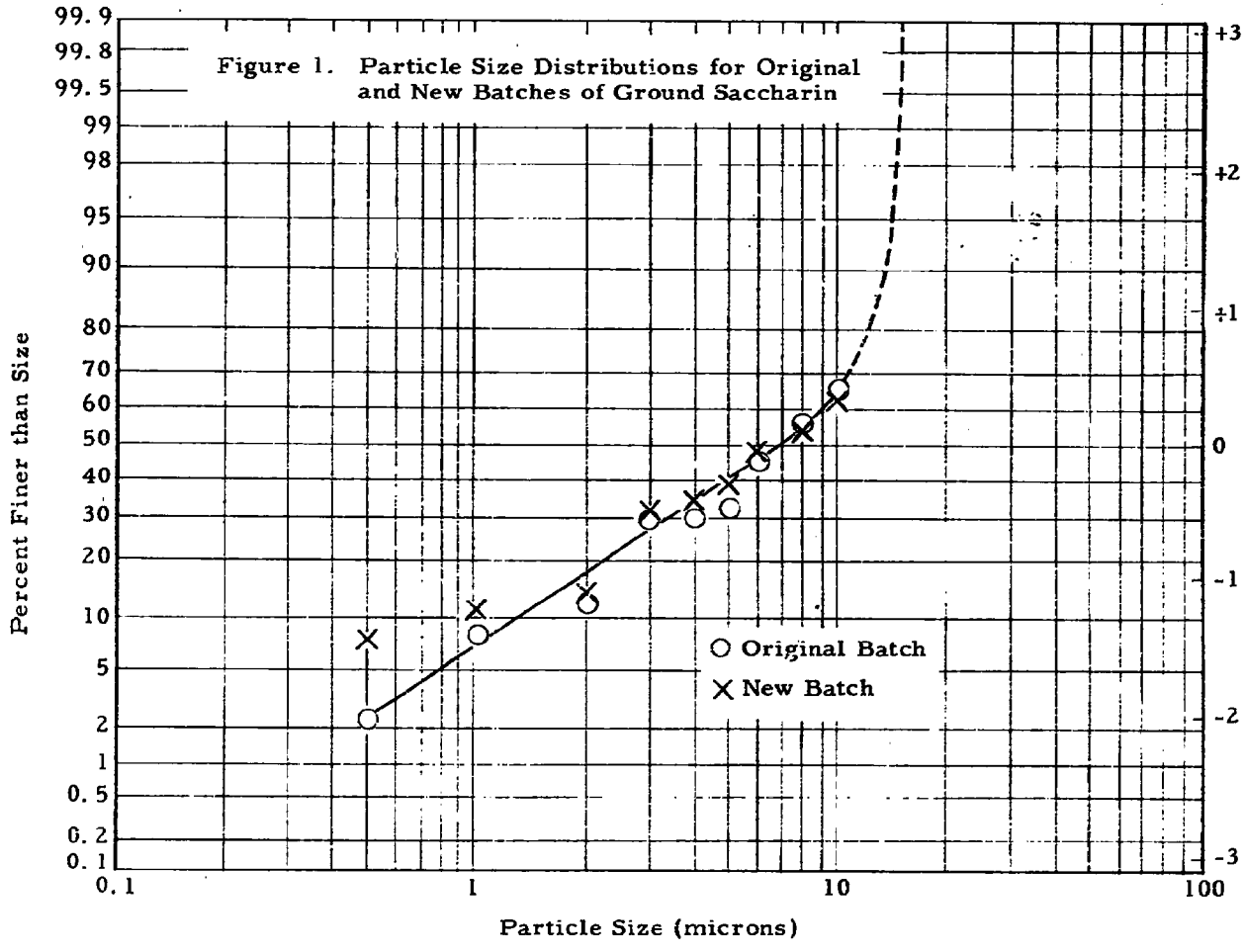
Figure 1. Particle Size Distributions for Original and New Batches of Ground Saccharin
Percent Finer than Size
99.9
99.8
99.5
99
98
95
90
80
70
60
50
40
30
20
10
5
2
1
0.5
0.2
0.1
+3
+2
+1
0
-1
-2
-3
0.1
1
10
100
Particle Size (microns)
Original Batch
New Batch

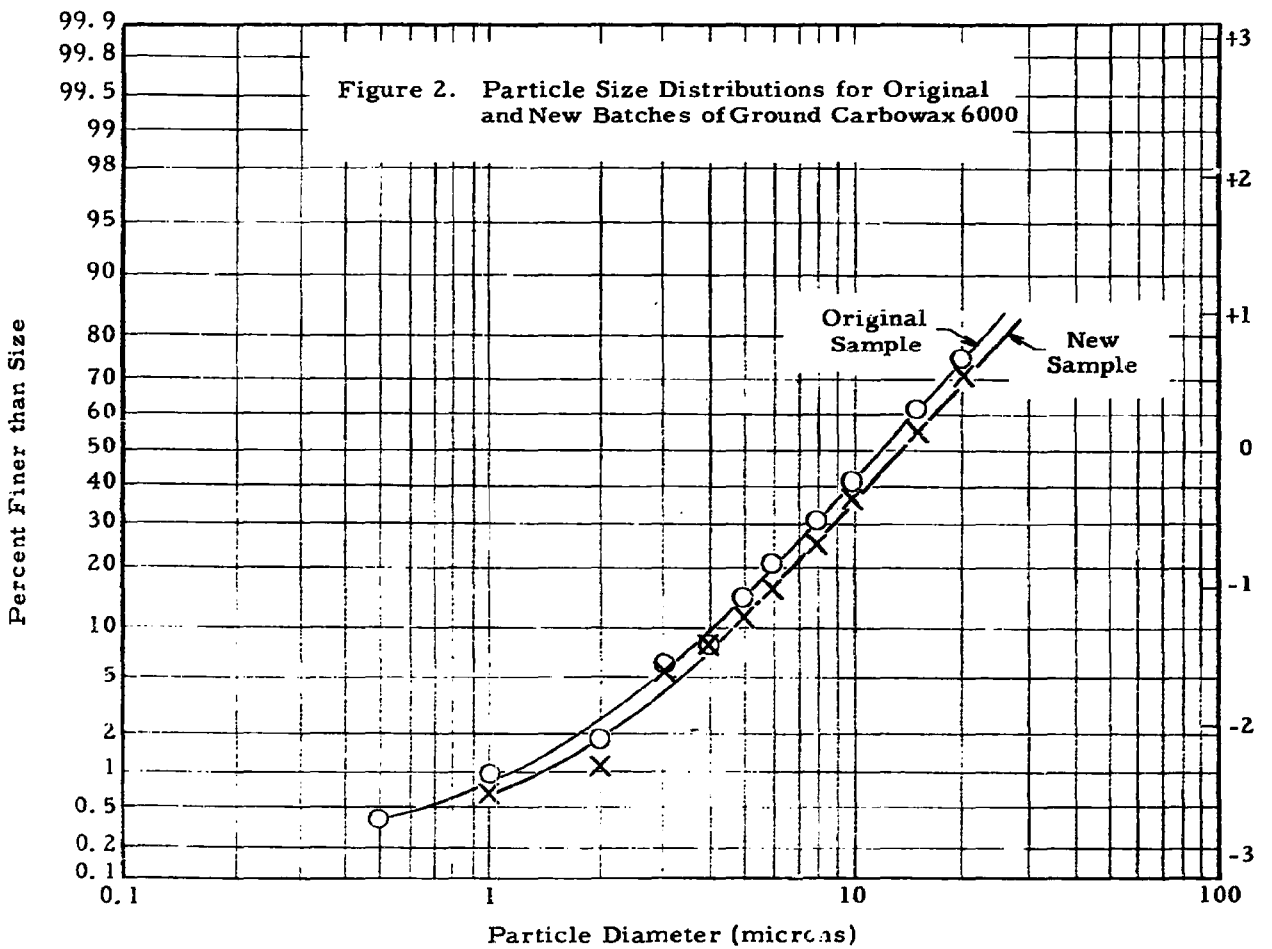
Figure 2. Particle Size Distributions for Original and New Batches of Ground Carbowax 6000
Original Sample
New Sample
Percent Finer than Size
99.9
99.8
99.5
99
98
95
90
80
70
60
50
40
30
20
10
5
2
1
0.5
0.2
0.1
+3
+2
+1
0
-1
-2
-3
0.1
1
10
100
Particle Diameter (microns)

Van der Waals forces are significant only for small particles that are either in contact or are in very close proximity with each other. Hamaker[1] derived the following equation for van der Waals force between two spheres of diameters d_1 and d_2:

$$F = \frac{\pi^2 q^2 \lambda}{12 a^2} \quad \frac{d_1 d_2}{d_1 + d_2} \quad , \tag{1}$$

where:

F = interparticle force

q = number of molecules per unit volume

a = distance between particles

λ = van der Waals' constant for attraction

If $d_1 = d_2 = d$, then Equation (1) becomes:

$$F = \frac{\pi^2 q^2 \lambda}{24 a^2} \, d \quad . \tag{2}$$

The Lifschitz[2] equation indicates that the interparticle force between two spheres of equal size is inversely proportional to the cube of the distance separating the spheres as shown below:

$$F = - \frac{B d}{36 a^3} \quad , \tag{3}$$

where:

F = interparticle force

B = constant which depends upon particle composition and nature of surrounding medium

d = particle diameter

a = distance between particles

The rate at which agglomerates form is dependent upon, among other things, how much the powder is agitated and the size and concentration of agglomerates already present.[3] For this reason, a powder that has just recently been ground has different characteristics than one that has been allowed to stand for some time and has agglomerated as a result of normal vibrations present in any building.

This presented a problem. Tests conducted on a powder immediately after grinding probably would not agree with the same type of tests conducted on the same powder at a later time.

To meet this problem, we devised a technique to deagglomerate powders without changing their particle size distribution. Each time a series of tests is begun, the powder samples are deagglomerated. There still is the possibility of course for reagglomeration to occur while a series of tests is in progress. It is felt, however, that the amount of change that the samples underwent during any given series of tests conducted on this program was slight.

The apparatus for deagglomerating powders without changing their particle size distribution is basically a fluid energy mill with modified feeding and collection systems (see Figure 3). The feeding system was modified by attaching a 1-foot length of 1/4-inch-inside-diameter rubber tubing to the feeder hopper as shown in Figure 3. The collecting system was modified by removing the cyclone collector from the mill and closing the hole with a rubber stopper. A 6-inch length of thick-wall rubber hose was fitted over the mill exhaust tube. The opposite end of this hose fits in the opening of a disposable vacuum cleaner bag as shown.

Since the purpose of the fluid energy mill is not to grind the powder to smaller particle sizes but to break agglomerates apart, a relatively low operating pressure of 35 psig was used. Air used to operate the mill was prefiltered to remove oil and water contamination.

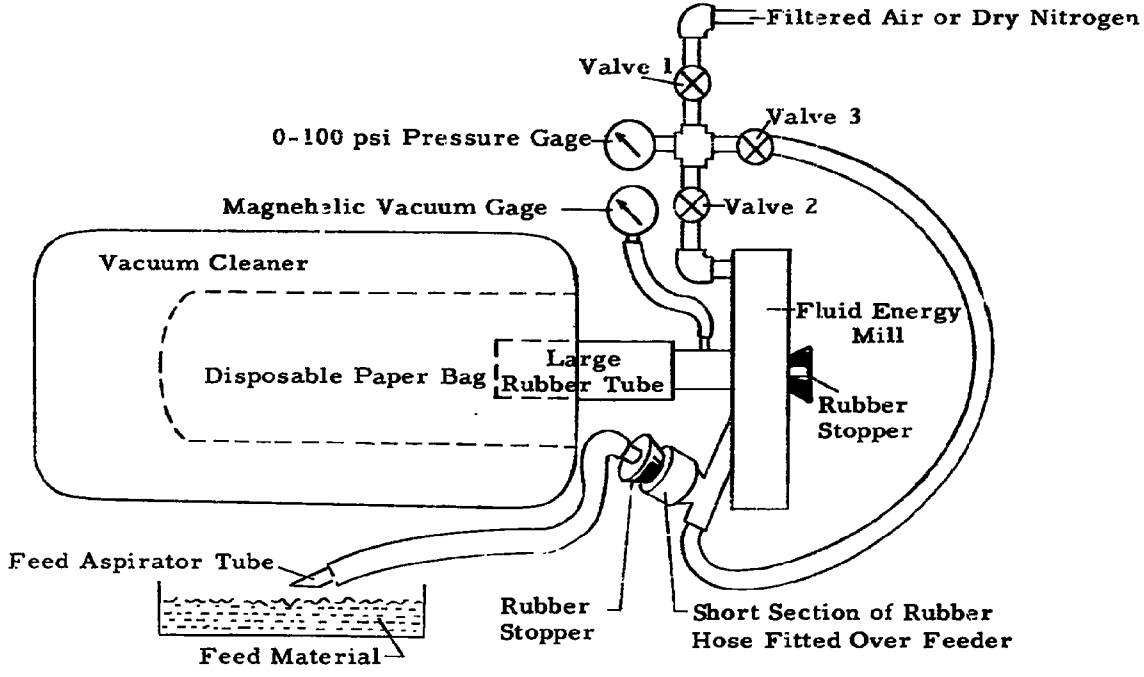

Figure 3. Modified Fluid Energy Mill System for Deagglomerating Powders

We used the following procedure to deagglomerate powders: Valves 1 and 3 are opened, and valve 2 is closed. The vacuum cleaner motor is turned on. Compressed air now enters the mill through the branch leading to the feeder. The aspirator action in the feeder causes a negative pressure inside the rubber tube attached to the feeder hopper. The tip of this tube is dipped into the feed material. Air rushing into the end of the tube dislodges feed material and transports it into the mill. As soon as material starts flowing into the mill, valve 2 is opened. Feed material continues flowing into the tube as long as the tip of the tube is submersed in the feed material. Feed rate is controlled by the rate at which the tip of the tube is advanced into the pile of feed material. Feed rates of approximately 100 g/min were used. The amount of material which can be deagglomerated before the vacuum cleaner bag clogs up is about 200 g.

At the completion of a run the compressed air is turned off, the vacuum cleaner motor turned off, and the disposable bag removed. The top of the bag is cut off and the contents emptied out into a container.

To determine if any particle size reduction occurs in the fluid energy mill during the deagglomerating process, a sample of talc was run through the mill, and particle size analyses were made on the sample prior to and after the deagglomerating process using the Whitby method. The two particle size distribution curves, when plotted on logarithmic normal graph paper, were practically superimposed. The sample which had not been deagglomerated in the fluid energy mill had a mass median diameter (MMD) of 2.55 microns and a geometric standard deviation (gsd) of 1.41, while the deagglomerated sample had a MMD of 2.45 microns and a gsd of 1.94. This small difference is not significant.

C. Technique for Blending Powders

Because of our work with antiagglomerant agents, it was necessary to have an effective method for blending powders. The method we used is this: The components to be blended are mixed together initially using a method

suggested by Flowler.[4] This method is recommended for cases where a small amount of one powder is to be mixed with a large amount of another. The method consists of mixing all the smaller component with an equal amount of the larger component. The mixture thus formed is mixed with an equal amount of the larger component, and so on, until all of each component is used up. Between each successive stage in the process, the powders are mixed by tumbling them back and forth in a polyethylene bag.

After the final mixture has been thoroughly mixed by means of the polyethylene bag technique, it is further blended by means of the modified fluid energy mill technique described in Section II-B.

An experiment was conducted to illustrate that it is indeed necessary to apply tortuous shear stresses to a powder mixture in order to obtain effective blending. A mixture consisting of 1 percent talc and 99 percent activated charcoal was prepared using Fowler's method. The final mixture was blended in a Patterson-Kelly twin-shell plastic blender for a period of one hour. A sample of the powder mixture was withdrawn by means of a spatula and placed on a sheet of white paper. The blade of the spatula was used to spread the sample across the paper. There was considerable evidence of unbroken agglomerants as indicated in Figure 4. The powder mixture was then deagglomerated in the fluid energy mill, and another sample was withdrawn and tested for unbroken agglomerates in the manner described. There was no evidence of unbroken agglomerates now as indicated in Figure 5.

D. Moisture Conditioning of Powders

In order to study the effects of moisture on powder properties, it was necessary to devise a unit in which powders could be stored and tested at any desired relative humidity. A diagram of this unit is shown in Figure 6. The basic idea of this unit is to mix very wet and very dry air together in the proper ratio to obtain any given humidity.

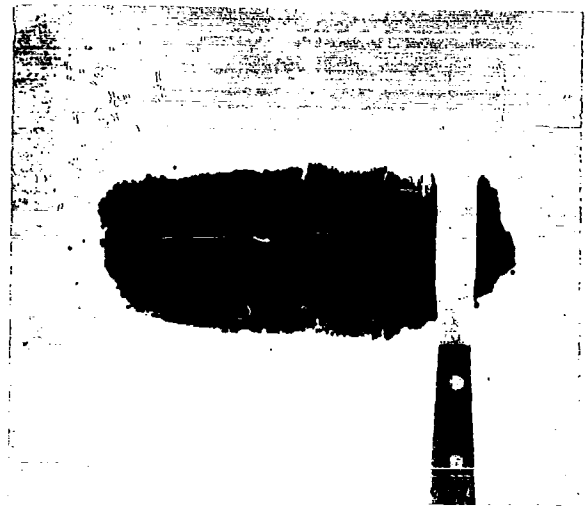

FIGURE 4
PHOTOGRAPH OF POORLY BLENDED POWDER SAMPLE

FIGURE 5
PHOTOGRAPH OF POWDER SAMPLE BLENDED
BY MEANS OF DESCRIBED TECHNIQUE

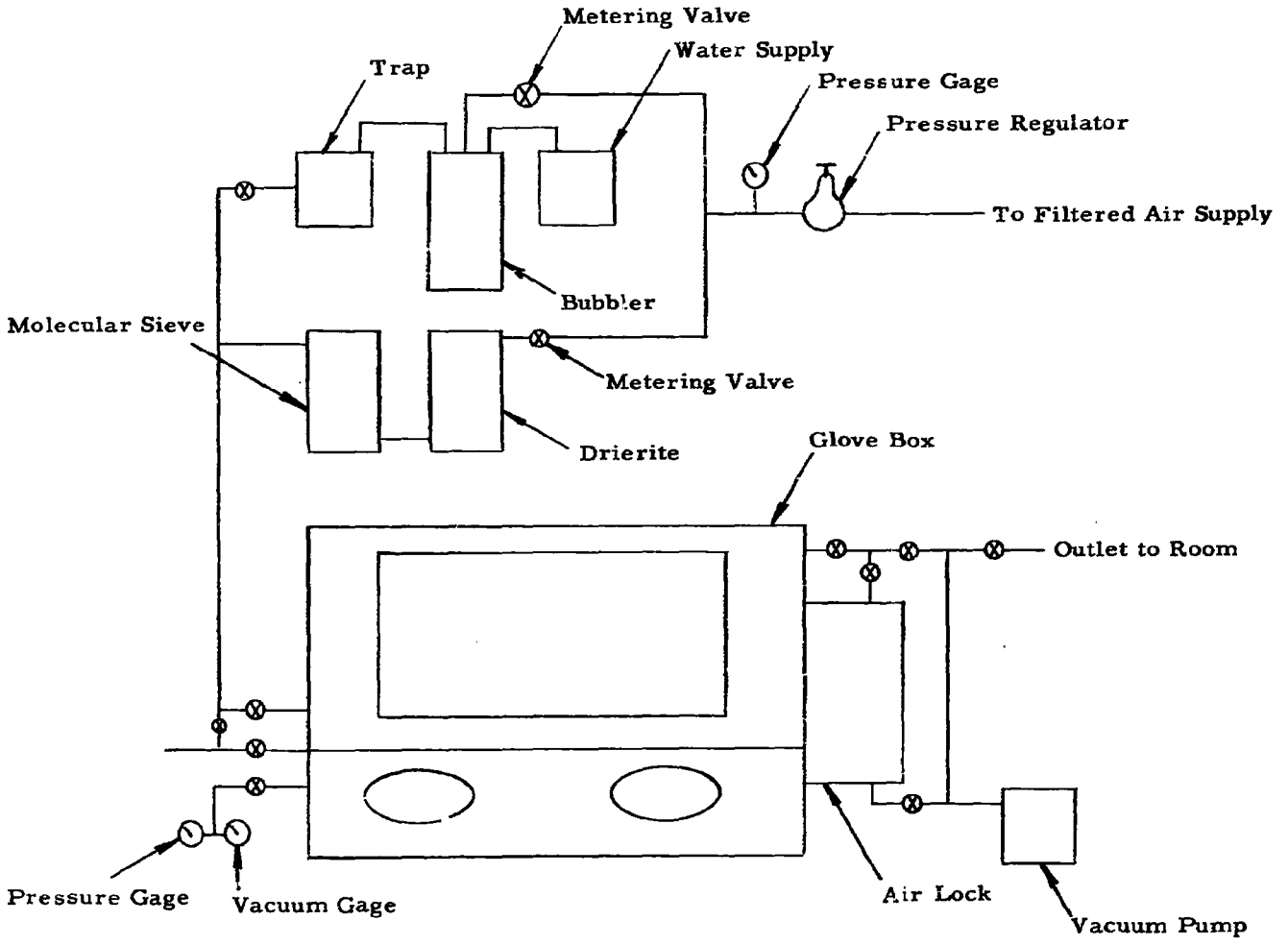

Figure 6. Controlled Humidity System

In practice, filtered compressed air is reduced in pressure to about 5 psig. The air line is divided with one part going through columns of Dierite and molecular sieve and the other part going through a bubbler and a water trap. The relative flow between the wet and dry air is controlled by means of two twenty-turn metering valves. The mixture of wet and dry air enters the glove box on one side, and the majority of the air leaves through an outlet on the other side of the box. A General Mills infrared hygrometer monitors the humidity of the system by continuously drawing a sample from either the glove box or the air line feeding the box by means of a valve arrangement. The air lock may be either connected to or isolated from the controlled humidity by means of another valve arrangement. In order to work comfortably in the glove box, the proper pressure must be maintained. This is accomplished by adjusting the input and output valves and, when a negative pressure is desired, a low capacity vacuum pump is used. Gages are used for measurement of the glove box pressure.

Since powders in general take a long time to equilibrate to a given humidity, all powders were stored at the proper humidity in shallow, open pans for a period of at least 48 hours prior to testing. In the case of shear strength, the tests were conducted in the glove box at the conditioning humidity while in the case of the aerosol decay and electrostatic charge tests, the conditioned powder was removed from the glove box and dispersed at room humidity.

E. Technique for Coating Powders with Surface Active Agents

A sizeable portion of this program was devoted to an investigation of effects of surface active agents on powder properties. For this reason, it was necessary to devise a suitable method for coating powders with liquid agents.

Initial attempts to coat powders with liquid agents were made using a Norgren Model 0-41-2 oil-fog lubricator in conjunction with a 2-inch-diameter Jet Pulverizer Model 02-503 fluid energy mill. The Norgren

lubricator served to inject a fine spray of liquid droplets into the air stream entering the mill. As the powder and liquid passed through the mill simultaneously, the powder became coated with a thin layer of the liquid.

In principle, this arrangement was satisfactory; however, in practice, there were two major disadvantages: 1) It was difficult to adjust the liquid flow rate so that a known amount of liquid could be added to a given amount of powder, and 2) the apparatus was difficult to disassemble for cleaning. Because of these disadvantages, a new device for injecting the liquid into the air stream was designed. This device is illustrated in Figure 7.

The procedure used in coating a powder sample with a liquid agent is as follows: The glass tube is removed from the apparatus and filled with the liquid to be used in the test. Valve 4 is closed, and the tube containing the liquid is replaced. A mark is made on the tube to indicate the level of the liquid. The density of the liquid must be known so that the desired amount can be metered out during the run by noting the change in height (ΔH) of the liquid in the glass tube. The bore of the tube used in the present apparatus is 2.82 mm; therefore, the ΔH corresponding to one gram of water ($\rho_1 = 1$ g/cm^3) is 16 cm. The ΔH corresponding to one gram of another liquid having a density ρ_2 can be calculated from the following relationship:

$$\Delta H = 16 \left(\frac{\rho_1}{\rho_2}\right) \text{cm} \quad . \tag{4}$$

When the proper ΔH has been determined, a second mark is made on the glass tube of distance $\Delta H \times g$ below the previous mark, where g is the number of grams of liquid to be added.

The powder sample to be coated is carefully weighed out and placed in a shallow container. The vacuum cleaner motor is turned on. Valve 1 is opened. Air now enters the mill through two different branches. The pressure at the feed aspirator tube will be positive. Valve 2 is closed momentarily, forcing all of the air to enter the mill through the feed aspirator branch. This will cause the pressure at the feed aspirator tube to change

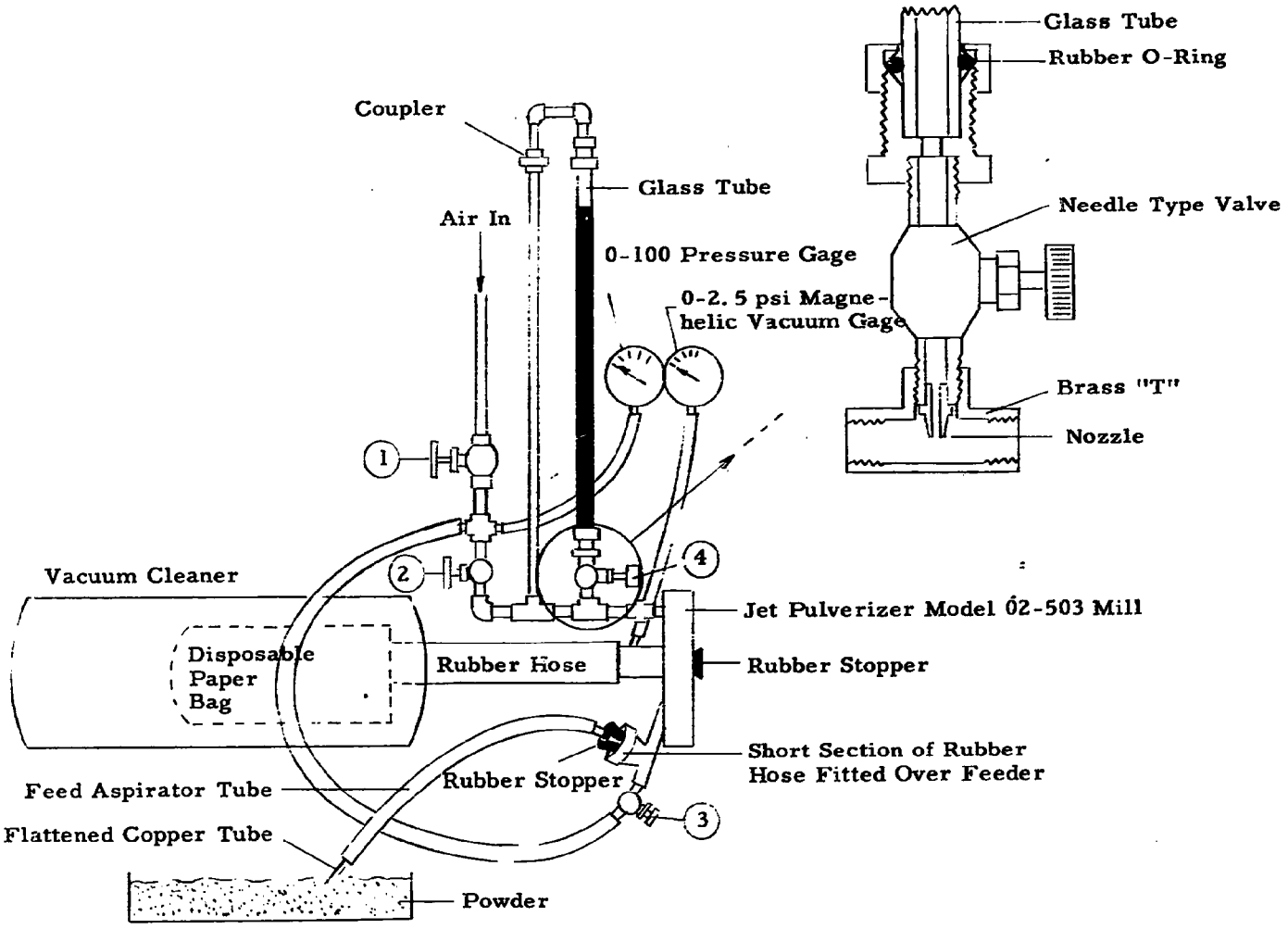

Figure 7. Apparatus for Coating Powders with Surface Active Agents

from positive to negative. The tip of the feed aspirator tube is dipped into the powder container. As soon as powder begins flowing into the mill, valve 2 is opened. The negative pressure at the feed aspirator tube will be maintained throughout the remainder of the run unless the mill outlet becomes clogged. Valve 4 is opened part way, allowing the liquid in the glass tube to flow slowly into the branch carrying the main air stream into the mill. The amount the valve is opened will depend upon the viscosity of the liquid. The high-velocity air stream breaks the liquid up into tiny droplets and transports them into the mill. During the run, the tip of the feed aspirator tube is moved back and forth in the powder container permitting the powder to be sucked up into the tube at a fairly uniform rate. The powder feed rate is controlled by the rapidity with which the tip is moved about. The powder feed rate should be such that the last trace of powder enters the mill at the same instant the level of the liquid reaches the lower mark on the glass tube. With a little practice, this can be accomplished without too much difficulty.

F. Technique for Adsorbing Foreign Vapors onto Powders

A system was devised for the purpose of allowing selected vapors to be absorbed onto powders. A schematic drawing of the system is shown in Figure 8.

The procedure used to treat a powder sample with a vapor is as follows: The powder to be treated is deagglomerated using the technique described in Section II-B and then is placed in the powder container shown in Figure 8. The volatile liquid whose vapors are to be adsorbed onto the powder is placed in the liquid container. With valves C and D closed and valves A and B open, the vacuum pump is started. The cold trap protects the pump from moisture and other vapors.

The powder is pumped down to a pressure of about 100 microns of mercury for a period of approximately 48 hours to remove as much water and vapors as possible before adding the vapor to be tested. The powder must

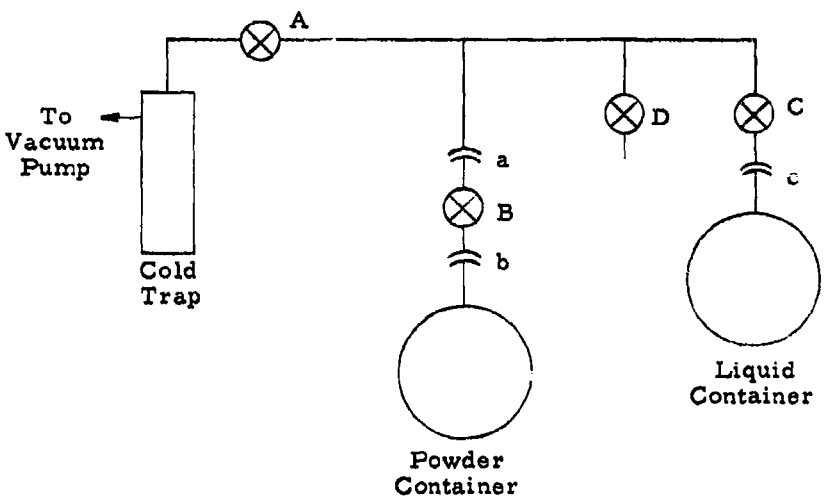

Figure 8. Apparatus for Adsorbing Vapors onto Powders

be stirred frequently during the pumping action. By closing valves A and B and opening bleeder valve D, the powder container can be separated from the rest of the system at ball and socket joint a. The powder container can then be shaken gently and replaced before the pumping is continued. In this manner, fresh powder is exposed to the vapor in the container.

Upon completion of the preliminary pumping phase, valve A is closed, the pump is stopped, and valve C is opened. Vapor from the volatile liquid rapidly fills the upper part of the system. The powder container is still under vacuum so, when valve B is opened, vapor enters the powder container and starts to adsorb onto the powder. At periodic intervals, the powder container is removed and gently shaken. At this time the pump is used to replenish the supply of vapor in the system. The powder is exposed to the vapor for a period of 48 hours before tests are begun.

III. TESTS AND PROCEDURES

A. Particle Size Analyses

Two different techniques have been used on this program to measure particle size distribution of powders. One is a microscopic technique, and the other is the Whitby centrifuge sedimentation technique.[5] Both techniques, along with any modifications required for specific powders, are discussed below.

1. Microscope Technique

With the exception of sample preparation, the basic microscope technique is the same for all powders analyzed. The basic technique is this: The sample is placed on the stage of a Unitron microscope. Photographs are taken of several random fields. The photographs are then analyzed by counting and measuring each particle. At least 200 particles are counted and measured in a single analysis. Particle diameters are determined by multiplying the measured diameter by the appropriate magnification factor.

Since sample preparation varied with different powders, it is necessary to discuss each powder separately.

a. Saccharin

Saccharin samples were prepared by adding a small amount (about 0.5 g) of powder to 150 ml hexane (Skelly B) and mixing in a Waring blender for 10 to 15 seconds. Immediately after mixing, an aliquot of the suspension was withdrawn by means of an eyedropper and placed in a Dunn cell. The Dunn cell was oriented with its cover slip facing downward and placed on the stage of the Unitron microscope. Sufficient time was allowed for the particles to settle on the cover slip before any photographs were taken.

b. Carbowax 6000

Sample preparation of Carbowax 6000 was essentially the same as that described above with the exception that heptane was used for the suspension liquid instead of hexane.

c. Span 60

Span 60 required a slightly different technique because no suitable suspension liquid could be found. The only liquids that would not dissolve Span 60 were either too dense or too viscous. The technique finally adopted was this: About 0.5 g of powder was added to 150 ml of cold water and mixed in a Waring blender for 10 to 15 seconds. An aliquot of the suspension was withdrawn by means of an eyedropper, and a single drop was placed on a glass cover slip. The water was allowed to evaporate. The cover slip was then placed on the stage of the microscope and analyzed in the manner described above.

d. Egg Albumin

Sample preparation of egg albumin was essentially the same as that used for Span 60 with the exception that benzene was used for the suspension liquid instead of water.

2. The Whitby Technique

The Whitby technique is a liquid sedimentation method in which the particles start settling from a thin layer at the top of the sedimentation liquid. This is accomplished by first dispersing the particles in a liquid that is miscible with the sedimentation liquid and has a slightly lower density and a slightly higher viscosity. A small aliquot of this suspension is introduced at the top of the sedimentation liquid by means of a special feeding

chamber, and the particles begin settling from the lighter liquid into the sedimentation liquid. The bottom of the settling tube is "necked down" into a narrow capillary. As the particles reach the bottom, they pile up in the capillary and form a column. Particle size distribution is determined by measuring the column height at predetermined intervals.

For powders containing relatively large-size particles, the entire analysis is made using gravity settling. For finer powders, the first portion of the analysis is made using gravitational force and the final portion using centrifugal force. For still finer powders, centrifugal force is used throughout the entire analysis. Three different centrifuge speeds are available, namely 600, 1200, and 1800 rpm.

For the gravitational portion of the analysis, the time schedule is calculated from Stokes' law:[6]

$$t_g = \frac{(18 \times 10^8)\,\eta_o\, h}{(\rho - \rho_o)\, g\, d^2} \quad , \tag{5}$$

where:

t_g = time in seconds for a particle to settle distance h

d = particle diameter, microns

h = settling height, cm

ρ = particle density, g/cm^3

ρ_o = density of sedimentation liquid, g/cm^3

η_o = viscosity of sedimentation liquid, poises

g = gravitational constant

For the centrifuge portion of the analysis, the time schedule is calculated using Svedberg's modification of Stokes' law.[7]

$$t_c = \frac{(18 \times 10^8)\eta_o}{(\rho - \rho_o)\omega^2 d^2} \ln \frac{r_2}{r_1} \quad , \tag{6}$$

where:

t_c = centrifuge running time, seconds

r_1 = starting radius of rotation of particle

r_2 = final radius of rotation of particle

ω = angular velocity

The first problem in performing a particle size analysis by this technique is to find suitable dispersing and settling liquids. In addition to the requirements for these liquids given above, there are the requirements that the particles must be practically insoluble in either liquid, and also that the particles must not flocculate in either liquid.

From the above statements, it is apparent that each powder presents a unique problem. For this reason, each powder analyzed is discussed separately.

a. Saccharin

The liquids found to work best for saccharin were naptha as the dispersing liquid and benzene as the sedimentation liquid. A small amount (one drop/100 cc) of Twitchell base 8240 (a product of Emery Industries, Inc.) was added to each liquid to disperse the particles.

The time schedule and other information pertinent to the particle size analyses of saccharin are given in Table 5. Since the particle sizes were quite small in all the saccharin samples analyzed, it was possible to dispense with gravity settling and begin the analyses at 600 rpm. The middle portion was made at 1200 rpm and the final portion at 1800 rpm.

Table 5. Particle Size Analysis Schedule for Saccharin

Material tested:	saccharin
Density of material:	1.426 g/cm^3
Dispersing liquid:	naptha
Sedimentation liquid:	benzene
Density of sedimentation liquid:	0.873 g/cm^3
Viscosity of sedimentation liquid:	0.00606 poises
Dispersing agent:	Twitchell base 8240 (1 drop/100 cc liquid)
Dispersing method:	mix in Waring blender for 10 sec

Particle Size (microns)	Centrifuge Speed (rpm)	Time (min, sec)	Centrifuge Correction* (sec)	Corrected Time (min, sec)
20	600	17.5	9	26.5
15	600	13.5	9	22.5
10	600	38.7	9	47.7
8	600	39.0	9	48.0
6	600	1:25.0	9	1:34.0
5	1200	22.6	10	32.6
4	1200	37.9	10	47.9
3	1200	54.6	10	1:04.6
2	1800	2:01.0	30	2:31.0
1	1800	6:29.0	30	6:59.0
0.5	1800	41:50.0	30	42:20.0

* Centrifuge corrections are made to compensate for starting and stopping times.

b. Carbowax 6000

The dispersing and settling liquids used in the analysis of Carbowax 6000 were hexane and heptane, respectively. A small amount (1 drop/100 cc liquid) of Span 20 was added to each liquid to disperse the particles.

The time schedule and other pertinent information are given in Table 6. Here again, the particle sizes in the samples analyzed were small enough to permit beginning the analysis at 600 rpm rather than under gravity.

Table 6. Particle Size Analysis Schedule for Carbowax 6000

Material tested:	Carbowax 6000
Density of material:	1.210 g/cm^3
Dispersing liquid:	hexane
Sedimentation liquid:	heptane
Density of sedimentation liquid:	0.679 g/cm^3
Viscosity of sedimentation liquid:	0.00409 poises
Dispersing agent:	Span 20 (1 drop/100 cc liquid)
Dispersing method:	mix in Waring blender for 10 sec

Particle Size (microns)	Centrifuge Speed (rpm)	Time (min, sec)	Centrifuge Correction (sec)	Corrected Time (min, sec)
20	600	12.2	9	21.2
15	600	9.5	9	18.5
10	600	27.2	9	36.2
8	600	27.5	9	36.5
6	600	59.7	9	68.7
5	1200	15.8	10	25.8
4	1200	26.6	10	36.6
3	1200	38.3	10	48.3
2	1800	1:25.1	30	1:55.1
1	1800	4:33	30	5:03
0.5	1800	29:27	30	29:57

c. Span 60

No suitable dispersing liquid-sedimentation liquid combination could be found for Span 60; therefore, no particle size analyses were made on this material using the Whitby technique.

d. Egg Albumin

The dispersing liquid used in the analysis of egg albumin was a mixture of 30 percent naptha and 70 percent benzene, and the settling liquid was benzene. A small amount (1 drop/100 cc liquid) of Twitchell base 8240 was added to each liquid to disperse the particles. Because of the different particle size ranges of the samples analyzed, it was necessary to use two schedules, one for coarse samples and one for fine samples. These schedules along with other pertinent information are given in Table 7.

B. Shear Strength Test

The apparatus for the powder shear strength test is illustrated in Figure 9. The letter A designates a small, flat table covered with No. 100 emery cloth. Item B is a mask consisting of a sheet of 1/16-inch aluminum with a 2-1/2-inch-diameter hole in its center. Letter C denotes a brass disc 1/16-inch thick and 2 inches in diameter. The bottom surface of the disc is covered with No. 100 emery cloth. Item D is a cord attached to the edge of the disc. The cord passes under pulley E and thence up to a force-measuring device.

The force-measuring device illustrated here is a modified Jolly balance. This device is one of the two force-measuring devices used in conjunction with shear strength tests. The other force-measuring device is the tilting beam apparatus. Both of these devices are discussed later.

Table 7. Particle Size Analysis Schedule for Egg Albumin

Material tested:	egg albumin
Density of material:	1.27 g/cm^3
Dispersing liquid:	30 percent naptha, 70 percent benzene
Sedimentation liquid:	benzene
Density of sedimentation liquid	0.873 g/cm^3
Viscosity of sedimentation liquid:	0.00606 poises
Dispersing agent:	Twitchell base 8240 (1 drop/100 cc liquid)
Dispersing method:	mix in Waring blender for 10 sec

Particle Size (microns)	Centrifuge Speed (rpm)	Time (min, sec)	Centrifuge Correction (sec)	Corrected Time (min, sec)
Schedule used for Coarse Samples				
200	gravity	7.0	none	7.0
150	gravity	5.5	none	5.5
100	gravity	15.6	none	15.6
75	gravity	21.8	none	21.8
50	gravity	1: 2.4	none	1: 2.4
40	gravity	1: 3.0	none	1: 3.0
30	gravity	2:16.3	none	2:16.3
20	gravity	6:29.5	none	6:29.5
10	600	57.5	9	1: 6.5
8	600	50.9	9	59.9
Schedule used for Fine Samples				
100	gravity	28.1	none	28.1
75	gravity	21.8	none	21.8
50	gravity	1: 2.4	none	1: 2.4
40	gravity	1: 3.3	none	1: 3.3
30	gravity	2:16.0	none	2:16.0
20	gravity	6:28.5	none	6:28.5
10	600	57.8	9	1: 6.8
8	600	50.7	9	59.7
6	600	1:54.6	9	2: 3.6
4	600	5:32.0	9	5:41.0
3	600	7:45.0	9	7:54.0
2	1200	5:38.0	10	5:48.0
1	1200	37:20.0	10	37:30.0

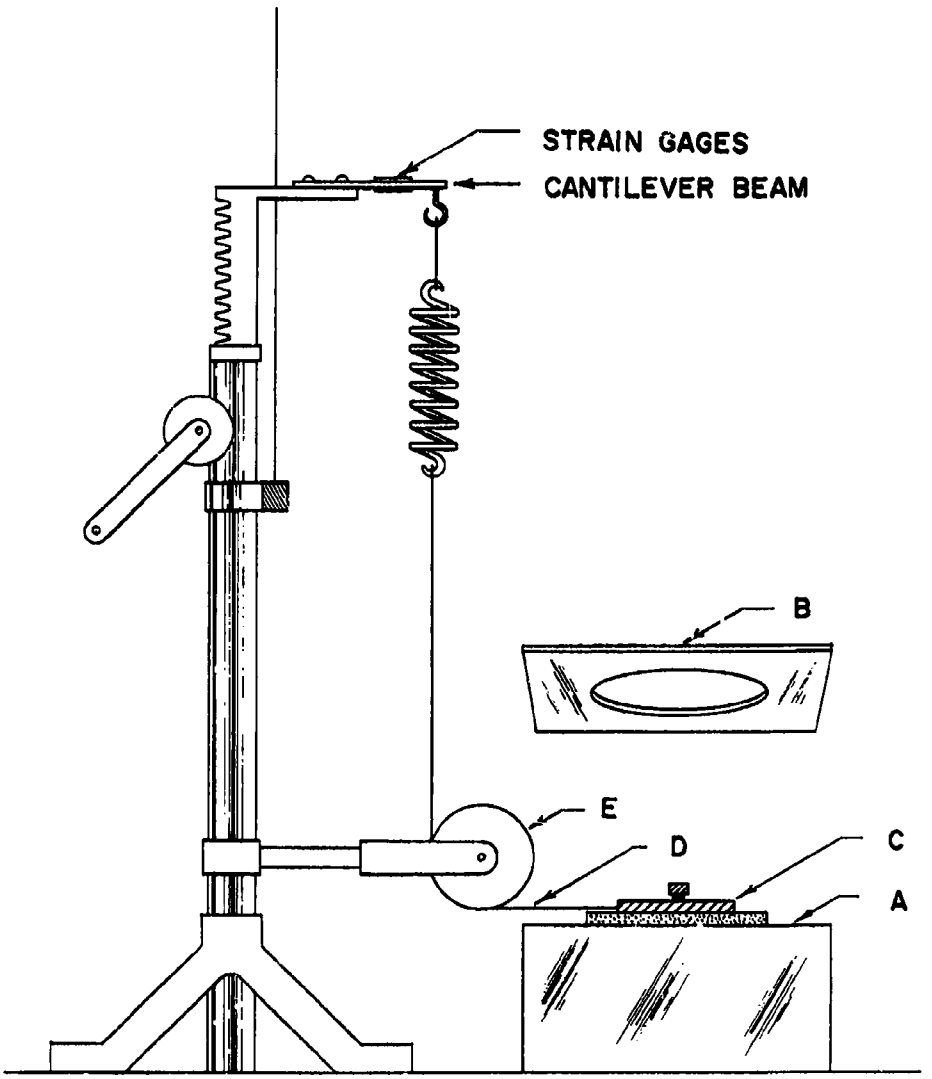

Figure 9. Powder Shear Strength Apparatus

The procedure used in conducting the shear strength test is this: The mask is placed on the emery cloth-covered table. A small amount of powder is sifted onto the mask and leveled off even with the top surface of the mask by means of a spatula. The mask is lifted off, leaving a thin layer of powder on the table. The brass disc is carefully set on the powder layer in such a manner that the point at which the cord is attached is lined up with the pulley. Weights are added to the disc to give the desired compressive load. The disc is displaced a short distance (about 1/4 inch) by pulling on the cord. This is to assure that the disc is seated properly on the powder layer and is oriented correctly with respect to the pulley. The recorder chart drive is turned on. Tension is applied to the cord by turning the crank of the Jolly balance at a slow, uniform rate of speed until the disc begins to slide, thus shearing the layer of powder sandwiched between the two emery cloth-covered surfaces. The chart drive is turned off, which completes the test. A series of such tests is made using various compressive loads. Plotting shear strength as a function of compressive load produces a linear relationship over a fairly wide range of compressive loads.

As mentioned previously, the force-measuring device illustrated in Figure 9 is a modified Jolly balance. The modification consists of transforming the device from a purely mechanical one to an electrical one. This is accomplished by adding a cantilever beam equipped with four strain gages. The main advantage with this modification is that it permits data to be recorded automatically by means of an electronic strip-chart recorder.

The strain gages are connected in a full bridge configuration as shown pictorially and schematically in Figure 10. Strain gage elements 2 and 4 are cemented to the top side of the beam, and elements 1 and 3 are cemented to the bottom side of the beam. Electrical connections are made according to instructions furnished by the manufacturer of the auxiliary equipment.

Two different makes of auxiliary equipment were used. One consisted of a Brush Electronics universal amplifier, Model BL-520; a Brush strain gage input box, Model BL-350; and a Brush oscillograph, Model BL-222. The other consisted of a Sanborn power supply, Model 150-400; a Sanborn carrier preamplifier, Model 150-1100AS; and a Sanborn 151 recorder.

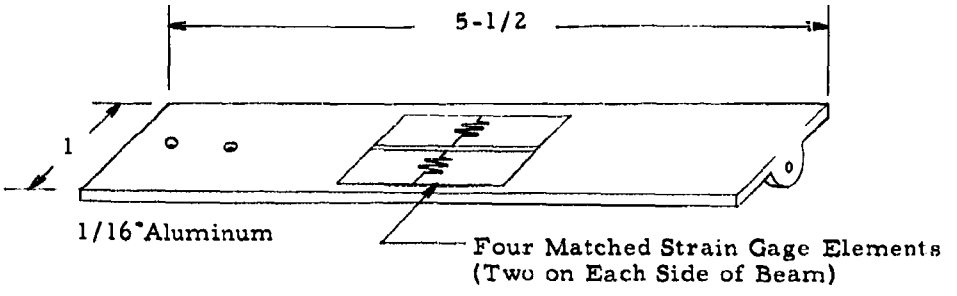

Note: Dimensions shown (in inches) are typical and may be varied with magnitude of forces to be measured.

(a) Cantilever Beam

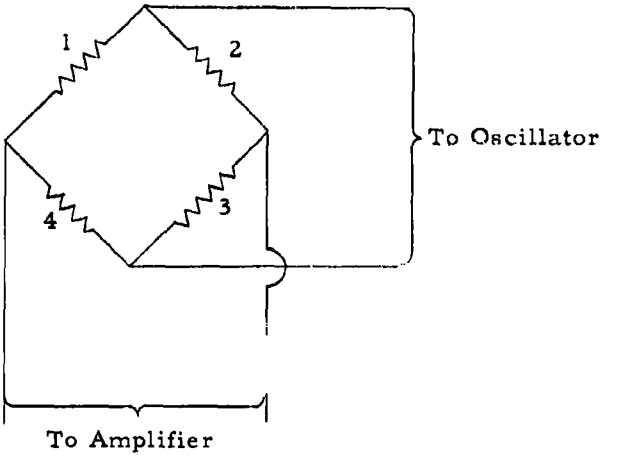

(b) Electrical Circuit for Strain Gages

Figure 10. Strain Gage-Cantilever Beam

Calibration of the strain gage-cantilever beam is accomplished simply by hanging known weights on the end of the beam and noting the deflection on the recorder.

Although the modified Jolly balance is fine for measurements made in the open laboratory, it is not suitable for glove box use because it is too tall. For this reason, a tilting-beam force-measuring device was constructed. This device is illustrated in Figure 11. The beam is supported by a vertical post 15 inches high, 2 inches wide, and 1/2 inch thick. The post is mounted in the center of a base plate 30 inches wide, 10 inches deep, and 1/2 inch thick. The beam itself is 24 inches long, 1 inch high, and 1/4 inch thick with a pivot point located 11 inches from the end attached to the spring. The spring, through which force is applied, has one end connected to the beam and the other end connected to a cord leading to a hand crank. (In a more recent version, the hand crank was replaced with a small d-c motor.) The cantilever beam, on which the strain gages are mounted, is fastened to the opposite end of the tilting beam.

Precautions must be taken to insure that the beam is in the horizontal position during calibration and use, and that the forces to be measured are applied straight downward at the tip of the cantilever beam.

1. Effect of Rate of Force Application on Powder Shear Strength

An investigation was conducted to determine whether rate of force application has any effect on powder shear strength. Rate of force application should not be confused with rate of shear. These two rates are entirely unrelated because force is applied before the powder begins to shear.

The force-measuring device used in this study was the tilting beam apparatus equipped with a small d-c motor. The d-c motor was connected to a variable voltage d-c power supply. Rate of force application was varied by varying the voltage which in turn varied the speed of the motor.

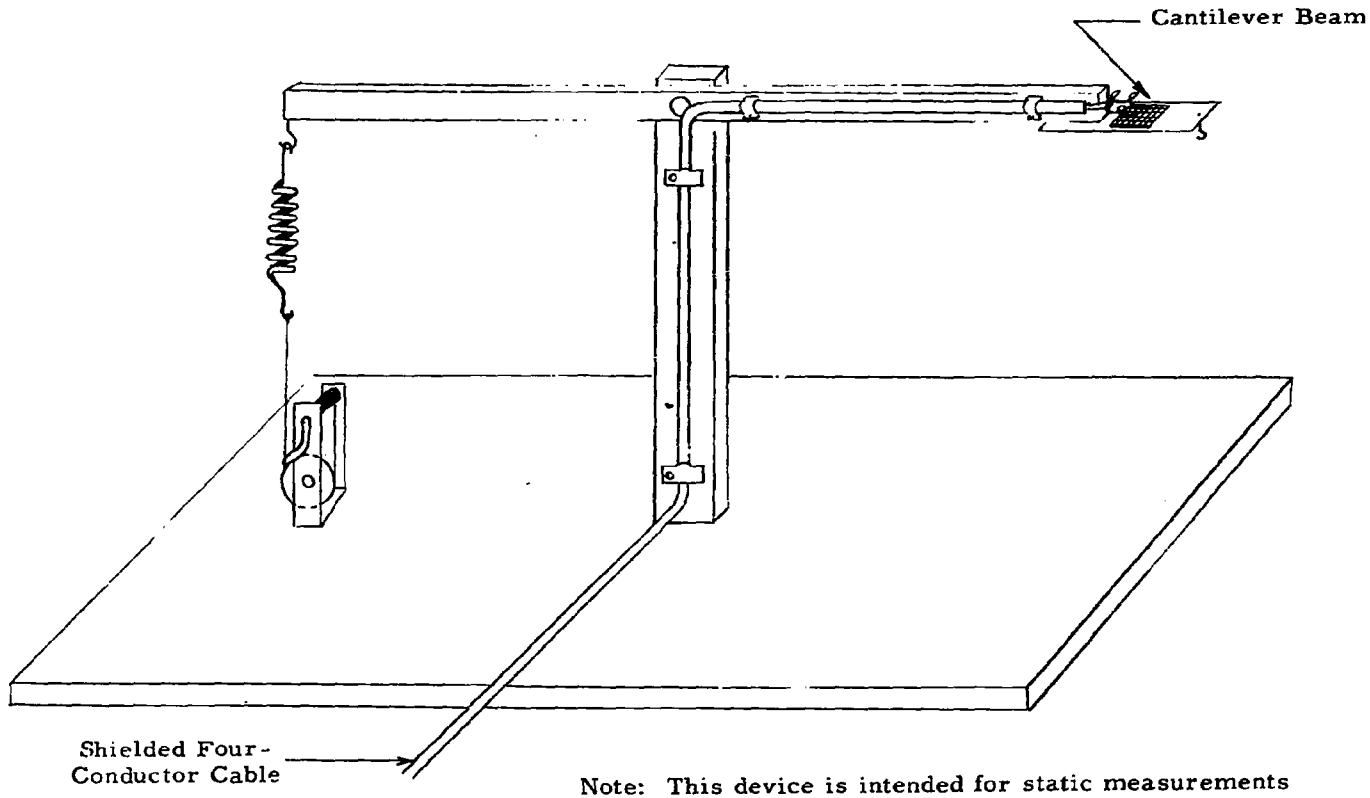

Note: This device is intended for static measurements only. Beam should be in horizontal position during calibration and use.

Figure 11. Tilting Beam Force-Measuring Device

A series of 59 runs was made on powdered Carbowax 6000 using a compressive load of 5950 dynes/cm^2 and varying the rate of force application from 4740 to 142,000 dynes/sec. Rate of force application was varied by varying the output voltage of the d-c power supply. Since the d-c motor ran at a fairly constant speed for any given test, it was possible to determine the rate of force application by analyzing the Sanborn strip charts on which shear strength data were recorded.

The results of the tests are presented in tabular form in Table 8 and in graphical form in Figure 12. The shaded area indicates the range of force application employed in previous shear strength tests in which the hand crank was used. The position of the line drawn through the points was determined by the method of least squares. The equation of the line was found to be:

$$y = 6870 - 0.00019\,x \qquad (7)$$

Since the slope of the line is nearly zero, it can be concluded that the rate of force application has no effect on the measured values.

2. Effect of Powder Bed Thickness on Powder Shear Strength

Tests were made to determine what effect, if any, the thickness of the powder bed has on powder shear strength. Three masks with thicknesses of 1.06, 1.66, and 3.29 mm respectively were used to produce powder beds with corresponding thicknesses. A total of 27 runs were made on powdered Carbowax 6000 using a compressive load of 5950 dynes/cm^2. The results are given in Table 9 and are presented graphically in Figure 13 where shear strength is plotted as a function of powder bed thickness.

It may be seen in Figure 13 that powder shear strength is practically independent of powder bed thickness over the range of 1.66 to 3.27 mm but begins to increase as powder bed thickness is decreased below 1.66 mm.

Table 8. Results of Tests to Determine Effect of Rate of Force Application on Powder Shear Strength

Force Rate (dynes/sec)	Shear Strength (dynes/cm^2)	Force Rate (dynes/sec)	Shear Strength (dynes/cm^2)
4,740	7,100	41,600	6,990
5,260	6,270	41,600	6,880
4,900	7,200	42,800	7,200
5,150	7,610	44,100	5,640
8,350	7,140	44,100	6,480
8,840	6,690	46,500	6,890
10,800	7,200	46,500	6,050
10,300	7,610	46,500	6,990
10,300	6,580	49,000	6,680
11,750	6,780	51,500	6,900
14,700	6,890	51,500	6,480
14,700	7,610	52,700	7,400
14,700	6,980	56,400	6,260
16,700	6,460	63,700	6,990
16,700	6,980	63,700	6,050
16,700	7,190	66,100	5,640
22,100	7,300	66,100	7,300
22,600	6,980	71,100	7,310
23,300	6,980	71,100	7,200
29,400	7,200	74,600	6,690
29,400	6,980	74,600	6,980
28,500	6,460	123,000	6,800
30,700	6,980	128,000	6,470
34,300	6,260	128,000	6,580
34,300	6,980	128,000	6,900
34,300	7,090	137,000	7,730
39,200	7,510	137,000	7,820
39,200	6,570	137,000	6,880
39,200	5,640	142,000	6,890
39,200	7,190		

The increase in shear strength when very thin layers of powder are used is due to the effect of the emery cloth on the table and disc. As the powder bed becomes very thin, asperities on one of the emery cloth surfaces protrude through the powder bed and rub against asperities on the other emery cloth surface. It is therefore important to use a powder bed thickness of at least 1.66 mm.

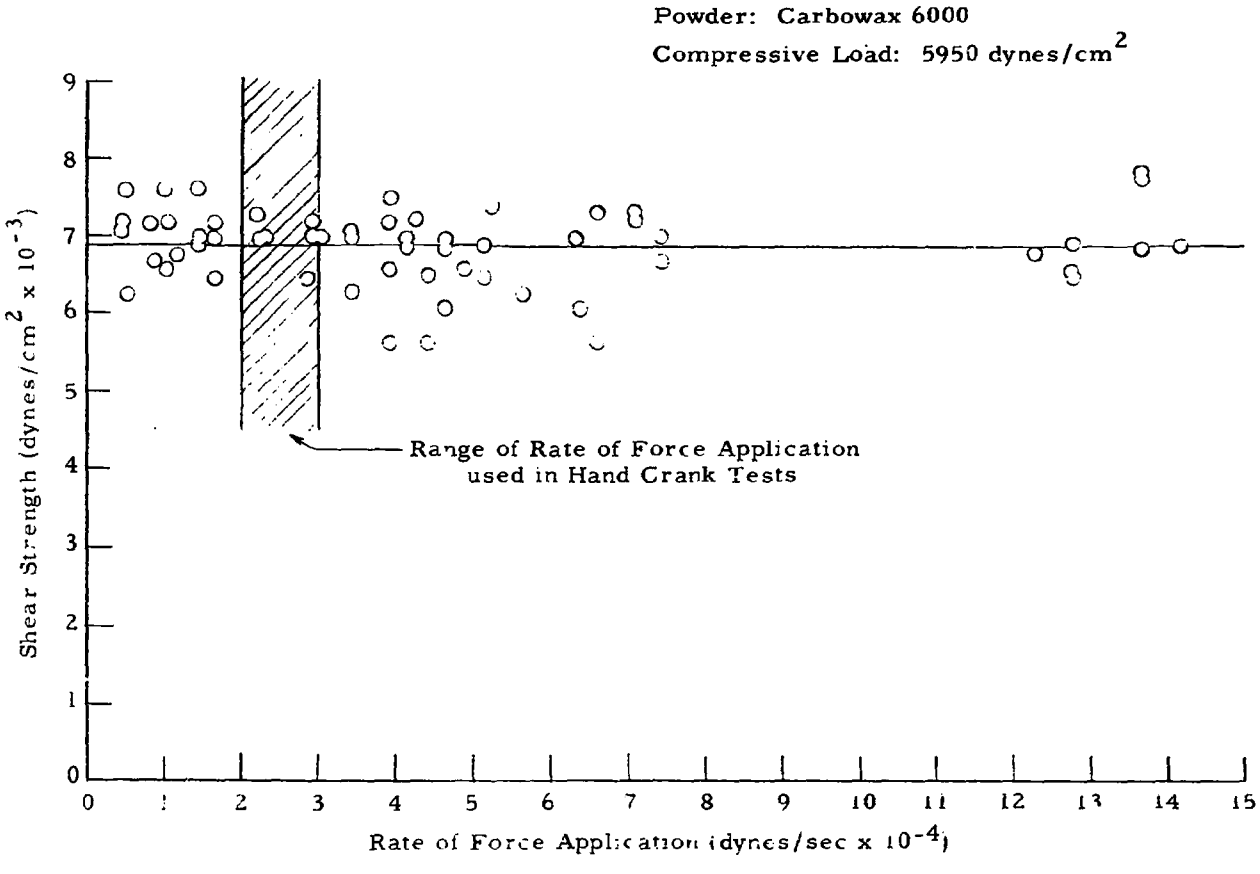

Figure 12. Powder Shear Strength versus Rate of Force Application

Table 9. Results of Tests to Determine Effect of Powder Bed Thickness on Shear Strength

Powder Bed Thickness (mm)	Shear Strength (dynes/cm^2)	Deviation in Shear Strength (dynes/cm^2)
1.06	7,065	224
1.66	6,580	324
3.29	6,420	238

On all powder shear strength tests reported elsewhere in this report, powder bed thickness was 1.66 mm.

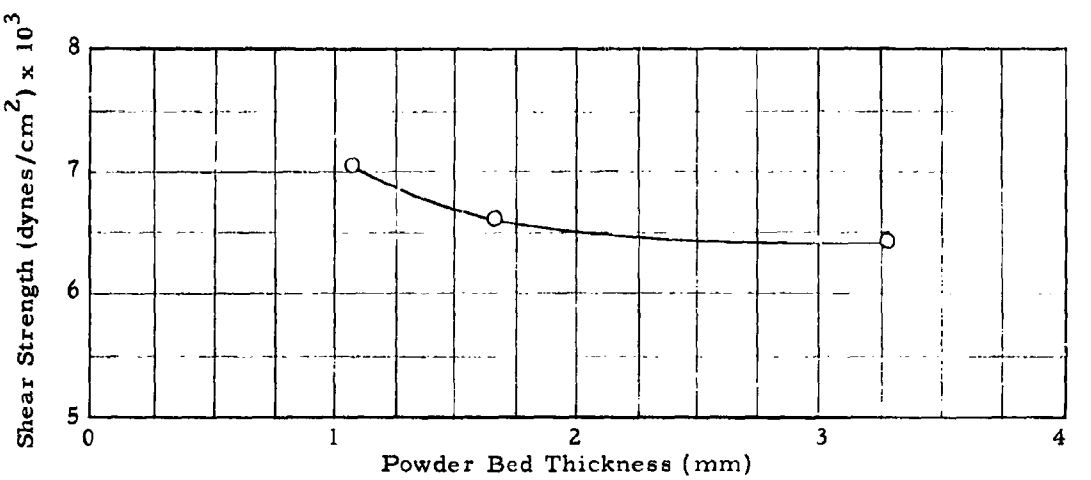

Figure 13. Shear Strength versus Powder Bed Thickness

C. Bulk Tensile Strength Test

The apparatus devised for the bulk tensile strength test is illustrated in Figure 14. Cylinders (1) and (2) are made of aluminum and have an inside diameter of 1.90 cm and a length of 5.08 cm. Cylinder (1) is attached at its lower end to a base plate, while cylinder (2) merely rests on top of cylinder (1) and is equipped with a "paint pail" wire handle at its upper end that permits it to be lifted off cylinder (1) by means of a sensitive force-measuring device. (Either the modified Jolly balance illustrated in Figure 9 or the tilting beam device illustrated in Figure 11 may be used for measuring the forces.) Cylinder (3), being made of brass, slides smoothly over cylinders (1) and (2) keeping them in concentric alignment. Two parallel guide rods prevent cylinder (3) from twisting as it slides over cylinders (1) and (2), and minimize the possibility of relative movement between the two cylinders before the tensile test is made. The knife-edge piston, which is constrained to move in a vertical direction, fits inside cylinder (2) for the purpose of compressing the powder.

Not shown in Figure 14 is an adjustable floor which fits inside cylinder (1). The distance at which this floor is set below the top of the cylinder is not critical; but the floor must be set far enough down to prevent the plug of compressed powder from pulling out of cylinder (1) when the tensile test is made. In this study the floor was arbitrarily set 1.27 cm below the top of cylinder (1).

We follow these steps in performing the test: The apparatus is assembled so that cylinder (2) rests on top of cylinder (1), and cylinder (3) is positioned so that it engages both cylinders (1) and (2). A measured amount of presifted powder is admitted at the top of cylinder (2). (The amount of powder to be used will be discussed later.) The piston is inserted at the top of cylinder (2), and weights necessary to produce the desired compressive load are placed on top of the piston. The period of time during which the load is applied should be such that essentially all settling has ceased, and the period should be the same for each test. In this study the load was

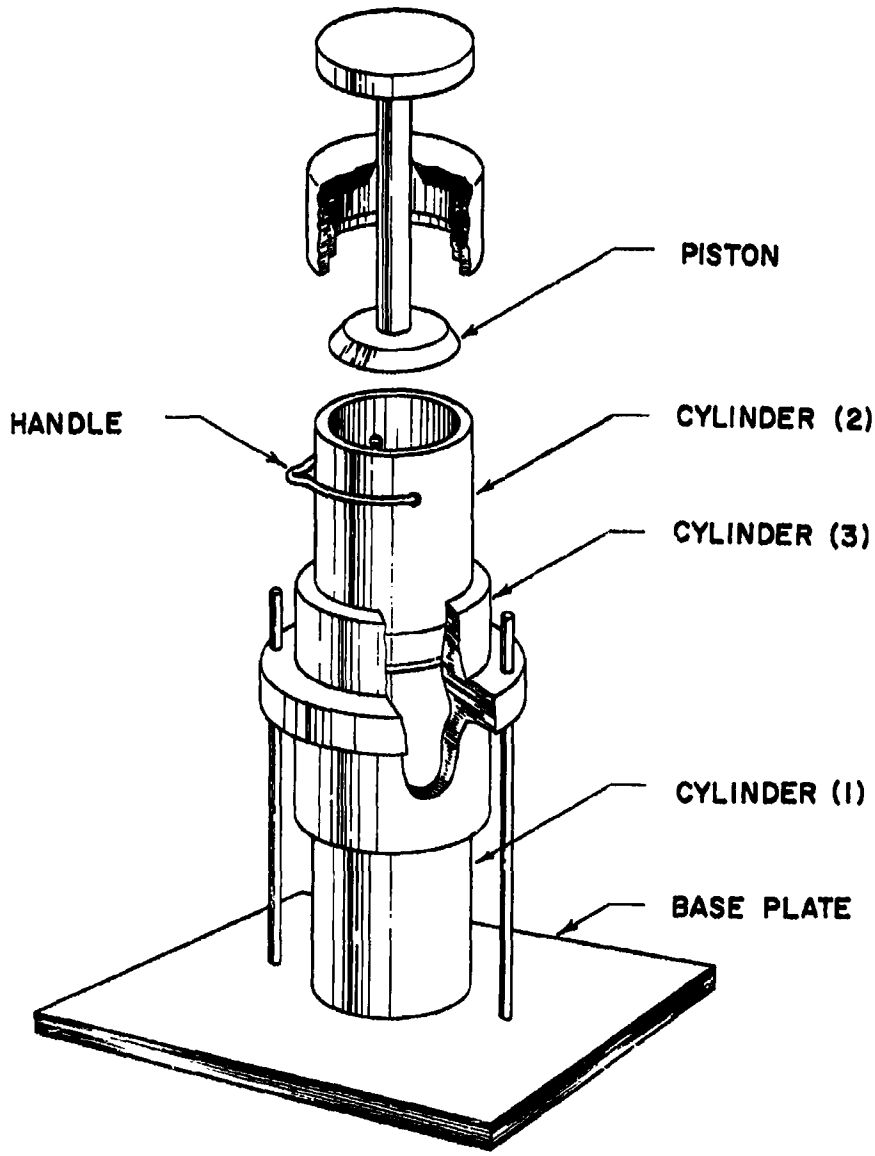

Figure 14. Apparatus for Bulk Tensile Strength Test

applied for a period of 30 seconds. While cylinder (2) is held down firmly against cylinder (1), weights and piston are removed, and the wire handle is raised to its vertical position. Care must be exercised during this act to prevent premature breakage of the powder column.

The apparatus is next placed under the force-measuring device. Cylinder (3) is slid downward until it no longer engages cylinder (2). By means of the force-measuring device, cylinder (2) is lifted off cylinder (1) thus severing the powder column at the plane where the two cylinders had touched each other. Part of the column remains in cylinder (1) and part in cylinder (2). Tensile strength is calculated by adding the weight of cylinder (2) and that of the powder remaining within it, subtracting the result from the total force required to lift cylinder (2) off cylinder (1), and dividing by the cross-sectional area of the powder column.

A series of tests is made at each compressive load using various amounts of powder. The reason for varying the amount of powder is to vary the distance between piston and fracture plane, a distance we refer to as column length.

Tests performed on a number of different powders have indicated that bulk tensile strength is an exponential function of column length. The following formula depicts the manner in which bulk tensile strength varies with column length (see Appendix A):

$$\sigma = \sigma_o e^{-kh} \quad , \tag{8}$$

where:

σ = bulk tensile strength at distance h from the piston

σ_o = bulk tensile strength immediately below the piston (zero column length)

k = a constant equal to $2\mu C/R$

μ = coefficient of friction between the powder and the cylinder wall

C = proportionality constant between the pressure acting in the horizontal direction and the pressure acting in the vertical direction at a point inside the powder column

This type of relationship has been found by other investigators[8, 9, 10, 11] to hold for pressure, density, and porosity of columns of compressed powder.

Plotting bulk tensile strength as a function of compressive load on semi-log graph paper yields a series of straight lines, one for each compressive load. (It is advisable to use the method of least squares when plotting the curves because a certain amount of scatter in the data points is unavoidable.) No data are available in the region corresponding to small column lengths because the powder column tends to pull out of the upper cylinder when column length becomes small. For this reason, the lines on the graph are extrapolated to the vertical axis. The points where the lines intersect the vertical axis have special significance because they represent bulk tensile strength at zero column length, in which case wall friction disappears. Finally, a plot is made of bulk tensile strength at zero column length as a function of compressive load. This yields a linear relationship over the range of compressive loads investigated in this program.

D. Techniques for Measuring Bulk Density of Powders

Two different techniques for measuring bulk density of powders were used on this program. One is a technique for measuring bulk density of loose, uncompacted powders; the other is a technique for measuring local bulk density with a column of compacted powder.

1. Bulk Density of Uncompacted Powder

When using the term "bulk density" with reference to a powder, one should specify the manner in which the measurements are made because rather large differences can result from different methods of measurement. For the same reason, when making a series of bulk-density measurements in which the results are to be compared with one another, it is quite important to follow the same procedure throughout the entire series of tests.

We used the following procedure for measuring bulk density of powders: Powder is sifted through a small funnel covered with 16-mesh screen and into a cylindrical container 7.62 cm high and 3.79 cm in diameter. The orifice of the funnel is held just above the top of the container. The container is filled to the brim, and excess powder is scraped off by means of a spatula. During this operation, the container is not shaken, tapped or otherwise disturbed. Finally, the container is weighed, and the powder bulk density calculated.

2. Local Bulk Density within a Column of Compacted Powder

When powder is compacted in a cylindrical container, the bulk density can easily be found from the mass of powder used, the cross-sectional area of container, and the final column height. This bulk density is only an average over the entire plug, however. No information as to the bulk density at localized regions within the plug can be determined by this method.

In order to study the variation of bulk density as a function of distance from the compacting piston, a special technique was devised. It consisted simply of making direct measurements of bulk density at regularly spaced intervals along the cylinder length. The special apparatus illustrated in Figure 15 was constructed in order to accomplish this. The cylinder in which the powder compaction takes place is made up of a series of fourteen 1-inch and eight 1/2-inch long sections of aluminum tubing. These sections

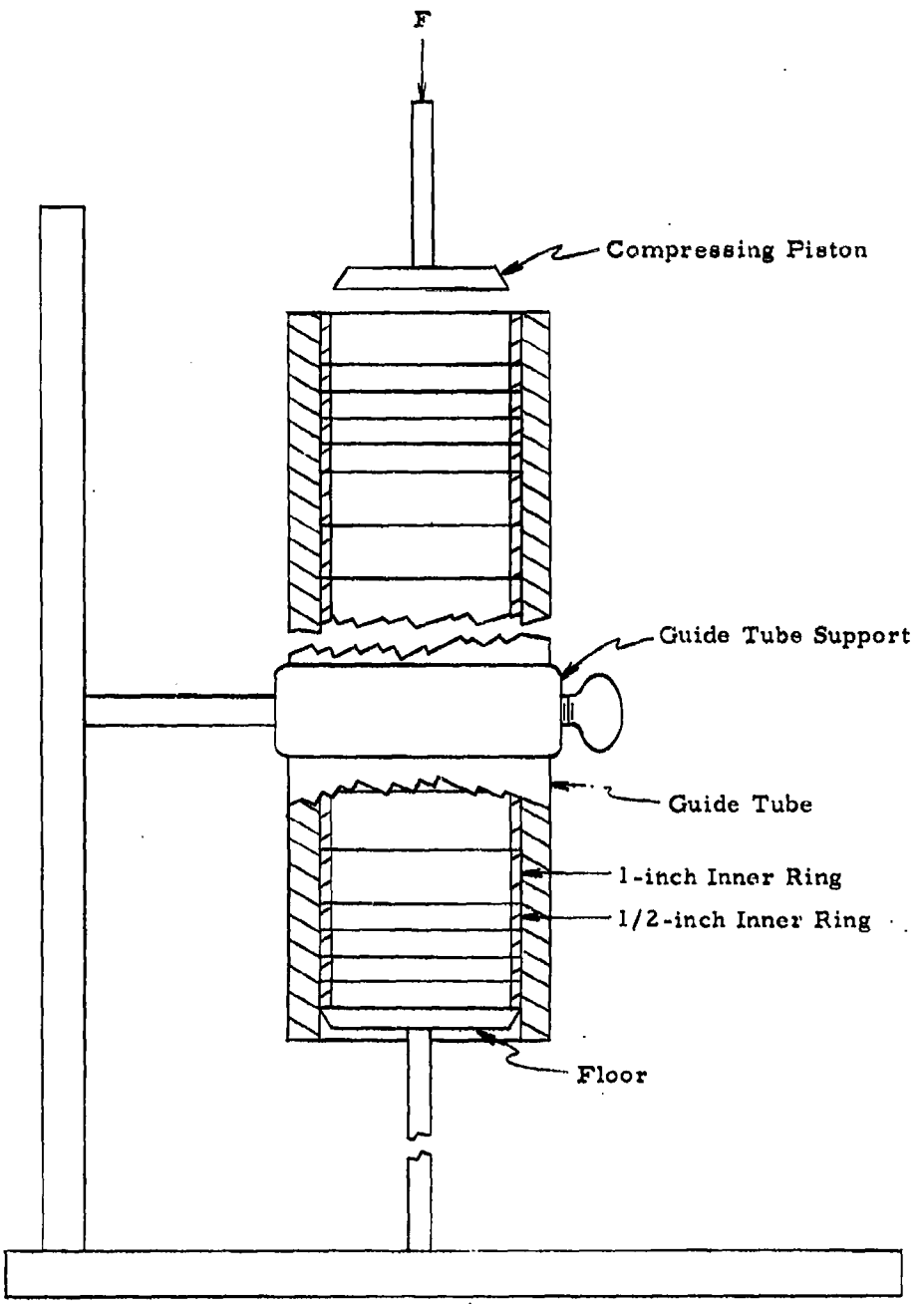

Figure 15. Apparatus for Investigating Variation in Local Bulk Density

are simply stacked one on top of the other to make up a single tube 18 inches long. A second tube is used to hold the stack of rings in axial alignment. This outer guide tube is 18 inches long and its inside diameter is slightly larger than the outside diameter of the rings. A special frame holds this guide tube in such a way that it can be slipped downward while the rings remain in place. In this way the rings can be removed one at a time.

a. Procedure

The guide tube is clamped in place in the frame and the cylinder flour is inserted. The rings are slipped into place in the guide tube in such a way that four of the 1/2-inch rings are located at the bottom and four at the top of powder column after compression. The reason for arranging the rings in this manner is to locate the 1/2-inch rings at the regions where bulk density changes most rapidly. (It may be necessary to make a trial run to properly locate the upper 1/2-inch rings.)

The cylinder is filled with the powder to be tested, and the piston is used to compact it with a known load. Compaction will, of course, decrease the length of the powder column leaving one or more of the upper rings empty. By loosening the frame clamp, the guide tube can be slipped downward exposing the empty rings and permitting them to be removed. The guide tube is slipped downward still further exposing the first filled ring and then reclamped. Using a piece of 0.003-inch shim stock, the powder column is sheared at the junction between the two uppermost rings. The upper ring and powder contained therein is weighed and the mass recorded. This procedure is repated until the entire series of rings has been removed.

Knowing the mass and volume of each ring, the average bulk density of powder contained in each ring is calculated. A graph is made in which bulk density is plotted against distance from the compressing piston. The bulk density is assumed to vary linearly over the short distances represented by the length of a ring, and the average bulk density of the powder in a ring is plotted as if it were the local bulk density at the center of the ring.

Each compressive load results in a different final plug length. By using percentage of final length rather than actual distance from the piston as the abscissa, it is possible to plot the results for a number of different compressive loads on the same graph. This makes comparison of effects of different loads easier.

E. Dynamic Angle of Repose Test

In the test for measuring dynamic angle of repose of powders, the powder flows rapidly out of a funnel onto a flat, horizontal surface. While the powder is flowing, a photograph is taken of the powder pile. The angle between the horizontal surface and the side of the conical-shaped pile, the angle we refer to as the dynamic angle of repose, is measured from the photograph.

The apparatus used in this test consists primarily of a small copper funnel attached to an electric vibrator (see Figure 16). The dotted lines represent a wooden box with windows on the top and one side. The main function of this box is to shield the falling powder from air draughts. The arm holding the funnel extends through a loose-fitting hole in the box. The spacing between the tip of the funnel and the top of the lab-jack onto which the powder falls is 4 cm. The diameter of the funnel orifice is 0.79 cm.

The test procedure is as follows: The powder to be tested is sifted through a 16-mesh screen to eliminate the large lumps. Approximately 20 cm^3 of this presifted powder is loaded into the funnel. The funnel outlet is closed during loading and then opened immediately thereafter. Care is taken so as not to bump the funnel causing the powder to flow out prematurely. After the funnel is loaded, the Plexiglas cover is placed on the box, and the light is positioned so that the inside of the box is well lighted. The vibrator is turned on and powder starts to flow through the funnel orifice. A photograph is taken of the powder pile while the powder is flowing, usually just before the funnel is empty. It has been found that when the powder

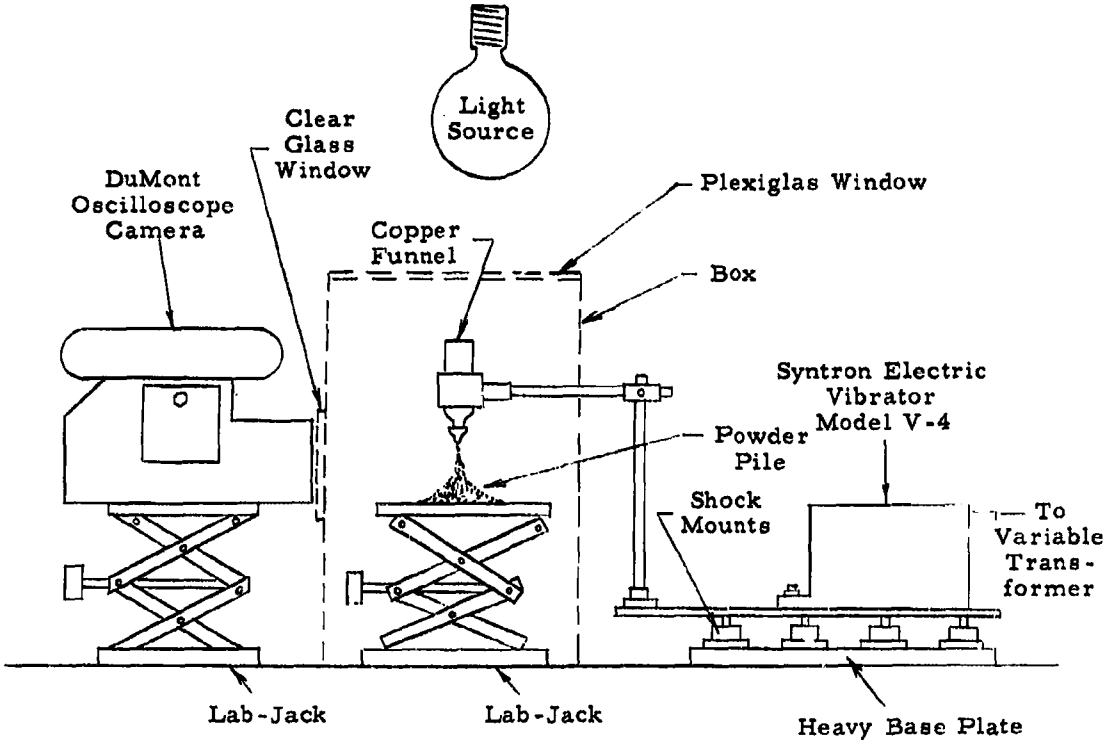

Figure 16. Dynamic Angle of Repose Apparatus

starts to flow, the angle of repose rapidly reaches a value which remains essentially constant as long as powder continues to flow. Sometimes the pile has a tendency to collapse and flatten out just after the powder has stopped flowing.

At least three tests are made on each powder, and new powder samples are used for each test. The angles are measured from the photographs, and the results averaged. The average deviation is used as a measure of error.

F. Dispersibility Test

A device patterned after the aerophilometer[12] was designed and constructed to test the dispersibility of various powders directly. The basic principle of this test consists simply of dispersing the powder sample into a special chamber and measuring two parameters which characterize the resulting aerosol.

A schematic drawing of the apparatus is shown in Figure 17. The apparatus consists of three major parts. First is the chamber itself; second is the detecting system consisting of a light source, photomultiplier tube with associated power supply and a strip chart recorder; last is the dispersing gun. Each of these will be described separately.

The final system herein described evolved throughout the program, with modifications and improvements being made from time to time.

1. Aerosol Chamber

The aerosol chamber is a large box into which samples of powder are dispersed. It is constructed of sheet aluminum and measures one meter on each side. The front is held in place by eight clamps and can be removed easily for access to the interior. Mounted on one side is a collimated beam light source, and directly opposite on the other side is a light trap. The trap is designed to minimize reflection from the interior of the box itself, thus reducing background level of the scattered light. A 1P21 photomultiplier tube is mounted directly in the center of the chamber top. A baffle is arranged so that the sensing element in the photomultiplier tube monitors the entire path of the light beam. Thus, the output of the photomultiplier tube at any time will be dependent on the number, size, and kind of particles in the path of the light beam.

A small electric fan sets on the floor of the box. This fan is turned on just before the powder sample is dispersed in the chamber and is turned off immediately after. The purpose of the fan is to create turbulence for a short period of time to thoroughly mix the aerosol evenly throughout the chamber.

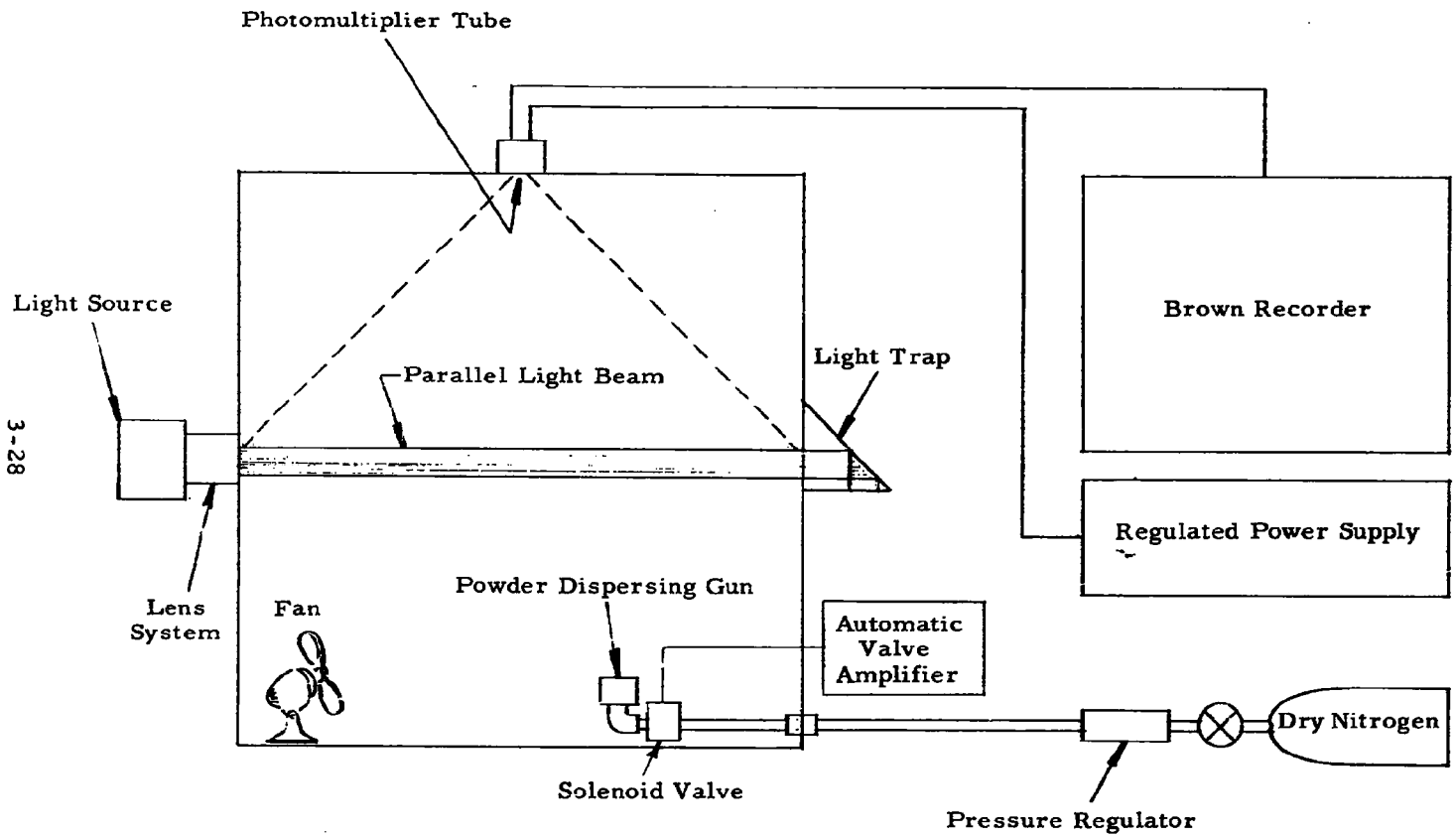

Figure 17. Apparatus for Measuring Dispersibility of Powders

2. Detecting System

A 200-watt projector bulb provides the light source for the system. Its intensity can be adjusted by means of a variable transformer to compensate for aging of the bulb. A constant voltage transformer is used to minimize the effects of line voltage fluctuations. A blower prevents overheating of the bulb and lengthens its life. The sensing element is the 1P21 photomultiplier tube. The potentials for its dynodes are obtained from a regulated power supply, which in turn is supplied by a constant voltage transformer. With this arrangement, normal line voltage fluctuations have negligible effect on the system. The output of the photomultiplier tube is indicated by a Brown recorder. The recorder has a position control for setting the zero or reference level. An adjustable span control enables one to vary the difference between recorder reading and reference level for a given signal. With the span control, one can always adjust the deflection to a convenient level.

3. Standardization of the Light Source

A technique was devised to compensate for aging of the light bulb. The basic idea is to insert a standard light-scattering object into the path of the light beam so that a reproducible amount of light can be scattered onto the photomultiplier tube. This is done when there is no aerosol in the chamber. The light intensity of the source is adjusted by means of the variable voltage transformer to produce some arbitrary reading on the recorder chart. Each time the light source is standardized, the variable voltage transformer is adjusted to produce the same reading on the recorder chart.

The specific steps to be followed are these: The chamber is cleaned with a vacuum cleaner, and any airborne dust particles are blown out with the electric fan. The glass windows covering the light source and photomultiplier tube are cleaned. The light-scattering object (in this case a sheet of Teflon) is inserted in the light beam at the point where light enters the chamber. With the chamber cover clamped in place and the photomultiplier

B+ turned off, the reference control is adjusted to give a convenient reading near the bottom of the recorder scale. The B+ is turned on, and the light intensity is adjusted to produce a convenient reading near the top of the scale. Both readings are purely arbitrary; however, the same ones must be used each time the light source is standardized. After standardizing, the Teflon sheet is removed and the apparatus is ready for testing aerosols.

4. Powder Dispersing Gun

The powder-dispersing apparatus used in conjunction with the aerosol chamber is of the bursting-diaphragm type. We call this apparatus the bursting-diaphragm gun. A sketch of the apparatus is shown in Figure 18. The retaining cap is made of hardened tool steel, while the rest of the device is made of brass. The edge of the retaining cap which fits down against the diaphragm is sharp so that it cuts the diaphragm when the pressure inside the powder chamber is sufficiently great. The dimensions of the powder chamber are 1.43 cm deep by 1.43 cm in diameter. The diameter of the capillary hole at the bottom is 0.061 cm.

The gun is connected by way of a high-pressure hose and a high-pressure regulator to a cylinder of dry nitrogen. The pressure inside the powder chamber of the gun is increased until the diaphragm shears. The sudden expansion of air entrapped in the void spaces between the powder particles tends to break up the agglomerates and disperse the powder. The energy expended in the dispersing process can be varied by varying the thickness of the diaphragm, thereby changing the bursting pressure. A perforated disc may be inserted underneath the diaphragm so that when the diaphragm bursts the particles must pass through the small holes in the disc. The only time this perforated disc was used was in the study of dispersibility of compacted plugs of powder (see Section IV-I).

In the early studies, the supply of dry nitrogen was turned off by hand after the powder was dispersed. Thus, a certain amount of gas escaped into the chamber in the interval of time between the bursting of the diaphragm

and the closing of the valve. This escaping gas tended to pressurize the chamber slightly causing some of the airborne particles to be blown out through various leak holes. To eliminate this difficulty, an automatic shut-off valve was devised.

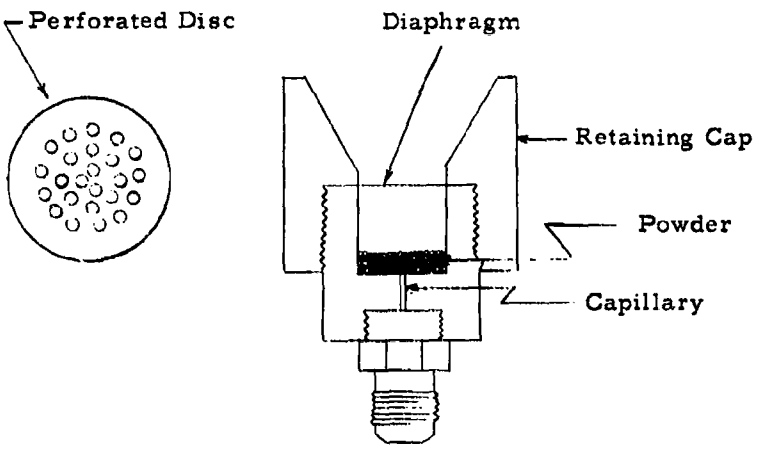

Figure 18. Bursting-Diaphragm Powder-Dispersing Gun

5. Automatic Shut-Off Valve

Operation of the automatic valve is based on the fact that when the diaphragm is burst, a definite shock wave results. This shock wave is transformed into an electrical pulse by means of a crystal phono cartridge (Astatic No. 6) which is mounted directly on the dispersing gun. A high-inertia pendulum is mounted in the stylus chuck so that when the cartridge vibrates, the stylus chuck is more-or-less stationary, and an electrical

signal is produced. This electrical signal is amplified by means of a three-stage transistor amplifier. The amplified signal actuates a sensitive relay which in turn releases a locking relay. The locking relay shuts off the power to a normally-closed solenoid valve, stopping the flow of nitrogen.

In use, switch S_2 (Figure 19) is pushed to lock open the solenoid valve. Switch S_3 (Figure 20) is turned on, and potentiometer R_1 is advanced until the background current through the first relay is just under the relay pull-in current. The diaphragm is then burst in the usual manner. Switch S_1 may be pushed if it ever becomes necessary to shut off the flow of nitrogen manually.

6. Dispersibility Test Procedure

The equipment must be warmed up thoroughly before a test is started. The time required for equipment warmup may be utilized for such purposes as preparing the powder dispersing gun. The powder sample is carefully weighed out and placed in the gun. (The amount of powder used in most tests performed on this program was 0.1 g.) The gun is assembled with brass diaphragm properly inserted. The light source is standardized in the manner previously described. The variable span control on the Brown recorder is adjusted to the desired level, and the reference is positioned at a convenient point near the bottom of the chart. The solenoid valve which shuts off the flow of nitorgen after powder dispersal is opened by closing switch S_2 in Figure 19. The fan inside the chamber is turned on, and pressure to the dispersing gun is increased until the diaphragm bursts. The resulting shock wave causes the solenoid valve to close preventing excess gas from escaping into the chamber. The fan is turned off immediately after the powder is dispersed.

The test continues for one hour unattended, with the results being recorded on the Brown recorder chart. Then the chamber is opened and flushed of any remaining aerosol. The chamber is closed again, and a final

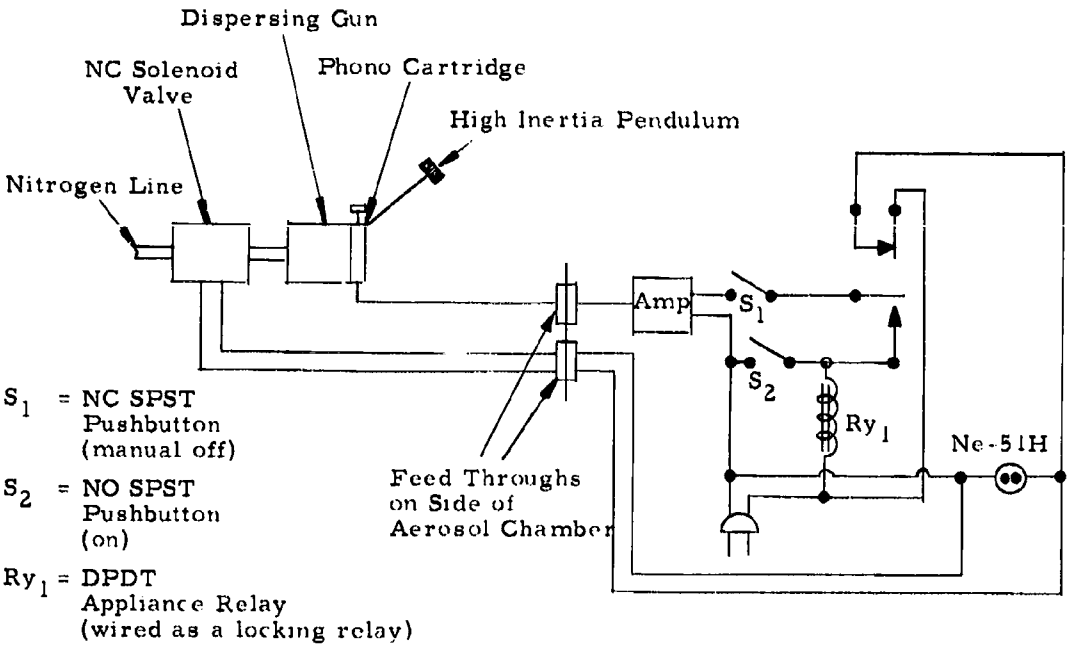

Figure 19. Automatic Valve Assembly

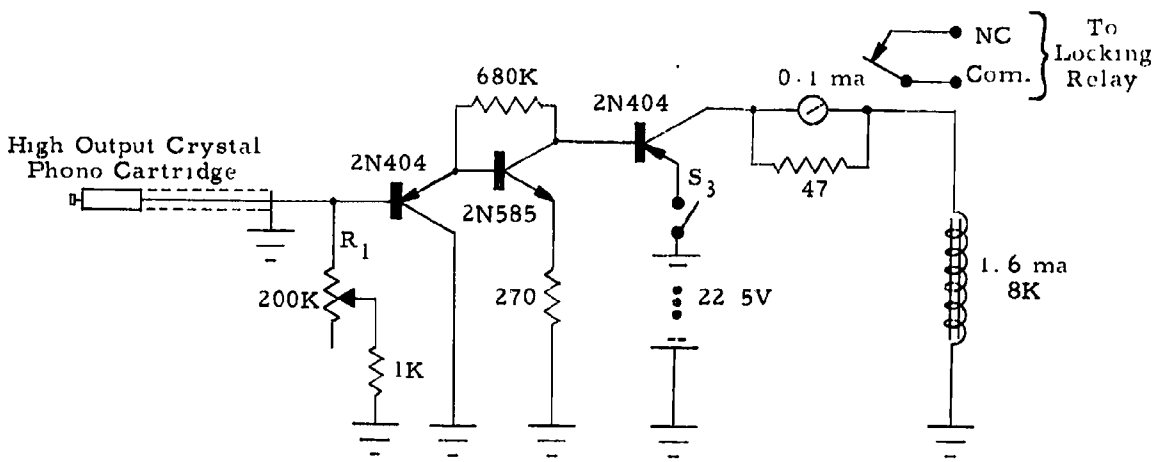

Figure 20. Amplifier for Automatic Valve

reference level is found. On some occasions the final reference might differ from the initial reference. When this occurs, it is assumed that the change took place linearly with time, and a base line connecting the two reference levels is drawn. Amplitude measurements are made from this base line. Since the difference in references is usually small little or no error should result from this source.

A typical decay curve is shown in Figure 21. Knowing the chart speed, the amplitudes of the decay curve are measured at points corresponding to 5-minute-time increments starting at t = 5. The amplitudes are plotted against the square root of time on semilog paper. The plot corresponding to this decay curve is shown in Figure 22. The resulting curve is a straight line, implying an equation of form:

$$A = A_0 e^{-\lambda t^{\frac{1}{2}}} \tag{9}$$

where:

A = amplitude at time t

A_0 = amplitude at time t = 0

t = time

Although time is normally expressed in seconds, λ has a more convenient magnitude if minutes are used as units of time. Thus A_0 has units of centimeters, and λ has units of minutes$^{-\frac{1}{2}}$. The physical significance of λ and A_0 will be discussed in the following section

7. Discussion of Aerosol Decay Constant and Initial Amplitude A_0

We call λ the decay constant. It is obtained from the slope of the line on a plot of ln A versus $t^{\frac{1}{2}}$ and has the units of time$^{-\frac{1}{2}}$. The decay constant is a measure of the rate of decrease of the output of the photomultiplier tube and is consequently a measure of the decrease of number of particles per unit volume within the monitored region of the aerosol chamber.

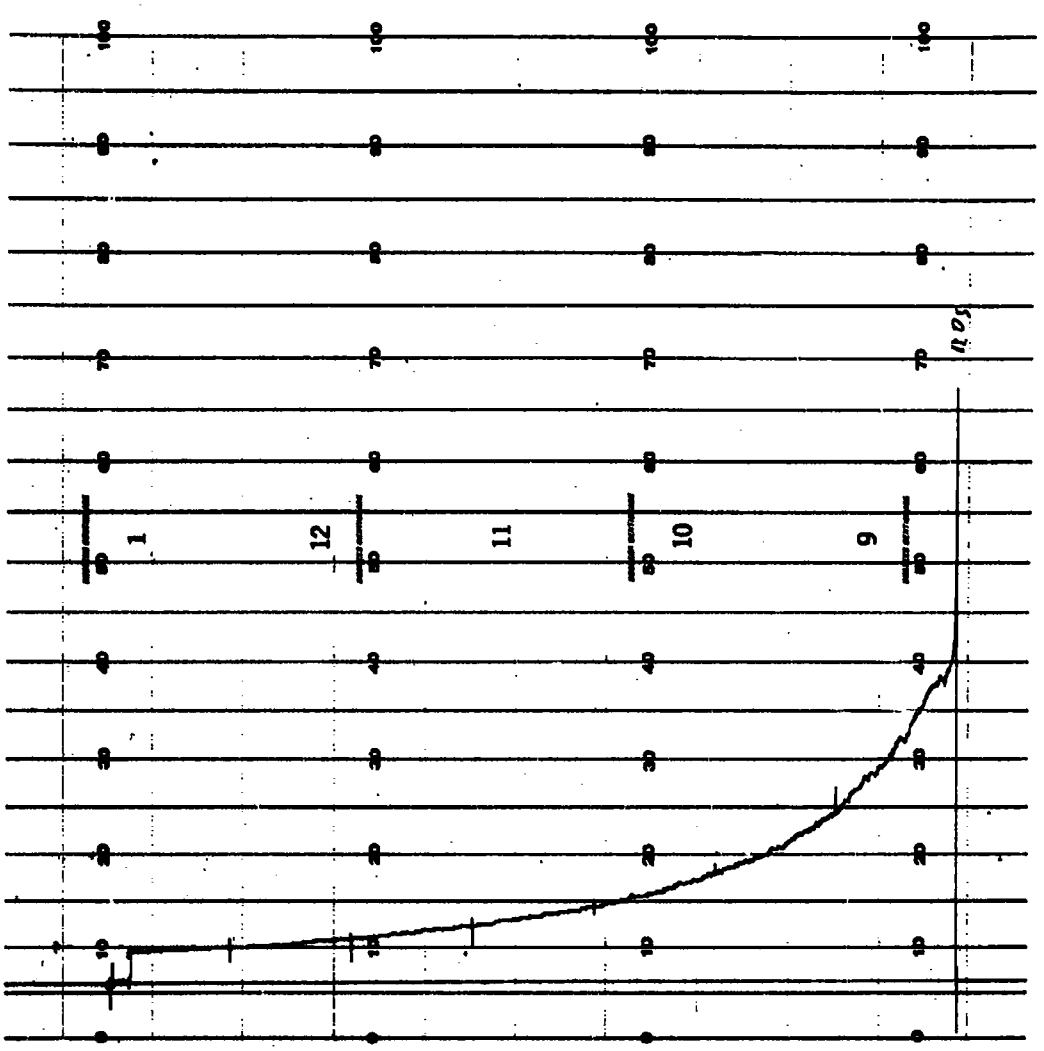

Figure 21. Typical Aerosol Decay Curve

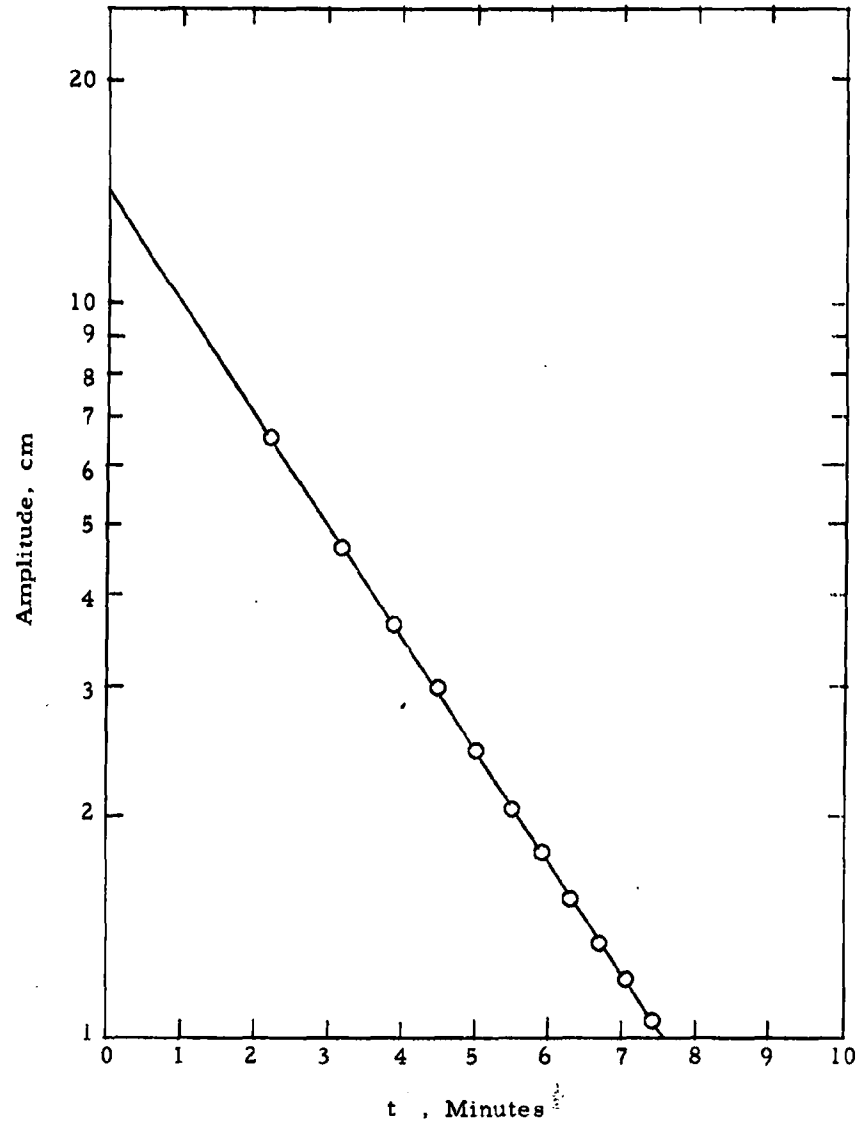

Figure 22. Amplitude as a Function of Time Raised to the One-Half Power

This decrease in number of particles can come about in two ways:

1) Natural settling of aerosols. In this case, λ provides a measure of the ease of dispersibility. If a powder is dispersed easily, all agglomerates are broken up resulting in a low settling rate and a low value for λ. A powder not so easily dispersed produces an aerosol containing many agglomerates which fall out rapidly, producing a large value for λ.

2) Reagglomeration of aerosol particles. Even if a powder is easily dispersed and all agglomerates are completely broken up, the number of particles present decreases rapidly if reagglomeration takes place during settling.

We call A_o the initial amplitude. It is a measure of the number of particles present in the aerosol immediately after powder dispersal. A_o is obtained from the plot of ln A versus $t^{\frac{1}{2}}$ by extrapolating back to t = 0. Thus it has more of a mathematical rather than physical existence.

8. Difficulties Encountered with the Dispersibility Test

Slightly different values for the decay constant λ and the initial amplitude A_o for the three base powders are given in several places in this report. The reason these values differ somewhat, even though the powders are the same, can be attributed to three main factors:

1) Amount of powder dispersed

2) State of agglomeration of the sample

3) Humidity conditions with which the sample is in equilibrium

Let us consider each factor separately.

The amount of powder dispersed affects both λ and A_o, particularly the latter. For this reason, it is important to use the same amount of powder throughout a given series of tests. This has been done in every series, although it has not always been possible to use the same amount of powder from one series of tests to the next. The actual amount of powder dispersed

is not critical so long as it is kept within certain limits. If the sample is too small, weighing errors become significant and also background noise becomes appreciable. If the sample is too large, the aerosol density may exceed 10^5 particles/cc in which case aggregation of particles by direct contact due to thermal turbulence may occur during settling. The most important consideration, besides keeping the sample size within these limits, is to use the same amount of powder throughout a given series of tests so that valid comparisons can be made.

The state of agglomeration of the sample greatly affects both λ and A_o. In order to insure that all of the samples to be tested in a given series are in the same state of agglomeration, it has been standard practice to deagglomerate all samples according to the procedure described in Section II-B. Although this deagglomeration procedure has been used in every series of tests performed, there is still a possible source for error in the fact that some samples must stand longer than others before being tested. Thus, there is a chance for some of the samples to reagglomerate to some extent before being tested.

As mentioned above, it has been found that the humidity conditions with which the powder sample is in equilibrium affects both λ and A_o. Obviously then, tests made on a given powder at a time of the year when the humidity is high, will give different results from tests made on the same powder when the humidity is low, assuming the powder has been stored at room humidity.

Thus, rigid comparisons of λ and A_o should not be made from one series of tests to another unless all conditions are identical.

The initial amplitude A_o has some value as a measure of the initial density of an aerosol but also presents certain problems. To illustrate, let us consider two aerosols which have approximately the same density at time t' and consequently the same amplitude on the Brown recorder chart (see Figure 23). Assume also that λ_2 is appreciably greater than λ_1. At time t', both straight lines pass through the same point, but line 2 has a considerably

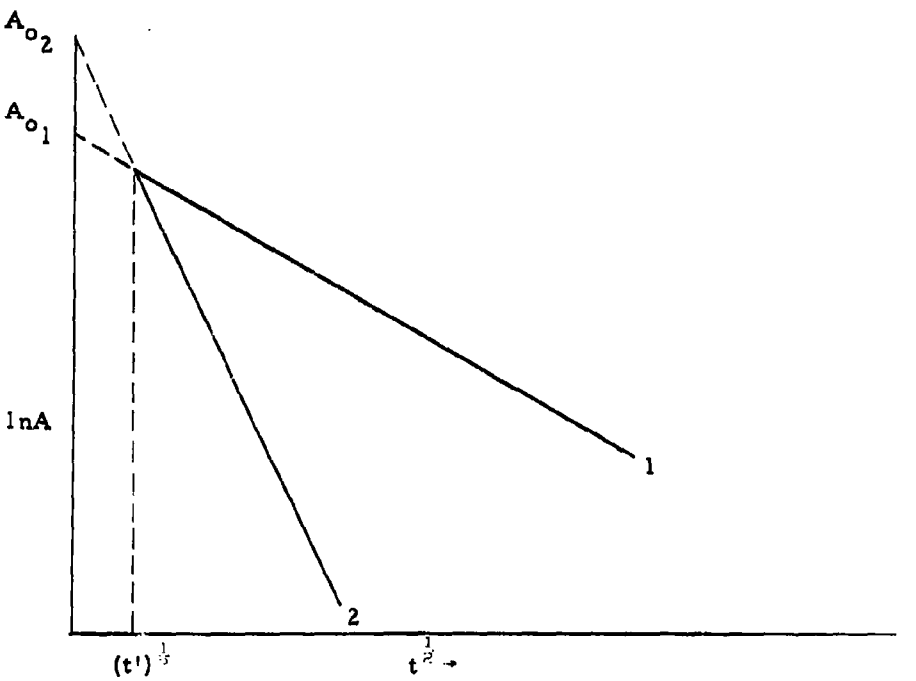

Figure 23. Example of Two Aerosol Decay Curves having Different A_o's and Equal Densities at Time t'

greater slope than line 1. It may be seen in this case that A_o for aerosol 2 will be considerably larger than A_o for aerosol 1, even though the actual aerosol density is approximately equal at t = t'.

One cannot expect the equation which holds for the latter part of the test to hold for the early part as well (when conditions are more turbulent). Prior to t', the aerosol decay may not follow Equation (9) but should follow it more and more closely as t' is approached. The results of many tests indicate that the value for t' should lie somewhere between 0 and 5 minutes.

G. Electrostatic Charge Tests

Two different techniques have been used on this program to study electrostatic charge on particles. One is a quantitative technique for measuring electrostatic charge on airborne particles; the other is a qualitative (but rapid) technique for measuring electrostatic charge on bulk powders.

1. Technique for Measuring Electrostatic Charge on Airborne Particles

The apparatus we constructed for measuring electrostatic charge on airborne particles was patterned after a design by Gillespie.[13] The electrostatic charge analyzer (see Figure 24) consists of two aluminum plates held parallel to each other by the polystyrene body of the instrument. Each plate is covered by two microscope slides placed end-to-end. The slides and the polystyrene body form a channel (1.20 cm wide by 0.50 cm deep by 15.2 cm long) through which the aerosol is passed. The aerosol is introduced into the channel through a No. 16 hypodermic needle which is positioned exactly in the center of the cross section of the channel at its top. A stream of clean air enters the channel at the base of the hypodermic needle through two arms which protrude from the sides of the instrument. This stream of air forms a sheath around the aerosol stream and minimizes the tendency for the aerosol to diffuse throughout the channel after leaving the needle. The flow is laminar.

The two aluminum plates are connected to a d-c power supply so that an electric field appears between the plates. The needle is maintained at ground potential while one plate is above and the other below ground. This tends to minimize distortion of the field. A Sorenson Model 9015-5 power supply makes possible the use of potential differences up to 15 kv.

When an aerosol passes through the channel, charged particles are deflected toward one or the other of the plates (depending upon their sign) and are deposited on the glass slides covering the plates. Uncharged particles,

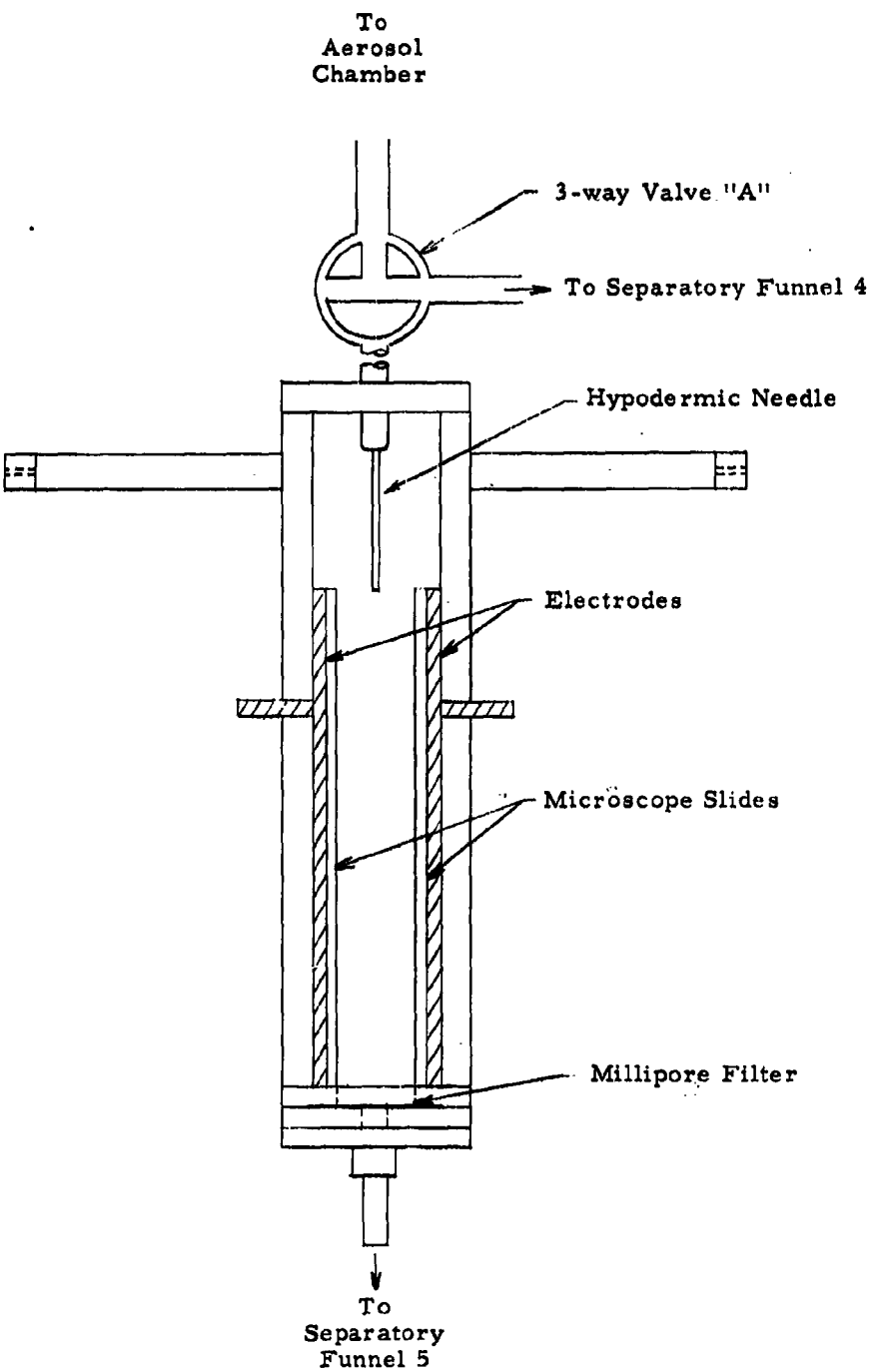

Figure 24. Electrostatic Charge Analysis Apparatus for Airborne Particles

being unaffected by the electric field between the plates, pass through the channel and are deposited on a millipore filter at the bottom of the channel.

a. Operating Procedure

During operation, the electric charge analyzer is mounted directly beneath the aerosol chamber as shown in Figure 25. The analyzer is lined up in a perfectly vertical position by means of the ring stand (1) and the small bubble level (2) mounted at the lower end. Valves A and B are turned in such a manner that there is an open path directly from the aerosol chamber through the tube (3) to the open air of the room. The powder sample is dispersed in the aerosol chamber. The setting of valves A and B permit excess air to escape into the room. When pressure inside the aerosol chamber has equilibrated with room pressure, valve B is turned providing an open path from the aerosol chamber through the tube (3) to the separatory funnel (4). The stopcock on this funnel is then opened, allowing water to run out. The increasing volume above the water creates a low-pressure region, and the aerosol is drawn from the aerosol chamber into the tube (3).

Valve A is then turned so as to connect the tube to the charge analyzer. The stopcock of separatory funnel (5) is opened allowing water to run out through hypodermic needle (6). This hypodermic needle acts as a restriction making it easier to control the flow rate. As water runs out of separatory funnel (5), the aerosol is drawn from the tube into the charge analyzer. The voltage across the plates is adjusted to the desired level. This is accomplished by adjusting the variable transformer (7) which in turn adjusts the input voltage to the d-c power supply (8).

After the run is completed, the charge analyzer is taken from its position and the microscope slides and millipore filter are carefully removed for analysis.

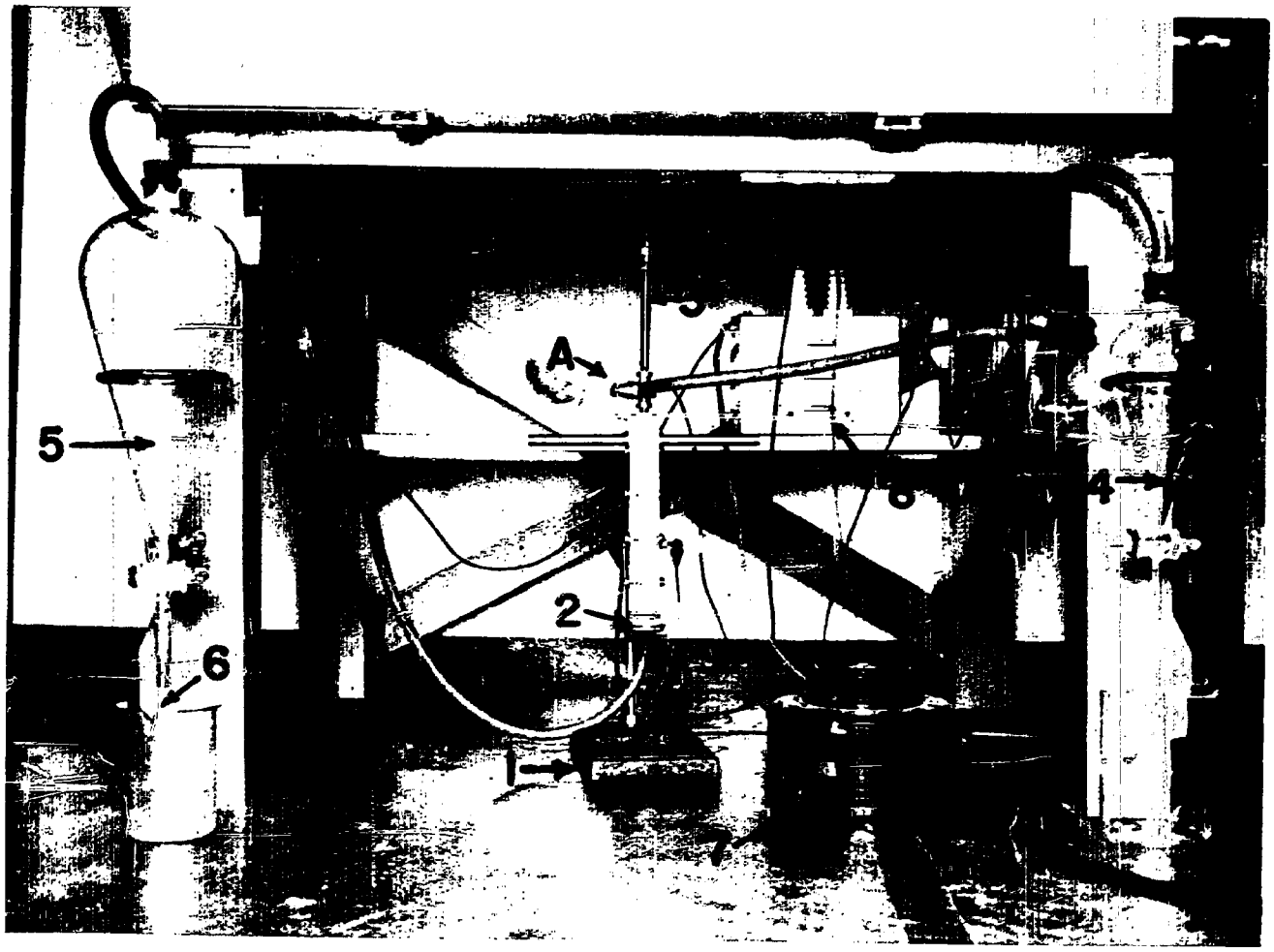

Figure 25. Electrostatic Charge Analyzer and Associated Equipment

b. Preliminary Tests

Preliminary tests were conducted to determine if the apparatus was functioning properly.

First a test was conducted with both plates and needle at ground potential. In these tests the plates remained free of particles, and all particles were deposited on a fairly localized area near the center of the millipore filter. This lends support to the belief that the charged particles are deposited primarily by electrostatic means and that thermal or Brownian motion effects are negligible.

A second reason for the preliminary tests was to obtain approximate values for the three parameters which control the density and distribution of particles deposited on the slide.

The first parameter is the potential between the two plates. If this is too high, particles will be deflected too rapidly and will be deposited in a region of short length just below the opening of the needle. On the other hand, a potential which is too low might permit some charged particles to reach the filter before being deflected sufficiently to impinge on the slides.

The approximate potential required to deflect the particles onto the slides can be calculated using the following equation:

$$V = 11,500 \frac{VR}{n} \quad , \tag{10}$$

where:

V = potential in volts

v = particle velocity in cm/sec

R = particle radius in microns

n = number of charges on particles

The derivation of this equation appears in Appendix D. This is not means to be a rigorous solution to the problem but rather an estimate of the necessary potential.

The second parameter is the particle velocity or flow rate through the analyzer channel. This has an effect inverse to that of the potential. The two are interdependent and must be adjusted together to spread particles over the desired track length. Average velocity of the aerosol passing through the channel can be calculated from the following equation:

$$v = \frac{U}{At} \quad , \tag{11}$$

where:

v = average particle velocity

U = volume of air drawn through channel in time t

A = cross-sectional area at channel

While this average velocity will differ slightly from the velocity of a particle at the exact center of the channel as used in the derivation of Equation (11), it should be sufficiently accurate for the present purposes.

The third parameter is the duration of the run. This depends on the particle density of the aerosol in the chamber and also on the degree to which the particles are charged. Too long a run will cause particles to pile up on top of one another making counting difficult or impossible.

c. Analysis of Data

Visual observation of the glass slides after a trial run revealed several things. The particles were confined to a narrow track approximately 1 mm wide along the length of the slide. The particle density (particles per unit area) was quite high near the beginning of the track and decreased rapidly

with distance along the track. Beyond about 2 cm, the density was so low that the track of particles was no longer visible to the naked eye. Thus nearly all particles were distributed along the first 2 cm of track, and a large percentage of the total was in the first 2 mm. Furthermore, the total number of particles deposited on the slides was too large to make a direct count feasible. It was necessary, therefore, to devise an indirect method to determine the total number of particles on each slide.

The indirect method we devised for counting particles is this: The track is divided into a series of narrow strips perpendicular to the track length starting at its beginning. These strips are of known width and separation. All particles within each strip are counted under a microscope. Having determined the number of particles in each strip and knowing strip width, one can compute linear density. The linear density is the number of particles per unit distance along the track. The value obtained is obviously the average linear density over the width of the strip, but since the strips are very narrow, it should approximate closely the linear density at the center of the strip. Knowing strip widths and spacing between strips, one can calculate the coordinate (distance from start of track) to which a linear density corresponds. A plot is made of linear density versus distance along the track. The area under the curve is equal to the total number of particles. This area can be found easily by application of Simpsons' Rule.

In the case of the millipore filter, the number of particles found was relatively small; therefore, it was possible in every test made to count all the particles on the filter by visual examination under a microscope.

Knowing the total number of particles on each slide and on the millipore filter, one can calculate the percentage of positively-charged particles, the percentage of negatively-charged particles, and the percentage of non-charged particles.

2. Technique for Measuring Electrostatic Charge on Bulk Powders

Because the electrostatic charge test described in the previous section is very time consuming, a simpler and more rapid test was devised. The information this test provides is not quantitative; however, it is of some value. For example, it indicates whether the net charge on a powder sample is positive, negative, or zero. If the net charge is zero, the test tells whether the sample is completely uncharged or is charged bipolarly. By bipolar, we mean that for every particle carrying a charge q_i, there is a corresponding equal sized particle carrying a charge $-q_i$.

The test apparatus is shown in Figure 26. The small copper funnel at the top is supported by an arm leading to an electric vibrator. Directly underneath the funnel are two parallel aluminum plates space 6.35 cm apart and mounted on an insulating support. The support rests on top of a 600-ml glass beaker so that the plates extend downward inside the beaker. The plates are connected to the terminals of a Sorenson 15,000-vdc power supply. One plate is maintained at 7500 volts above ground and the other at 7500 volts below ground; and the funnel is maintained at ground potential. The electric field produced in the region between the plates is 2360 v/cm.

The first step in the test procedure is to sift the powder through a 16-mesh screen to eliminate any large lumps. In a series of tests, all powder samples should be treated in the same manner prior to testing in order to minimize the possibility of charging one sample more than another. For the same reason, when replicate tests are made on a given powder, new samples should be used each time, otherwise the sample may become more highly charged with each successive test.

With the funnel outlet closed, a quantity (about 25 cm^3) of presifted powder is loaded into the funnel. The funnel outlet is opened taking care not to bump the funnel and cause the powder to flow out prematurely. The glass beaker containing the plates is positioned underneath the funnel as shown in Figure 26. Proper connections are made to the power supply. The power

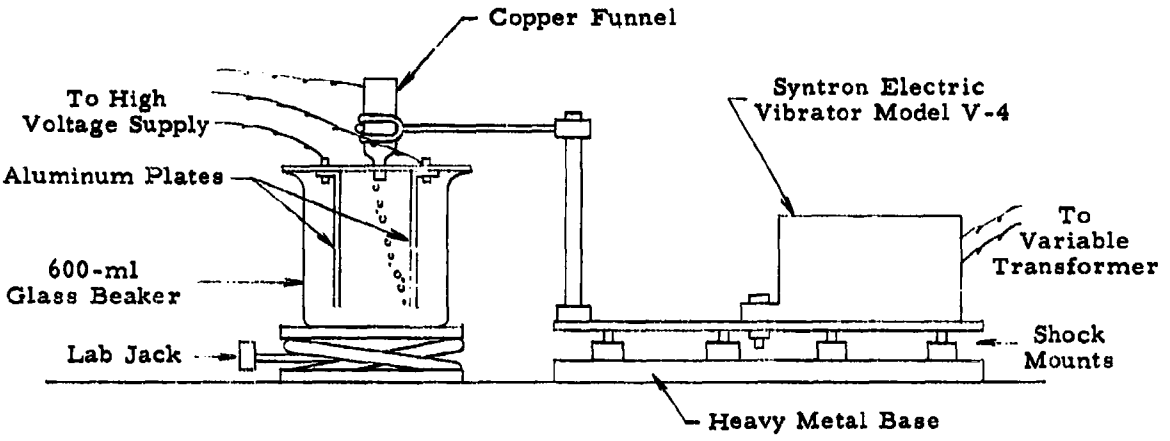

Figure 26. Electrostatic Charge Analysis Apparatus for Bulk Powders

supply and vibrator are then turned on simultaneously. Vibration transmitted to the funnel through the supporting arm causes the powder to flow downward between the plates. As the powder particles sift down between the plates, they migrate either to the positive or negative plate depending upon their charge or fall straight downward if uncharged. While the powder is falling, a photograph is taken of the region between the plates using a Polaroid Land camera. The photograph then serves as a permanent record of the test and may be analyzed at a later time.

The technique for analyzing the photographs involves the use of a Welch densichron. The photograph is clamped in a metal frame which rests on the densichron table and is constrained to move in a straight line across the table by means of a pair of guide tracks. The photograph is positioned in the frame in such a manner that the light beam scans a narrow horizontal band located about midway between the top and the bottom edges of the plates.

A 1/10-rpm synchronous motor pulls the frame at a slow, constant speed across the table. The output from the photocell is fed into a Brown recorder, which in turn records the intensity of the light passing through the photograph as a function of lateral displacement of the photograph relative to the light beam. The completed Brown recorder trace has three major peaks, one corresponding to the edge of each plate and one corresponding to the stream of powder flowing down between the plates.

Photographs of typical tests on each of the three base powders and the corresponding Brown recorder charts are shown in Figure 27. In all cases the plate on the left is negative and that on the right is positive with respect to ground. The dimension labeled "A" on the Brown recorder chart represents the distance from the edge of the negative plate to the densest portion of the powder stream. The dimension labeled "B" represents the distance from the edge of the positive plate to the densest portion of the powder stream. Knowing the A/B ratio and knowing the actual distance between the plates (6.35 cm), one can calculate the actual distance from the edge of the negative plate to the densest portion of the powder stream (a) and the actual distance from the edge of the positive plate to the densest portion of the powder stream (b). The quantity (b - a) indicates what type of net charge the powder sample has. If (b - a) < 0, the net charge is negative; if (b - a) > 0, the net charge is positive; if (b - a) = 0, the net charge is zero. A net charge of zero may mean one of two things. Either the powder has no charge at all or it is charged bipolarly. A bipolar charge means that for every particle carrying a charge q_i, there is a corresponding, equal-size particle carrying a charge $-q_i$.

The dimension labeled $W_{\frac{1}{2}}$ is measured from the Brown recorder trace. It is the width of the peak corresponding to the powder stream at one-half maximum amplitude. It is useful only in cases where the net charge on the powder is zero. In such cases, a small value for $W_{\frac{1}{2}}$ indicates that the powder is virtually noncharged, whereas a large value for $W_{\frac{1}{2}}$ indicates that the powder is charged bipolarly.

(A)

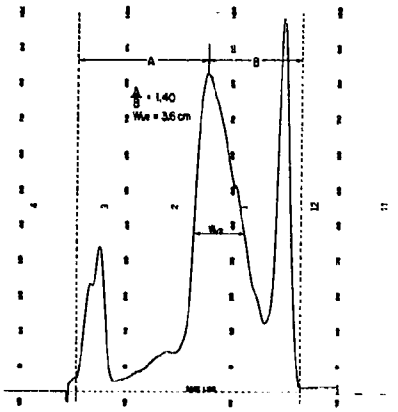

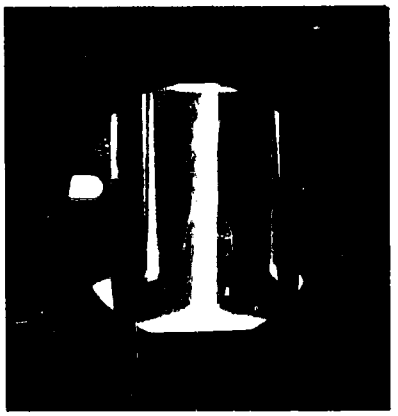

(B)

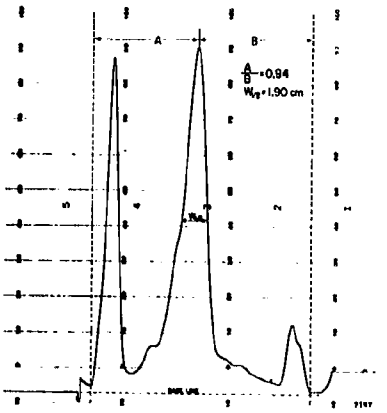

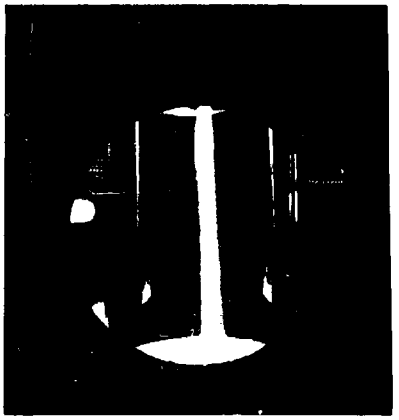

(C)

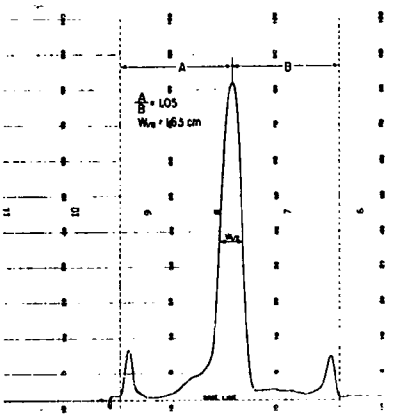

Figure 27. Photographs of Typical Electrostatic Charge Tests on Saccharin, Carbowax 6000, and Span 60

IV. MAJOR STUDIES

A. Bulk Tensile Strength Tests

The bulk tensile strength test described in Section III-C was not used to any great extent because the test is rather difficult to perform and is a time consuming one. Tests were made, however, on the following powders: zinc cadmium sulfide, saccharin, Carbowax 6000, Span 60, egg albumin, and samples of Carbowax 6000 and Span 60 containing 1 percent Cab-O-Sil.

The reason for testing zinc cadmium sulfide was to develop the technique. The data obtained from these tests are not pertinent to the program and, therefore, will not be presented here. These data may be found in a previous report.[14]

Results of the tests on saccharin, Carbowax 6000, Span 60, and egg albumin are plotted in Figures 28, 29, 30, and 31, respectively. These curves were plotted using the method of least squares. The bulk tensile strengths at zero column length (obtained by extrapolating the curves to the vertical axis) are plotted as a function of compressive load in Figure 32. It is seen that Span 60 has the highest bulk tensile strength, and egg albumin has the lowest bulk tensile strength of these four powders.

Results of the tests on Carbowax 6000 and Span 60 containing 1 percent Cab-O-Sil are presented in Section IV-C.

B. Effects of Humidity on Powder Properties

Electrostatic charge of airborne particles, shear strength, and aerosol decay were the three tests conducted at various relative humidities in order to determine what effect, if any, relative humidity has on powder properties. The shear strength tests were made at the conditioning humidity while the aerosol decay and electrostatic charge tests were conducted at room humidity using preconditioned powders.

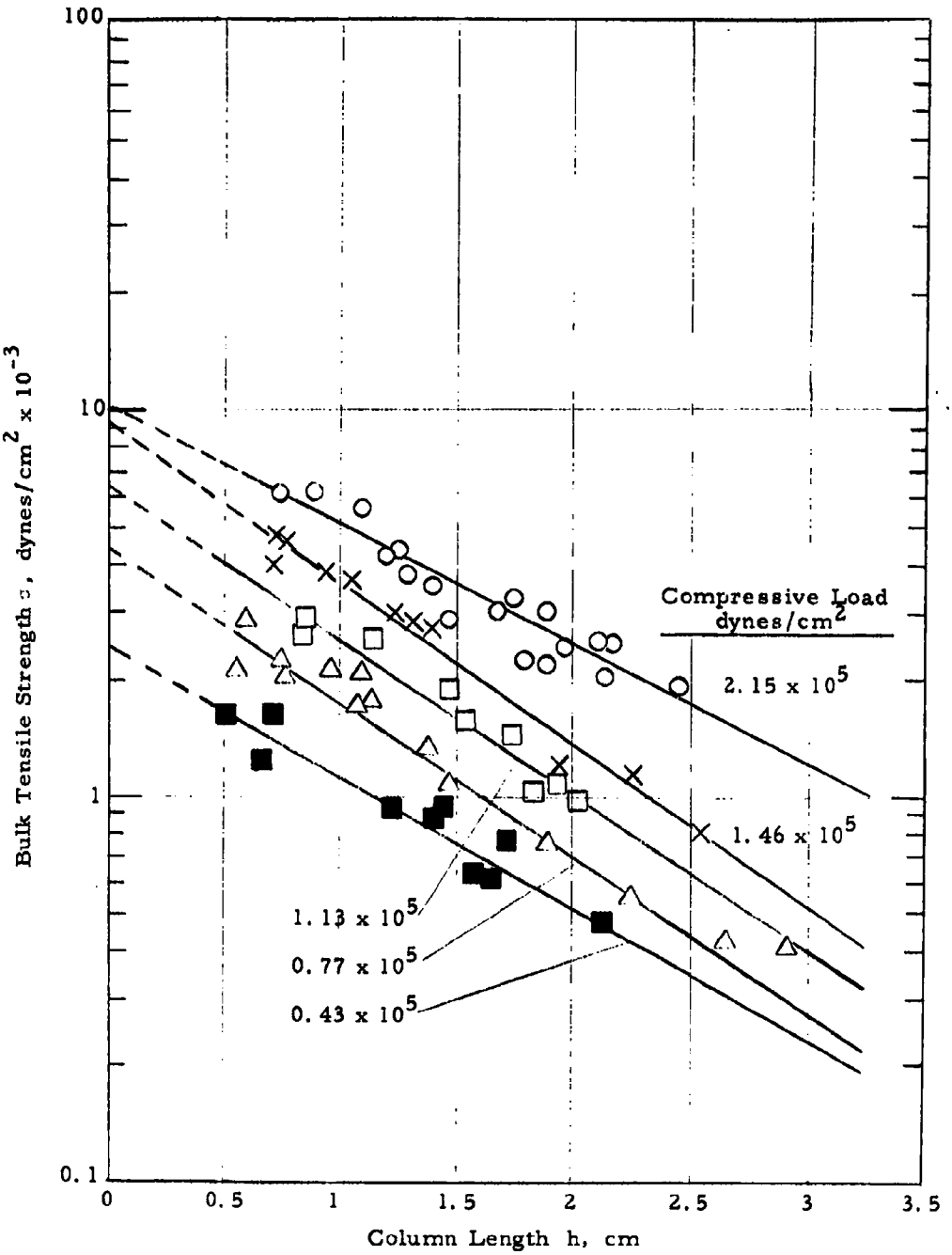

Figure 28. Bulk Tensile Strength of Saccharin as a Function of Column Length for Various Compressive Loads

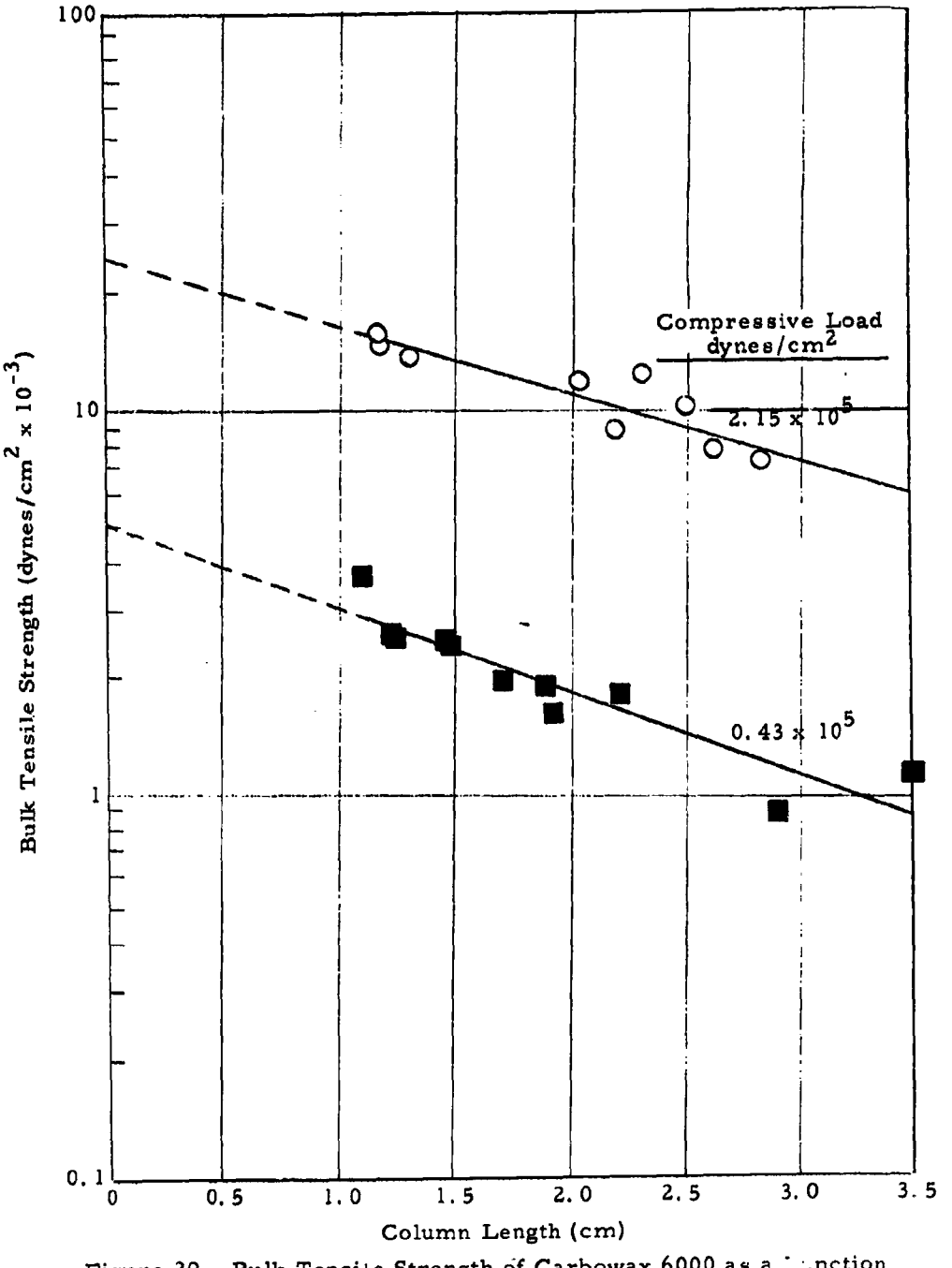

Figure 29. Bulk Tensile Strength of Carbowax 6000 as a function of Column Length for Various Compressive Loads

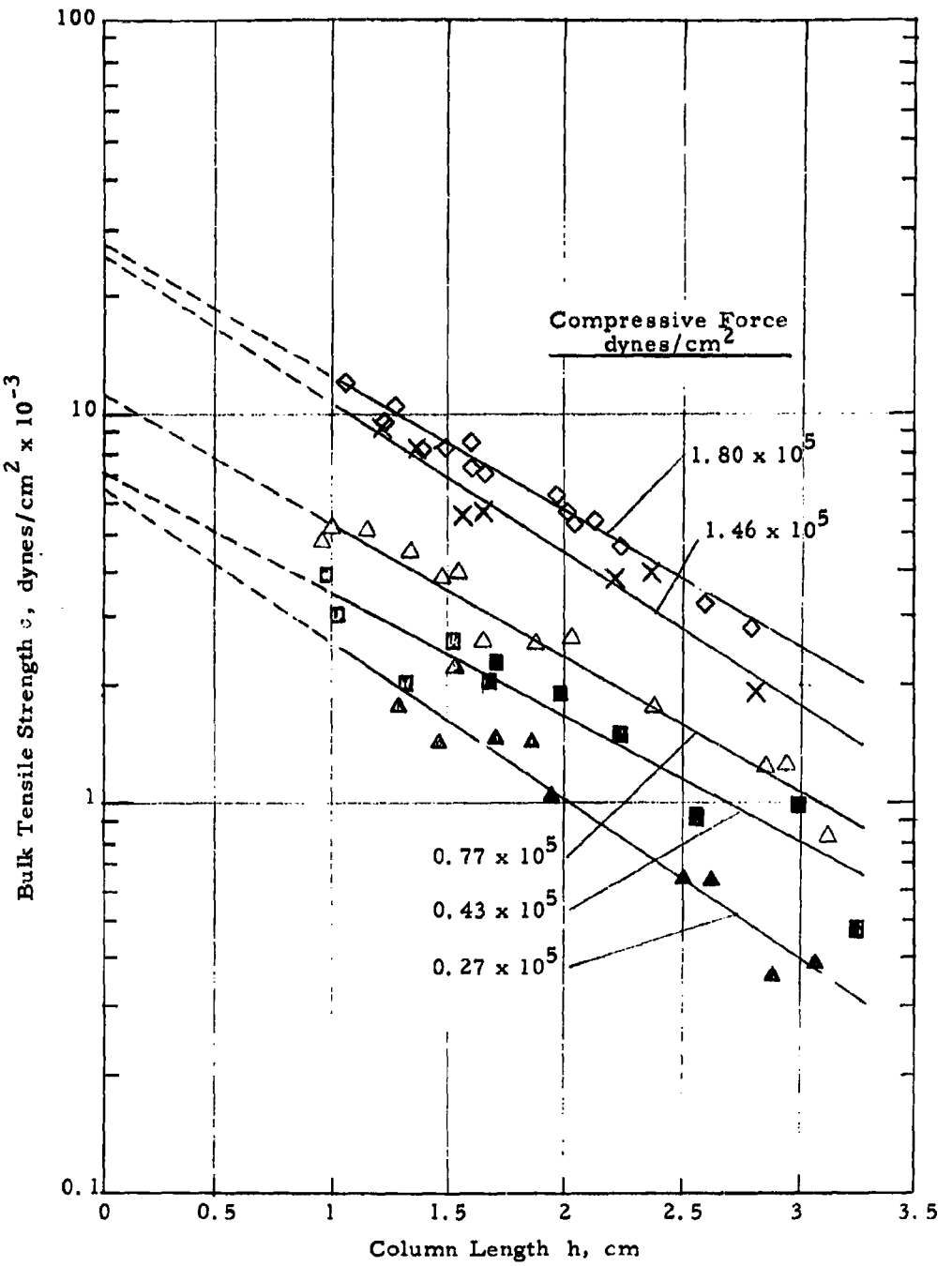

Figure 30. Bulk Tensile Strength of Span 60 as a Function of Column Length for Various Compressive Loads

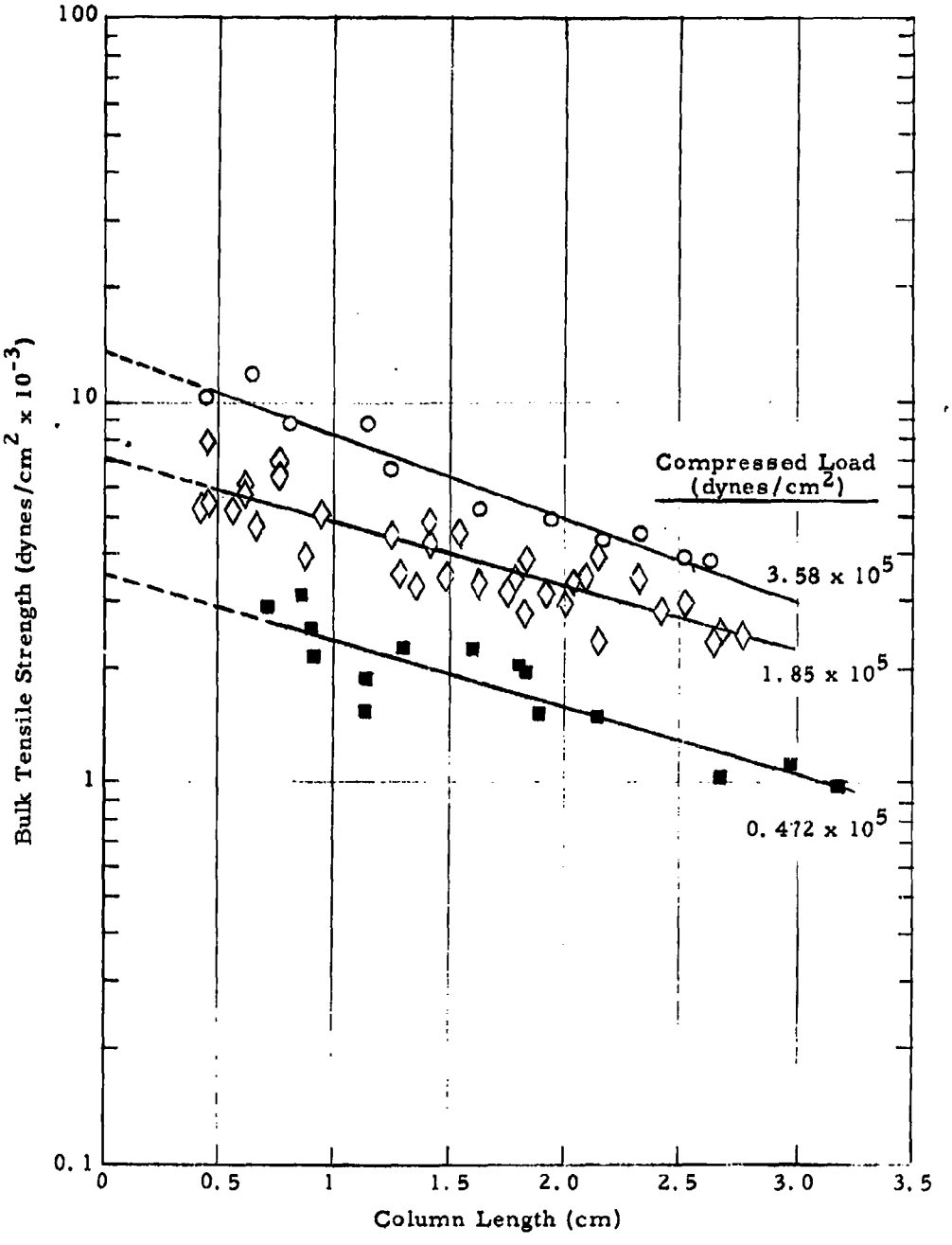

Figure 31. Bulk Tensile Strength of Egg Albumin as a Function of Column Length for Various Compressive Loads

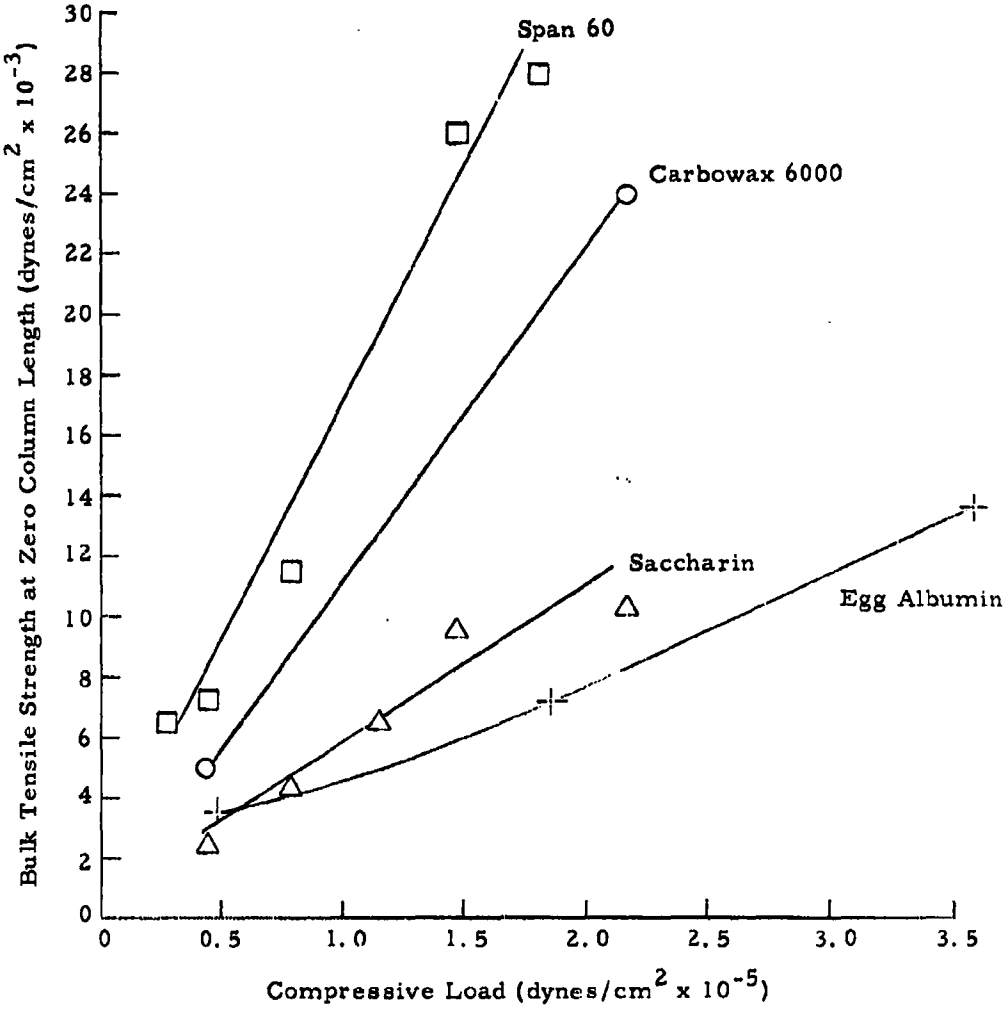

Figure 32. Bulk Tensile Strength of Various Powders at Zero Column Length as a Function of Compressive Loads

The shear strength tests were conducted at eight different compressive loads ranging from 1500 to 14,900 dynes/cm^2. The tests were conducted in triplicate and the results averaged. The results are tabulated in Table 10 and three representative loads are presented as a function of relative humidity in Figures 33, 34, and 35. It is seen that in the case of saccharin (Figure 33), shear strength has a minimum value at about 25 percent humidity; in the case of Carbowax 6000 (Figure 34), shear strength has a maximum value at about 25 percent relative humidity; and in the case of Span 60 (Figure 35), shear strength gradually decreases with increasing humidity. It is seen also that the effect of humidity is more pronounced at the higher compressive loads.

Table 10. Shear Strength Measurements for Saccharin, Carbowax 6000, and Span 60 at ~ 1%, at 25%, and at 75% Relative Humidities

Compressive Load (dynes/cm^2)	Shear Strength (dynes/cm^2)	Compressive Load (dynes/cm^2)	Shear Strength (dynes/cm^2)
Saccharin at ~ 1% RH		Saccharin at 25% RH	
1,500	1,200	1,500	1,200
2,200	1,800	2,200	1,800
3,700	3,000	3,700	2,700
6,000	5,200	6,000	4,700
8,200	6,800	8,200	6,600
10,500	8,700	10,500	7,700
12,700	12,600	12,700	10,000
14,900	14,800	14,900	10,900
Saccharin at 75% RH		Carbowax 6000 at ~ 1% RH	
1,500	1,300	1,500	1,100
2,200	2,100	2,200	1,800
3,700	3,400	3,700	3,400
6,000	5,900	6,000	6,100
8,200	8,300	8,200	8,500
10,400	10,600	10,500	10,500
12,700	12,800	12,700	13,100
14,900	14,500	14,900	15,500

Table 10 (Continued)

Compressive Load (dynes/cm^2)	Shear Strength (dynes/cm^2)	Compressive Load (dynes/cm^2)	Shear Strength (dynes/cm^2)
Carbowax 6000 at 25% RH		Carbowax 6000 at 75% RH	
1,500	1,200	1,500	1,100
2,200	2,100	2,200	1,600
3,700	3,600	3,700	3,000
6,000	6,100	6,000	5,300
8,200	9,200	8,200	7,500
10,500	11,700	10,500	10,200
12,700	14,000	12,700	12,900
14,900	16,000	14,900	14,400
Span 60 at < 1% RH		Span 60 at 25% RH	
1,500	1,100	1,500	900
2,200	1,500	2,200	1,400
3,700	2,600	3,700	2,400
6,000	4,200	6,000	4,000
8,200	5,700	8,200	5,500
10,500	7,700	10,500	6,900
12,700	9,000	12,700	8,900
14,900	10,800	14,900	10,900
Span 60 at 75% RH			
1,500	900		
2,200	1,500		
3,700	2,300		
6,000	3,700		
8,200	5,200		
10,500	6,700		
12,700	8,400		
14,900	10,000		

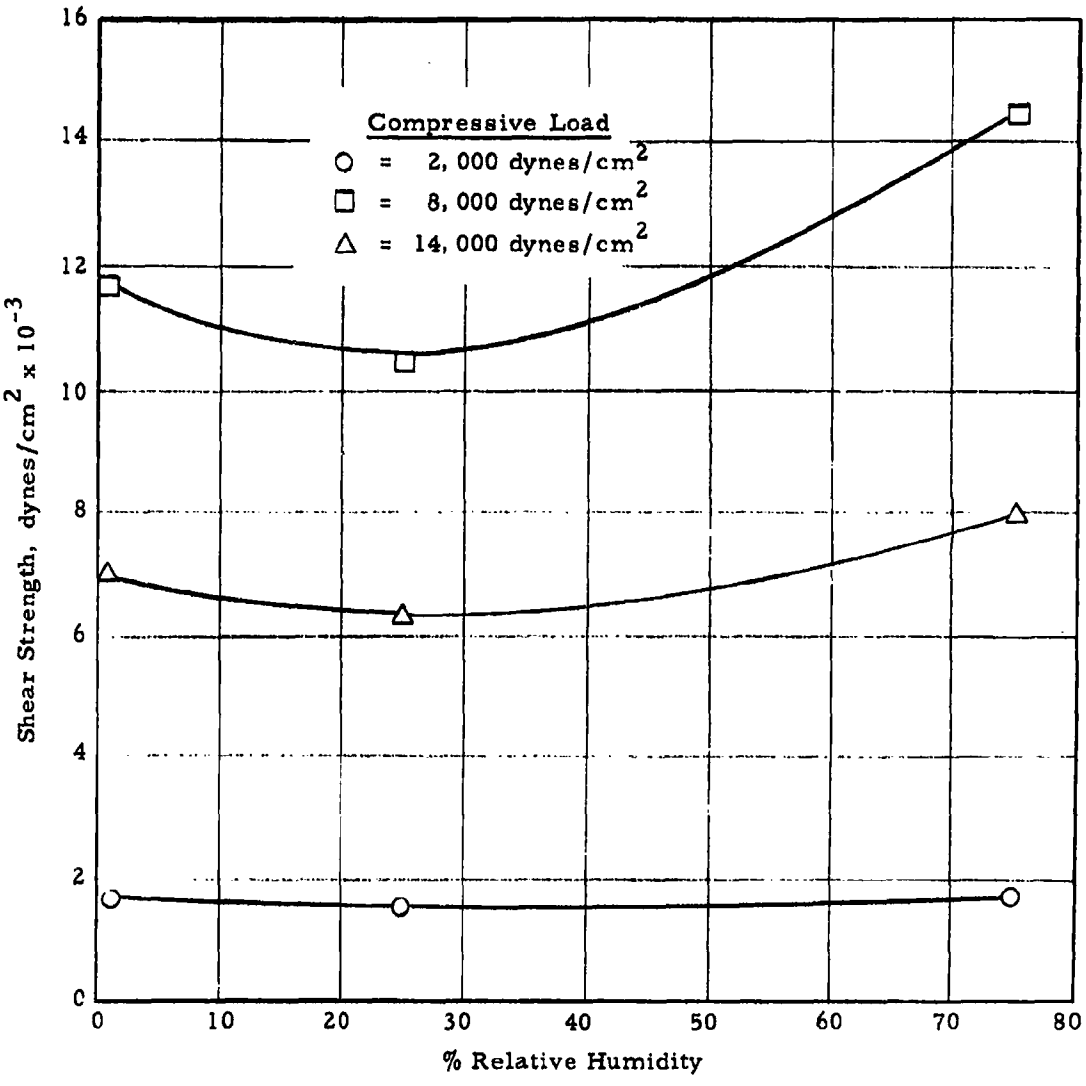

Figure 33. Shear Strength of Saccharin as a Function of Humidity

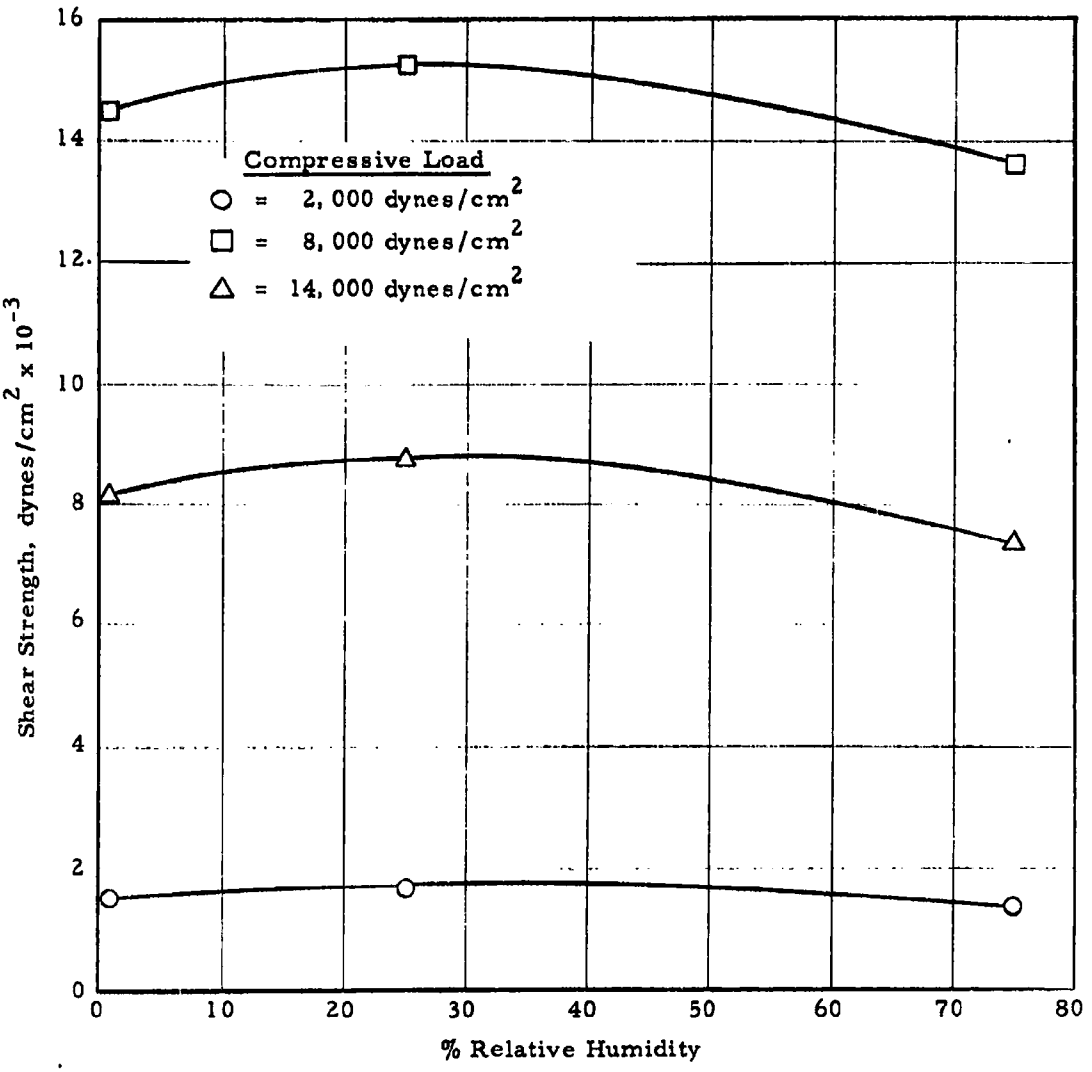

Figure 34. Shear Strength of Carbowax 6000 as a Function of Humidity

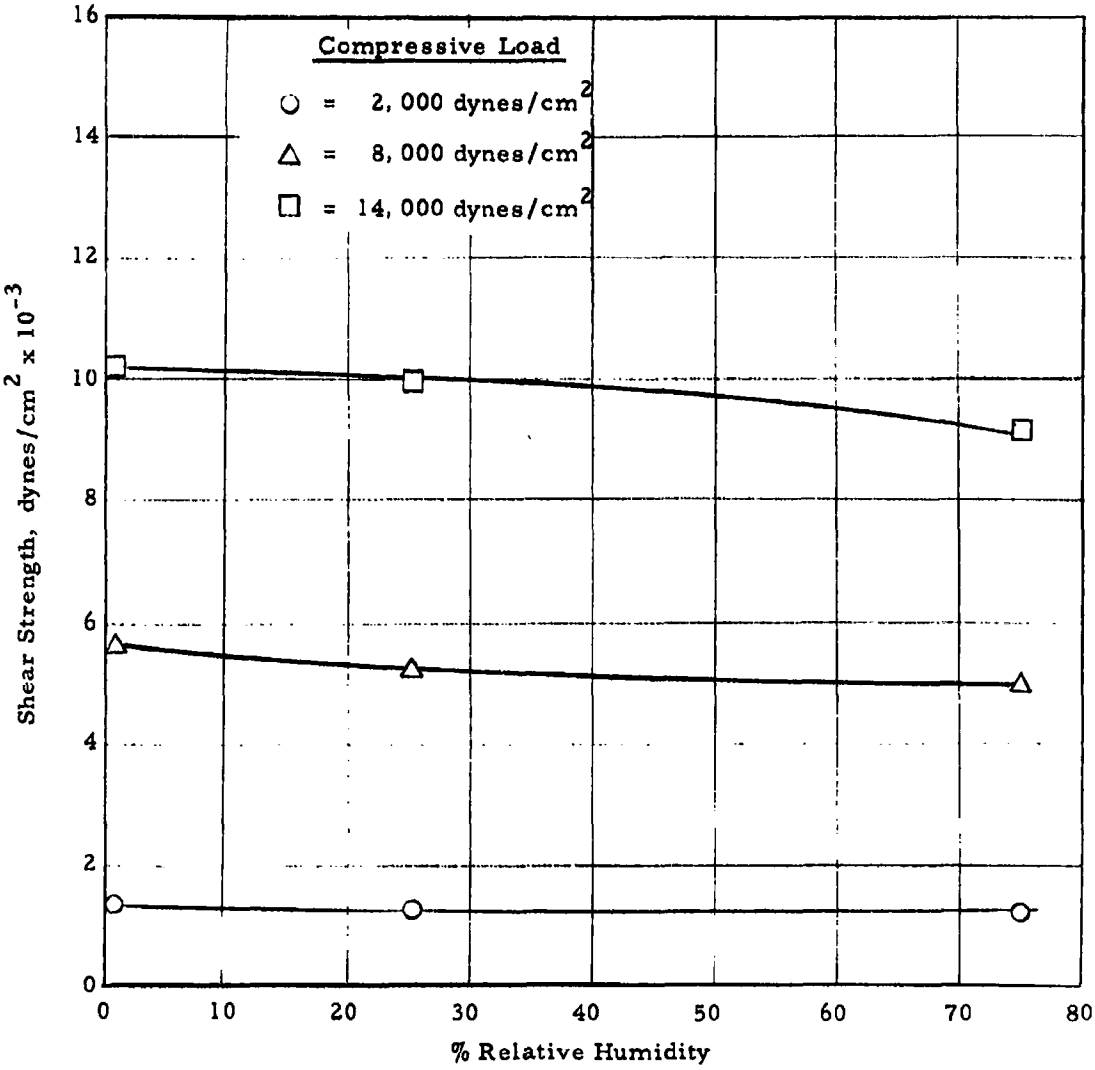

Figure 35. Shear Strength of Span 60 as a Function of Humidity

Dispersibility tests were performed in conjunction with the study of properties of powders preconditioned at relative humidities of 1, 25, and 75 percent. In the present tests, the powder could not be weighed inside the glove box, and careful weighing outside the glove box would have resulted in a longer exposure of the powder to the room air than was desirable. The problem was solved by the use of No. 1 gelatin capsules. The capsules were filled inside the glove box, passed out through an airlock, loaded into the bursting diaphragm dispersing gun, and quickly dispersed inside the aerosol chamber in the usual manner. This method makes it possible to use approximately the same amount of powder each time and to minimize the time of exposure to room air.

Several runs were made and the results averaged. The results so obtained are listed in Table 11.

The test results are also presented graphically in Figures 36 and 37. Figure 36 is a plot of the decay constant as a function of percent relative humidity to which the powder samples were conditioned prior to the test. It is seen that is an increasing function of conditioning relative humidity in all three cases. In effect, this means the higher the humidity to which the powder is conditioned the faster the aerosol settles out. For saccharin and Carbowax 6000, increases slowly with increasing conditioning humidity, while for Span 60, increases rapidly with increasing conditioning humidity.

Figure 37 shows a plot of the initial amplitude A_o as a function of conditioning relative humidity for the three powders. The curves indicate that for saccharin and Carbowax 6000, A_o is practically independent of conditioning humidity, while for Span 60, A_o decreases rapidly with increasing conditioning humidity.

The adverse effect of high humidity on the dispersibility of Span 60 was demonstrated quite effectively when the aerosol chamber was opened after the aerosol decay test had been performed on the sample of Span 60 that had been preconditioned at 75 percent relative humidity. Normally, there is still

Table 11. Results of Aerosol Decay Tests Performed on Powders Conditioned at Various Humidities

Relative Humidity, %	Decay Constant, λ
Saccharin	
<1	0.273
25	0.293
75	0.343
Carbowax 6000	
<1	0.264
25	0.279
75	0.319
Span 60	
<1	0.322
25	0.337
75	0.481

an aerosol present in the chamber after an hour's settling time; however, in this case the aerosol had completely settled out, and furthermore the ceiling of the chamber directly above the bursting diaphragm gun was literally speckled with lumps of Span 60. Apparently, the powder was so wet and sticky that most of it discharged from the bursting diaphragm gun in the form of lumps which pelted the ceiling of the chamber and adhered there upon impact.

Electrostatic charge analyses were made on samples of each of the three base powders preconditioned at relative humidities of <1, 25, and 75 percent. The experimental work was carried out at the same time as the investigation of effects of conditioning relative humidity on dispersibility.

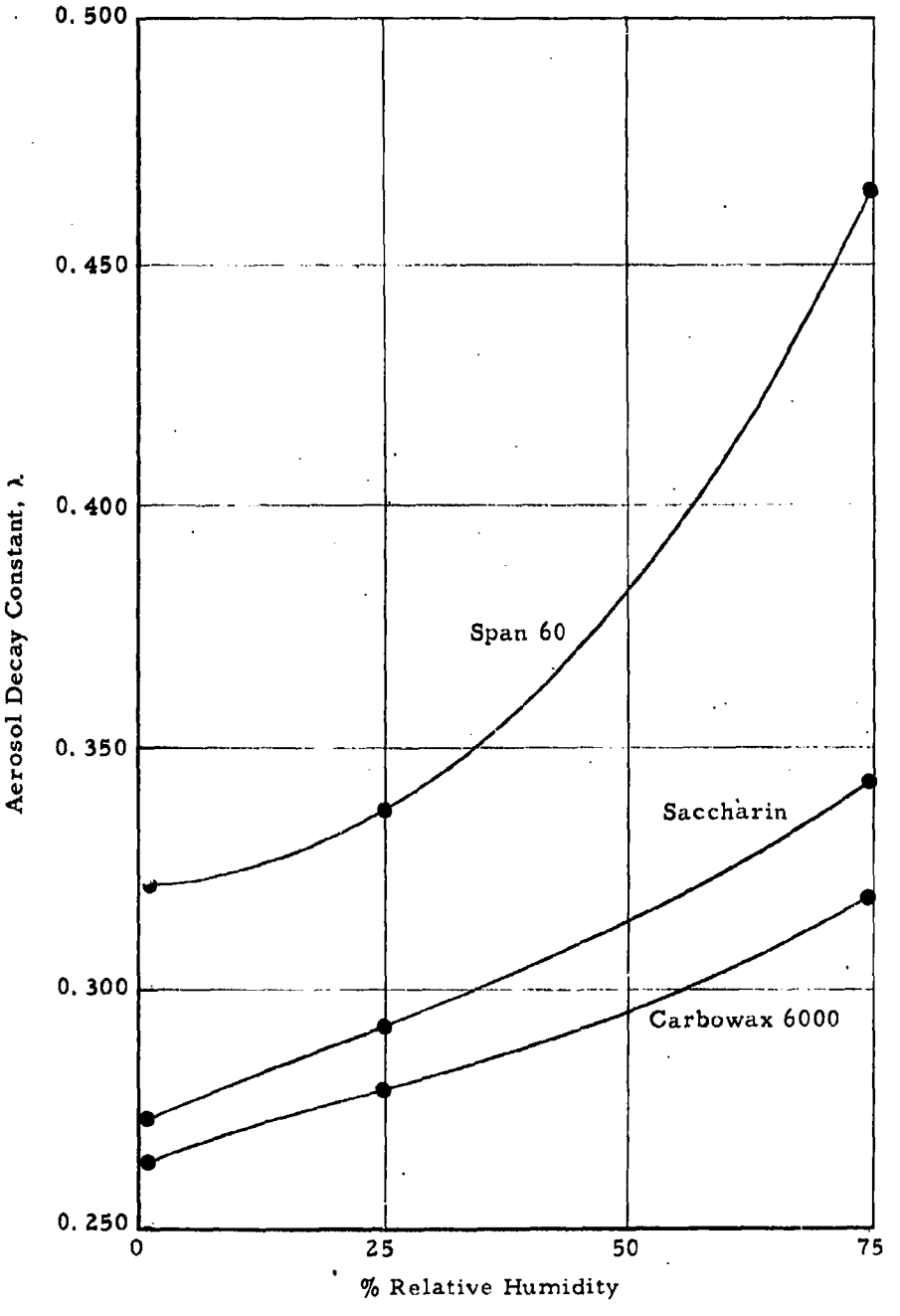

Figure 36. Aerosol Decay Constant as a Function of Humidity

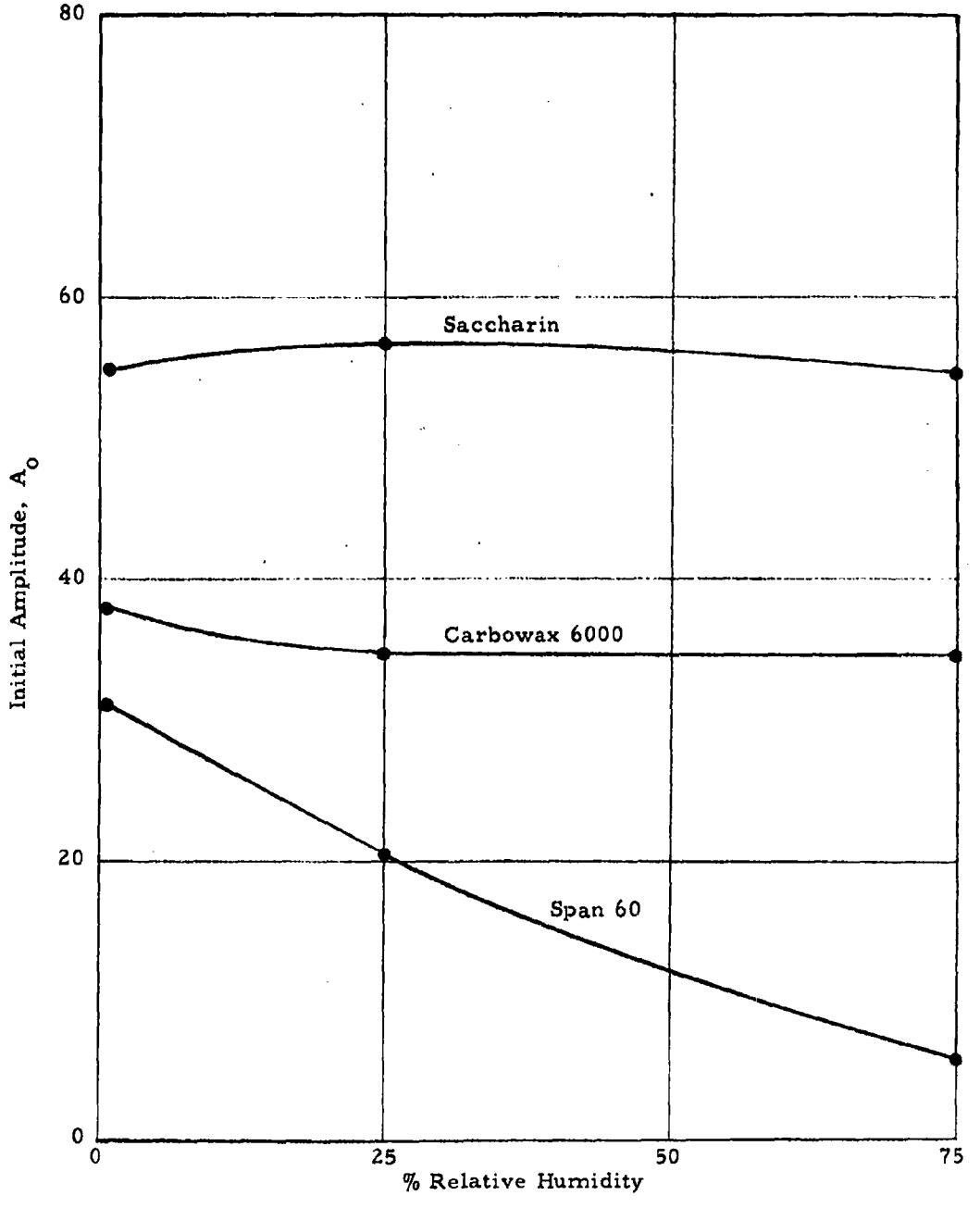

Figure 37. Initial Amplitude as a Function of Humidity

The technique used in preconditioning the powder samples and transfering them from the glove box to the powder dispersing gun was the same as that used in the dispersibility tests.

The graphs in Figure 38 indicate that the three powders are affected in somewhat the same manner as the relative humidity is varied. In all cases, the percentage of neutral particles is small, and the variation of this percentage with relative humidity is insignificant. It may be seen that in the case of saccharin there is always an excess of negatively-charged particles regardless of humidity, but in the case of Carbowax 6000 and Span 60 there may be an excess of negatively-charged or positively-charged particles depending upon humidity. A solid line is drawn through the 50 percent point to indicate where the changeover from an excess of one polarity to the other occurs.

The finding that very few particles are uncharged, and that the numbers of positively-charged and negatively-charged particles are nearly equal agrees with Kunkel's[15] findings.

C. Effects of Antiagglomerant Agents on Powder Properties

1. Shear Strengths of the Agents Themselves

The first step in the investigation of antiagglomerant agents was a series of screening tests to determine which agent (or agents) merited further investigation. The agents investigated are listed in Table 12. The test used for screening purposes was the powder shear strength test described in Section III-B. The first screening tests were conducted on the agents themselves. These tests were conducted at room conditions of temperature and humidity (Temp = 75 - 77°F, RH = 35%). Five different compressive loads ranging from 1450 dynes/cm^2 (the disc alone) to 6360 dynes/cm^2 were used.

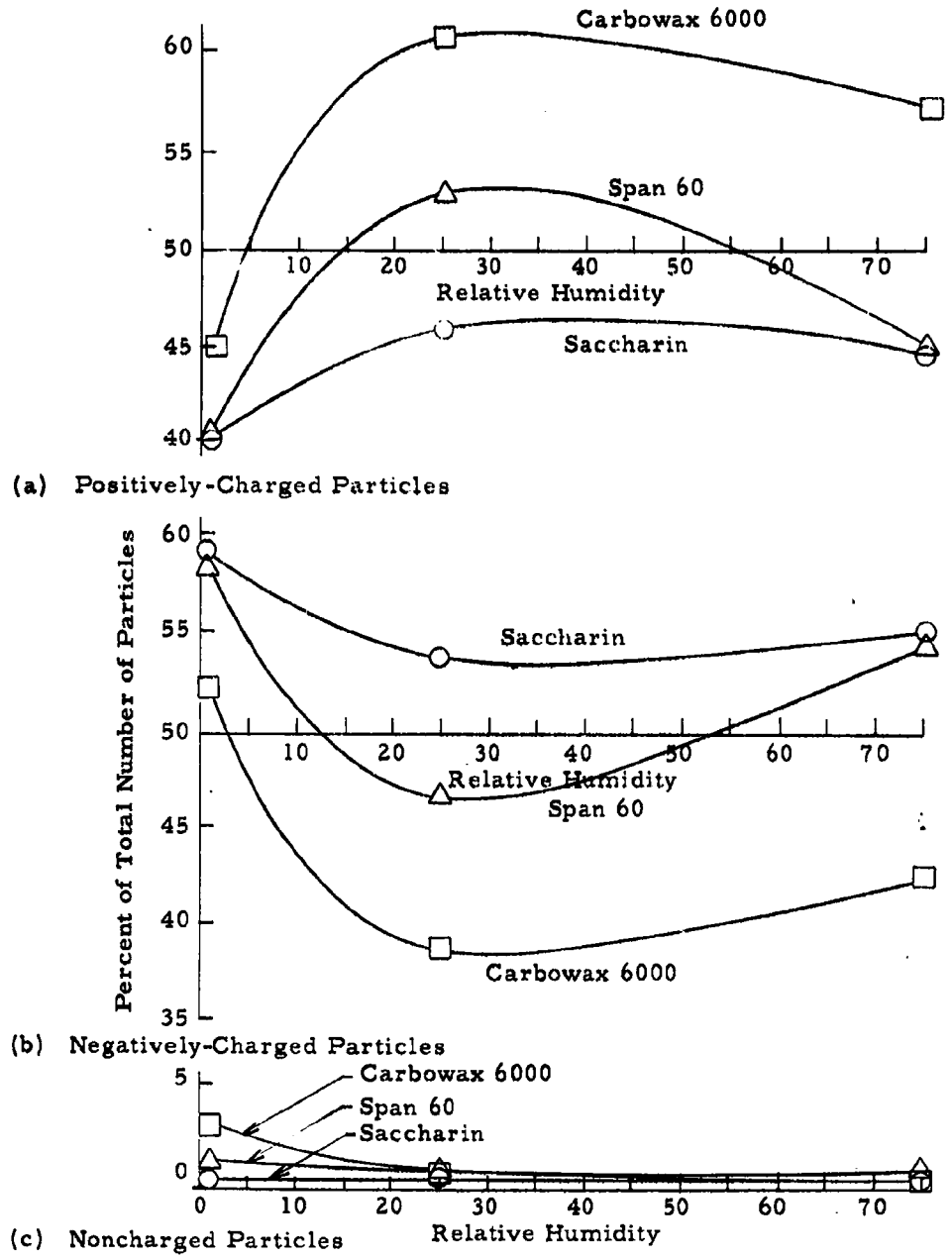

Figure 38. Electrostatic Charge on Particles as a Function of Relative Humidity

Table 12. Antiagglomerant Agents Tested

Agent	Material	Manufacturer
Cab-O-Sil	silica	Godfrey L. Cabot, Inc.
P-25	titanium dioxide	Godfrey L. Cabot, Inc.
Alon-C	aluminum oxide	Godfrey L. Cabot, Inc.
Santocel	silica	Monsanto Chemical Corp.
Tri-Calcium Phosphate	$Ca_3 (PO_4)_2$	Monsanto Chemical Corp.
Micria AL	alumina	Monsanto Chemical Corp.
Calcium Stearate	$Ca (C_{18} H_{35} O_2)_2$	Mallinckrodt Chemical Works
Kalite	surface-coated $CaCO_3$	Diamond Alkali Co.
Multifex MM	ultra-fine $CaCO_3$	Diamond Alkali Co.
Super Multifex	ultra-fine surface-coated $CaCO_3$	Diamond Alkali Co.
ASP-101	alumina silicate (0.5% stearate)	Minerals & Chemicals Philipp Corp.
Attasorb LVM	Attapulgus clay	Minerals & Chemicals Philipp Corp.
Attagel 20	Attapulgus clay	Minerals & Chemicals Philipp Corp.
Attacote C	Attapulgus clay	Minerals & Chemicals Philipp Corp.

The results of these tests are given in Table 13 and presented graphically in Figure 39. It is seen that several of the agents have nearly the same shear strength. These are represented on the graph by heavy vertical bars with the curve drawn through the mean values of shear strength at each compressive load. Four agents have shear strengths that are considerably different from that of the large group. These are Multifex MM, ASP-101, Alon-C, and Cab-O-Sil. Data for these four agents are plotted separately on

the graph. Multifex MM and ASP-101 have higher shear strengths, while Alon-C and Cab-O-Sil have lower shear strengths than that of the large group. It is apparent that Cab-O-Sil has the lowest shear strength of all agents tested.

Table 13. Shear Strength Data for Various Antiagglomerant Agents

Average Shear Strength (dynes/cm^2)	Deviation (dynes/cm^2)	Compressive Load (dynes/cm^2)
Cab-O-Sil		
916	36.6	1448
1660	33.3	2775
2440	36.6	4060
2995	30.0	5305
3673	22.3	6360
P-25		
1051	23.0	1448
1838	7.3	2775
2970	106.6	4060
3705	46.6	5305
4513	102.3	6360
Alon-C		
954	37.3	1448
1790	20.0	2775
2653	17.6	4060
3390	16.6	5305
3902	91.0	6360
Santocel		
1121	60.0	1448
2102	124.0	2775
2760	70.0	4060
3433	124.0	5305
4136	54.6	6360

Table 13 (Continued)

Average Shear Strength (dynes/cm^2)	Deviation (dynes/cm^2)	Compressive Load (dynes/cm^2)
Tri-Calcium Phosphate		
1013	21.6	1448
1967	76.6	2775
2923	92.3	4060
3713	117.6	5305
4715	160.0	6360
Micria AL		
1105	35.2	1448
2027	2.6	2775
2893	9.0	4060
3662	11.0	5305
4360	13.3	6360
Kalite		
1265	71.6	1448
2170	0.0	2775
2970	40.0	4060
3826	164.6	5305
4416	302.0	6360
Multifex MM		
1378	36.3	1448
2655	26.6	2775
3768	21.0	4060
4778	99.0	5305
6005	70.0	6360
Super Multifex		
1182	20.5	1448
2212	87.6	2775
3140	126.6	4060
3738	42.3	5305
4606	142.2	6360

Table 13 (Continued)

Average Shear Strength (dynes/cm^2)	Deviation (dynes/cm^2)	Compressive Load (dynes/cm^2)
ASP-101		
1288	21.6	1448
2413	37.6	2775
3304	54.6	4060
4348	92.3	5305
5243	37.6	6360
Attasorb LVM		
1111	50.0	1448
1905	47.0	2775
2725	86.6	4060
3667	91.0	5305
4187	119.0	6360
Attagel 20		
1151	35.0	1448
1979	54.3	2775
2821	53.0	4060
3422	41.0	5305
4152	54.3	6360
Attacote C		
1090	47.3	1448
1914	36.3	2775
2816	115.3	4060
3615	113.3	5305
4713	186.0	6360
Calcium Stearate		
1040	0.0	1448
2040	46.6	2775
3018	37.6	4060
3728	33.0	5305
4423	84.3	6360

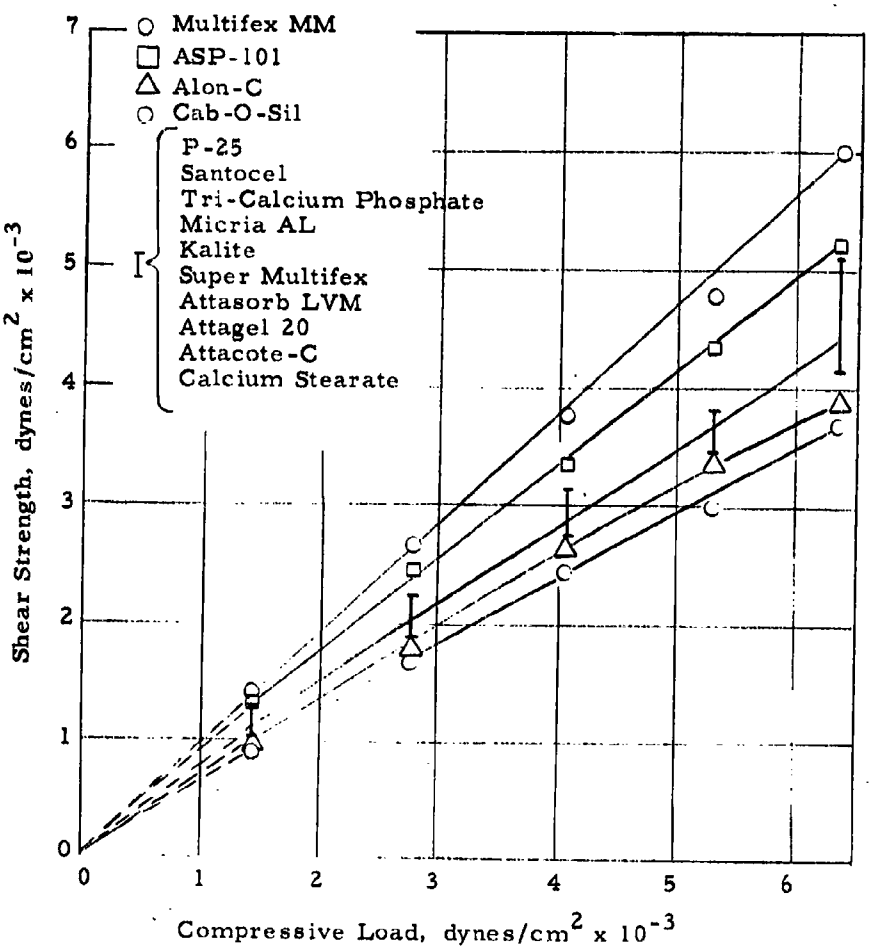

Figure 39. Shear Strength of Various Antiagglomerant Agents as a Function of Compressive Load

2. Shear Strengths of Powders Containing 1 Percent Agent

Although these tests indicate that the agents themselves have quite a wide range of shear strengths, with Cab-O-Sil having the lowest, they do not indicate what effects the agents may have on powder properties. For this reason, shear strength tests were conducted on samples of the three base powders containing 1 percent by weight of each of the antiagglomerant agents listed in Table 12. The results are given in Tables 14, 15, and 16 and are presented graphically in Figures 40, 41, and 42. Separate plots are shown for the control samples (powders with no additive) and for the mixtures which have significantly lower shear strengths than the control samples. It is seen that agents Cab-O-Sil, Alon-C, and P-25 are the most promising for the base powders saccharin and Carbowax 6000. With Span 60, however, none of the agents produced a clear-cut reduction in shear strength, although tri-calcium phosphate seems to be the most promising agent tested.

3. Optimum Concentration

Several different tests were used to determine optimum concentration of the more promising antiagglomerant agents. These were shear strength, bulk density, dynamic angle of repose, electrostatic charge, and dispersibility. For saccharin and Carbowax 6000, the agents tested were Cab-O-Sil, Alon-C, and P-25. For Span 60, the agents tested were Cab-O-Sil and tri-calcium phosphate. In all cases, the concentrations investigated were 0, 1, 5, 10, 30, and 100 percent agent. All powder samples were blended prior to testing by means of the technique described in Section II-C.

a. Shear Strength Tests

The shear strength tests were made at two different times and at two different compressive loads. The compressive load used in the first series was 5300 dynes/cm^2, and the agent tested was Cab-O-Sil. The results of

Table 14. Shear Strengths of Saccharin Samples Containing Various Antiagglomerant Agents

Compressive Load = 1510 dynes/cm^2		Compressive Load = 6200 dynes/cm^2	
Additive	Shear Strength (dynes/cm^2)	Additive	Shear Strength (dynes/cm^2)
Alon-C	750	Alon-C	3020
Cab-O-Sil	860	P-25	3530
P-25	950	Cab-O-Sil	4210
Santocel	1150	Santocel	4630
Calcium Stearate	1200	Super Multifex	5680
Attagel	1240	Tri-Calcium Phosphate	5710
No Additive	1290	Calcium Stearate	5750
Tri-Calcium Phosphate	1320	Attagel	5850
Multifex MM	1370	Kalite	5950
Attasorb	1500	Micria AL	6150
Kalite	1510	Attasorb	6240
ASP 101	1560	ASP 101	6260
Micria AL	1580	No Additive	6270
Super Multifex	1620	Multiflex MM	6360

Compressive Load = 10900 dynes/cm^2

Additive	Shear Strength (dynes/cm^2)
Alon-C	5510
P-25	5600
Cab-O-Sil	7070
Santocel	8500
Tri-Calcium Phosphate	8890
Super Multifex	9560
No Additive	9700
Calcium Stearate	10100
ASP 101	10200
Attagel	10300
Multifex MM	10400
Micria AL	10600
Attasorb	10900
Kalite	10900

Table 15. Shear Strengths of Carbowax 6000 Samples Containing Various Antiagglomerant Agents

Compressive Load = 1510 dynes/cm^2		Compressive Load = 6200 dynes/cm^2	
Additive	Shear Strength (dynes/cm^2)	Additive	Shear Strength (dynes/cm^2)
Cab-O-Sil	800	Alon-C	4390
P-25	960	P-25	4430
Alon-C	1030	Cab-O-Sil	4670
Micria AL	1460	Super Multifex	5150
ASP 101	1480	Santocel	5200
Santocel	1510	Tri-Calcium Phosphate	5760
Super Multifex	1530	ASP 101	5850
Tri-Calcium Phosphate	1530	Kalite	5940
Attagel	1620	Micria AL	6320
Calcium Stearate	1690	Calcium Stearate	6360
Kalite	1710	Multifex MM	6570
Multifex MM	1800	No Additive	6890
No Additive	1920	Attagel	8260

Compressive Load = 10900 dynes/cm^2

Additive	Shear Strength (dynes/cm^2)
P-25	6800
Alon-C	7950
Cab-O-Sil	8890
Super Multifex	9640
Santocel	9980
Tri-Calcium Phosphate	10000
Kalite	10500
Multifex MM	10500
Micria AL	11000
Calcium Stearate	11000
No Additive	11200
Attagel	15300

Table 16. Shear Strengths of Span 60 Samples Containing Various Antiagglomerant Agents

Compressive Load = 1510 dynes/cm^2	
Additive	Shear Strength (dynes/cm^2)
Alon-C	610
P-25	700
Attagel	760
Calcium Stearate	760
No Additive	790
Santocel	790
Kalite	800
Tri-Calcium Phosphate	810
Micria AL	840
ASP 101	840
Multifex MM	880
Cab-O-Sil	950
Super Multifex	980

Compressive Load = 6200 dynes/cm^2	
Additive	Shear Strength (dynes/cm^2)
Alon-C	3110
Micria AL	3300
No Additive	3340
Attagel	3510
Calcium Stearate	3540
P-25	3580
Tri-Calcium Phosphate	3580
Multifex MM	3940
Santocel	4060
ASP 101	4300
Cab-O-Sil	4310
Super Multifex	4590

Compressive Load = 10900 dynes/cm^2	
Additive	Shear Strength (dynes/cm^2)
Tri-Calcium Phosphate	5040
No Additive	5670
Multifex MM	5850
Attagel	5940
ASP 101	6040
Micria AL	6250
Kalite	6330
Calcium Stearate	6450
Alon-C	6510
Santocel	6520
P-25	6700
Cab-O-Sil	6900
Super Multifex	7080

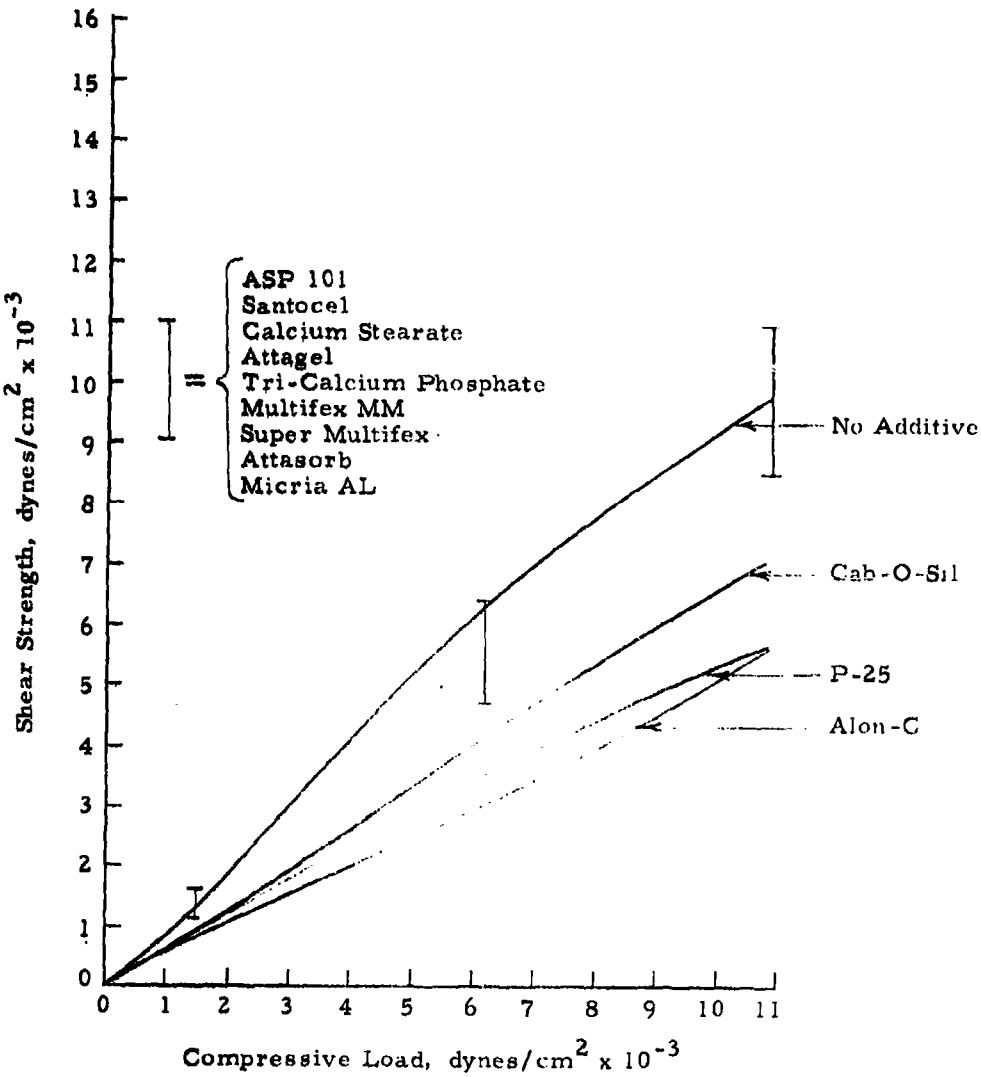

Figure 40. Shear Strength of Saccharin Samples Containing 1 Percent by Weight of Various Antiagglomerant Agents

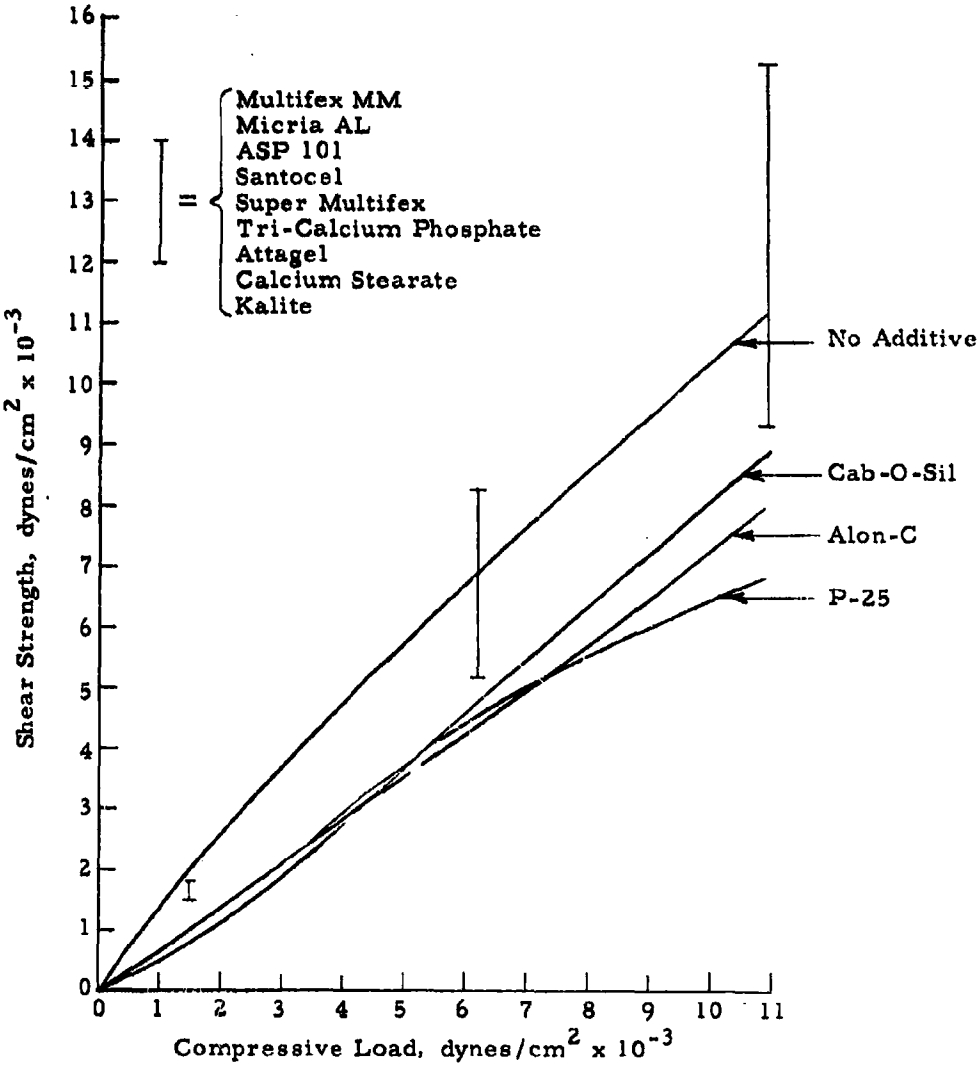

Figure 41. Shear Strength of Carbowax 6000 Samples Containing 1 Percent by Weight of Various Antiagglomerant Agents

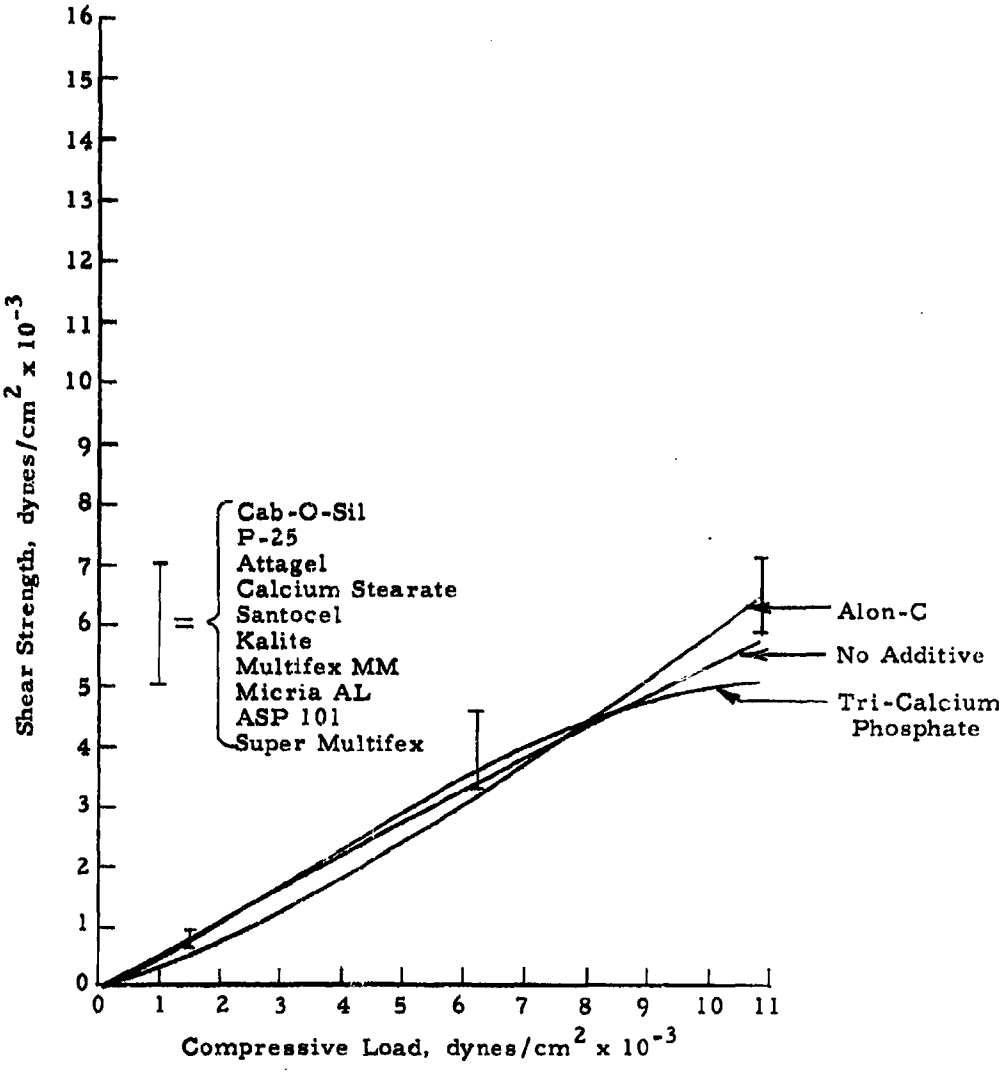

Figure 42. Shear Strength of Span 60 Samples Containing 1 Percent by Weight of Various Antiagglomerant Agents

these tests are given in Table 17. The compressive load used in the second series was 6000 dynes/cm^2 and the agents tested were Alon-C, P-25, and Tri-Calcium Phosphate. The results of these tests are given in Table 18.

Table 17. Shear Strengths of Powder Samples with Various Concentrations of Cab-O-Sil$_2$ (Compressive Load = 5300 dynes/cm^2)

Additive	Concentration (%)	Shear Strength (dynes/cm^2)	Percent Change in Shear Strength
Saccharin			
Cab-O-Sil	0	5060	0
	1	4010	-20.7
	5	3970	-21.7
	10	3930	-22.4
	30	3770	-25.5
	100	3000	-40.9
Carbowax 6000			
Cab-O-Sil	0	6070	0
	1	4190	-31.0
	5	4040	-33.5
	10	3770	-38.0
	30	3580	[illegible]
	100	3000	-50.[illegible]
Span 60			
Cab-O-Sil	0	5370	0
	1	5230	- 2.6
	5	4920	- 8.3
	10	4560	-15.0
	30	3900	-27.3
	100	3000	-44.2

Table 18. Shear Strengths of Powder Samples with Various Concentrations of Alon-C, P-25, and Tri-Calcium Phosphate (Compressive Load = 6000 dynes/cm^2)

Additive	Concentration (%)	Shear Strength (dynes/cm^2)	Percent Change in Shear Strength
Saccharin			
Alon-C	0	4860	0
	1	4120	-15.2
	5	4540	- 6.6
	10	4790	- 1.4
	30	5250	+ 6.4
	100	3805	-21.7
P-25	0	4860	0
	1	3900	-19.7
	5	3665	-24.6
	10	4760	- 2.1
	30	4710	- 3.1
	100	4160	-14.4
Carbowax 6000			
Alon-C	0	6100	0
	1	5270	-13.7
	5	4000	-34.4
	10	3575	-41.4
	30	4360	-28.5
	100	3805	-37.7
P-25	0	6100	0
	1	4970	-16.9
	5	4160	-31.8
	10	3970	-34.9
	30	4430	-27.4
	100	4160	-31.8
Span 60			
Tri-Calcium Phosphate	0	3630	0
	1	3600	- 0.8
	5	3270	- 9.9
	10	4120	+13.5
	30	4280	+17.9
	100	4120	+13.5

In order to plot the data for both series on the same graph, it is necessary to express them in terms of percent. This is a valid manipulation since shear strength is a linear function of compressive load over this range of compressive loads. Plots of percent change in shear strength as a function of concentration are shown in Figures 43, 44, and 45.

We see, in the case of saccharin, the optimum concentration is 1 percent for Cab-O-Sil, 1 percent for Alon-C, and between 1 and 5 percent for P-25. For Carbowax 6000, the optimum concentration is 1 percent for Cab-O-Sil, 10 percent for Alon-C, and 10 percent for P-25. In the case of Span 60, the optimum concentration is 5 percent for tri-calcium phosphate and indeterminable for Cab-O-Sil. When we speak of optimum concentration here, we mean the concentration which produces the greatest reduction in shear strength, considering of course that agent concentration should be small.

b. Bulk Density Tests

To investigate what effect agent concentration has on powder bulk density and also to help determine optimum agent concentration, bulk density tests were made on the prepared powder samples. The technique used for this test is described in Section III-C-1. The results of the bulk density tests are given in Table 19 and are plotted in graphical form in Figures 46, 47, and 48. We see, in the cases of both saccharin and Carbowax 6000, the maximum bulk density occurs at a concentration of 1 percent for Cab-O-Sil, 5 percent for Alon-C, and 10 percent for P-25. For Span 60, the bulk density curves all dip before rising to a maximum, and the maximum occurs at a concentration of 5 percent for Cab-O-Sil, 10 percent for Alon-C, about 25 percent for P-25, and at 100 percent for tri-calcium phosphate.

The significance of the concentration at which maximum bulk density occurs is discussed in greater detail in Section IV-D-1.

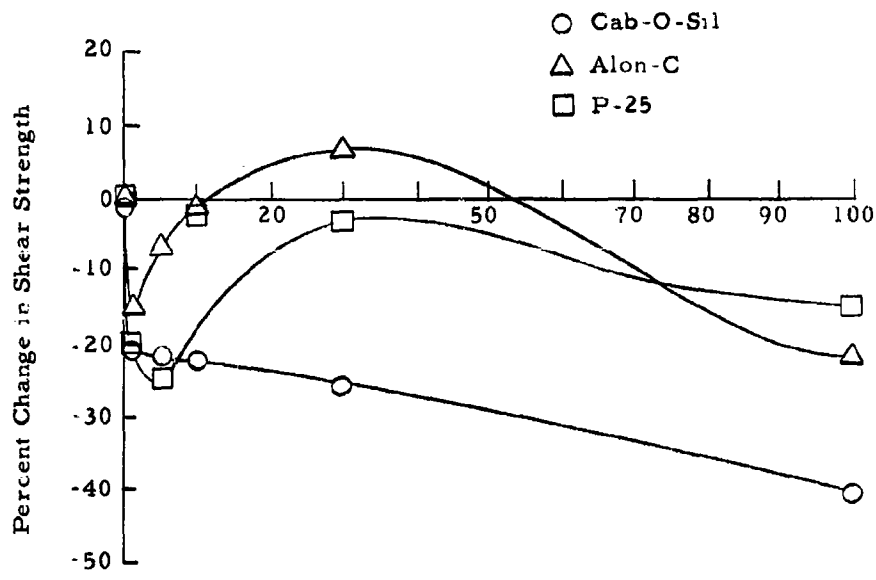

Figure 43. Percent Change in Shear Strength of Saccharin as a Function of Additive Concentration

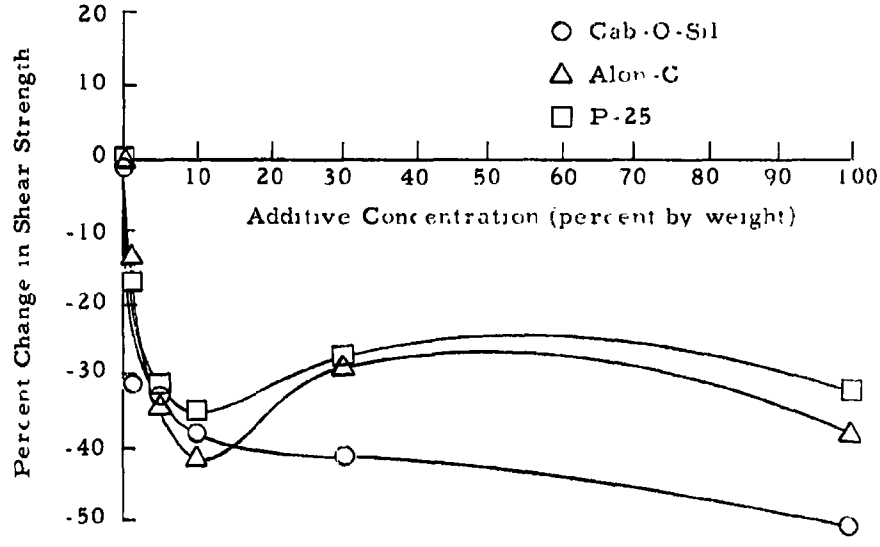

Figure 44. Percent Change in Shear Strength of Carbowax 6000 as a Function of Additive Concentration

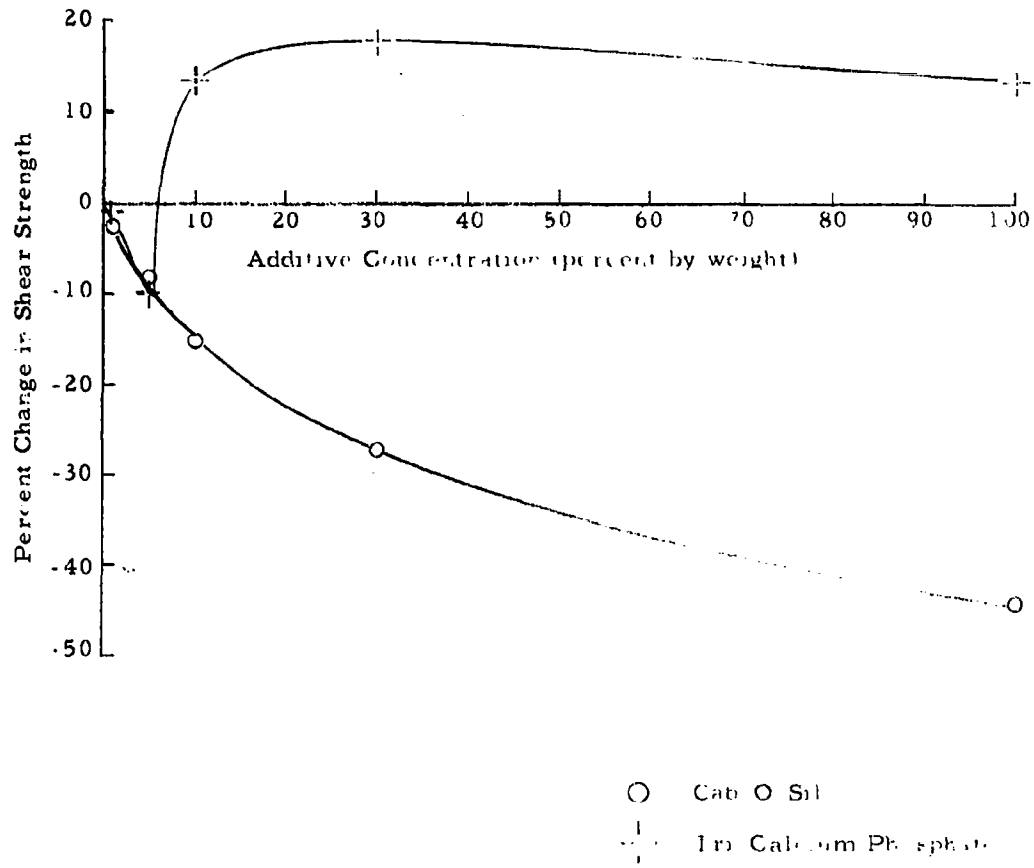

Figure 45 Percent Change in Shear Strength of Spar 60 as a Function of Additive Concentration

Table 19 Bulk Density of Powder Samples Containing Various Anti-agglomerant Agents

Concentration % by Weight	Additive			
	Cab-O-Sil g/cm³	Aloxide C g/cm³	P-25 g/cm³	Tri-Calcium Phosphate g/cm³
Saccharin				
0	0.181	0.181	0.181	
1	0.192	0.254	0.238	
5	0.156	0.279	0.280	
10	0.125	0.240	0.292	
30	0.069	0.156	0.203	
100	0.030	0.038	0.060	
Carbowax 6000				
0	0.243	0.243	0.243	
1	0.318	0.263	0.268	
5	0.222	0.318	0.301	
10	0.209	0.306	0.309	
30	0.100	0.194	0.241	
100	0.030	0.038	0.060	
Span 60				
0	0.193	0.193	0.193	0.193
1	0.183	0.183	0.200	0.180
5	0.210	0.187	0.175	0.178
10	0.203	0.217	0.207	0.191
30	0.093	0.154	0.228	0.236
100	0.030	0.038	0.060	0.475

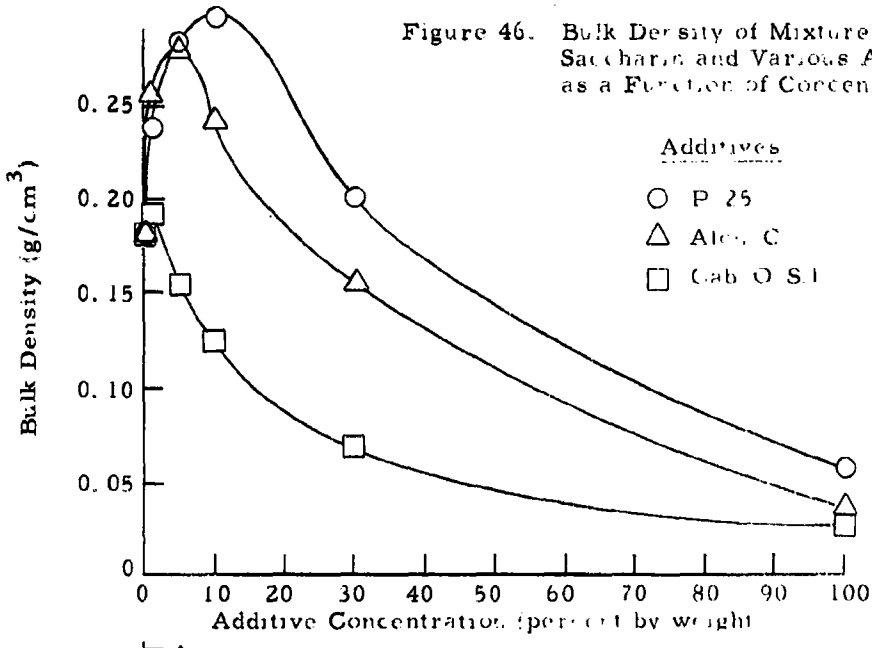

Figure 46. Bulk Density of Mixtures of Saccharin and Various Additives as a Function of Concentration

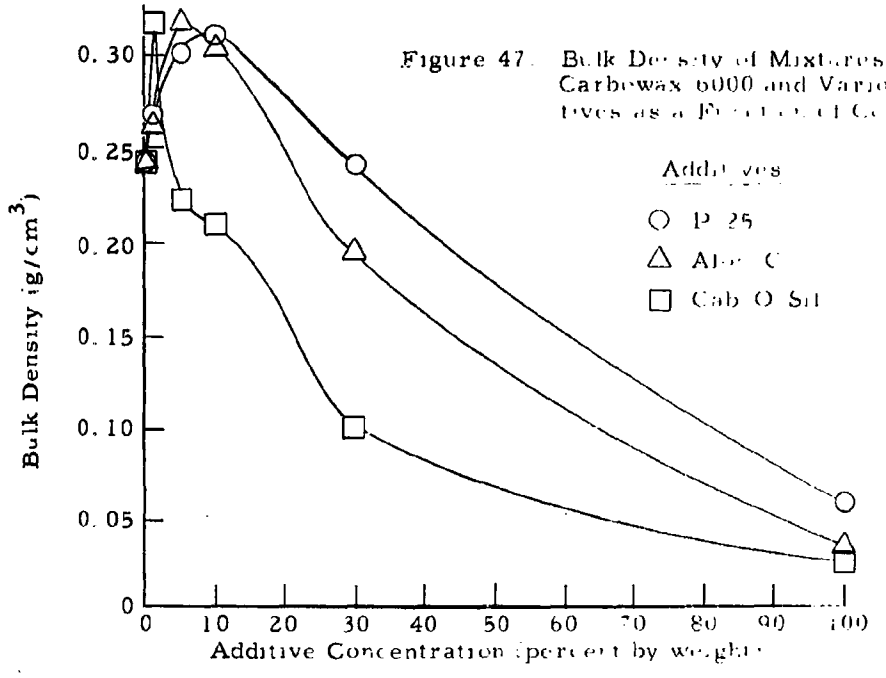

Figure 47. Bulk Density of Mixtures of Carbowax 6000 and Various Additives as a Function of Concentration

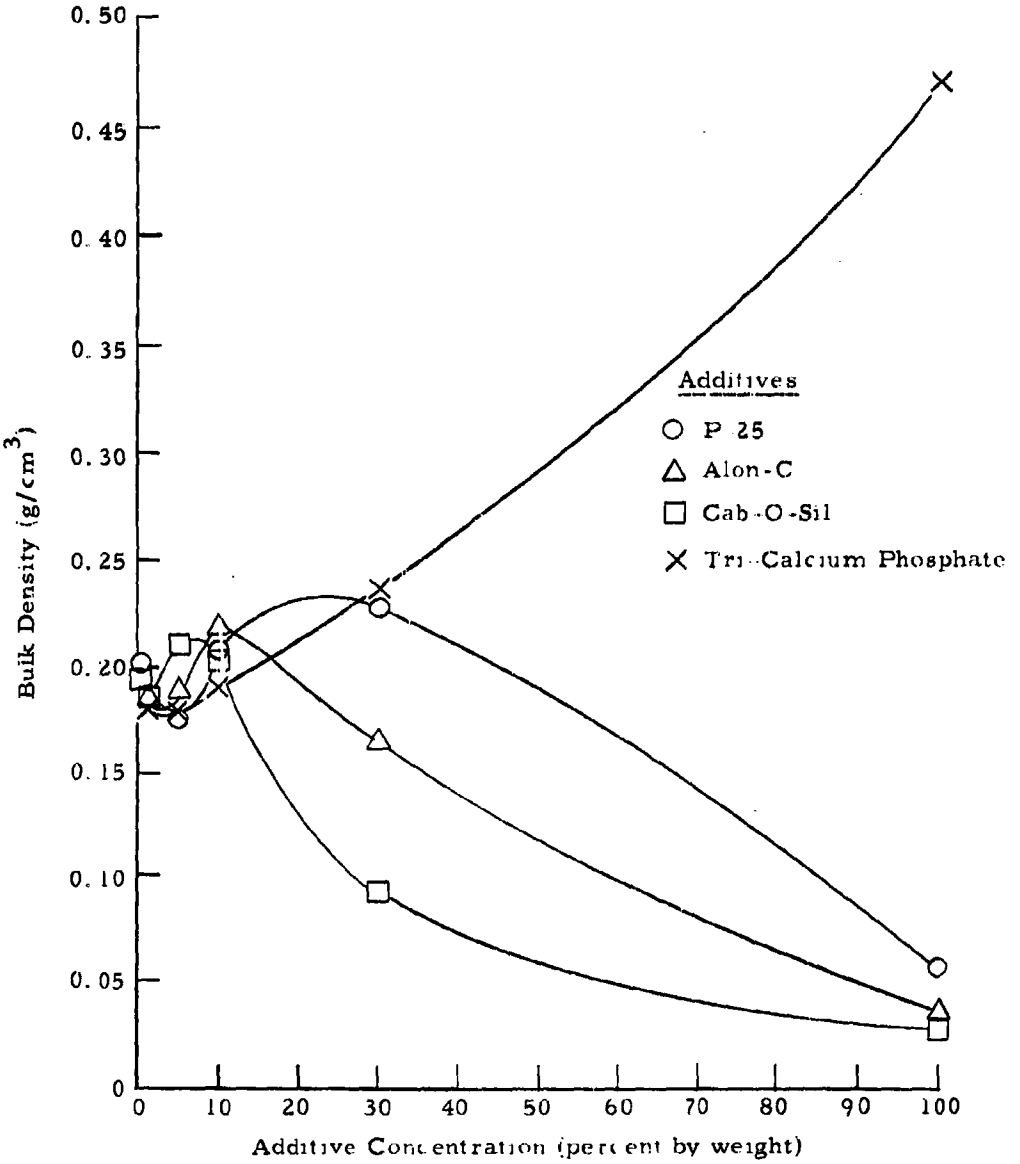

Figure 48. Bulk Density of Mixtures of Spar 60 and Various Additives as a Function of Concentration

c. Dynamic Angle of Repose Tests

To help establish optimum concentration of the more promising anti-agglomerant agents, the prepared powder samples were tested by means of the dynamic angle of repose test described in Section III-E. At least three tests were made on each sample, and new samples were used for each test. The results are given in Table 20 and are plotted graphically in Figures 49, 50, and 51.

We see, in the case of saccharin, the maximum dynamic angle of repose occurs at a concentration of 1 percent for all three agents. For Carbowax 6000, the maximum occurs at a concentration of 5 percent for Cab-O-Sil, 10 percent for Alon-C, and 30 percent for P-25. In the case of Span 60, the maximum occurs at a concentration of 1 percent for Cab-O-Sil and 5 percent for tri-calcium phosphate.

Table 20. Dynamic Angle of Repose of Powder Samples Containing Various Antiagglomerant Agents

Antiagglomerant Agent	Concentration (%)	Dynamic Angle of Repose (Degrees)
Saccharin		
Cab-O-Sil	0	40.4 ± 0.9
	1	52.1 ± 1.4
	5	49.1 ± 1.4
	10	35.2 ± 2.1
	30	32.9 ± 2.1
	100	31.1 ± 1.1
Alon-C	0	40.4 ± 0.9
	1	48.9 ± 2.0
	5	42.3 ± 1.5
	10	37.5 ± 1.6
	30	34.6 ± 1.0
	100	51.4 ± 1.5

Table 20 (Continued)

Antiagglomerant Agent	Concentration (%)	Dynamic Angle of Repose (Degrees)
Saccharin (Continued)		
P-25	0	40.4 ± 0.9
	1	46.7 ± 1.4
	5	44.2 ± 1.3
	10	38.3 ± 1.1
	30	39.1 ± 1.7
	100	49.3 ± 1.2
Carbowax 6000		
Cab-O-Sil	0	30.5 ± 1.0
	1	43.9 ± 1.5
	5	45.7 ± 1.6
	10	44.8 ± 1.7
	30	41.1 ± 0.8
	100	31.1 ± 1.1
Alon-C	0	30.5 ± 1.0
	1	44.5 ± 1.3
	5	47.8 ± 1.2
	10	48.6 ± 1.7
	30	43.2 ± 1.6
	100	51.4 ± 1.6
P-25	0	30.5 ± 1.0
	1	44.5 ± 3.4
	5	43.6 ± 2.2
	10	48.1 ± 1.4
	30	49.8 ± 1.1
	100	49.3 ± 1.2
Span 60		
Cab-O-Sil	0	46.8 ± 0.8
	1	50.6 ± 1.1
	5	47.0 ± 2.5
	10	46.1 ± 1.6
	30	44.6 ± 0.8
	100	31.1 ± 1.1

Table 20 (Continued)

Antiagglomerant Agent	Concentration (%)	Dynamic Angle of Repose (Degrees)
Span 60 (Continued)		
Tri-Calcium Phosphate	0	46.8 ± 0.8
	1	48.3 ± 1.7
	5	51.0 ± 1.8
	10	45.8 ± 1.5
	30	45.3 ± 1.2
	100	46.8 ± 1.3

d. Dispersibility Tests

The same powder samples used in the previous tests were tested for dispersibility using the technique described in Section III-F. As with the shear strength tests, the dispersibility tests were conducted at different times and under different conditions. Data corresponding to powder samples containing various concentrations of Cab-O-Sil are tabulated in Table 21, and those corresponding to powder samples containing various concentrations of Alon-C, P-25, and tri-calcium phosphate are tabulated in Table 22. The same test procedure was used in both series, but sensitivity settings were different. The sensitivity setting should not affect the aerosol decay constant λ, but it should affect the initial amplitude A_o. This is borne out in the data corresponding to the control samples given in Tables 21 and 22.

In order to plot all the data on a single graph, it is necessary to express in terms of percent. Figures 52, 53, and 54 show plots of percentage change in λ as a function of additive concentration. We see, in the case of saccharin, the optimum concentration is 5 percent for Cab-O-Sil, between 10 and 30 percent for Alon-C, and 30 percent for P-25. For Carbowax 6000, the optimum concentration is 5 percent for Cab-O-Sil, 30 percent for Alon-C, and approximately 30 percent for P-25. In the case of Span 60, the optimum concentration is about 10 percent for Cab-O-Sil and 1 percent for tri-calcium phosphate.

Figure 49. Dynamic Angle of Repose of Mixtures of Saccharin and Various Additives as a Function of Additive Concentration

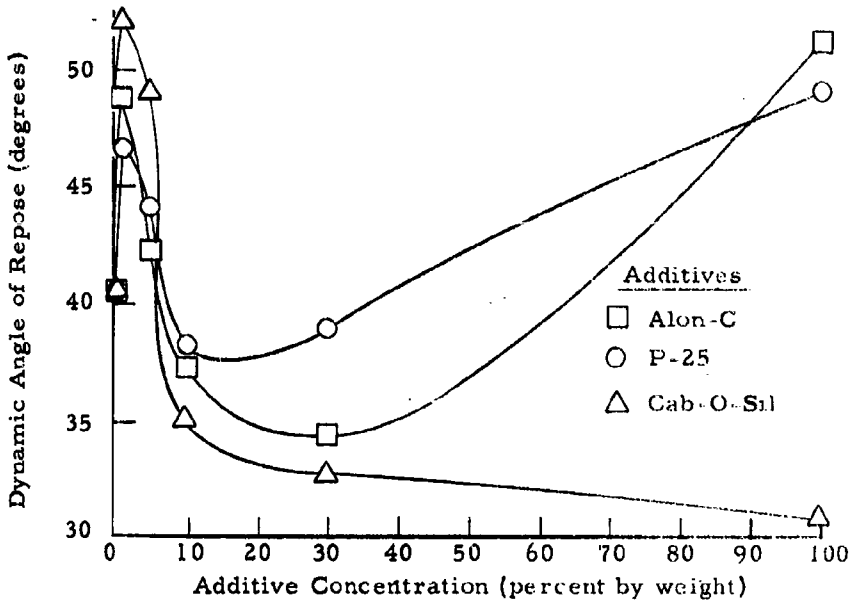

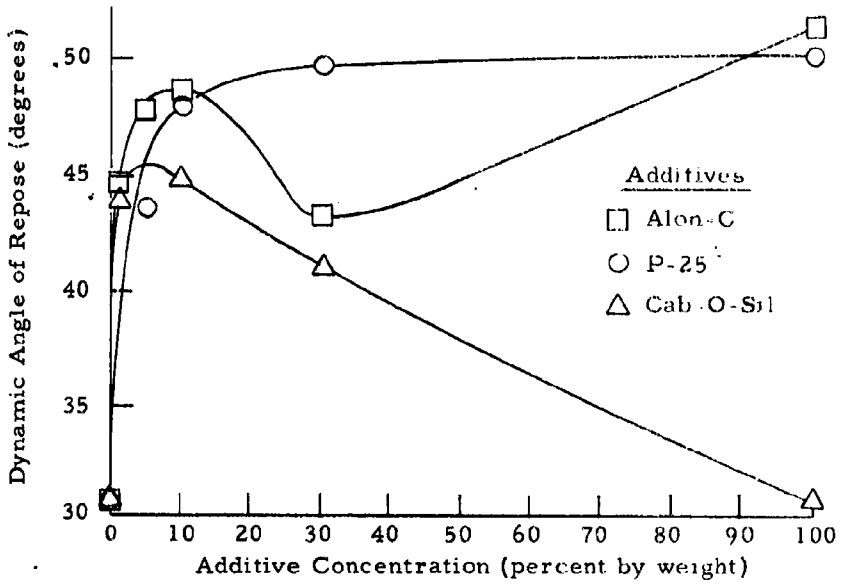

Figure 50. Dynamic Angle of Repose of Mixtures of Carbowax 6000 and Various Additives as a Function of Additive Concentration

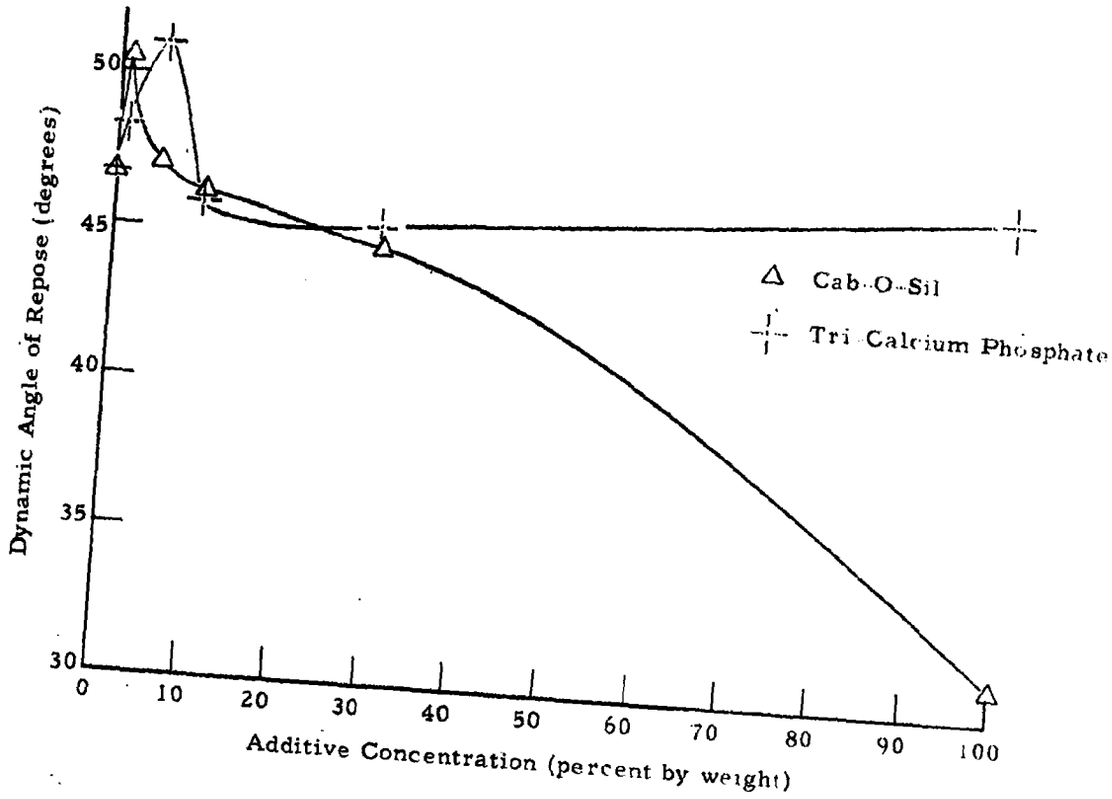

Figure 51. Dynamic Angle of Repose of Mixtures of Span 60 and Various Additives as a Function of Additive Concentration

Table 21. Dispersibility of Powder Samples with Various Concentrations of Cab-O-Sil

Additive	Concentration (%)	Aerosol Decay Constant, λ	Initial Amplitude, A_o
Saccharin			
Cab-O-Sil	0	0.268	29.75
	1	0.237	38.50
	5	0.219	37.75
	10	0.223	37.50
	30	0.254	34.00
	65	0.290	15.00
	100	0.305	5.50
Carbowax 6000			
Cab-O-Sil	0	0.291	13.25
	5	0.258	13.00
	10	0.255	14.00
	30	0.250	14.25
	65	0.286	12.50
	100	0.305	5.50
Span 60			
Cab-O-Sil	0	0.308	4.40
	1	0.230	19.15
	5	0.204	31.60
	10	0.168	38.00
	30	0.157	36.00
	65	0.220	29.00
	100	0.305	5.50

Table 22. Dispersibility of Powder Samples with Various Concentrations of Alon-C, P-25, and Tri-Calcium Phosphate

Antiagglomerant Agent	Concentration (%)	Aerosol Decay Constant, λ	Initial Amplitude, A_o
Saccharin			
Alon-C	0	0.235	53.00
	1	0.210	51.75
	5	0.211	50.50
	10	0.194	47.00
	30	0.181	42.60
	100	0.244	9.35
P-25	0	0.235	53.00
	1	0.208	44.00
	5	0.208	60.50
	10	0.168	56.20
	30	0.142	57.50
	100	0.176	36.50
Carbowax 6000			
Alon-C	0	0.291	33.50
	1	0.277	30.30
	5	0.272	28.60
	10	0.252	30.00
	30	0.288	28.00
	100	0.244	9.35
P-25	0	0.291	33.50
	1	-----	-----
	5	0.284	28.40
	10	0.276	27.50
	30	0.206	32.00
	100	0.176	36.50
Span 60			
Tri-Calcium Phosphate	0	0.306	5.50
	1	0.250	16.20
	5	0.236	25.80
	10	0.226	32.10
	30	0.189	36.25
	100	0.166	20.60

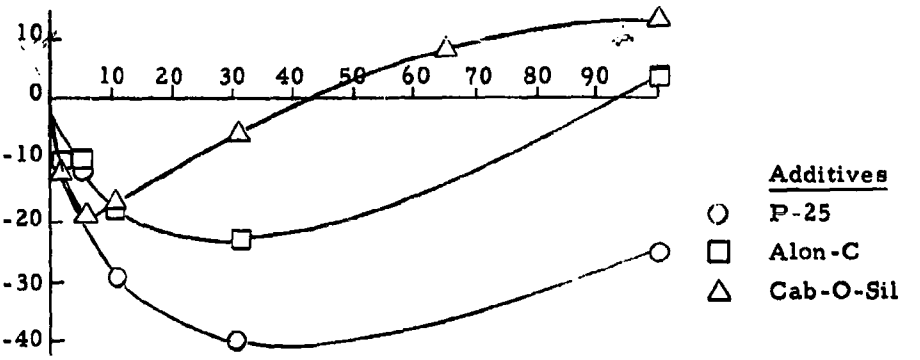

Figure 52. Percentage Change in λ versus Additive Concentration for Saccharin

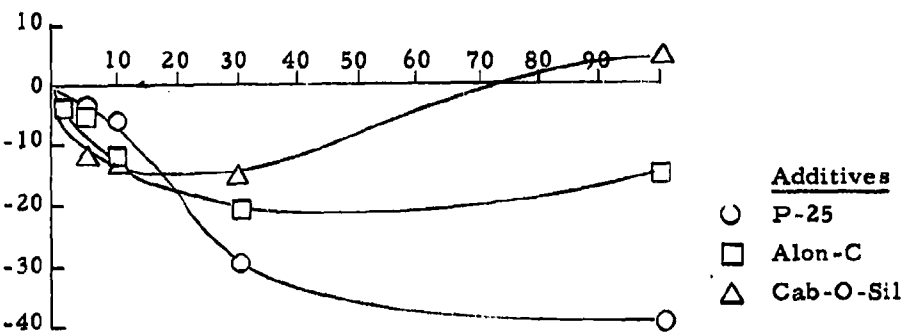

Figure 53. Percentage Change in λ versus Additive Concentration for Carbowax 6000

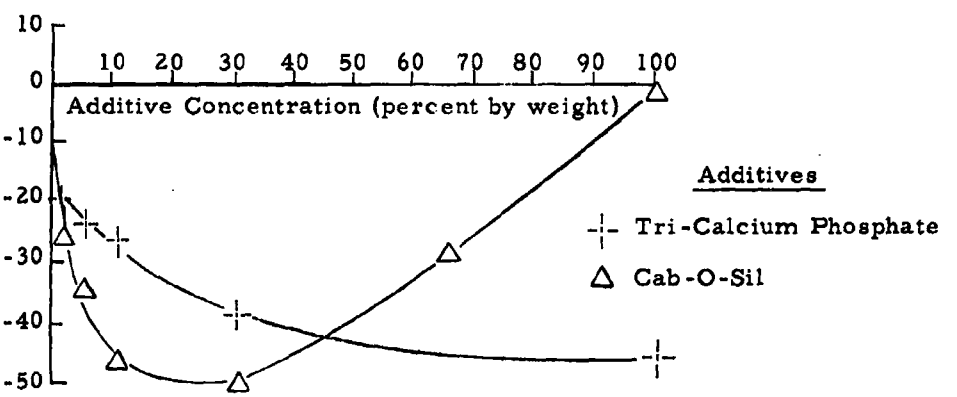

Figure 54. Percentage Change in λ versus Additive Concentration for Span 60

e. Electrostatic Charge Tests

To determine what effect agent concentration has on electrostatic charge and also to help determine optimum agent concentration, electrostatic charge tests were performed on the specially prepared powder samples. The procedure used in performing this test is described in Section III-G-2. In all cases, at least two tests were made on each sample, and the results were averaged. The results are presented in tabular form in Table 23.

With one possible exception, the most neutral sample in each group is the one having an agent concentration of 1 percent. The one possible exception is found in the group of saccharin samples containing Alon-C. Here the most neutral sample appears to be the one having a concentration of 5 percent. As indicated in Section III-G-2, the criterion used to determine the most neutral sample is a value near zero for the quantity (b - a) together with a low value for $W_{\frac{1}{2}}$.

f. Summary

The results of the various tests to determine optimum concentration of the more promising antiagglomerant agents are summarized in Table 24.

4. Effect of 1 Percent Cab-O-Sil on Bulk Tensile Strength of Powders

An investigation was conducted to determine the effect of 1 percent Cab-O-Sil bulk tensile strength of the three base powders. Although it would have been interesting to investigate the whole range of Cab-O-Sil concentrations as was done in the previous section, the time-consuming nature of the test precluded any such undertaking. The investigation, therefore, was limited to the 1 percent concentration.

Table 23. Electrostatic Charge Characteristics of Powder Samples with Various Concentrations of Cab-O-Sil, Alon-C, P-25, and Tri-Calcium Phosphate

Additive	Concentration (%)	A/B	a (cm)	b (cm)	b - a (cm)	$W_{\frac{1}{2}}$
Saccharin						
Cab-O-Sil	0	1.44	3.75	2.60	-0.85	3.94
	1	1.04	3.24	3.11	-0.13	2.67
	5	1.11	3.34	3.01	-0.33	2.67
	10	1.78	4.07	2.28	-1.79	4.44
	30	2.39	4.48	1.87	-2.61	*
	100	very large	6.35	0	-6.35	*
P-25	0	1.44	3.75	2.60	-0.85	3.94
	1	1.27	3.55	2.80	-0.75	1.55
	5	1.09	3.31	3.04	-0.27	2.00
	10	0.98	3.14	3.21	+0.07	1.95
	30	1.08	3.30	3.05	-0.25	2.79
	100	1.00	3.17	3.17	0.00	*
Alon-C	0	1.44	3.75	2.60	-0.85	3.94
	1	1.01	3.19	3.16	-0.03	2.31
	5	0.94	3.08	3.27	+0.19	2.08
	10	0.97	3.13	3.22	+0.09	2.59
	30	0.62	2.43	3.92	+1.49	5.23
	100	1.00	3.11	3.17	0.00	*
Carbowax 6000						
Cab-O-Sil	0	0.92	3.04	3.31	+0.27	1.78
	1	1.08	3.30	3.05	-0.25	1.47
	5	1.09	3.31	3.04	-0.27	1.98
	10	1.01	3.19	3.16	-0.03	2.41
	30	1.06	3.26	3.09	-0.17	2.46
	100	very large	6.35	0.00	-6.35	*
P-25	0	0.92	3.04	3.31	+0.27	1.78
	1	1.08	3.30	3.05	-0.25	1.29
	5	0.92	3.04	3.31	+0.27	1.60
	10	1.03	3.22	3.13	-0.09	1.85
	30	1.00	3.17	3.17	0.00	2.10
	100	1.00	3.17	3.17	0.00	*

Table 23 (Continued)

Additive	Concentration (%)	A/B	a (cm)	b (cm)	b - a (cm)	$W_{\frac{1}{2}}$
Carbowax 6000 (Continued)						
Alon-C	0	0.92	3.04	3.31	+0.27	1.78
	1	0.87	2.96	3.39	+0.43	1.45
	5	0.95	3.09	3.26	+0.17	2.69
	10	0.97	3.13	3.22	+0.09	5.41
	30	0.96	3.11	3.24	+0.13	8.17
	100	1.00	3.17	3.17	0.00	*
Span 60						
Cab-O-Sil	0	1.05	3.26	3.09	-0.17	1.80
	1	1.07	3.28	3.07	-0.21	1.67
	5	1.06	3.27	3.08	-0.19	1.98
	10	1.02	3.21	3.14	-0.07	2.11
	30	1.29	3.58	2.77	-0.81	4.22
	100	very large	6.35	0.00	-6.35	*
Tri-Ca. .um Phosphate	0	1.05	3.26	3.09	-0.17	1.80
	1	0.99	3.16	3.19	+0.03	1.70
	5	1.04	3.24	3.11	+0.13	1.7
	10	1.03	3.23	3.12	+0.11	2.00
	30	0.86	2.94	3.41	+0.47	2.00
	100	1.17	3.43	2.92	-0.51	1.62

Notes:

* = not measurable

$A/B = \frac{\text{Distance from edge of negative plate to densest portion of powder stream}}{\text{Distance from edge of positive plate to densest portion of powder stream}}$

$W_{\frac{1}{2}}$ = Width of middle peak at one-half maximum amplitude

a = Actual distance from edge of negative plate to densest portion of powder stream

b = Actual distance from edge of positive plate to densest portion of powder stream

The sign of the quantity (b - a) is the sign of the net charge of the sample.

Table 24. Summary of Tests to Determine Optimum Concentration of the More Promising Antiagglomerant Agents

Test	Saccharin	Carbowax 6000	Span 60
Optimum Concentration of Cab-O-Sil (%)			
Shear Strength	1	1	Indeterminable
Bulk Density	1	1	5
Dynamic Angle of Repose	1	5	1
Electrostatic Charge	1	1	1
Dispersibility	5	5	10
Optimum Concentration of Alon-C (%)			
Shear Strength	1	10	--
Bulk Density	5	5	10
Dynamic Angle of Repose	1	10	--
Electrostatic Charge	5	1	--
Dispersibility	10-30	30	--
Optimum Concentration of P-25 (%)			
Shear Strength	1-5	10	--
Bulk Density	10	10	25
Dynamic Angle of Repose	1	10-30	--
Electrostatic Charge	1	1	--
Dispersibility	30	30	--
Optimum Concentration of Tri-Calcium Phosphate (%)			
Shear Strength	--	--	5
Bulk Density	--	--	Indeterminable
Dynamic Angle of Repose	--	--	5
Electrostatic Charge	--	--	1
Dispersibility	--	--	1

The results of bulk tensile strength tests on the three base powders are given in Section IV-A. Similar tests were made on samples of these powders containing 1 percent Cab-O-Sil. For saccharin plus 1 percent Cab-O-Sil, the bulk tensile strength was so low that it was very difficult to measure without using extremely high compressive loads. For this reason, no data were obtained for this sample. Data for the tests on Carbowax 6000 plus 1 percent Cab-O-Sil and Span 60 plus 1 percent Cab-O-Sil are plotted in Figures 55 and 56, respectively. Figure 57 shows plots of bulk tensile strength at zero column length as a function of compressive load for both unadulterated samples and samples containing 1 percent Cab-O-Sil. It is seen that the bulk tensile strength of the samples containing 1 percent Cab-O-Sil is less than half that of the unadulterated samples.

D. Mechanism by Which Cab-O-Sil Functions

Experimental data presented in Section IV-C indicate that Cab-O-Sil is one of the most, if not the most, effective antiagglomerant agent we have tested. For this reason, we conducted a study to learn more about the mechanism by which Cab-O-Sil functions. This study consists mainly of a close examination of the effects of 1 percent Cab-O-Sil on various properties of Carbowax 6000. Carbowax 6000 was chosen as the base powder to be investigated in this study because its properties are affected more markedly by small amounts of Cab-O-Sil than most powders. The 1 percent concentration was given greatest attention because four different tests in Section IV-C indicated this to be the optimum concentration.

1. Bulk Density Tests

Referring to Figure 47, we see that the bulk density of powdered Carbowax 6000 is 0.243 g/cm^3. The density of solid Carbowax 6000 is 1.21 g/cm^3. From this it can be shown that about 80 percent of the volume occupied by the powder is void space. In like manner, we see that the bulk density of

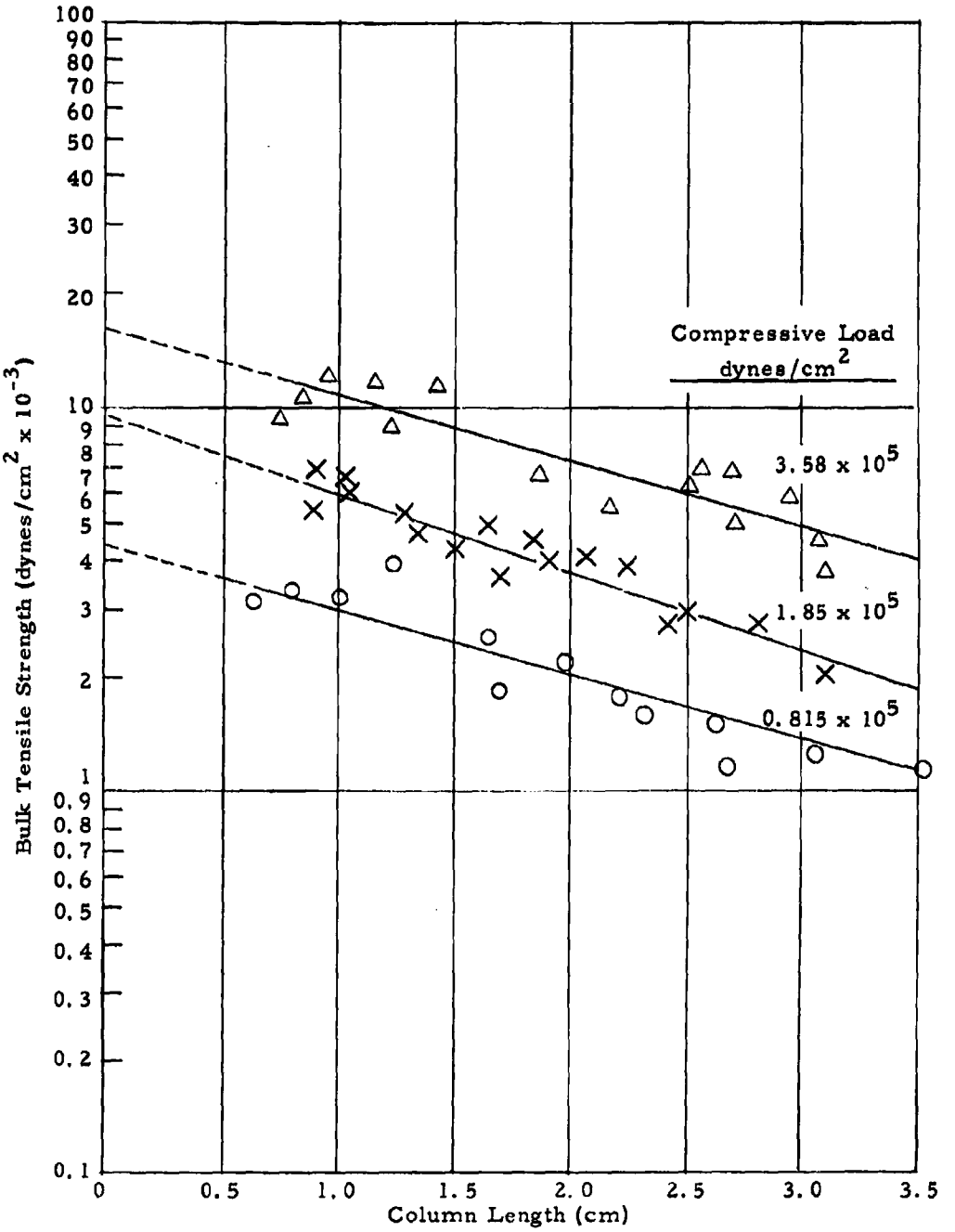

Figure 55. Bulk Tensile Strength of Carbowax 6000 Containing 1 Percent Cab-O-Sil as a Function of Column Length

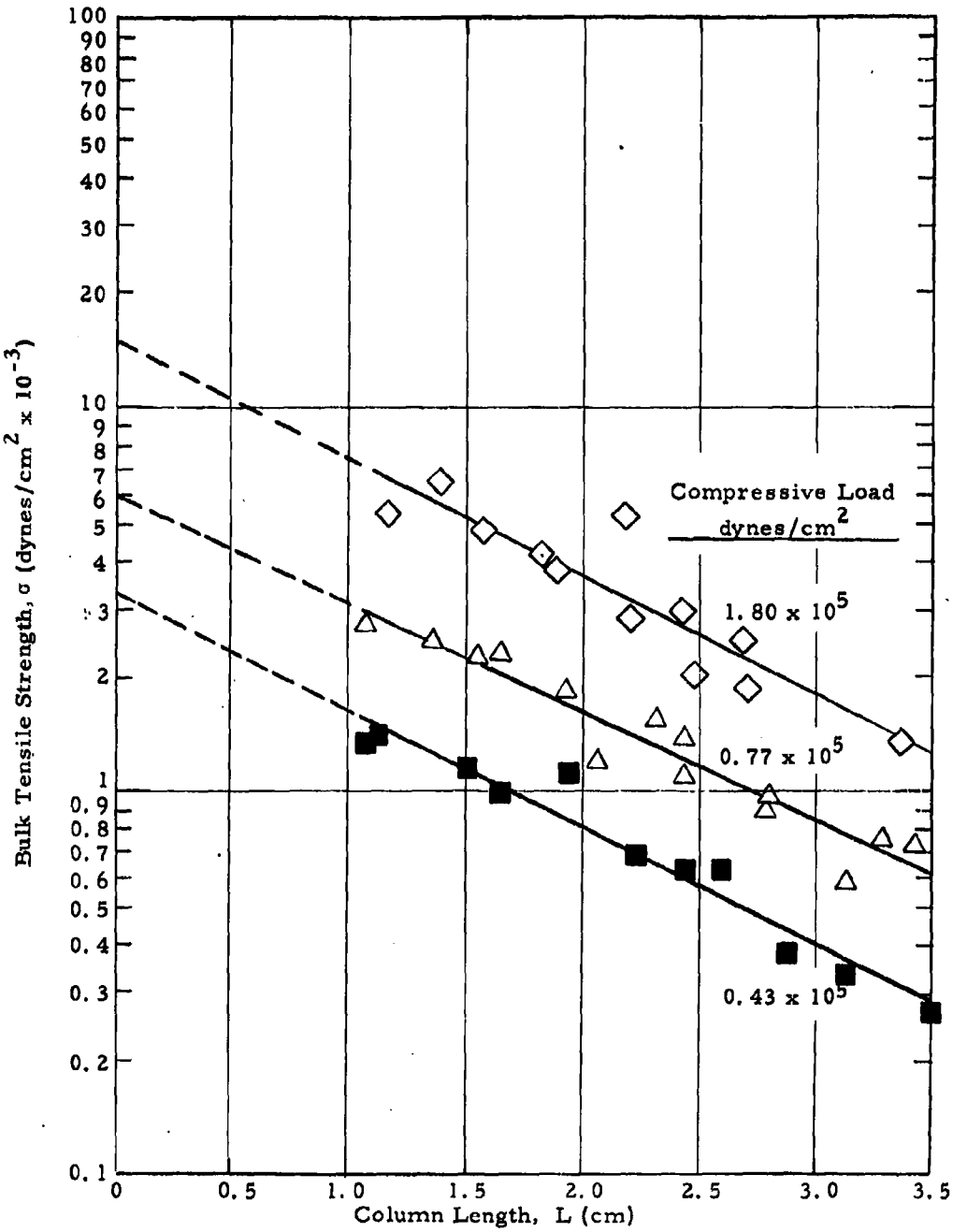

Figure 56. Bulk Tensile Strength of Span 60 Containing 1 Percent Cab-O-Sil as a Function of Column Length

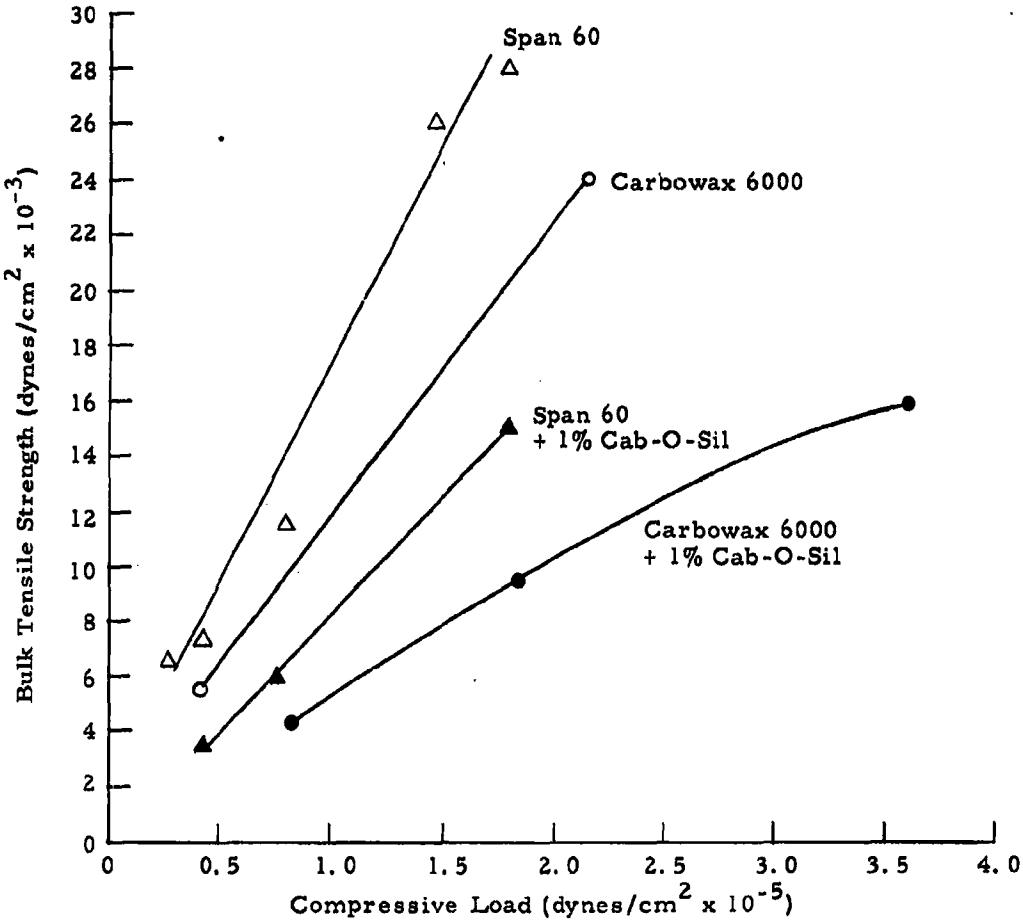

Figure 57. Bulk Tensile Strength of Powders at Zero Column Length as a Function of Compressive Load

Cab-O-Sil is 0.030 g/cm^3. The actual density of SiO_2 is 2.3 g/cm^3. From this we can show that about 99 percent of the volume occupied by Cab-O-Sil is void space. If the void space in a sample of powdered Carbowax 6000 were to be filled with Cab-O-Sil, which itself is 99 percent void space, the weight increase of the sample would be only about 9 percent. Thus we see that in order to increase bulk density by 31 percent, Cab-O-Sil must have some function other than just filling in the void spaces. Additional data will be presented later which will help to explain this function.

2. Use of Electron Micrographs

To gain further knowledge of the mechanism whereby Cab-O-Sil functions, a number of electron micrographs were taken of samples of plain Cab-O-Sil, plain Carbowax 6000, and a mixture consisting of 1 percent Cab-O-Sil and 99 percent Carbowax 6000. The specimens were obtained by exposing collodion-coated electron microscope screens to aerosols of the three powders. The specimens were then shadow-cast with chromium prior to being photographed. A magnification of 20,000 was used. The negatives were enlarged an additional four times, providing a total magnification of 80,000 for the final enlargements. A distance of 8 cm on the final enlargements thus corresponds to 1 micron on the specimens. The final enlargements appear as Figures 58, 59, and 60. Figure 58 is a micrograph of a Cab-O-Sil agglomerate. The diameters of the primary particles making up this agglomerate are between 15 and 25 millimicrons. Figure 59 is a micrograph of a Carbowax 6000 particle. Note that its surface is irregular in shape but generally quite smooth. Figure 60 is a micrograph of a specimen from the mixture consisting of 1 percent Cab-O-Sil and 99 percent Carbowax 6000. Note that the entire surface of the Carbowax 6000 particle is covered with a layer of tiny Cab-O-Sil particles.

This layer provides a clue as to why the sample having a concentration of 1 percent Cab-O-Sil has a higher bulk density than the other samples. Referring to Section IV-C, we see that Cab-O-Sil has a much lower shear

Figure 58. Electron Micrograph of Cab-O-Sil Agglomerate

Figure 59. Electron Micrograph of Carbowax 6000 Particle

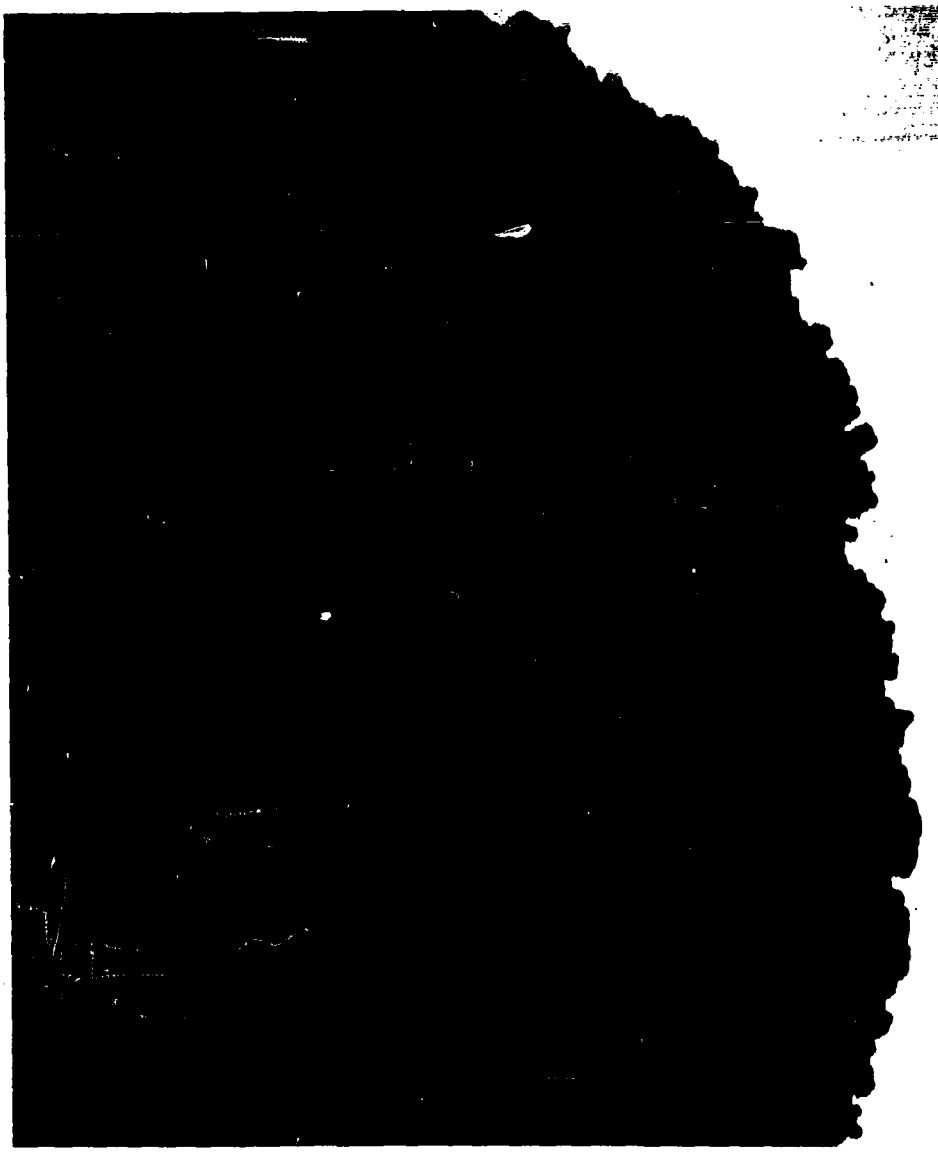

Figure 60. Electron Micrograph of Carbowax 6000 Particle Coated with Cab-O-Sil

strength than Carbowax 6000. It seems reasonable then that this layer acts as a lubricant, permitting the Carbowax 6000 particles to pack together more tightly, thereby increasing the bulk density of the sample. As concentration increases, Cab-O-Sil, which itself has a very low bulk density, separates the Carbowax 6000 particles farther and farther, reducing the overall bulk density of the sample.

3. Theoretical Determination of Concentration Required to Coat Carbowax 6000 Particles with Cab-O-Sil

The electron micrograph of the mixture of Cab-O-Sil and Carbowax 6000 (Figure 60) indicates clearly that the Cab-O-Sil particles form a closely packed layer around the Carbowax 6000 particles. It was decided, therefore, to determine theoretically how much Cab-O-Sil would have to be added to a sample of Carbowax 6000 in order to coat the entire surface of every Carbowax 6000 particles with a layer of Cab-O-Sil particles. These computations appear in Appendix B. Two types of coatings are considered. One is a layer of Cab-O-Sil particles arranged in a square packing and the other in a hexagonal packing. It is shown that, in the case of square packing, the Cab-O-Sil concentration required is 1.20 percent, and in the case of hexagonal packing, it is 1.37 percent. These theoretical values compare quite favorably with the experimentally determined value of approximately 1 percent for the optimum concentration.

4. Electrostatic Charge Test

Examination of the electron micrograph of the mixture of Cab-O-Sil and Carbowax 6000 (Figure 60) leads one to believe that Cab-O-Sil and Carbowax 6000 have a strong mutual attraction. To determine how electrostatic charge contributes to this attraction, we conducted electrostatic charge tests on samples of Carbowax 6000, Cab-O-Sil, and a mixture consisting of 1 percent Cab-O-Sil and 99 percent Carbowax 6000. Photographs of the tests are

shown in Figure 61. It is seen that Carbowax 6000 tends to migrate toward the plate on the left, which is negative in this case, indicating that the net charge on this sample is positive. Cab-O-Sil, on the other hand, migrates toward the positive plate immediately upon entering the electric field, indicating that the net charge on the sample is strongly negative. The mixture consisting of 1 percent Cab-O-Sil and 99 percent Carbowax 6000 flows straight downward between the plates with almost no deflection to either side, indicating that all charges have been neutralized.

The top and bottom photographs in Figure 61 provide an indication of how the addition of 1 percent Cab-O-Sil affects the flow properties of Carbowax 6000. The powder in the top photograph trickles down rather slowly, while that in the bottom photograph flows more like a liquid than a powder. (Note evidence of splashing against the sides of the beaker in the bottom view.)

5. How Cab-O-Sil Prevents Agglomeration

It is believed that the main mechanism by which Cab-O-Sil prevents or reduces agglomeration is its ability to coat the surface of the host particles with a layer of closely packed silica particles. The silica particles are of collodial dimensions; therefore, the particle size distribution of the host powder is not changed appreciably. The layer thus formed alters the powder's properties by reducing its bulk tensile strength and shear strength. In addition, it tends to neutralize electrostatic charge.

Evidence that Cab-O-Sil is indeed an effective antiagglomerant agent is portrayed in Figure 62. The powder at the left is a sample of unadulterated Carbowax 6000, while that at the right is a mixture of 1 percent Cab-O-Sil and 99 percent Carbowax 6000. Both samples have had the same amount of agitation. Obviously the powder at the left is highly agglomerated compared with that at the right.

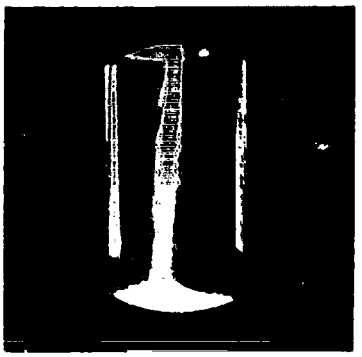

CARBOWAX 6000

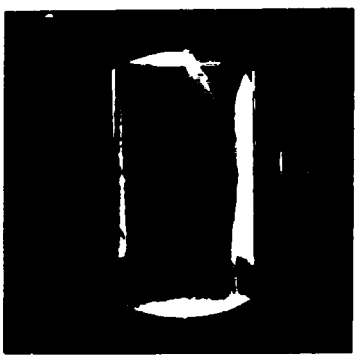

CAB-O-SIL

CARBOWAX 6000 + 1% CAB-O-SIL

FIGURE 7
ELECTROSTATIC CHARGE TESTS
ILLUSTRATING EFFECT OF CAB-O-SIL

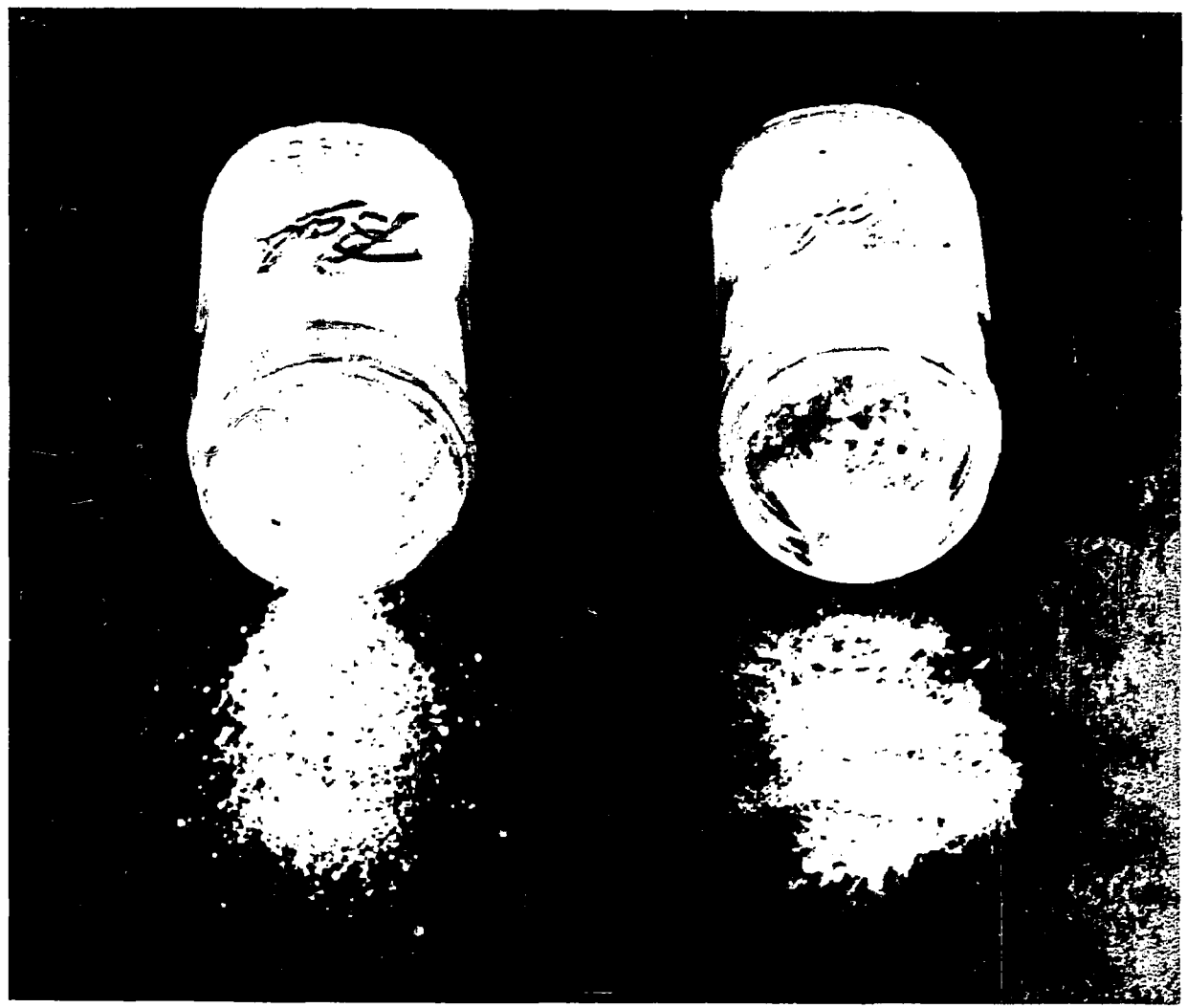

Figure 62. Photograph of Samples of Carbowax 6000 (left) and Carbowax 6000 Containing 1 Percent Cab-O-Sil (right)

E. Effects of Surface Active Agents on Powder Properties

One of the major studies undertaken on this program was an investigation of effects of surface active agents on powder properties.

The term surface active agent applies to certain solutes whose presence, even in small concentrations, markedly reduces the surface energy of a given substance. The molecular structure of most surface active agents is linear, with one end of the structure being composed of radicals having weak valence forces or low residual affinity and the other end being composed of radicals having strong valence forces or high residual affinity.

Chemically, there are four main classes of surface active agents: anionic, cationic, non-ionic, and amphoteric (or ampholytic). The anionic class is characterized by the fact that the low-affinity end of the molecule is included in the anion in aqueous solution. Anionic molecules bear a negative charge in solution and migrate toward the anode. In the cationic class, the low-affinity end of the molecule is included in the cation in aqueous solution. Cationic molecules bear a positive charge in solution and migrate toward the cathode. In the non-ionic class, the molecules have non-ionizable high-affinity end groups and carry no electric charge. In the amphoteric class, the molecule contains both acidic and basic functional groups, and the charge on the molecule as a whole depends upon the pH of the solution. In acidic solutions, they exhibit cationic properties, and in basic solutions they exhibit anionic properties.

A number of samples of surface active agents was obtained from various manufacturers. The number of samples was too large for all to be tested; therefore, it was decided to choose several from each of the four main classes and determine what effects these have on each of the three base powders. In addition, one agent which is not classified as surface active (L-45 Silicone) was tested along with the others. The trade names of these agents, their chemical names, activity, concentration, type, and manufacturer are given in Table 25. Much of the information in Table 25 was compiled by McCutcheon.[16]

Table 25. Surface Active Agents Used

Trade Name	Chemical Name	Activity	Concentration	Type	Manufacturer
Deriphat 151	sodium N-coco β-aminopropionate	100%	67% solids 33% water	Amphoteric	General Mills
Deriphat 154	disodium N-tallow β-iminodi-propionate	100%	75% solids 25% water	Amphoteric	General Mills
Tween 20	polyoxyethylene (2) sorbitan monolaurate	100%	as is	Non-ionic	Atlas
Span 20	sorbitan monolaurate	100%	as is	Non-ionic	Atlas
Span 80	sorbitan monooleate	100%	as is	Non-ionic	Atlas
Triton X-100	aklyl aryl polyether alcohol	100%	as is	Non-ionic	Rohm & Haas
Diglycol Laurate S	diethylene glycol laurate	100%	as is	Non-ionic	Glyco
Santomerse S	alkyl aryl sodium sulfonate	30%	as is	Anionic	Monsanto
Santomerse SX	alkyl aryl sodium sulfonate	30%	as is	Anionic	Monsanto
Triton X-200	sodium salt of alkyl aryl polyether sulfonate	28%	as is	Anionic	Rohm & Haas
Zelec NE	fatty alcohol phosphate composition	100%	50% solids 50% water	Anionic	DuPont
Zelec NK	fatty alcohol phosphate composition	100%	50% solids 50% water	Cationic	General Mills
Diam 26	N-tallow 1, 3-propylene diamine	100%	50% solids 50% isopropanol	Cationic	General Mills

Table 25 (Continued)

Trade Name	Chemical Name	Activity	Concentration	Type	Manufacturer
Aliquot 26	tallow trimethyl ammonium chloride	50%	as is	Cationic	General Mills
Alamine H26D	distilled primary hydrogenated tallow amine	100%	50% solids 50% isopropanol	Cationic	General Mills
BTC - 2125	alkyl dimethyl ethylbenzyl ammonium chloride plus alkyl dimethylbenzyl ammonium chloride	50%	as is	Cationic	Onyx
Alamine 570	coco dimethyl amine	100%	as is	Cationic	General Mills
G-3634	quaternary ammonium derivative	100%	as is	Cationic	Atlas
Armour Agent 100-V	(unknown)		as is	Cationic	Armour
L-45 Silicone		(not a surface active agent)			Union Carbide

The technique described in Section II-E was used to coat powder samples with the selected agents. In all cases, the concentration used was 1 percent active agent and 99 percent powder. The term "active agent" pertains to the active portion of the agent. For example, if the agent is 100 percent active and contains no solvent, then 1 g agent is added to 99 g powder. If the agent is 50 percent active and contains no solvent, then 2 g agent is added to 99 g powder. If the agent contains solvent, then an appropriately larger amount of agent is added to 99 g powder.

The samples thus treated were tested in several different ways to determine the effects of the agents. The types of tests conducted were: 1) shear strength, 2) dispersibility, and 3) electrostatic charge.

1. Shear Strength Tests

The shear strength tests were conducted in a glove box maintained at a relative humidity of 15 percent at room temperature (75 to 82°F). The testing procedure is described in Section III-V. In all cases the compressive load was 5950 dynes/cm^2, and the mask thickness was 1.7 mm. Tests were made in triplicate and the results averaged. Data for the tests on the three base powders treated with the various surface active agents are given in Tables 26, 27, and 28. In addition to the actual shear strength values, the percentage change in shear strength values are given. The following equation is used to calculate percent change in shear strength.

$$\text{Percent change} = -\frac{S_o - S_c}{S_o} \times 100 \qquad (12)$$

where:

S_o = shear strength of unadulterated sample

S_c = shear strength of treated sample

Table 26. Shear Strengths of Saccharin Samples Treated with Various Surface Active Agents

Agent	Type	Shear Strength ($dynes/cm^2$)	Percent Change in Shear Strength
Diglycol Laurate S	non-ionic	3340	-31.2
Tween 20	non-ionic	3980	-18.2
Deriphat 151	amphoteric	4220	-13.2
Zelec NK	anionic	4300	-11.5
Santomerse S	anionic	4370	-10.0
Span 20	non-ionic	4470	- 8.0
Alamine H26D	cationic	4490	- 7.6
Span 80	non-ionic	4550	- 6.3
Triton X-200	anionic	4700	- 3.3
Diam 26	cationic	4710	- 3.0
Aliquot 26	cationic	4740	- 2.4
G-3634	cationic	4830	- 0.7
Santomerse SX	anionic	4840	- 0.4
Deriphat 154	amphoteric	4840	- 0.4
Triton X-100	non-ionic	4850	- 0.2
Control Sample (no additive)		4860	---
L-45 Silicone		4900	- 0.7
Zelec NE	anionic	4980	2.4
Alamine 570	cationic	5000	2.8
Armour Agent 100-V	cationic	5010	3.0
BTC-2125	cationic	5080	4.6

Figures 63, 64, and 65 show the percent change in shear strength for each treated sample as compared with the control samples.

In some instances the shear strength test is misleading. One example of this is the saccharin sample treated with Diglycol Laurate (see Table 26). We see that the shear strength of this sample is relatively low. The reason for this lies in the fact that the sample contained many hard agglomerates. When a sample containing hard agglomerates is tested by the shear strength method, a low value is obtained because the disc simply rolls on top of the hard agglomerates instead of shearing the powder.

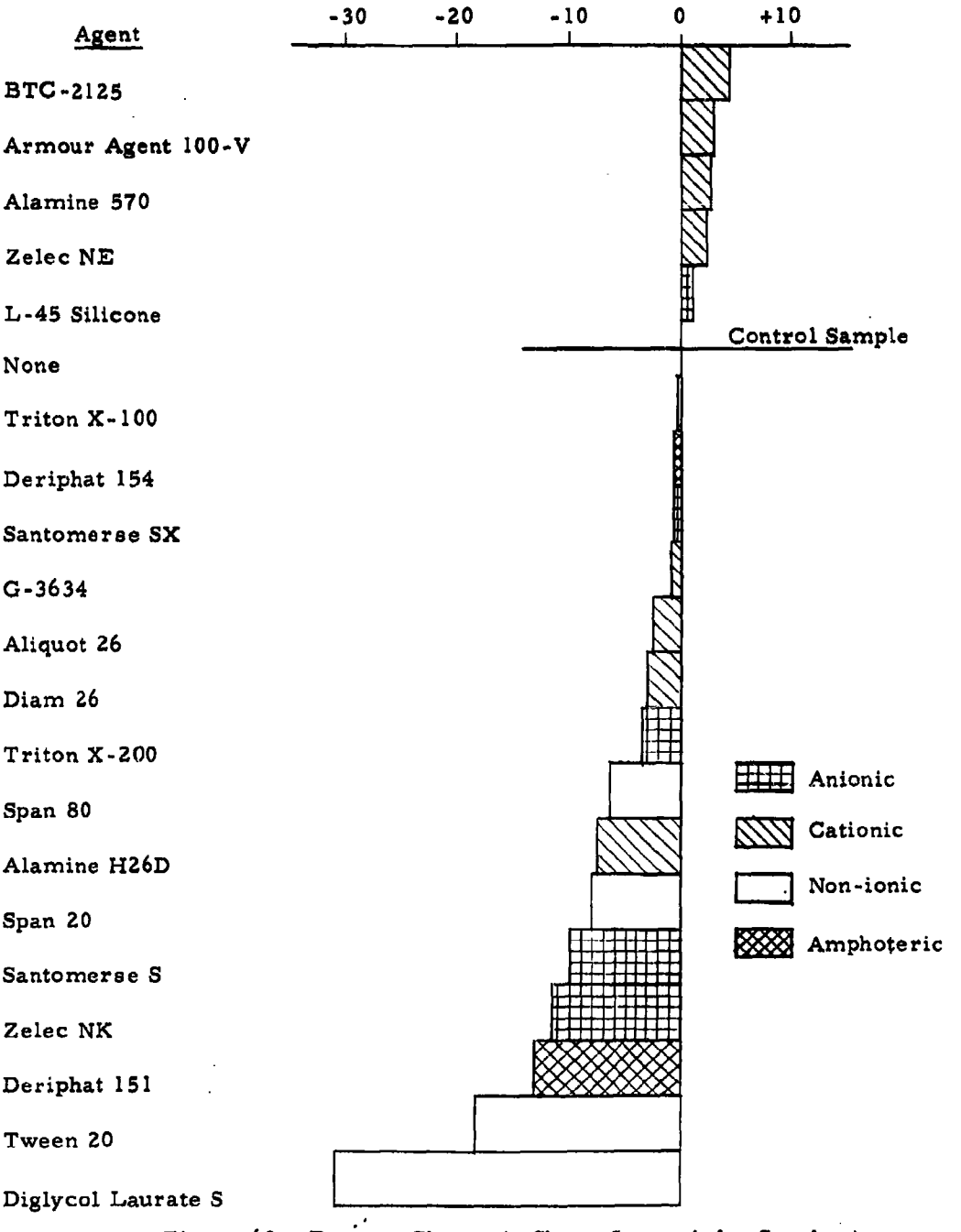

Figure 63. Percent Change in Shear Strength for Saccharin Samples Coated with Various Surfactants

Table 27. Shear Strengths of Carbowax 6000 Samples Treated with Various Surface Active Agents

Agent	Type	Shear Strength (dynes/cm^2)	Percent Change in Shear Strength
Alamine 570	cationic	6240	-13.2
G-3634	cationic	6300	-12.3
Armour Agent 100-V	cationic	6480	- 9.9
BTC-2125	cationic	6550	- 8.8
Deriphat 151	amphoteric	6640	- 7.6
Santomerse S	anionic	6720	- 6.5
Triton X-200	anionic	6740	- 6.1
Triton X-100	non-ionic	6770	- 5.7
Tween 20	non-ionic	6790	- 5.4
Deriphat 154	amphoteric	6880	- 4.2
Zelec NE	anionic	6900	- 4.0
Span 80	non-ionic	6940	- 3.4
Santomerse SX	anionic	6980	- 2.9
Diam 26	cationic	7020	- 2.3
Aliquot 26	cationic	7070	- 1.6
Diglycol Laurate S	non-ionic	7120	- 0.9
Zelec NK	anionic	7170	- 0.2
Alamine H26D	cationic	7180	0.0
Control Sample (no additive)		7180	---
Span 20	non-ionic	7510	4.5

In the case of saccharin, we see there is no apparent grouping of agents according to their classes if we discount the sample treated with Diglycol Laurate. For Carbowax 6000, we see that all samples, with the exception of the one treated with Span 20, have lower shear strengths than the control, and that the three samples having the lowest shear strengths were all treated with cationic-type agents. Beyond this, there is no apparent grouping of samples into their respective categories. In the case of Span 60, we see a definite grouping of the cationic agents on one side and amphoteric agents on the other. The cationic agents have the effect of increasing shear strength, and the amphoteric agents have the effect of decreasing shear strength.

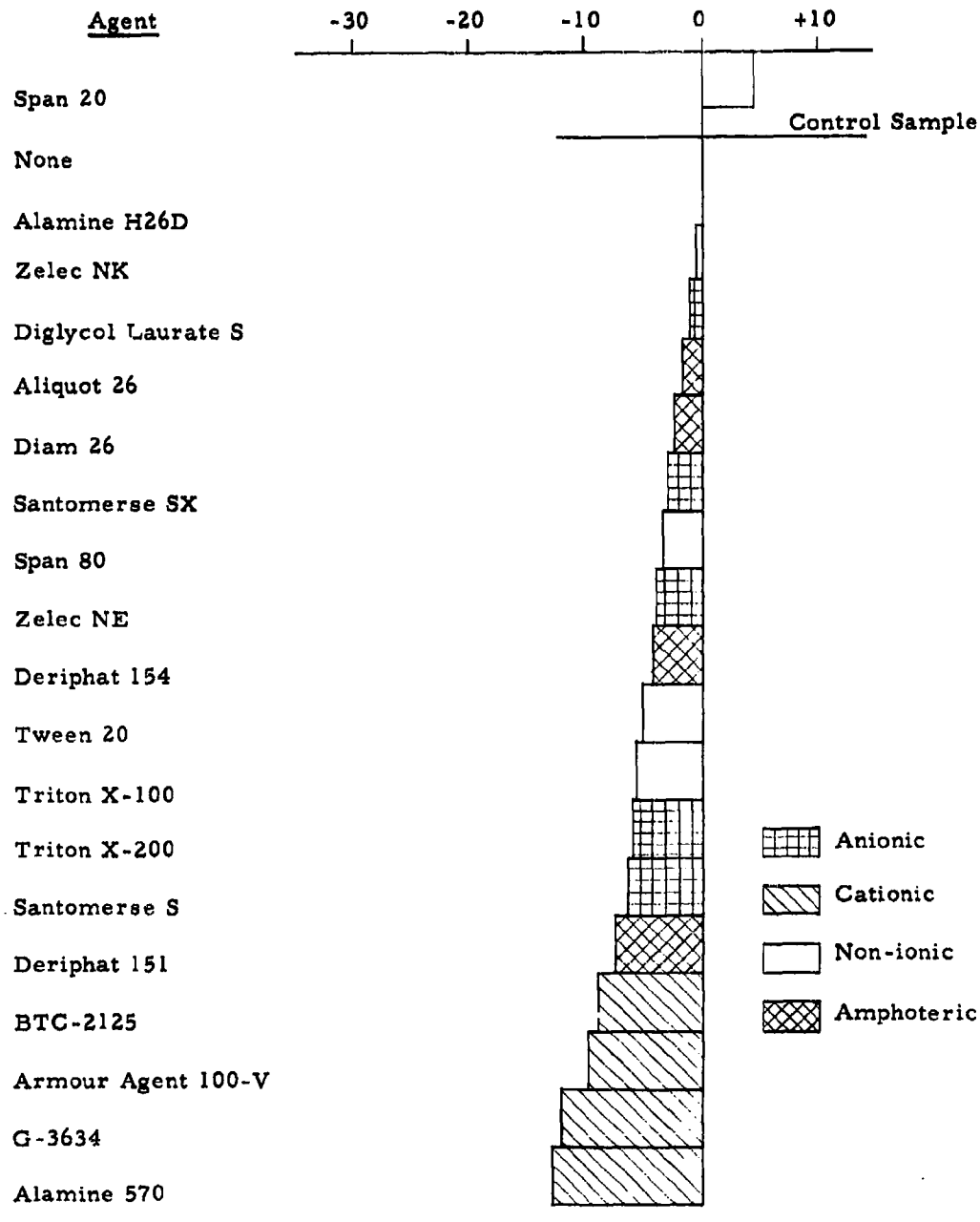

Figure 64. Percent Change in Shear Strength for Carbowax 6000 Samples Coated with Various Surfactants

Table 28. Shear Strengths of Span 60 Samples Treated with Various Surface Active Agents

Agent	Type	Shear Strength (dynes/cm^2)	Percent Change in Shear Strength
Deriphat 151	amphoteric	3580	-16.5
Zelec NK	anionic	4080	- 4.9
Deriphat 154	amphoteric	4150	- 3.3
Span 20	non-ionic	4200	- 2.1
Tween 20	non-ionic	4220	- 1.7
Triton X-100	non-ionic	4230	- 1.4
Silicone L-45		4250	- 0.9
Control Sample (no additive)		4290	---
Santomerse S	anionic	4290	0.0
Diglycol Laurate S	non-ionic	4340	1.2
Triton X-200	anionic	4380	2.1
Zelec NE	anionic	4380	2.1
Alamine 570	cationic	4410	2.8
Aliquot 26	cationic	4440	3.5
Santomerse SX	anionic	4450	3.7
G-3634	cationic	4510	5.1
Span 80	non-ionic	4550	6.1
Alamine H26D	cationic	4550	6.1
Armour Agent 100-V	cationic	4560	6.3
BTC-2125	cationic	4610	7.5
Diam 26	cationic	4660	8.6

2. Dispersibility Tests

Samples of the three base powders treated with selected surface active agents were tested for dispersibility using the test described in Section III-F. Tests were conducted at room conditions (Temperature = 72 - 80°F, RH = 35 - 50%). The amount of powder dispersed in each test was 0.1 g. The results are tabulated in Tables 29, 30, and 31 and are presented graphically in terms of percent change in λ and A_o in Figures 66, 67, 68, 69, 70, and 71.

In discussing these results, let us consider each base powder separately starting with saccharin.

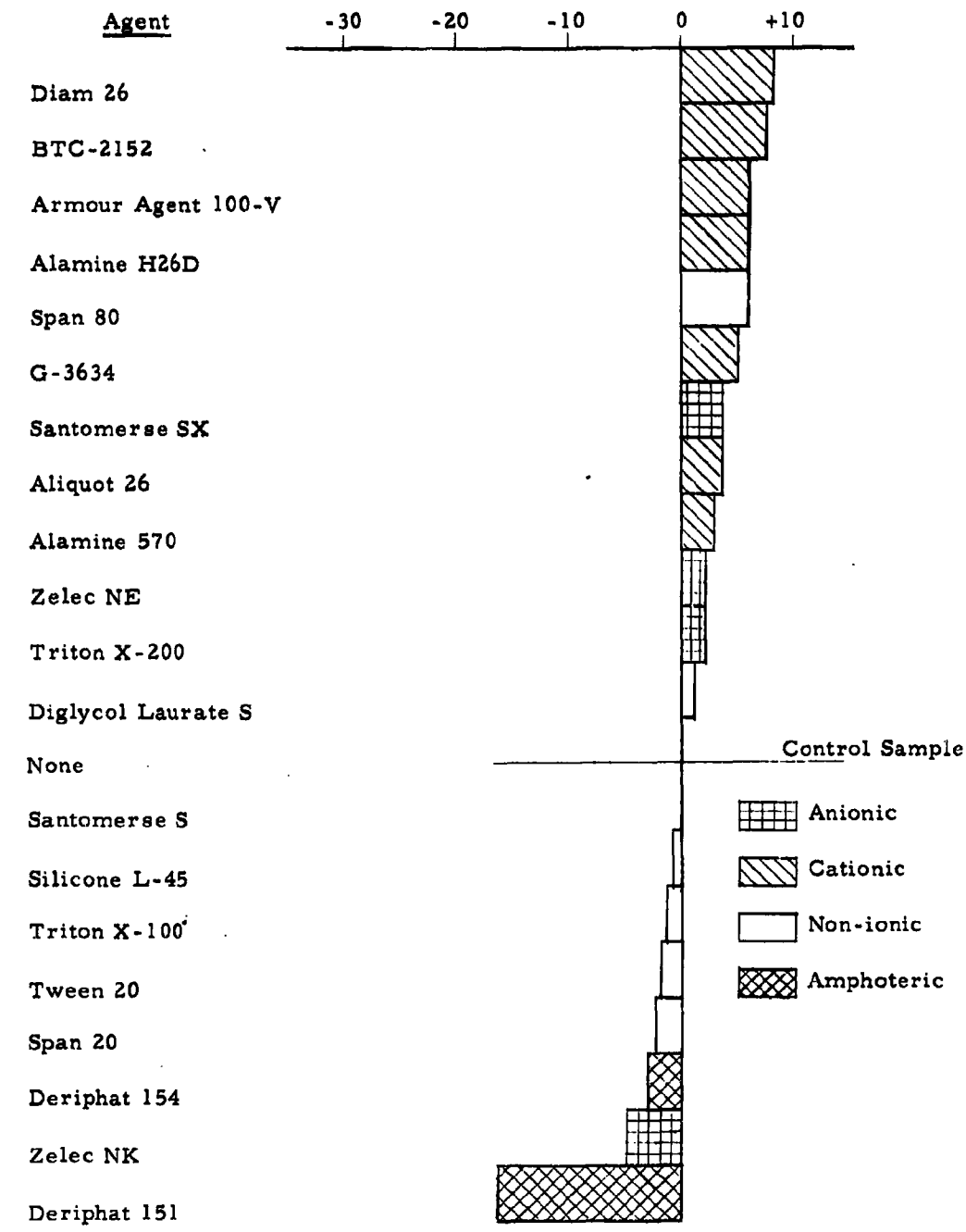

Figure 65. Percent Change in Shear Strength for Span 60 Samples Coated with Various Surfactants

a. Saccharin

From Table 29 it is obvious that all amphoteric and non-ionic agents tested, with the single exception of Span 20, have detrimental effects on the dispersibility of saccharin. The anionic agents appear to have no noticeable effect with the possible exception of Zelec NE which seems to improve the dispersibility somewhat. As a group, the cationic agents appear to be the most beneficial. The initial amplitudes of all agents in this group are higher and the decay constants lower than those of the untreated powder.

Even more revealing as to the beneficial effects of the cationic agents is the length of time which the Brown recorder remains at full scale reading. While testing the cationic agents, it was noticed that the time at which the recorder remained at full scale reading, T_{fs}, was considerably longer than for the other types of agents. The cationic group was tested last. All agents tested prior to this produced a smaller T_{fs}. This indicated the possibility that some equipment change might have taken place just before the cationic group was started. To check this possibility, another series of tests was made on the previously tested agents to determine T_{fs}, and it was found that the results of the second series agreed quite closely with those of the previous series. From this it was concluded that the effect was real and not due to an equipment change. The average values of T_{fs} are listed in Table 32. It may be seen that the lowest value of T_{fs} in the cationic group is higher than the highest value in any other group.

b. Carbowax 6000

Comparing the dispersibility characteristics of the untreated Carbowax 6000 sample with those of the treated samples (Table 30), we see that the amphoteric agents and L-45 Silicone have little or no effect, the non-ionic agents appear to have a beneficial effect (lower λ and higher A_o), and the anionic and cationic agents both have detrimental effects (higher λ and lower A_o).

Table 29. Dispersibility of Saccharin Samples Treated with Various Surface Active Agents

Agent	λ	A_o
Control Sample		
None	0.234	61.75
Non-Surface Active		
L-45 Silicone	0.206	70.00
Amphoteric		
Deriphat 151	0.254	47.25
Deriphat 154	0.239	64.30
Non-ionic		
Diglycol Laurate S	0.241	37.80
Triton X-100	0.268	69.00
Span 80	0.258	66.00
Span 20	0.227	59.40
Tween 20	0.264	49.70
Anionic		
Santomerse SX	0.230	50.50
Santomerse S	0.239	55.50
Triton X-200	0.236	53.10
Zelec NE	0.224	60.50
Zelec NK	0.233	63.10
Cationic		
Alamine 570	0.221	70.50
Diam 26	0.228	75.00
Aliquot 26	0.228	70.30
BTC-2125	0.209	64.30
Alamine H26D	0.205	72.30
G-3634	0.208	69.30
Armour Agent 100-V	0.195	63.30

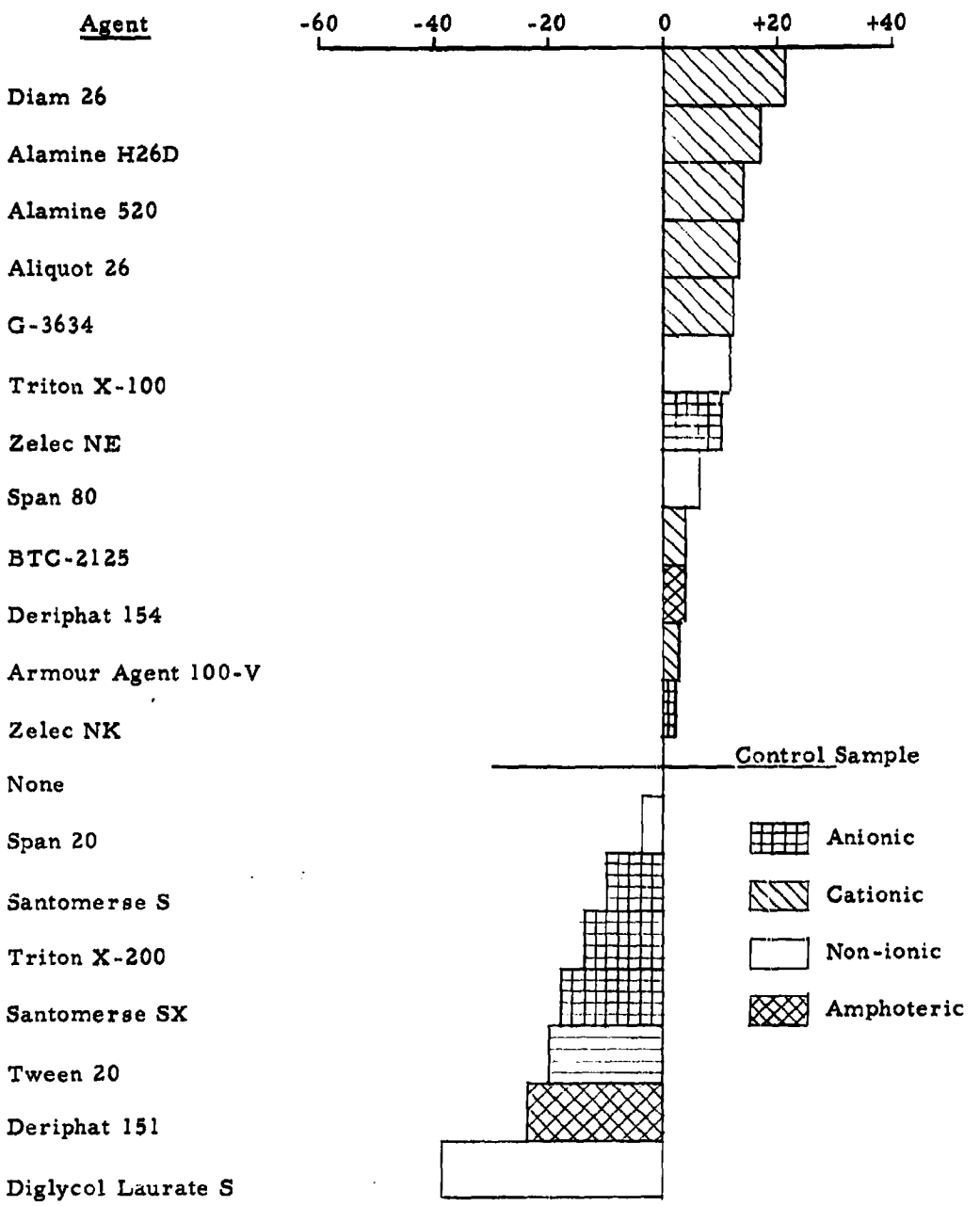

Figure 66. Percent Change in A_o for Saccharin Samples Coated with Various Surfactants

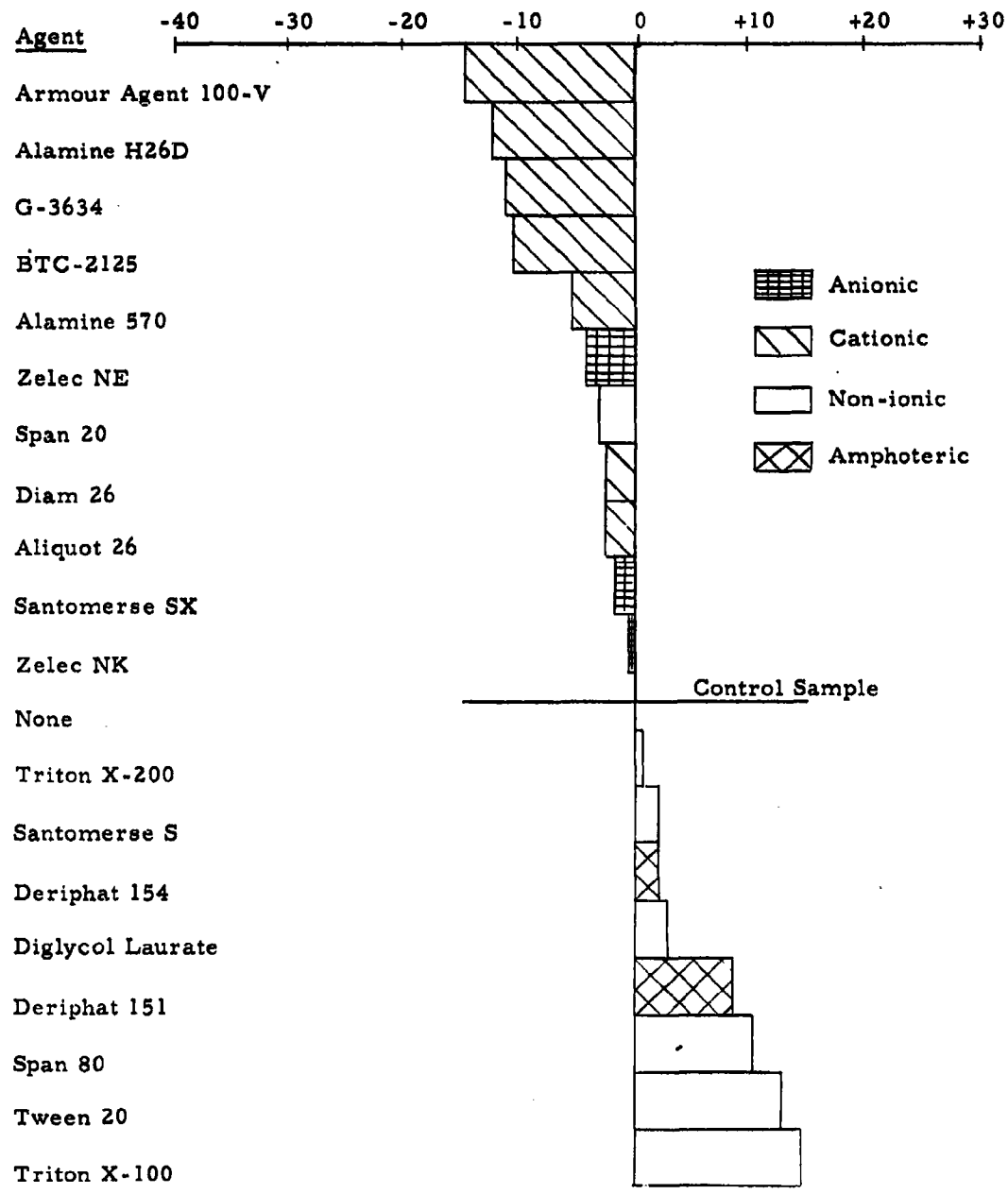

Figure 67. Percent Change in λ for Saccharin Samples Coated with Various Surfactants

Table 30. Dispersibility of Carbowax 6000 Samples Treated with Various Surface Active Agents

Agent	λ	A_o
Control Sample		
None	0.286	26.00
Non-Surface Active		
L-45 Silicone	0.248	24.50
Amphoteric		
Deriphat 154	0.285	23.60
Deriphat 151	0.294	24.60
Non-ionic		
Triton X-100	0.252	23.00
Span 80	0.262	27.50
Span 20	0.262	22.25
Tween 20	0.273	24.00
Diglycol Laurate S	0.352	21.40
Anionic		
Zelec NK	0.262	23.75
Zelec NE	0.298	21.25
Santomerse S	0.315	17.00
Triton X-200	0.351	22.00
Santomerse SX	0.360	21.00
Cationic		
Diam 26	0.280	20.75
Alamine H26D	0.288	22.00
Armour Agent 100-V	0.295	14.30
G-3634	0.296	14.25
Alamine 570	0.299	13.30
Aliquot 26	0.310	20.60
BTC-2125	0.319	16.95

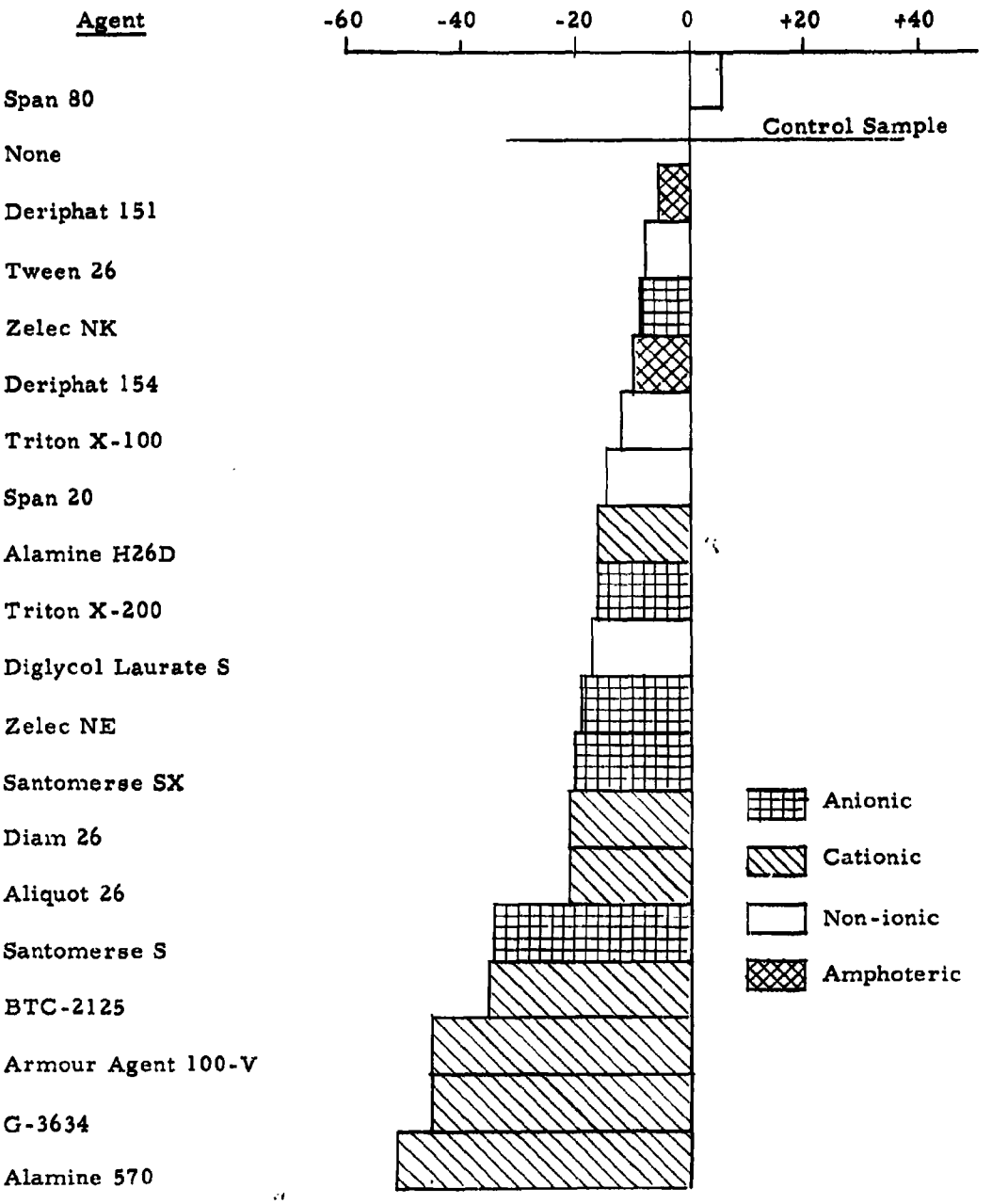

Figure 68. Percent Change in A_o for Carbowax 6000 Samples Coated with Various Surfactants

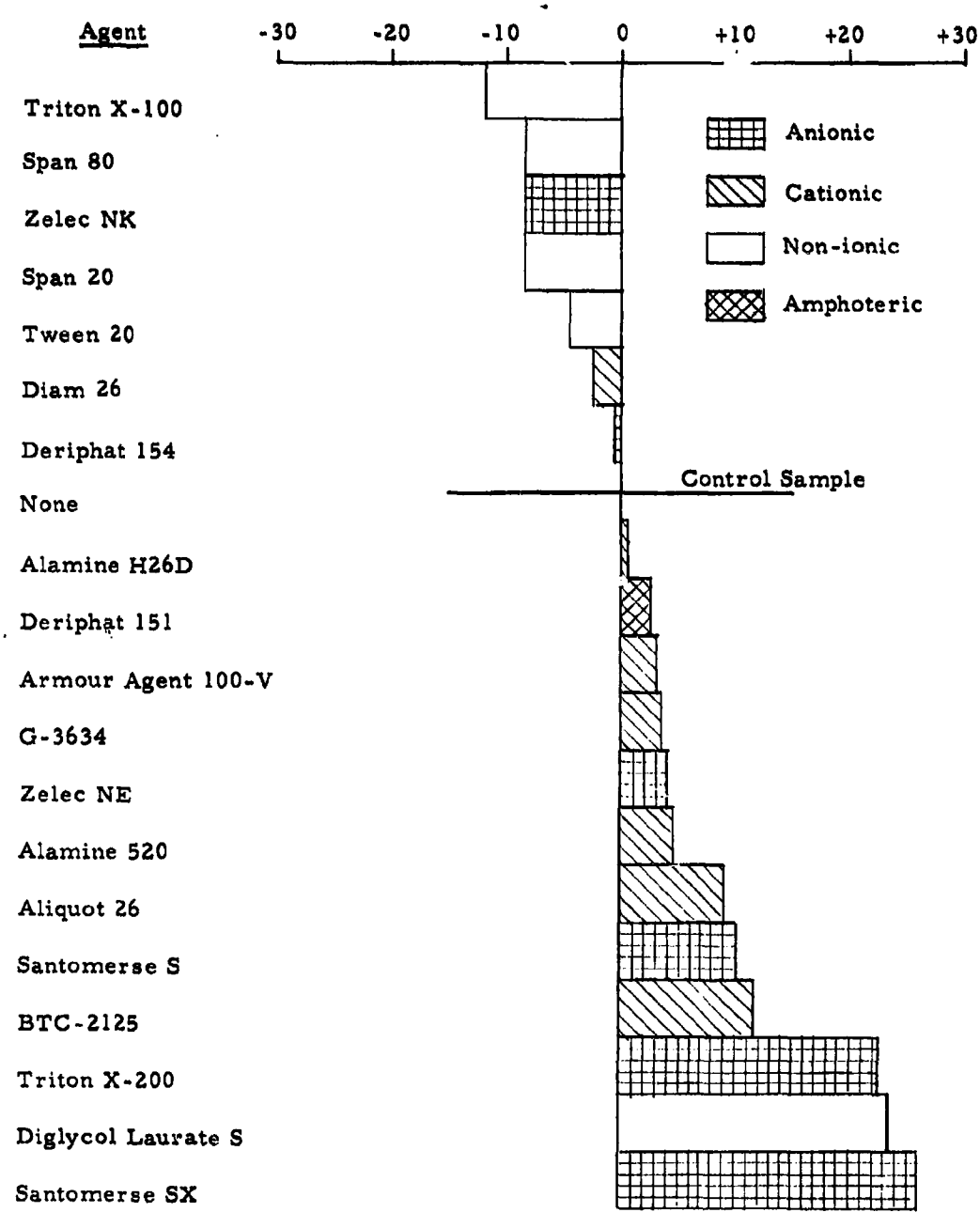

Figure 69. Percent Change in λ for Carbowax 6000 Samples Coated with Various Surfactants

Table 31. Dispersibility of Span 60 Samples Treated with Various Surface Active Agents

Agent	λ	A_o	Mass Dispersed (g)
Control Sample			
None	0.302	37.00	0.1
Non-Surface Active			
L-45 Silicone	0.308	26.40	0.1
Amphoteric			
Deriphat 154	0.293	22.40	0.1
Deriphat 151	0.307	16.65	0.1
Non-ionic			
Span 20	0.270	28.60	0.1
Triton X-100	0.293	21.00	0.1
Span 80	0.296	32.40	0.1
Tween 20	0.303	32.60	0.1
Diglycol Laurate	0.310	22.15	0.1
Anionic			
Santomerse SX	0.259	41.60	0.1
Santomerse S	0.273	36.30	0.1
Zelec NE	0.278	48.10	0.1
Zelec NK	0.293	51.80	0.1
Triton X-200	0.301	52.00	0.1
Cationic			
Armour Agent 100-V	0.272	35.15	0.1
Diam 26	0.272	44.00	0.1
G-3634	0.276	46.30	0.1
BTC-2125	0.279	41.00	0.1
Aliquot 26	0.287	37.20	0.1
Alamine	0.308	44.65	0.1
Alamine H26D	0.324	44.35	0.1

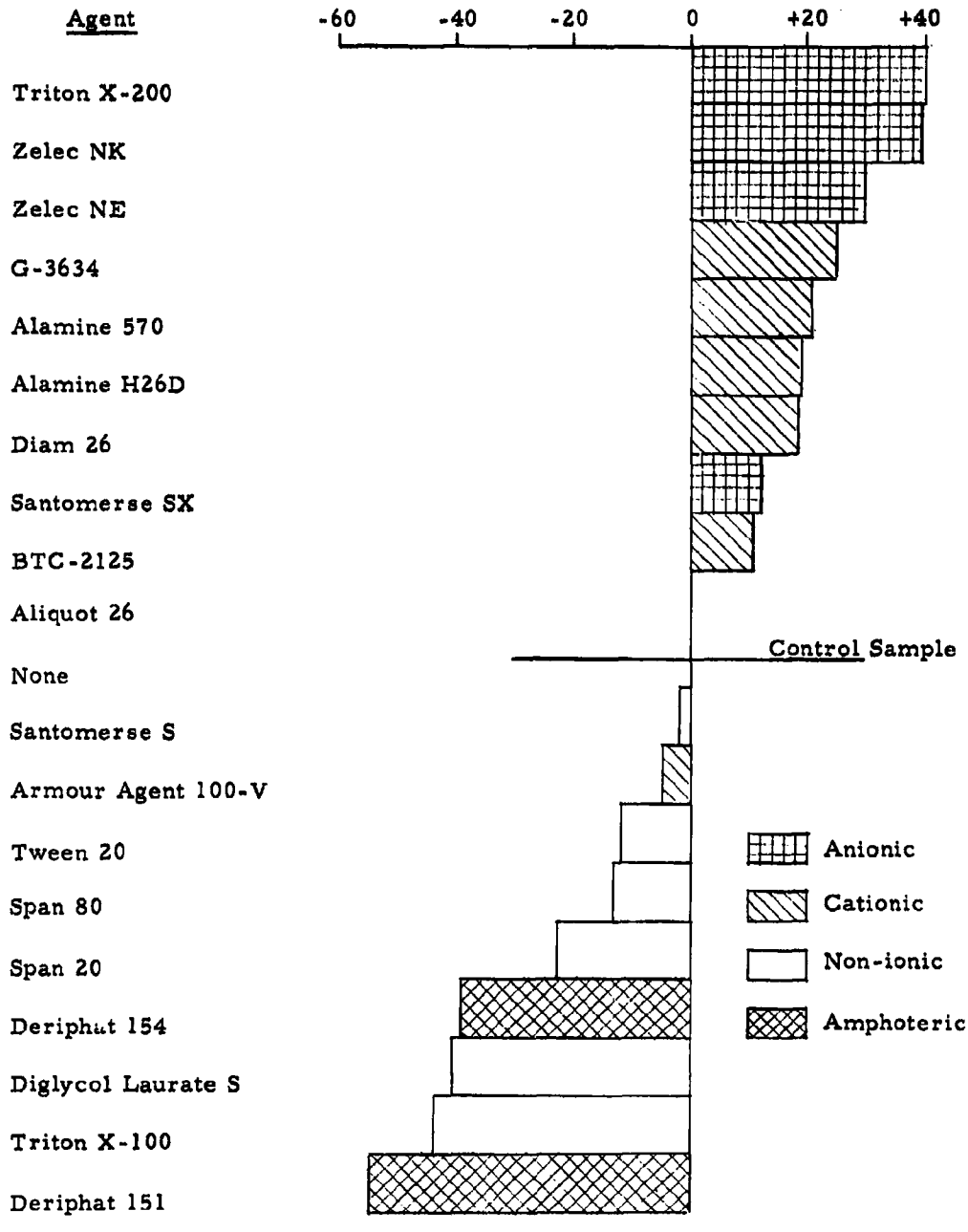

Figure 70. Percent Change in A_o for Span 60 Samples Coated with Various Surfactants

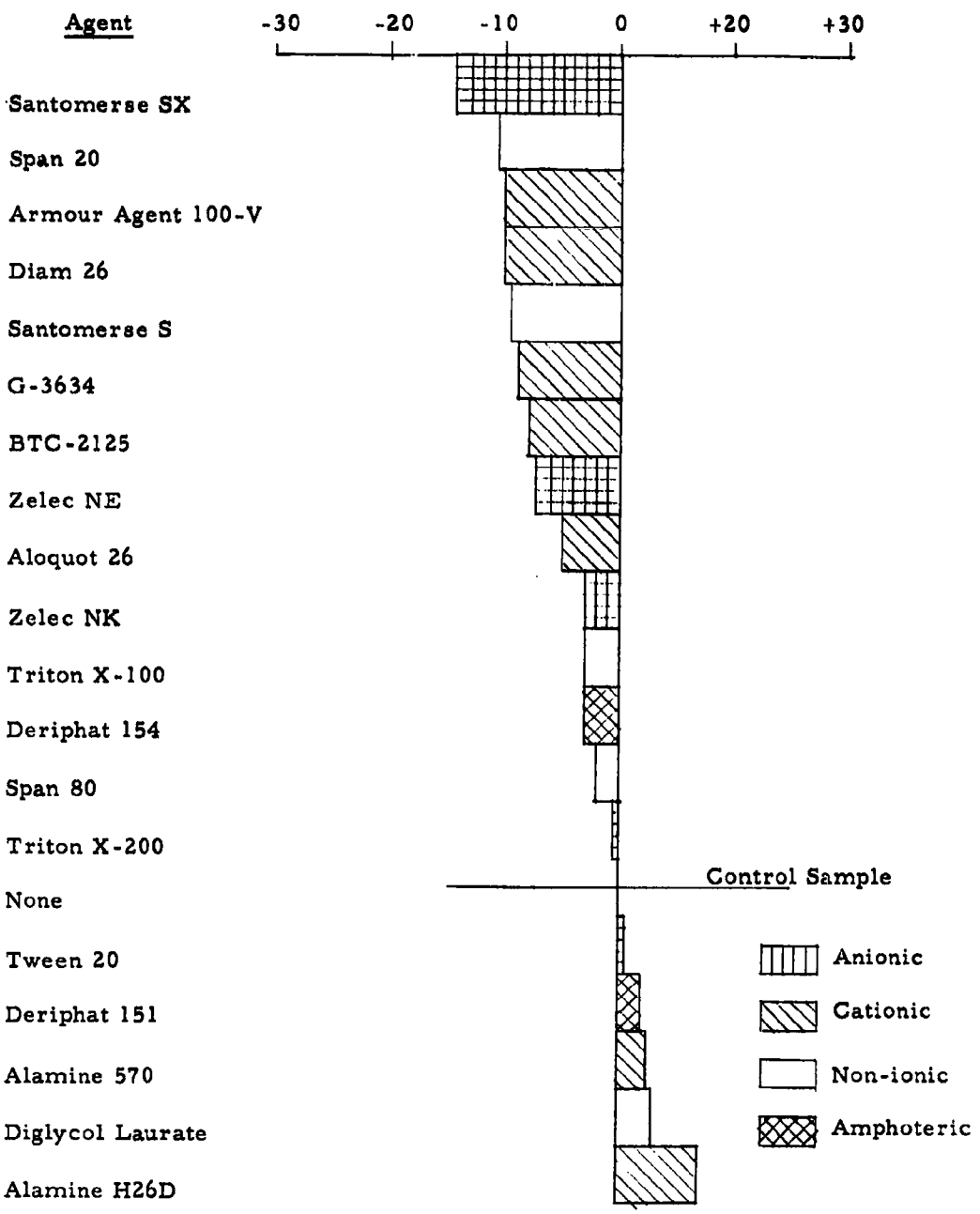

Figure 71. Percent Change in λ for Span 60 Samples Coated with Various Surfactants

c. Span 60

In the case of Span 60, we see from Table 31 that little is to be gained by coating the particles with amphoteric agents, non-ionic agents, or L-45 Silicone. The anionic and cationic agents both improve the dispersibility characteristics by decreasing ` and increasing A_o.

3. Electrostatic Charge Tests

Electrostatic charge tests (see Section III-G-2) were made on the saccharin and Carbowax 6000 samples treated with selected surface active agents. No tests were made on the treated Span 60 samples because previous tests indicated that Span 60 acquires little, if any, electrostatic charge (see Section IV-C). The results of the electrostatic charge tests are tabulated in Tables 33 and 34.

It is difficult to draw any definite conclusions regarding the electrostatic charge tests. In the case of saccharin, all the treated samples are more neutral than the untreated control sample. One agent in particular reaches the electrostatic charge of saccharin significantly. This agent is Alamine 570 which is of the cationic type. Note that the quantity (b - a) for this agent is nearly zero indicating that the net charge is nearly zero, and the $W_{\frac{1}{2}}$ dimension is low indicating that the sample does not fan out as it falls through the electric field.

In the case of Carbowax 6000, several agents of different types produce a significant reduction in electrostatic charge. They are Span 20 and Span 80 (non-ionic agents), Zelec NK (anionic agent), and Aliquot 26 (cationic agent).

Table 32. T_{fs} Values for Saccharin Samples Treated with Various Surface Active Agents

Agent	Type	T_{fs} (sec)
Deriphat 151	amphoteric	5.1
Deriphat 154	amphoteric	12.7
Diglycol Laurate S	non-ionic	0
Triton X-100	non-ionic	14.8
Span 80	non-ionic	12.5
Span 20	non-ionic	13.9
Tween 20	non-ionic	6.7
Santomerse SX	anionic	10.0
Santomerse S	anionic	12.0
Triton X-200	anionic	8.5
Zelec NE	anionic	17.5
Zelec NK	anionic	13.5
Alamine 570	cationic	22.0
Diam 26	cationic	23.0
Aliquot 26	cationic	19.5
BTC-2125	cationic	20.0
Alamine H26D	cationic	28.0
G-3634	cationic	24.5
Armour Agent 100-V	cationic	21.5
L-45 Silicone		25.0
Unadulterated Saccharin		12.0

4. Explanation of Effects of Surface Agents on Powder Properties from the Chemical Viewpoint

A study has been made to determine to what extent the changes in powder properties resulting from coating the base powders, saccharin, Carbowax 6000, and Span 60 with surface active agents can be explained on the basis of the chemical characteristics of these materials. The effects of these surface coatings upon shear strength, dispersibility (λ and A_o), and electrostatic charge were considered.

Table 33. Electrostatic Characteristics of Saccharin Samples Treated with Surface Active Agents

Agent	A/B	a (cm)	b (cm)	b - a (cm)	$W_{\frac{1}{2}}$
Control Sample					
None	1.45	3.76	2.59	-1.17	3.73
Amphoteric					
Deriphat 151	0.99	3.16	3.19	+0.03	2.95
Deriphat 154	1.24	3.52	2.83	-0.69	3.58
Non-ionic					
Triton X-100	1.05	3.25	3.10	-0.15	3.81
Span 20	1.28	3.57	2.78	-0.79	3.66
Span 80	1.12	3.35	3.00	-0.35	3.91
Tween 20	0.99	3.16	3.19	+0.03	3.43
Diglycol Laurate S	0.93	3.06	3.29	+0.23	2.33
Anionic					
Santomerse SX	0.96	3.11	3.24	+0.13	2.77
Santomerse S	0.98	3.14	3.21	+0.07	4.27
Triton X-200	1.16	3.41	2.94	-0.47	3.68
Zelec NE	1.30	3.59	2.76	-0.83	4.80
Zelec NK	1.06	3.27	3.08	-0.19	3.51
Cationic					
Alamine 570	0.97	3.13	3.22	+0.09	1.97
Diam 26	1.04	3.24	3.11	-0.13	3.78
Aliquot 26	1.18	3.44	2.91	-0.53	4.83
Alamine H26D	1.14	3.38	2.97	-0.41	3.45
BTC-2125	1.22	3.49	2.86	-0.63	3.18
G-3634	1.31	3.60	2.75	-0.85	5.20
Armour Agent 100-V	1.02	3.21	3.14	-0.07	4.93

Table 34. Electrostatic Charge Characteristics of Carbowax 6000 Samples Treated with Surface Active Agents

Agent	A/B	a (cm)	b (cm)	b - a (cm)	$W_{\frac{1}{2}}$
Control Sample					
None	0.96	3.11	3.24	+0.13	3.11
Amphoteric					
Deriphat 151	0.95	3.10	3.25	+0.15	3.65
Deriphat 154	0.97	3.13	3.22	+0.09	3.10
Non-ionic					
Triton X-100	0.88	2.97	3.38	+0.41	4.77
Span 20	0.99	3.16	3.19	+0.03	2.88
Span 80	0.98	3.15	3.20	+0.05	2.93
Tween 20	0.88	2.97	3.38	+0.41	4.19
Diglycol Laurate S	0.97	3.13	3.22	+0.09	3.80
Anionic					
Santomerse SX	1.16	3.41	2.94	-0.47	2.99
Santomerse S	1.11	3.34	3.01	-0.33	2.45
Triton X-200	1.02	3.21	3.14	-0.07	3.95
Zelec NE	1.06	3.27	3.08	-0.19	3.42
Zelec NK	1.01	3.19	3.16	-0.03	2.85
Cationic					
Alamine 570	1.11	3.34	3.01	-0.33	3.45
Diam 26	1.11	3.34	3.01	-0.33	2.69
Aliquot 26	0.97	3.13	3.22	+0.09	2.97
Alamine H26D	0.94	3.08	3.27	+0.19	2.51
BTC-2125	1.05	3.25	3.10	-0.15	6.66
G-3634	0.95	3.10	3.25	+0.15	5.58
Armour Agent 100-V	1.14	3.38	2.97	-0.41	5.91

The shear strength and dispersibility data are presented for comparative purposes in Figure 72. Although upon thorough examination of these data, sweeping generalizations relating changes in powder properties to the chemical characteristics of the materials under study cannot be made, the following presentation includes a discussion of the useful information gained from such a study.

The base powders used in this study were selected primarily for their physical properties (cyrstalline, waxy, and gummy). Since the powders used are chemically rather unreactive, great changes in powder properties resulting from chemical interaction are not to be expected. Saccharin (benzosulfimide) is characterized by its acidic hydrogen; Carbowax 6000 (polyethylene glycol) is a high molecular weight molecule made up predominantly of multiple ether linkages ($-O-CH_2-CH_2-O$) with a glycolic hydroxyl group at each end of a long chain; and Span 60 (sorbitan monostearate) is an ester of a long chain fatty acid and a polyhydric alcohol.

The surface active agents used in this study have been placed in the following classifications consistent with the ionic character of the molecule: cationic, anionic, non-ionic, and amphoteric. The cationic surfactants studied are mainly amines, whereas the anionic surfactants are organic phosphates and sulfonates. Organic esters and alcohols make up the non-ionic classification and the two amphoteric surfactants are sodium salts of complex organic acids.

Experimentally, the base powders were coated with liquid surfactant by simultaneously feeding the two materials through a fluid energy mill. Assuming the powder particles are uniformly coated, the amounts used correspond to a monolayer or less of surfactant. When the powder and surfactant were placed in intimate contact in the fluid energy mill, the interaction may have been a chemical or physical adsorption or merely a mechanical coating process resulting from interparticle bombardment. To experimentally determine what actually has occurred would require extensive adsorption studies together with chemical and/or instrumental analysis to

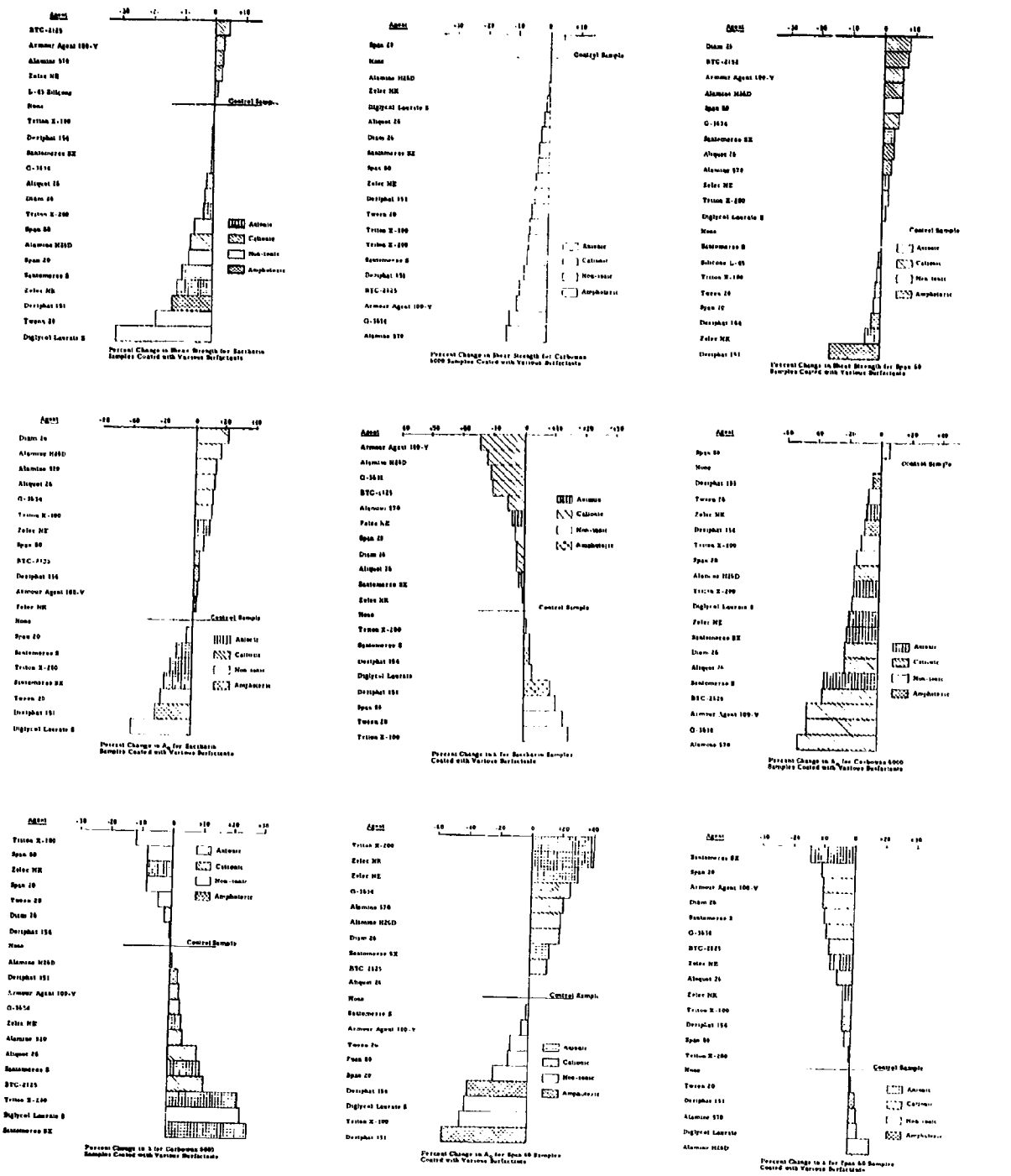

Figure 72

Montage of Shear Strength and Dispersibility Test Results

prove the existence or absence of a new chemical species resulting from reactions between surfactant and base powder. Such an experimental effort is beyond the scope of the current project.

Ultimately, the behavior of bulk powders whether in the compacted or loose state is determined by the nature of the physiochemical forces between particles in contact. The magnitude of these forces is determined in part by the nature of the reactive sights on the primary particle as well as the geometry of the primary particle itself and the particle size distribution. Thus the rate of the surface coating would be to change the nature of these reactive sights. The geometry of the primary particle would not be substantially changed by a monomolecular coating, but if serious agglomeration occurred as a result of the coating process the powder would then have essentially a different particle size distribution which would be reflected in changes of powder properties. Another function of the surfactant would be to change the electrostatic behavior of the particle resulting from changes in surface conductivity of the particle. Finally, the surface coating could act as a mechanical lubricant between particles.

The factors affecting shear strength, dispersibility, and electrostatic charge of powders are complex. In order to predict the chemical effects of the surface active agents, we must examine the powder properties individually.

Changes in shear strength would result from changes in primary interparticle forces as well as from changes in effective particle size distribution due to agglomeration caused by the coating process.

The dispersibility of the powder is not only affected by interparticle bonding and size distributions but may be affected by high electrostatic charge generation as the individual particles are separated as they leave the dispersing gun. The level of electrostatic charge generated during dispersion would not necessarily be comparable in sign and magnitude to that displayed in the electrostatic charge test, since this test measures chiefly the electrostatic charge on the powder, whereas during the dispersing process, the electrostatic charge generated would be in part a function of the design of the dispersing device as well as the energy level of dispersion.

If the base powders are considered only as nuclei for the coating process, then the characteristics of the surfactant should predominate to such an extent that the change caused by the surfactant should be independent of the base powder. That is, the change in powder property should be the same for all three powders studied. Upon examination of the data, such a pattern does not emerge. From a chemical standpoint, the greatest chance for chemical interaction would appear to be between the cationic agents (which were amines in this case) and saccharin with its active hydrogen. It is quite possible that this has in fact occurred because it does seem to be reflected by changes in powder properties. As seen from the data, the cationic agents behave more predictably as a group, but frustratingly they do not maintain the same order within the group.

In summary, desirable change in powder properties such as lowering of shear strength and producing a more stable aerosol by lowering λ can be accomplished by coating the base powders with surfactants; but at this point in our study, the data indicate that predictions of these changes according to broad chemical classifications should be supplemented by experiments involving the specific base powder and surfactant.

Future work including studies to determine the effect of changing the amount of surfactant used, studies to determine what chemical interaction takes place, and to determine what changes in particle size distribution, agglomeration, and particle shape took place should help make the picture clearer.

F. Investigation of Effects of Adsorbed Foreign Vapors on Powder Properties

An investigation was conducted to determine the effects of a number of different adsorbed foreign vapors on powder properties. The powders which we investigated are saccharin, Carbowax 6000, and Span 60; the vapors whose effects we investigated are n-butylamine, phenol, acetone, and propionaldehyde. The technique for treating a powder sample with a given vapor is described in Section II-D.

1. n-butylamine Vapors

The first vapor to be investigated was n-butylamine. This vapor was chosen because other workers[17] have found that a monolayer of n-butylamine molecules adsorbed onto two sputter-cleaned titanium surfaces reduces the coefficient of friction between the surfaces by 37 percent.

Samples of the three base powders were treated with n-butylamine vapors in the manner described. In the case of saccharin and Span 60, the n-butylamine vapors reacted with the powders rendering them unusable for further tests. The saccharin sample dissolved into a syrupy liquid, and the Span 60 sample foamed up. There was no apparent chemical reaction in the case of Carbowax 6000; therefore, tests were conducted on this sample to determine the effects of the adsorbed vapor.

Attempts to measure shear strength of the sample inside a glove box were unsuccessful because the n-butylamine vapors softened the glue which held the strain gages onto the cantilever beam, thereby disabling the force-measuring device.

Dispersibility tests (see Section III-F) were made on the treated samples. In order to minimize the possibility of water vapor from the room air readsorbing on the sample prior to its dispersal, the gelatine capsule technique described earlier was used to transfer samples from the glove box to the dispersing gun. Since the samples were not weighed out, care was taken to fill all capsules as nearly the same as possible.

Results of these tests, along with those for untreated samples of Carbowax 6000 which had been preconditioned at less than 1 percent relative humidity, are given in Table 35. It is seen that λ and A_o are essentially the same (within experimental error) for both samples.

An electrostatic charge analysis using the method described in Section III-G-1 was made on the Carbowax 6000 sample treated with n-butylamine vapor. These results along with those for a Carbowax 6000 sample which

Table 35. Effect of Adsorbed n-butylamine Vapors on Dispersibility of Carbowax 6000

Sample	λ	A_o
Untreated sample	0.264	38.0
Treated sample	0.261	33.8

had been preconditioned at less than 1 percent relative humidity (see Section IV-B) are given in Table 36. It is seen that the samples treated with n-butylamine vapor have a larger number of positively charged particles and a smaller number of negatively charged particles than the untreated samples.

Table 36. Effect of Adsorbed n-butylamine Vapors on Electrostatic Charge of Carbowax 6000

Carbowax 6000 Preconditioned at < 1% RH	
Positively Charged Particles, Percent of Total	44.9
Negatively Charged Particles, Percent of Total	52.2
Noncharged Particles, Percent of Total	2.9
Carbowax 6000 Exposed to n-butylamine Vapors	
Positively Charged Particles, Percent of Total	59.0
Negatively Charged Particles, Percent of Total	40.7
Noncharged Particles, Percent of Total	0.3

The most noticeable effect caused by the n-butylamine vapor is the manner in which it affected the aggregation of the Carbowax 6000 particles as they entered the electric field in the charge analyzer. In the case of the untreated sample, the particles tended to form linear aggregates. This tendency was especially pronounced at the higher voltages. In the case of

the sample treated with n-butylamine vapor, there was no evidence of chain-like aggregates, even at voltages three times higher than that used in previous tests.

In order to explain this phenomenon, let us consider the mechanism by which a linear aggregate can form in an electric field. First of all, the particles making up the aggregate must exhibit a dipole moment in an electric field. In substances where this is possible, there are three main factors which contribute to the total dipole moment. These are as follows:

1) Orientation polarization due to rotation of polar molecules such that, statistically, there is a net dipole moment.

2) Electronic polarization due to deformation of electronic distributions about the nucleus.

3) Atomic polarization due to displacement of ions or groups of ions within the molecules.

In general, polar molecules have limited mobility in solids, and the effect of orientation polarization (Item 1 above) is reduced, if present at all. However, high polymers containing polar groups often do display orientation polarization due to changes in orientation of molecular segments in the presence of an electric field without change in orientation of the whole molecule. It is possible, therefore, for such a phenomenon to occur in the case of Carbowax 6000.

Having concluded that Carbowax 6000 particles can become dipoles in an electric field, let us consider the mechanism by which the dipoles make up linear aggregates. A dipole in an electric field orients itself so that its lengthwise axis is parallel to the direction of the field. When two such dipoles come into near proximity of each other, they tend to coagulate, forming a "twin" with the lengthwise axis still parallel to the direction of the field. In this position, its dipole moment is considerably greater than that of a primary particle. As coagulation progresses, other primary dipoles attach themselves to the twin's ends, and soon a linear aggregate is formed. This phenomenon has been observed in the case of certain smokes.[18]

Most likely, the linear aggregates stand up on end with one end resting against the glass microscope slide in the charge analyzer. When the electric field is turned off, the linear aggregates fall over but still maintain their linear configuration because the particles adhere to one another by van der Waals forces.

Now let us consider the case of Carbowax 6000 treated with n-butylamine vapor. Carbowax 6000 is a high molecular weight polyethylene glycol having the following generalized formula:

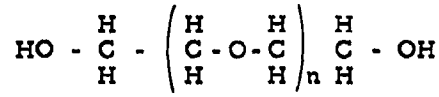

where n represents the average number of oxyethylene groups. n-butylamine is a highly polar compound having the following structural formula:

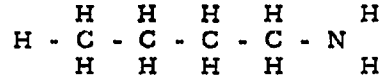

An n-butylamine molecule may be illustrated schematically in the following manner:

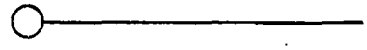

Amine Group (polar) Methyl Group

When n-butylamine vapor comes into contact with a Carbowax 6000 particle, the polar groups (NH_2) of the n-butylamine molecules are strongly attracted to the surface of the Carbowax 6000 particle, the result being the formation of a monolayer of vertically oriented n-butylamine molecules as illustrated on the following page.

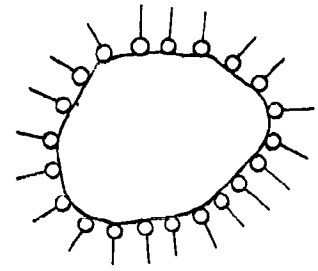

It is conceivable that Carbowax 6000 particles coated with a monolayer of n-butylamine molecules may exhibit a dipole moment in an electric field, and if this is the case, it is possible also for linear aggregates to form. But because of the low energy surface consisting of methyl groups, the particles do not adhere to one another after the electric field is turned off. Thus the linear aggregates would collapse and loose their linear configuration leaving no evidence of ever having been formed.

2. Phenol, Acetone, and Propionaldehyde Vapors

Samples of the three base powders (saccharin, Span 60, and Carbowax 6000) were treated with phenol, acetone, and propionaldehyde vapors. In some cases, the vapors reacted chemically with the powder samples rendering them useless for further tests. This occurred in the following cases:

acetone - saccharin
acetone - Span 60
propionaldehyde - saccharin

In these cases, the powder samples agglomerated into hard balls and were subsequently discarded.

The remaining treated samples (those not noticeably affected by the vapors) and untreated control samples were tested for shear strength, dispersibility, and electrostatic charge. These tests are described in

Sections III-B, III-F, and III-G-2, respectively. Each vapor was investigated separately, i.e., the entire series of tests on one vapor was completed before tests on the next vapor were begun.

The shear strength tests were conducted in a glove box maintained at a relative humidity of less than 1 percent at room temperature. The reason for keeping the relative humidity low was to prevent readsorption of water vapor onto the powder. Tests were made in triplicate and the results averaged. These data are given in Table 37.

Table 37. Effect of Adsorbed Foreign Powders on Powder Shear Strength

Powder	Shear Strength (dynes/cm^2)	Percent Change in Shear Strength
Phenol		
Saccharin control	4860	---
Saccharin + phenol	3630	-25.3
Carbowax 6000 control	6100	---
Carbowax 6000 + phenol	6370	+ 4.5
Span 60 control	3630	---
Span 60 + phenol	3990	+ 9.9
Acetone		
Carbowax 6000 control	7080	---
Carbowax 6000 + acetone	6080	-14.0
Propionaldehyde		
Carbowax 6000 control	7150	---
Carbowax 6000 + propionaldehyde	6680	- 6.5
Span 60 control	3570	---
Span 60 + propionaldehyde	4220	+18.2

Dispersibility tests were made on samples of the treated powders. To minimize the possibility of water vapor readsorbing onto the samples prior to dispersal, the gelatin capsule technique was used to transfer samples from the glove box to the powder dispersing gun. The conditions of temperature and humidity inside the aerosol chamber were essentially room conditions (temperature = 72 to 80°F, RH = 35 to 50%). The test results along with those for untreated control samples are given in Table 38.

Table 38. Effect of Adsorbed Foreign Vapors on Powder Dispersibility

Powder	Aerosol Decay Constant, λ	Initial Amplitude, A_o
Phenol		
Saccharin control	0.234	83.00
Saccharin + phenol	0.240	60.00
Carbowax 6000 control	0.292	36.00
Carbowax 6000 + phenol	0.278	39.00
Span 60 control	0.273	21.50
Span 60 + phenol	0.273	20.50
Acetone		
Carbowax 6000 control	0.296	65.50
Carbowax 6000 + acetone	0.299	65.50
Propionaldehyde		
Carbowax 6000 control	0.293	32.50
Carbowax 6000 + propionaldehyde	0.270	31.20
Span 60 control	0.344	48.40
Span 60 + propionaldehyde	0.325	54.80

It may be seen that the values for λ and A_o corresponding to the control samples vary somewhat from one series of tests to the next. The reason for this is that the amount of powder dispersed varied somewhat from one series to the next. Within a given series, however, the amount of powder dispersed did not vary by more than a few milligrams.

Electrostatic charge tests were made on the vapor-treated samples and on control samples. The technique used here is the one for measuring electrostatic charge on bulk powders (Section III-G-2). The tests were conducted in a glove box maintained at a relative humidity of about 1 percent at room temperature. The results are given in Table 39.

Table 39. Effect of Adsorbed Foreign Vapors on Electrostatic Charge of Powders

Powder	A/B	a (cm)	b (cm)	b - a (cm)	$W_{\frac{1}{2}}$
Phenol					
Saccharin control	2.02	4.25	2.10	-3.23	4.54
Saccharin + phenol	1.13	3.37	2.98	-0.39	4.38
Carbowax 6000 control	0.71	2.64	3.71	+1.07	4.05
Carbowax 6000 + phenol	0.79	2.81	3.54	+0.73	4.24
Span 60 control	1.03	3.23	3.12	-0.11	1.80
Span 60 + phenol	1.06	3.27	3.08	-0.19	2.03
Acetone					
Carbowax 6000 control	0.94	3.08	3.27	+0.19	1.90
Carbowax 6000 + acetone	1.03	3.23	3.12	-0.11	2.82
Propionaldehyde					
Carbowax 6000 control	0.94	3.08	3.27	+0.19	1.90
Carbowax 6000 + propionaldehyde	0.95	3.10	3.25	+0.15	2.42
Span 60 control	1.05	3.25	3.10	-0.15	1.63
Span 60 + propionaldehyde	0.98	3.15	3.20	-0.05	1.89

G. Effects of Removal of Adsorbed Gases and Vapors

An investigation was made to determine effects of removal of adsorbed gases and vapors from powders. Unfortunately, this work was performed during the early part of the program before the more successful tests for studying powder properties had been developed.

The test used in this study was the disc-lifting test.[19,20] This test consists of imbedding a disc of known dimensions and weight in a bed of powder of known depth and measuring the force required to lift the disc out of the powder. The main problem with this test is the difficulty in interpreting its data. A few general statements can be made, however, regarding the resistance offered by the powder to the disc-lifting force. The greatest portion of this resistance is due to the weight of the powder resting on the disc and, therefore, is a function of powder bulk density. Some small portion of this resistance is due to adhesive forces between particles, but this portion cannot be determined precisely. For this reason, little work was done with the test, and it was later abandoned.

The effect of removal of adsorbed gases and vapors was investigated by performing disc-lifting tests on samples of the three base powders under normal laboratory conditions (temperature = 72 to 74°F, RH = 15 to 20%) and under high vacuum conditions (temperature = 72 to 74°F, pressure 2×10^{-5} mm Hg) and comparing results.

In order to conduct tests under high vacuum conditions, it was necessary to place the entire disc-lifting apparatus including a torsion balance, powder container, and disc inside a large high-vacuum system.* A flexible shaft was coupled between the reduction gear on the balance and a high-vacuum seal on the pump stand to permit operation of the balance from outside the chamber.

*National Research Corporation evaporating stand and 180-liter metal bell jar.

Powders to be tested under high vacuum conditions were preconditioned in a vacuum oven for a period of at least 24 hours to remove most of the adsorbed gases and vapors. The oven was set at 50°C for saccharin, but no heat (in excess of room heat) was used for the other two powders because of their low melting points.

Disc-lifting tests were performed using a 2.50-cm-diameter disc at depths of 2 and 4 cm. The results are given in Table 40.

Table 40. Results of Disc-Lifting Tests Performed Under Laboratory and High Vacuum Conditions

		Disc-Lifting Force (g)	
	Bed Depth (cm)	Vacuum Conditions	Laboratory Conditions
Saccharin	2	6.27 ± 0.23	7.47 ± 0.23
	4	18.10 ± 0.65	21.20 ± 1.20
Carbowax 6000	2	8.12 ± 0.19	9.87 ± 0.27
	4	26.20 ± 0.50	33.10 ± 2.30
Span 60	2	10.58 ± 0.56	6.40 ± 0.17
	4	33.58 ± 1.82	19.17 ± 0.50

We see that for Span 60 , the force required to lift the disc from the bed of powder is greater for high vacuum conditions than for laboratory conditions, while the opposite is true for saccharin and Carbowax 6000.

Before we can explain these phenomena, we must mention some additional measurements that were made along with the disc-lifting measurements. Samples of each powder were placed in glass weighing jars and placed under a bell jar which was subsequently evacuated to a pressure of 2×10^{-5} mm Hg. Every day for a period of one week, the samples were removed and weighed. No day-to-day weight change was observed with

saccharin or Carbowax 6000, but the Span 60 sample lost weight at the rate of approximately 0.4 percent per day. It is quite certain that this weight loss was due to sublimination because the rate was fairly constant throughout the entire week.

With this added information, we can explain why the force required to lift the disc from the Span 60 sample was greater for high vacuum conditions than for laboratory conditions. Since the material was subliming, its surface was very clean and free from contamination. It is well known that bonding forces between clean surfaces are considerably higher than those between surfaces exposed to air. Proceeding on the assumption that the force required to remove the disc from a bed of powder is a measure of adhesive forces between particles, one would expect this force to be higher for a powder that is subliming under high vacuum conditions than for the same powder exposed to air.

Now in the case of saccharin and Carbowax 6000, the disc-lifting force was lower for high vacuum conditions than for laboratory conditions. Since these two powders did not sublime under high vacuum conditions, they probably did not reach the condition where all of the surface contaminants were removed. Therefore, bonding between particles did not occur in the same sense that it did with Span 60. Most of the adsorbed water was probably removed, however. Under laboratory conditions, the layer of adsorbed water surrounding each particle may serve to hold the particles together by means of capillary action. When this layer is removed, or partially removed, the forces between particles decrease.

This explains why the force required to remove the disc from the Span 60 sample was greater for high vacuum conditions than for laboratory conditions, while the opposite was true for the saccharin and Carbowax 6000 samples.

H. Energy Required to Disperse a Powder Sample

1. Theoretical Study

A theoretical study was made to determine the relationship between the bursting pressure in the powder dispersing gun and the actual energy that goes into dispersing the powder sample.

The powder to be dispersed occupies only a small part of the chamber in the dispersing gun (see Figure 10). Compressed gas (dry, water-pumped nitrogen was used in this study) enters the chamber through a small capillary at the bottom. When the pressure inside the chamber is sufficiently great, the brass diaphragm shears around the edge, releasing the gas which in turn disperses the powder.

In producing an aerosol, the breakup of agglomerates occurs when the gas trapped in the voids rapidly expands as the diaphragm ruptures. The term "voids" refers to the spaces between particles in the bulk powder as well as the vacant spaces inside the agglomerates. It is necessary, therefore, to have a reasonable estimate of the voids volume V_V. We know

$$V_A = \frac{m}{\rho_A} \tag{13}$$

and

$$V_B = \frac{m}{\rho_B} \tag{14}$$

where:

V_A = actual volume occupied by powder material

V_B = bulk volume occupied by powder

ρ_A = actual density of powder material

ρ_B = bulk density of powder

m = mass of powder

Voids volume is obviously:

$$V_V = V_B - V_A = \frac{m}{\rho_B} - \frac{m}{\rho_A} \tag{15}$$

$$V_V = m\left(\frac{1}{\rho_B} - \frac{1}{\rho_A}\right) \tag{16}$$

Since the voids volume is only a small part of the total volume of the chamber, the major part of the gas in the powder chamber does no useful work.

The process by which the aerosol is dispersed involves a gaseous system, passing from a state P_1, V_1, T_1 to the state P_2, V_2, T_2 and doing work. It is necessary to make some assumption as to the nature of the gas and as to the process by which it goes from state 1 to state 2. We therefore make the following assumptions:

1) The gas can be considered to obey the van der Waals' equation

2) The process is adiabatic

The van der Waals' equation is a good compromise, since it agrees with a real gas fairly well and is at the same time simple enough to make calculations possible. Since the expansion is quite rapid, the second assumption also seems reasonable. The equation of state is:

$$\left(P + \frac{a}{V^2}\right)(V - b) = RT \tag{17}$$

where:

P = pressure in atmospheres

V = specific volume in cm^3/mole

T = temperature in °K

R = universal gas constant, 82 (cm^3 atm)/(mole degree)

a = 1.39×10^6 (cm^6 atm)/($mole^2$) for nitrogen

b = 39.1 (cm^3)/(mole) for nitrogen

Starting with the internal energy as a function of T and V

$$du = \left(\frac{\partial u}{\partial T}\right)_V dT + \left(\frac{\partial u}{\partial V}\right)_T dV \quad , \tag{18}$$

we can arrive at

$$W = -\int_{T_1}^{T_2} C_V \, dT - a\left(\frac{1}{V_1} - \frac{1}{V_2}\right) \quad . \tag{19}$$

This is the working equation from which energy claculations are made. A derivation of this equation and an evaluation of the integral are included in Appendix C.

The results of the calculations are presented in graphical form as shown in Figure 73.

To calculate the energy required to disperse a powder sample, one proceeds as follows: Knowing the mass of powder used, V_V is calculated using Equation (16). Diaphragm bursting pressure is measured. From Figure 73 the energy per unit initial volume is found. The product of this factor and V_V gives the desired information.

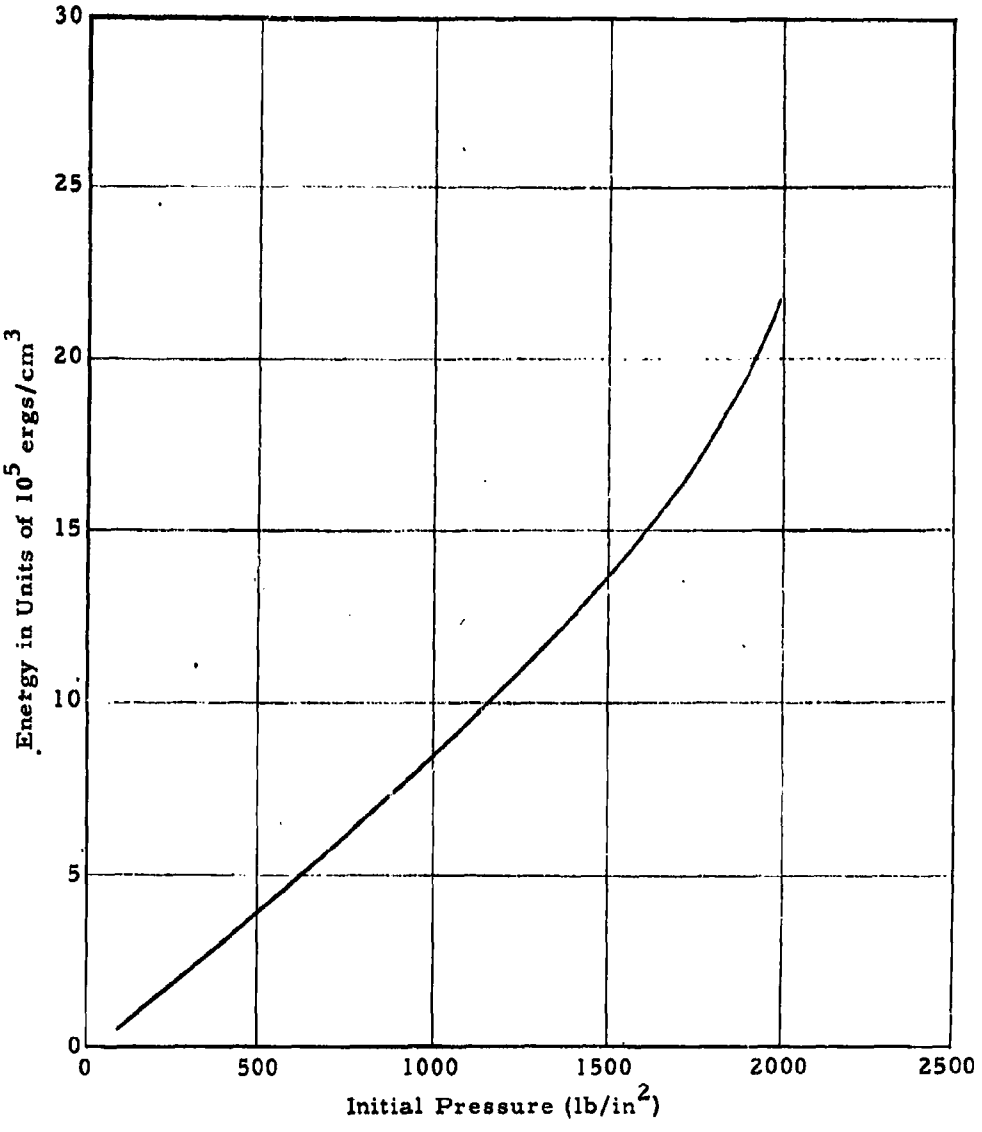

Figure 73. Energy Released when Nitrogen (van der Waals gas) Initially at Pressure P Expands Adiabatically to Pressure of One Atmosphere

2. Experimental Program

By performing the above calculations, one can determine how much energy goes into dispersing a given powder sample. But this does not tell if the powder has been dispersed effectively. To determine the energy required to disperse a powder effectively, one must determine experimentally the threshold bursting pressure.

Let us consider what happens as the energy available is increased. If the energy is too small, there will be many agglomerates which will not be broken up and the resulting aerosol will decay rapidly due to the large average particle size. As the energy available is increased the breakup of agglomerates becomes more and more complete, and the decay constant will decrease with the decreasing average particle size. Finally, a point is reached at which the energy is just sufficient to break up all agglomerates. Further increase of energy should have little effect (unless sufficient energy is used to actually fracture the primary particles). This point is the threshold value or energy necessary to effectively disperse a given powder sample.

An example is given below to illustrate how the energy required to effectively disperse a sample of Span 60 is determined.

A series of tests was conducted in which the decay constant was measured as a function of bursting pressure. Bursting pressure was varied over the range of 205 to 1660 psig using brass shim stock diaphragms with thicknesses ranging from 0.001 to 0.007 inch. For each test, 0.20 g of Span 60 was dispersed, and λ was determined. Several runs were made for each diaphragm thickness and the results averaged. The results are presented in Table 41. A plot of this data is presented in Figure 74. It is seen that the decay constant λ decreases rapidly until a bursting pressure of about 600 psig is reached. Beyond this point the decay constant decreases very slowly with increasing pressure.

Table 41. Decay Constants for Span 60 using Various Bursting Pressures

Diaphragm Thickness (inches)	Bursting Pressure (psig)	Decay Constant, λ
0.001	205	0.370
0.003	500	0.246
0.005	1200	0.227
0.007	1550	0.220

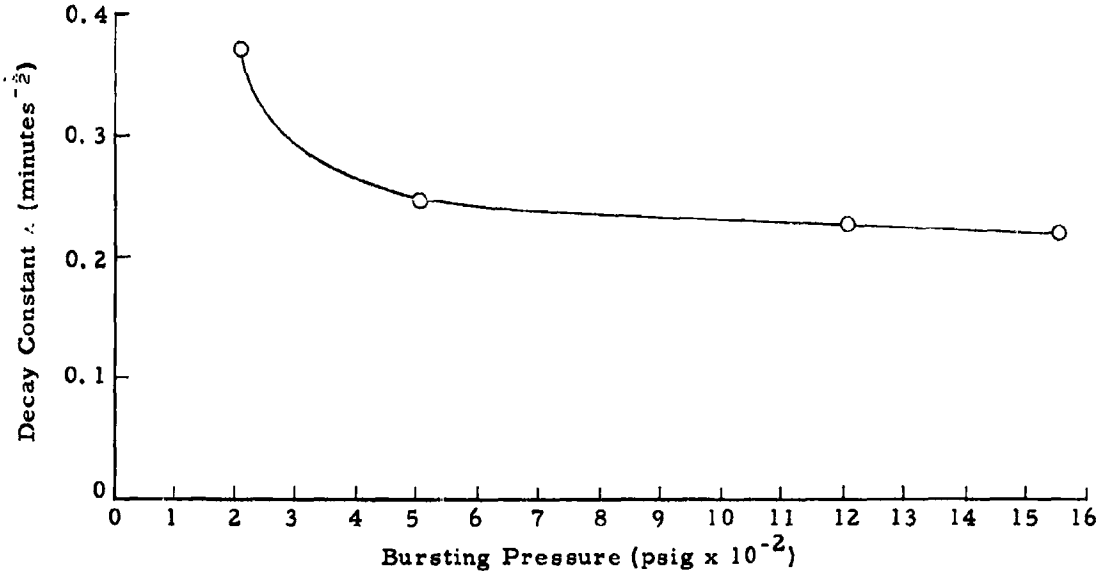

Figure 74. Plot of Decay Constant λ as a Function of Bursting Pressure

Having determined the threshold bursting pressure (600 psig), we can calculate the energy required to disperse a 0.20 g sample of Span 60 effectively. From Table 19, we see ρ_B = 0.193 g/cm. The actual density of Span 60, ρ_A, is known to be 1.0 g/cm^3. Substituting these values into Equation (16), we calculate the voids volume.

$$V_V = 0.20 \left(\frac{1}{0.193} - \frac{1}{1.0} \right) = 0.836 \text{ cm}^3 \qquad (20)$$

From Figure 73, we find the energy per unit volume corresponding to 600 psig to be 4.7 x 10^5 ergs/cm^3. Thus the energy required to disperse a 0.20 g sample of Span 60 effectively is:

$$(0.836 \text{ cm}^3)(4.7 \times 10^5 \text{ ergs/cm}^3) = 3.93 \times 10^5 \text{ ergs}$$

I. Properties of Compacted Powders

A limited amount of effort was invested in studying properties of compacted powders. Two studies were undertaken. These are: 1) local bulk density within columns of compacted powder, and 2) dispersibility of compacted plugs of powder.

1. Local Bulk Density within a Column of Compacted Powder

Using the technique described in Section III-D-2, tests were made to study the variation of local bulk density along the axial direction in a column of compacted powder. The results of measurements on each of the three base powders at several compressive loads are plotted in Figures 75, 76, and 77. Examination of the curves reveals quite different behavior for each powder as compressive load is increased. The uncompressed (except by its own weight) column is seen to have a maximum bulk density at the lower end. This is barely noticeable in the case of Span 60, evident but gradual for Carbowax 6000, and very predominant for saccharin as evidenced by the sharp "spike".

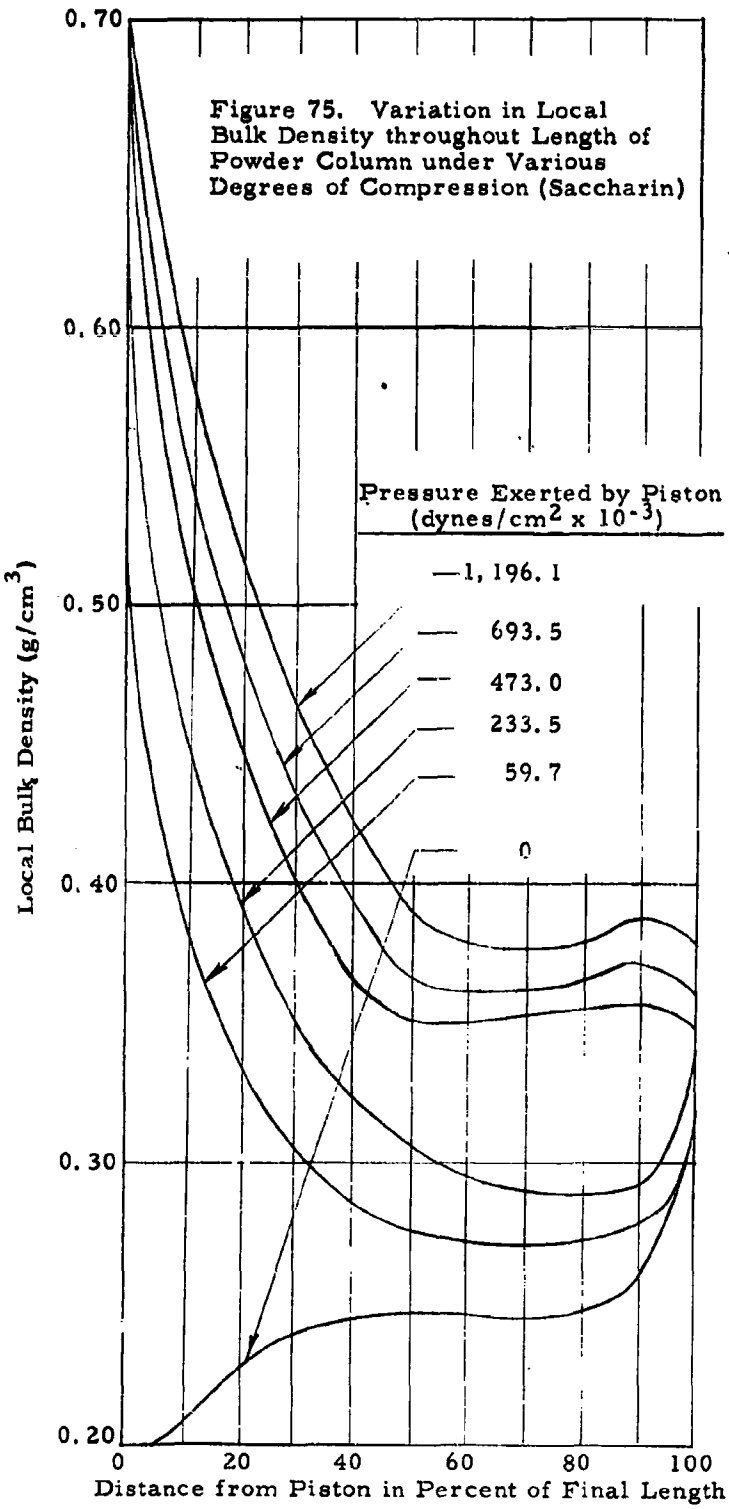

Figure 75. Variation in Local Bulk Density throughout Length of Powder Column under Various Degrees of Compression (Saccharin)

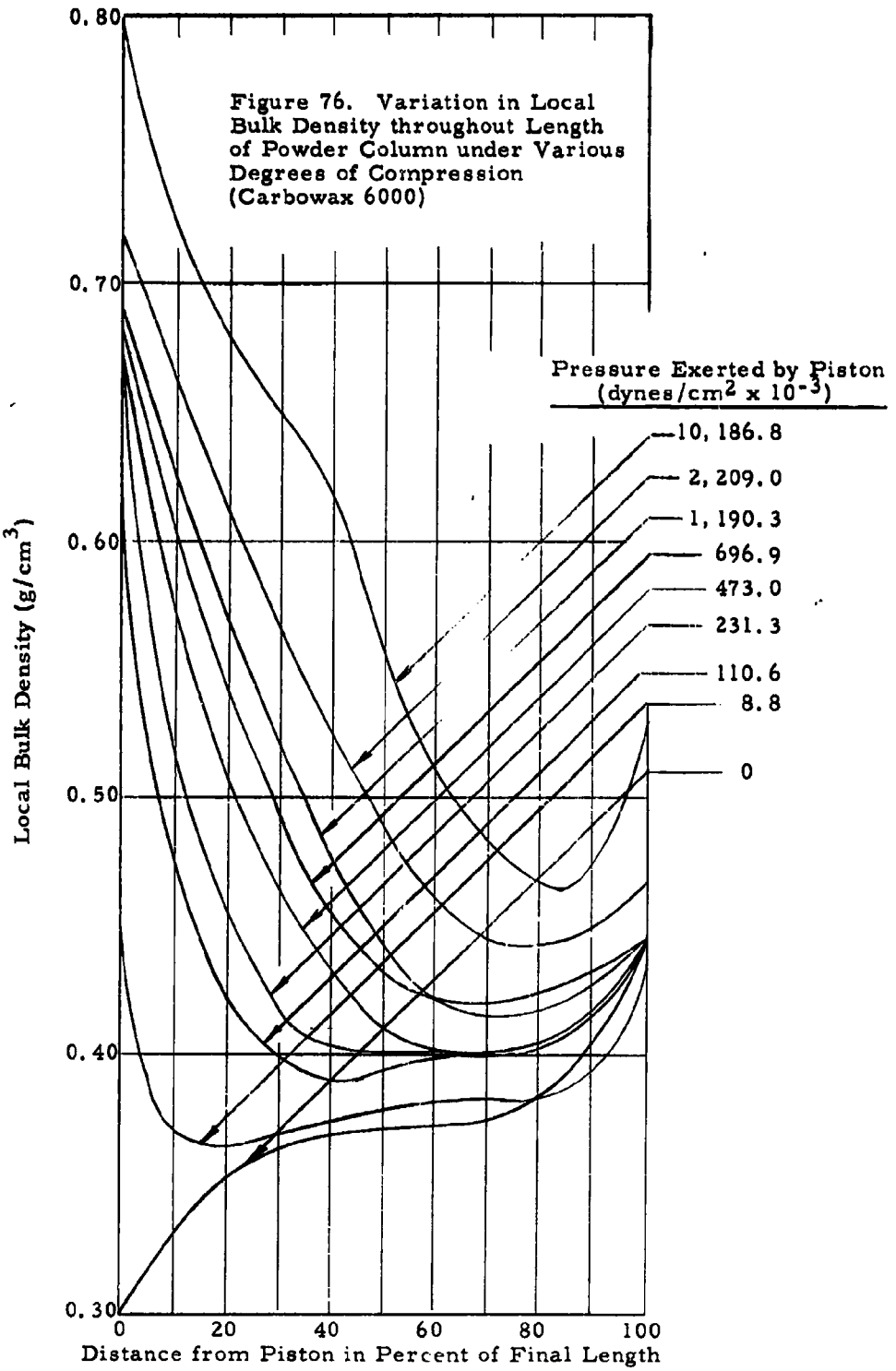

Figure 76. Variation in Local Bulk Density throughout Length of Powder Column under Various Degrees of Compression (Carbowax 6000)

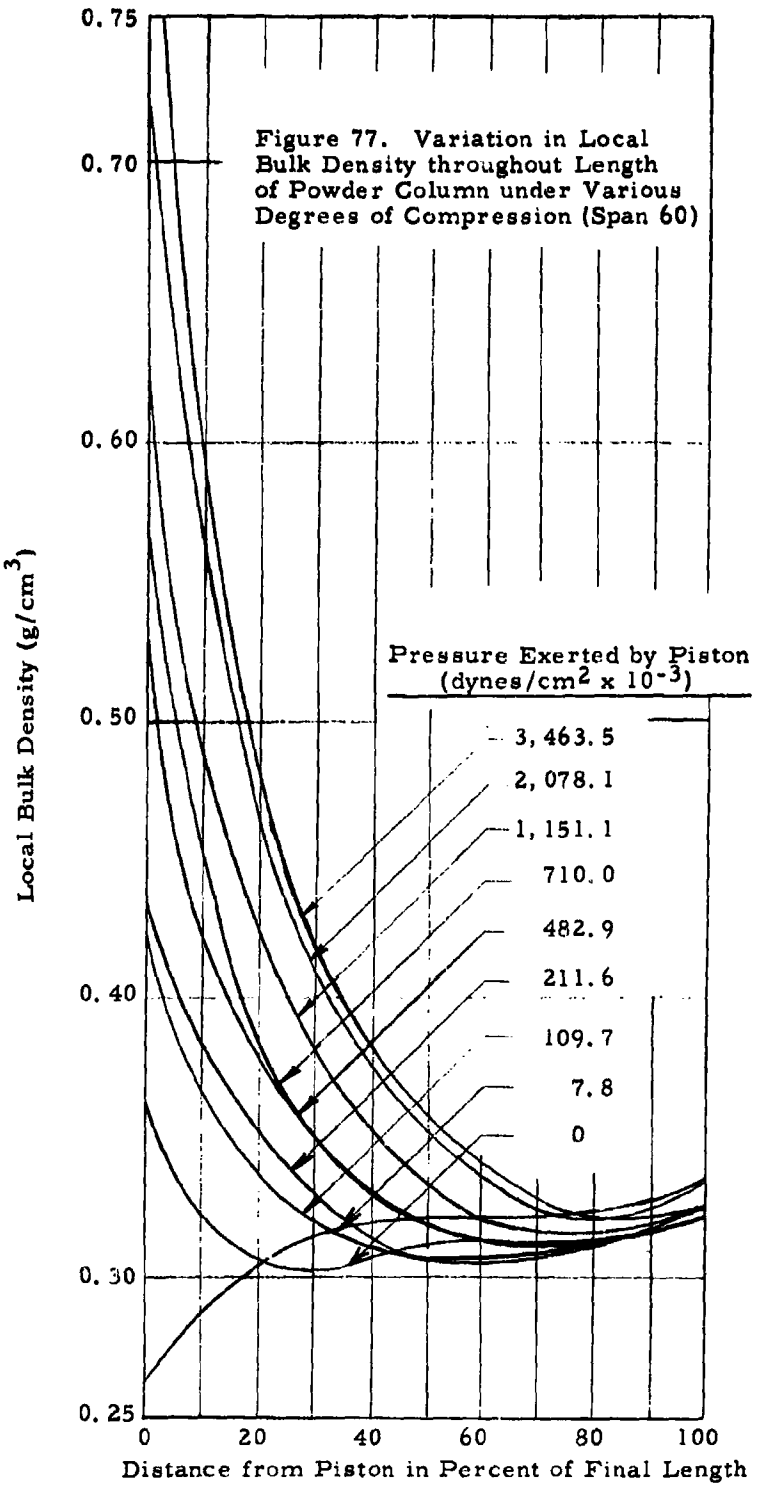

Figure 77. Variation in Local Bulk Density throughout Length of Powder Column under Various Degrees of Compression (Span 60)

As the compressive load is increased, the major effect in all three cases is confined to the first 50 percent or so of final plug length. No change occurs at the extreme bottom of the column until the density throughout the entire column length is at least as great as the initial density at the very bottom.

The measurements were found to be quite reproducible over the first half of the powder column with moderate scatter over the remainder of the length.

2. Dispersibility of Compacted Plugs of Powder

Normally all dispersibility tests were conducted on samples of finely ground, loose powder. At the request of the sponsor, a study was initiated to investigate the dispersibility characteristics of compacted plugs of powder. The first step in this investigation was a preliminary study to determine if the bursting diaphragm technique, which proved satisfactory for loose powders, could be adapted for compacted plugs of powder.

A special device was used to prepare the compacted plugs of powder. A diagram of the device is shown in Figure 78. It consists of a piston, a cylinder, a cap which fits into the bottom of the cylinder to facilitate extracting the plug after compaction, and a base.

Carbowax 6000 was selected as the powder to be used in these tests because its dispersibility characteristics fall somewhere between those of the other two base powders.

A number of plugs having a wide range of bulk densities were prepared. Each plug contained 0.25 g powder. The compacted plugs were cylindrically shaped and measured 1 cm in diameter, and the height was, of course, determined by the bulk density. In practice, the height was measured with a cathetometer and the bulk density calculated.

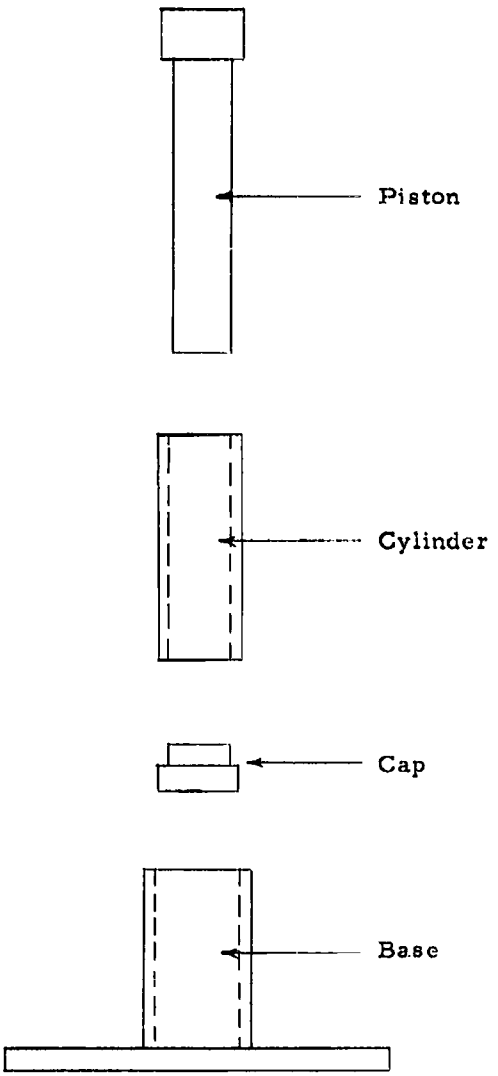

Figure 78. Apparatus for Compacting Powder Plugs

Dispersibility tests were conducted in the usual manner with one exception; a perforated disc was inserted underneath the diaphragm to prevent the plug from being ejected from the gun intact when the diaphragm bursts. A sketch of the bursting diaphragm gun and perforated disc appears in Figure 18.

The probable sequence of events that occurs during the dispersion process is as follows: 1) the sample chamber is pressurized, 2) air permeates the plug, 3) the diaphragm bursts, 4) air which has permeated the plug expands rapidly causing the plug to break apart, 5) plug fragments are carried upward by the air escaping through the small holes in the perforated disc, and 6) plug fragments too large to pass through the small holes in the perforated disc are eroded away by the high velocity air stream.

Several tests were made at each of seven different bulk densities ranging from 0.29 g/cm^3 for loose powder to 0.94 g/cm^3 for a quite hard plug. The results are given in Table 42 and plotted in Figure 79.

Table 42. Results of Dispersibility Tests on Compacted Plugs

Bulk Density (g/cm^3)	λ	A_o
0.29	0.321	49.30
0.44	0.318	60.50
0.61	0.333	43.00
0.73	0.349	56.50
0.79	0.345	51.75
0.91	0.345	58.30
0.94*	0.294	32.75

* Note comments in text.

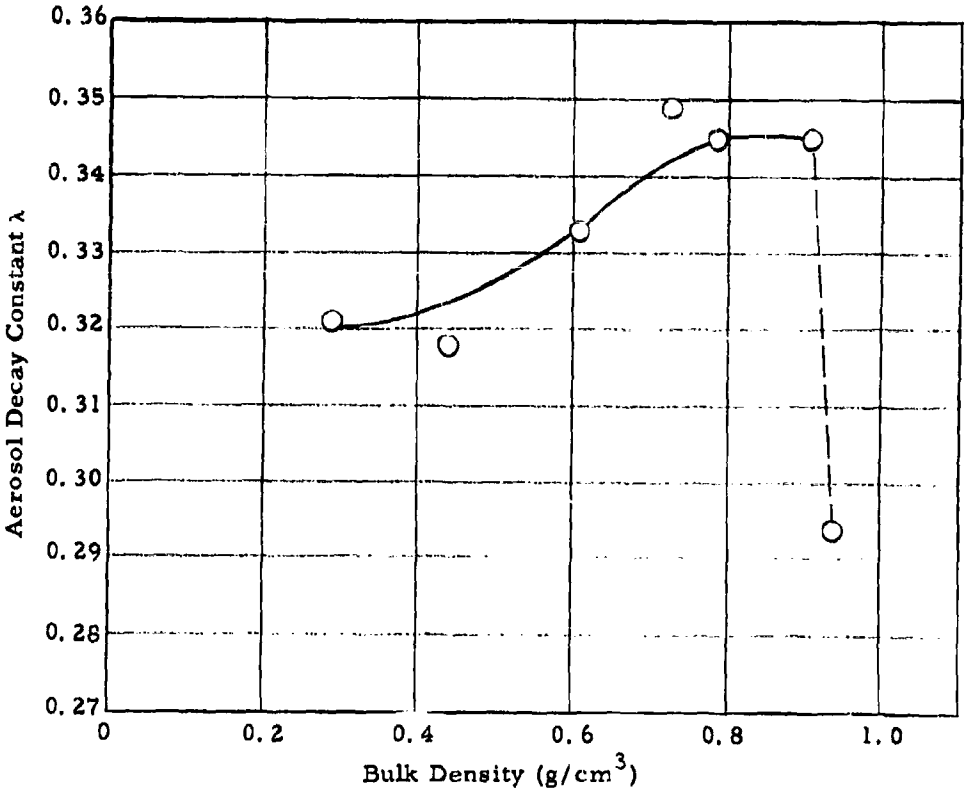

Figure 79. λ as a Function of Plug Bulk Density for Carbowax 6000

It may be seen that λ increases rather slowly with increasing bulk density until a bulk density of 0.91 g/cm^3 is reached. At higher bulk densities, λ decreases rapidly. This can be explained quite easily. When tests were made with $\rho = 0.91$ g/cm^3, all, or almost all, of the powder was dispersed. But on each test where $\rho = 0.94$ g/cm^3, hard lumps of powder were found in the dispersing gun after the test. This residue was weighed each time, and

it was found that only about 50 percent, on the average, of the powder was dispersed. This would lead to a less dense aerosol which in turn would cause both λ and A_o to be smaller. In general, however, the compacted plugs dispersed with surprisingly little loss of efficiency until bulk densities higher than 0.91 g/cm^3 were reached.

J. Egg Albumin Studies

By the request of the sponsor a fourth powder, egg albumin, was added to the list of powders to be investigated. Since this request was not made until the latter part of the program, egg albumin was not investigated as thoroughly as were the three base powders. All the work on the egg albumin, with the exception of bulk tensile strength tests (see Section IV-A), is reported in this section.

1. Grinding Experiments

Two attempts were made to grind egg albumin using the jet pulverizer 2-inch-diameter fluid energy mill and using bottled dry nitrogen as the grinding medium. Particle size analyses indicated that the ground products were not as fine as desired. The main reason for this was attributed to the fact that the maximum operating pressure available with the pressure regulator used was only 60 psig.

Later, two more grinding attempts were made using essentially the same mill setup as before but using compressed air from the blowdown wind tunnel air supply for the grinding medium. The maximum pressure obtainable with this supply is 100 psig, and the air is oil-free since the pumps are of the carbon piston type. In all cases, the mill was set up as illustrated in Figure 80.

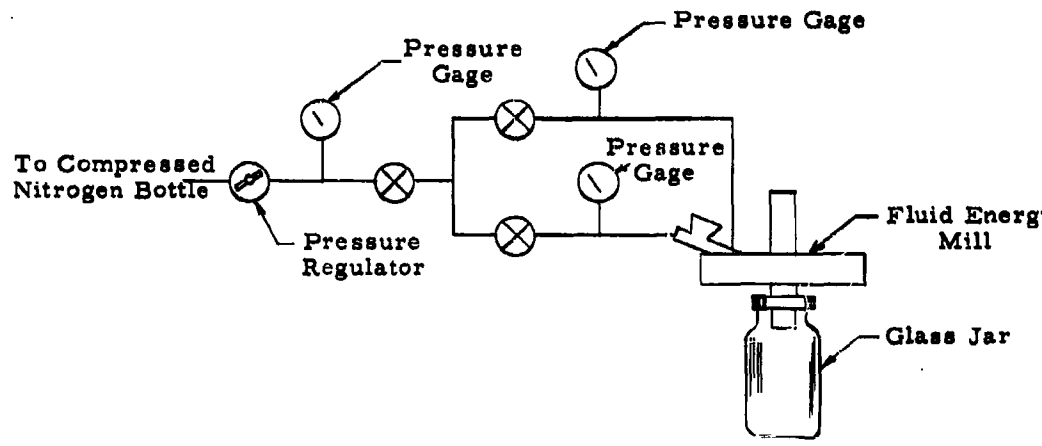

Figure 80. Mill Setup used for Grinding Egg Albumin

The grinding parameters used in the first grind are as follows:

Pressure at downstream side of regulator	60 psig
Pressure at mill outlet	40 psig
Pressure at feed aspirator inlet	52 psig
Powder feed rate	67 g/min

The same parameters were used in the second grind; the only difference is that the ground product from the first grind was used as feed material.

The grinding parameters used in the third grind are as follows:

Pressure at downstream side of regular	95 psig
Pressure at mill inlet	87 psig
Pressure at feed aspirator	73 psig
Powder feed rate	13 g/min

The feed material for this grind was a mixture of the coarse unground material and the ground product from the second grind.

The grinding parameters used in the fourth grind were the same as those for the third grind with the exception that the powder feed rate was only one-tenth as large.

Following each grind, particle size analyses were made on a sample of the ground product using the Whitby centrifuge sedimentation technique. An analysis was made also on the coarse, unground material.

The Whitby centrifuge sedimentation technique is described in Section III-A-2, and the time versus particle size schedules for egg albumin are given in Table 7. Because of the large particle sizes in the coarse, unground material, gravity settling was used throughout the entire analysis. A combination of gravity settling and centrifugal settling was used on the ground samples. The results of these analyses are plotted in Figure 81.

The peculiar size distribution corresponding to the third grind material is attributed to the fact that the feed material for this grind was a mixture of coarse and fine particles.

To check the Whitby technique against a more absolute method, particle size analyses were made on the first and second grind materials using the microscope technique described in Section III-A-1. The results of the microscope analyses are given in Table 43 and are plotted in Figures 82 and 83. The dashed lines are the particle size distributions calculated on the basis of the liquid sedimentation data using the following formula:[21]

$$D_c = D_m e^{-3 \ln^2 \sigma_g} \qquad (21)$$

where:

D_c = count median diameter

D_m = mass median diameter

σ_g = geometric standard deviation

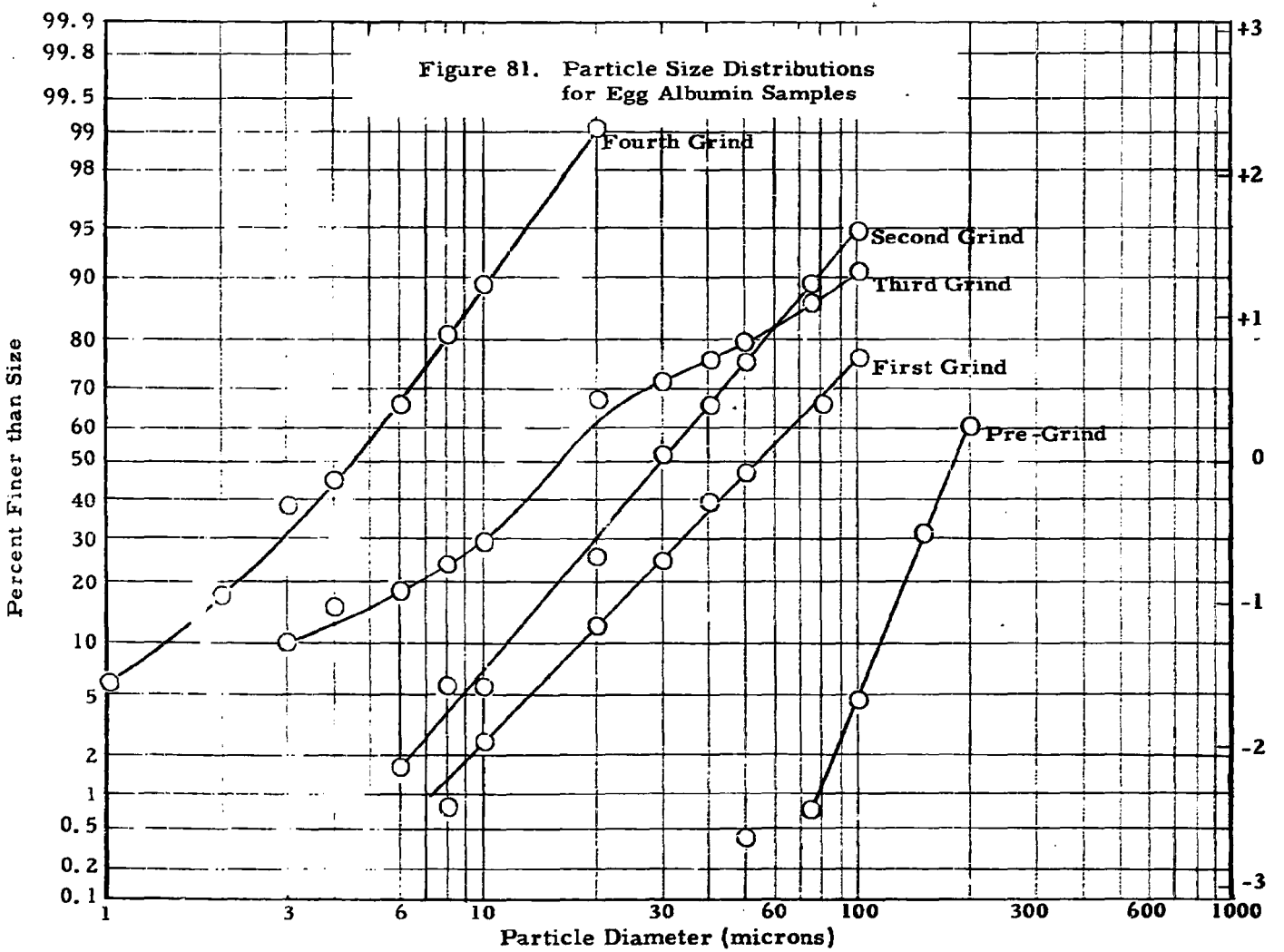
Figure 81. Particle Size Distributions for Egg Albumin Samples
Fourth Grind
Second Grind
Third Grind
First Grind
Pre-Grind
Percent Finer than Size
99.9
99.8
99.5
99
98
95
90
80
70
60
50
40
30
20
10
5
2
1
0.5
0.2
0.1
+3
+2
+1
0
-1
-2
-3
1
3
6
10
30
60
100
300
600
1000
Particle Diameter (microns)

Table 43. Microscopic Particle Size Analysis Data for Egg Albumin

Particle Diameter (microns)	Number of Particles Counted	Percent Finer than Size
First Grind		
2.15	60	14.1
4.30	81	33.0
6.45	87	53.4
8.60	73	70.5
10.74	37	79.2
12.89	27	85.5
15.04	16	89.3
17.19	13	92.3
19.32	11	94.9
21.50	9	96.9
23.65	2	97.4
25.80	5	98.6
27.90	2	99.0
30.10	1	99.2
32.20	1	99.5
67.80	1	99.7
79.50	1	100.0
	427	
Second Grind		
2.15	144	12.4
4.30	220	31.4
6.45	220	50.3
8.60	191	66.8
10.74	144	79.1
12.89	83	86.4
15.04	64	91.9
17.19	38	95.2
19.32	23	97.0
21.50	15	98.5
23.65	3	98.7
25.80	6	99.4
27.90	7	99.7
30.10	1	99.9
34.40	1	100.0
	1160	

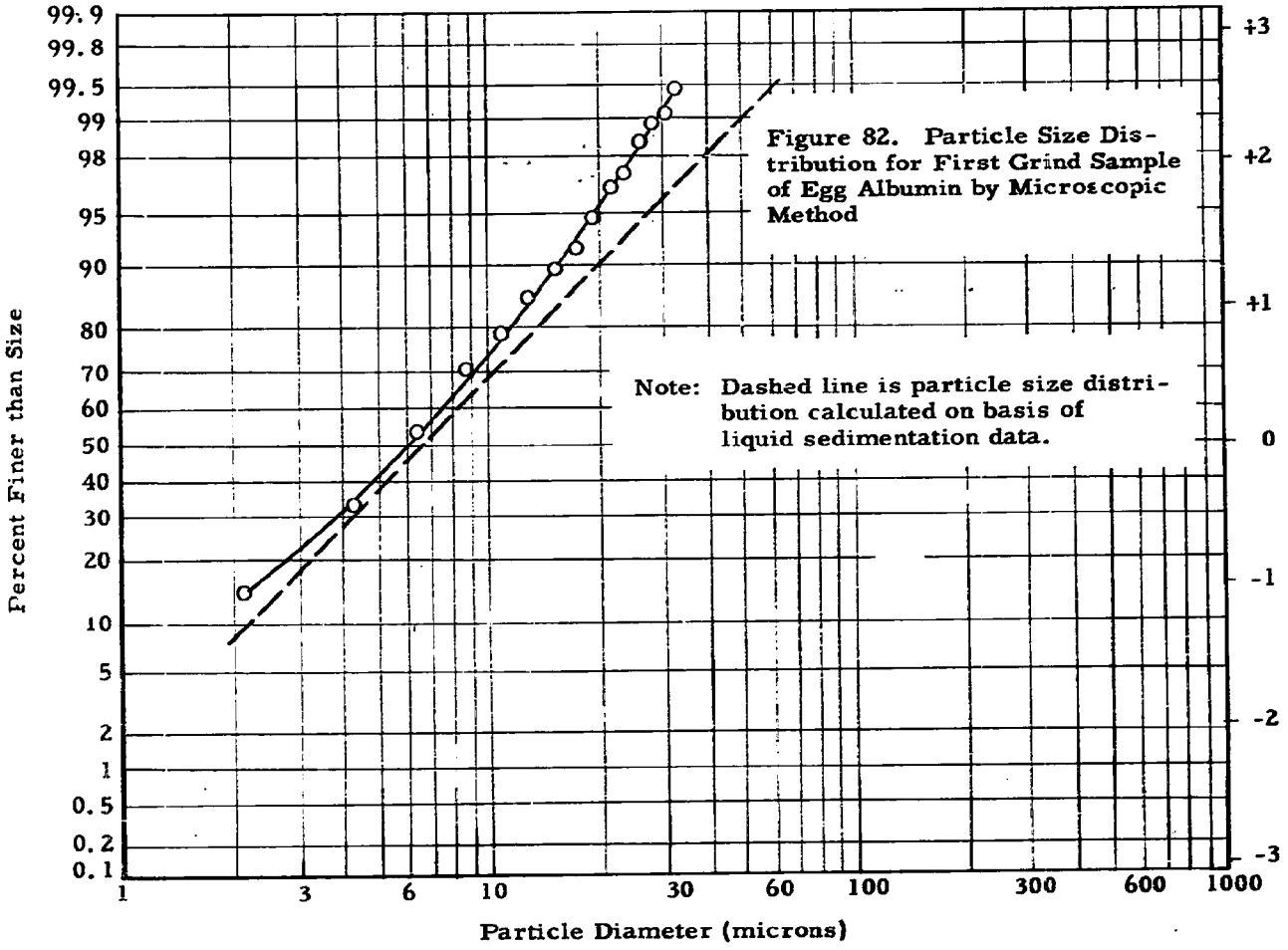

Figure 82. Particle Size Distribution for First Grind Sample of Egg Albumin by Microscopic Method

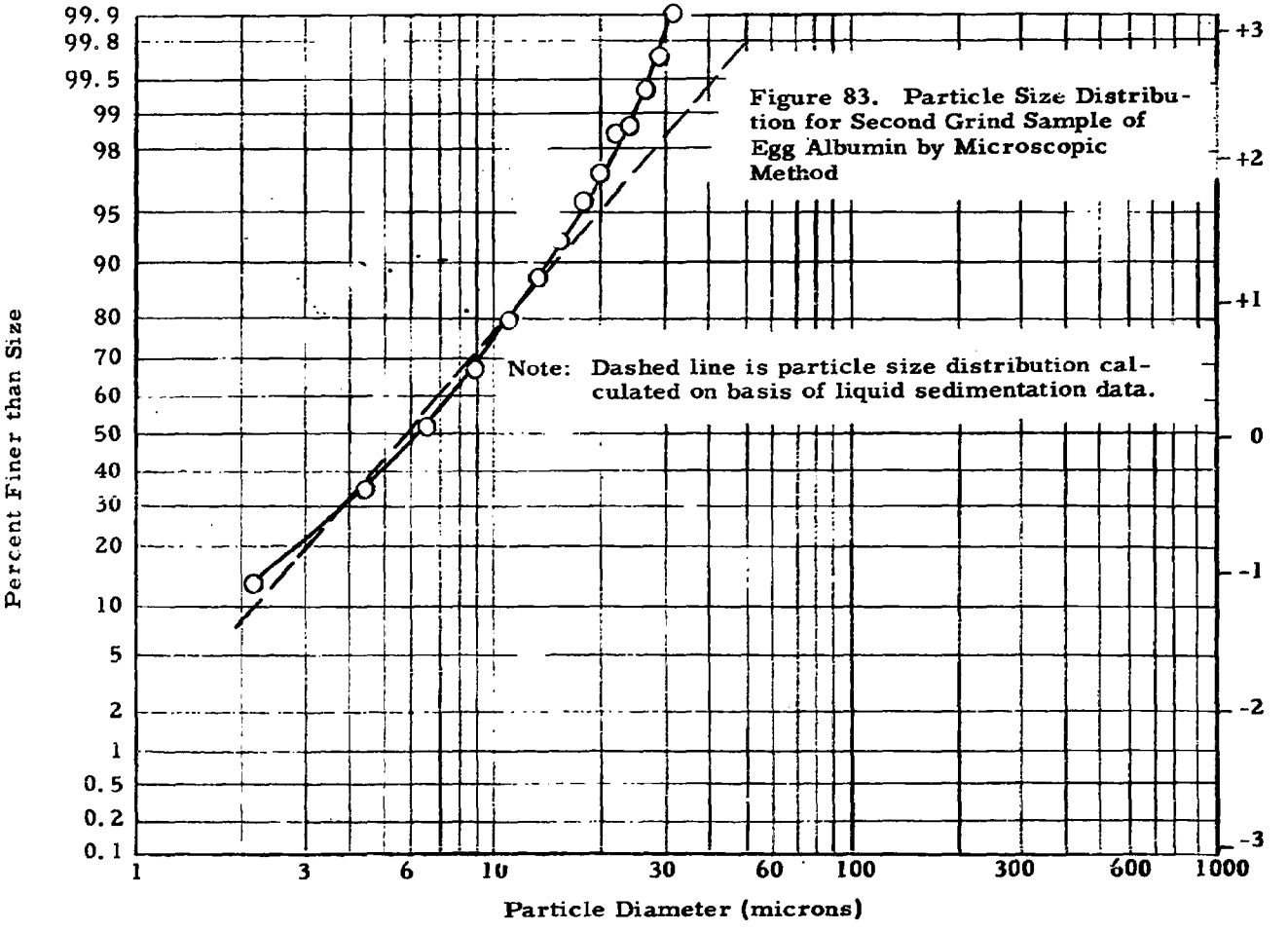

Figure 83. Particle Size Distribution for Second Grind Sample of Egg Albumin by Microscopic Method

It is seen that the size distribution as measured by the two different methods compare quite favorably.

The main reason for conducting the various grinding experiments was to obtain a sample whose particle sizes lie in the 2 to 5-micron range. The fourth grind material comes very close to meeting this requirement. From the particle size distribution curve plotted in Figure 81, it can be shown that 40 percent of its mass and 17 percent of its number lie in the 2 to 5-micron range. As long as we had several samples with known particle size distributions, we decided to determine what effect particle size has on such properties as shear strength and dispersibility.

2. Shear Strength

Shear strength measurements were made on samples of the second, third, and fourth grind materials using the technique described in Section III-B. The tests were made at six different compressive loads covering the range from 2690 to 30, 700 dynes/cm^2. The results are given in Table 44 and are plotted in Figure 84. It is seen that shear strength of egg albumin decreases as particle size decreases.

Table 44. Shear Strengths of Egg Albumin Samples at Various Compressive Loads

Compressive Load (dynes/cm^2)	Shear Strength (dynes/cm^2)			
	Unground Material	2nd Grind Material	3rd Grind Material	4th Grind Material
2, 690	2, 190	2, 220	2, 232	2, 292
4, 170	3, 560	3, 640	3, 338	3, 349
7, 120	6, 450	6, 130	6, 020	5, 336
13, 000	11, 600	11, 500	10, 294	8, 855
23, 400	21, 600	21, 500	18, 846	16, 651
30, 700	28, 500	27, 200	25, 236	21, 781

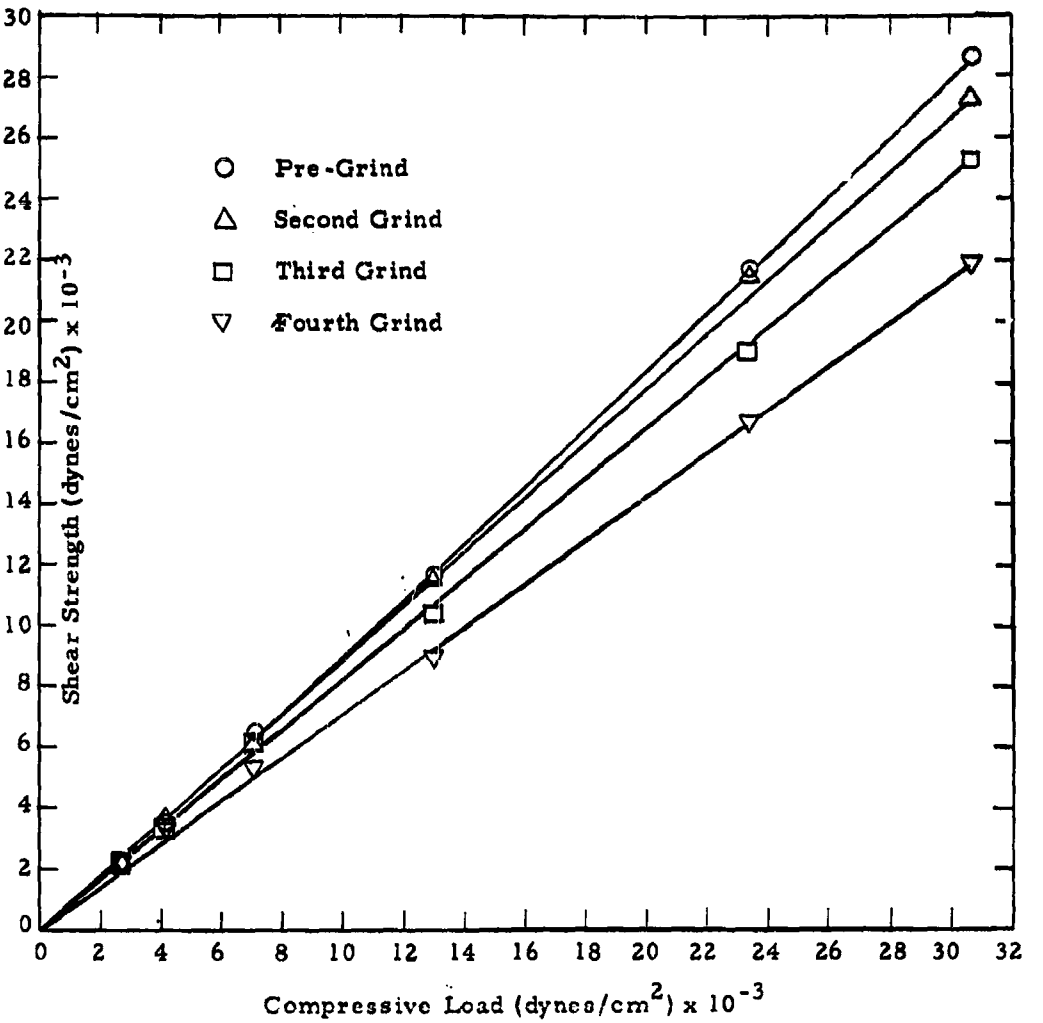

Figure 84. Shear Strength as a Function of Compressive Load for Egg Albumin

3. Dispersibility Tests

Dispersibility tests (see Section III-F) were made on samples of the first, second, third, and fourth grind materials. No tests were made on the unground material because its particle size was too large. The results are given in Table 45.

Table 45. Dispersibility Test Data for Egg Albumin Samples

Sample	λ	A_o	Mass Dispersed (g)
First grind material	0.387	7.45	0.1
Second grind material	0.337	12.35	0.1
Third grind material	0.332	27.50	0.1
Fourth grind material	0.156	82.00	0.1

As one would expect, λ decreases and A_o increases with decreasing particle size. The extreme fineness of the fourth grind material is portrayed by the fact that the Brown recorder used in the dispersibility test was "pegged" at full scale deflection for a period of one hour.

4. Effect of Cab-O-Sil on Properties of Egg Albumin

A limited amount of work was invested in determining how Cab-O-Sil affects various properties of egg albumin and also in determining approximately the optimum concentration. Samples of the fourth grind material were mixed with Cab-O-Sil in such proportions to produce Cab-O-Sil concentrations of 1, 5, and 10 percent by weight. Because of the small amount of egg albumin on hand, mixing was accomplished by tumbling the samples back and fourth in a polyethylene bag rather than by the fluid energy mill technique described in Section II-C. Thus the samples were not blended as thoroughly as they might have been.

These samples, as well as samples of unadulterated fourth grind egg albumin and unadultered Cab-O-Sil, were tested for shear strength using a compressive load of 5960 dynes/cm^2. The results are given in Table 46 and are presented graphically in Figure 85. These results indicate that the optimum concentration, insofar as reducing shear strength is concerned, lies between 1 and 5 percent.

Table 46. Shear Strengths of Egg Albumin Samples with Various Concentrations of Cab-O-Sil (compressive load = 5950 dynes/cm^2)

Cab-O-Sil Concentration (percent)	Shear Strength (dynes/cm^2)	Percent Change
Control Sample (no additive)	3840	0
1	2940	23
5	2800	27
10	3580	7
100	3800	1

a. Effects of Cab-O-Sil Concentration on Dispersibility of Egg Albumin

A series of dispersibility tests was made on the egg albumin samples containing various concentrations of Cab-O-Sil. The results of these tests are given in Table 47.

The data presented in Table 47 indicate that λ increases with increasing Cab-O-Sil concentration, while A_o reaches a maximum value at a concentration of 1 percent. No definite conclusions can be drawn from these few tests; however, it appears that Cab-O-Sil does little to improve the dispersibility of egg albumin.

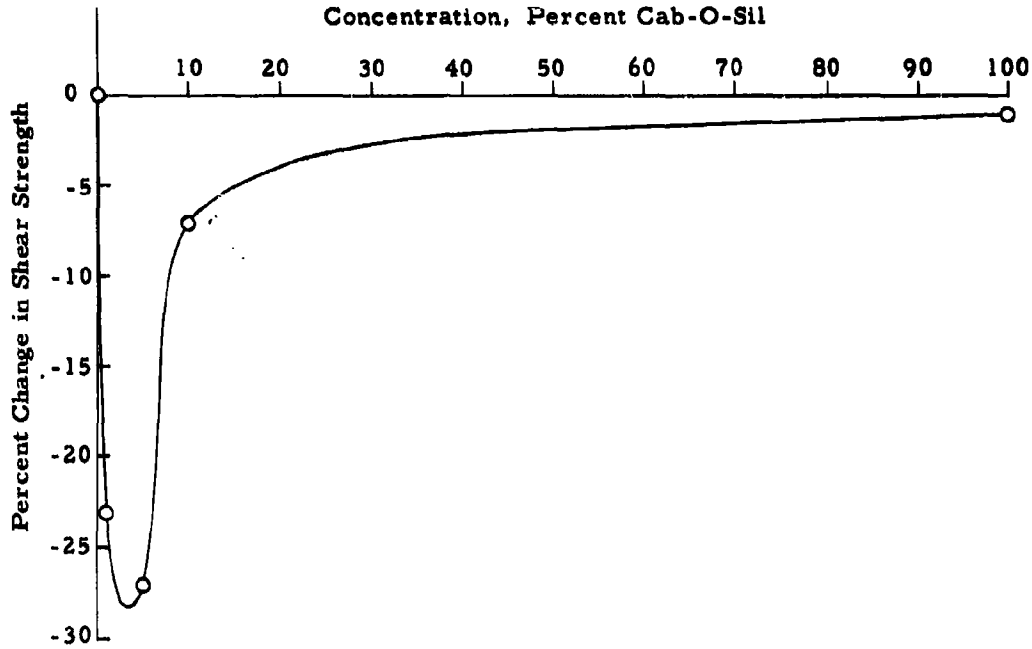

Figure 85. Percent Change in Shear Strength versus Cab-O-Sil Concentration

Table 47. Dispersibility of Egg Albumin with Various Concentrations of Cab-O-Sil

Cab-O-Sil Concentration	λ	A_o
Control sample (no additive)	0.190	43.20
1%	0.201	57.00
5%	0.245	36.00
10%	0.224	29.50

b. Effect of Cab-O-Sil Concentration on Electrostatic Charge of Egg Albumin

Electrostatic charge tests using the method described in Section III-G-2 were made on samples of egg albumin containing 0, 1, and 5 percent Cab-O-Sil. The results of these tests are presented in Table 48.

Table 48. Electrostatic Charge of Egg Albumin with Various Concentrations of Cab-O-Sil

Cab-O-Sil Concentration	A/B	a	b	(b - a)	$W_{\frac{1}{2}}$
Control sample (no additive)	1.13	3.37	2.98	-0.39	2.82
1%	1.01	3.19	2.16	-0.03	3.50
5%	1.09	3.31	3.04	-0.27	4.90

We see that the quantity (b - a) is negative in each case indicating that the net charge on each sample is negative. The $W_{\frac{1}{2}}$ dimension increases with increasing Cab-O-Sil concentration indicating that the samples fan out more as they flow through the electric field when Cab-O-Sil concentration is increased. This means that the samples become more highly charged in both + and - directions as Cab-O-Sil concentration is increased.

V. SUMMARY AND CONCLUSIONS

A. Preparation of Powders

The preparation of powders is discussed in Section II. Included here are such topics as 1) the initial grinding of three base powders, 2) a technique for deagglomerating powders, 3) a technique for blending powders, 4) a technique for conditioning powders at various known humidities, 5) a technique for coating powders with various surface active agents, and 6) a technique for absorbing foreign vapors onto powders.

B. Tests and Procedures

The tests and procedures used to investigate various powder properties are described in Section III. These are as follows: 1) tests for measuring particle size distribution (microscopic and Whitby centrifuge sedimentation methods), 2) shear strength test, 4) bulk tensile strength test, 4) bulk density tests (for uncompacted and compacted powders), 5) dynamic angle of repose tests, 6) dispersibility test, and 7) electrostatic charge tests (for airborne particles and bulk powders).

C. Major Studies

The largest section of the report (Section IV) is devoted to the major studies. The first of these deals with bulk tensile strength tests.

1. Bulk Tensile Strength Tests

Bulk tensile strength tests were made on samples of saccharin, Carbowax 6000, Span 60, and egg albumin. It was found that bulk tensile strength of a powder compressed in a cylinder is an exponential function of column length (distance from compressing piston to fracture plane). It was found

also that bulk tensile strength at zero column length (obtained by extrapolation) appears to be a linear function of compressive load over the range of loads investigated. Listing the powders in the order of highest to lowest bulk tensile strength, we obtain the following arrangement: Span 60, Carbowax 6000, saccharin, and egg albumin.

2. Effects of Humidity on Powder Properties

Effects of humidity on powder properties were investigated by conducting various tests on samples of the three base powders which had been conditioned at relative humidities of less than 1, 25, and 75 percent.

Results of shear strength tests indicate that, with saccharin, the value of the shear strength reaches a minimum at about 25 percent relative humidity, with Carbowax 6000 it reaches a maximum at about 25 percent, and with Span 60 it gradually decreases with increasing humidity.

Results of dispersibility tests indicate that the initial amplitude A_0 is practically independent of conditioning humidity for saccharin and Carbowax 6000 but decreases rapidly with increasing humidity for Span 60 and that the aerosol decay constant λ increases with increasing humidity for all three powders. In effect, this means that the aerosol becomes less dense and settles out faster as conditioning humidity is increased.

Results of electrostatic charge tests indicate the following: In all cases, the percentage of neutral particles is small. With saccharin, there is always an excess of negatively charged particles regardless of conditioning humidity. With Carbowax 6000 and Span 60, there may be an excess of negatively charged or positively charged particles, depending upon conditioning humidity.

3. Effects of Antiagglomerant Agents on Powder Properties

The investigation of effects of antiagglomerant agents began with a series of screening tests which ultimately eliminated ten of the fourteen agents under consideration. The four agents which merited further consideration are Cab-O-Sil, Alon-C, P-25, and tri-calcium phosphate. The agents found to be the most effective for saccharin and Carbowax 6000 were Cab-O-Sil, Alon-C, and P-25; those found to be the most effective for Span 60 were Cab-O-Sil and tri-calcium phosphate. Having found the most effective agents, we conducted a series of tests to determine the optimum agent concentration.

On the basis of shear strength tests, we can make the following statements: With saccharin, the optimum concentration is 1 percent for Cab-O-Sil, 1 percent for Alon-C, and between 1 and 5 percent for P-25. With Carbowax 6000, it is 1 percent for Cab-O-Sil, 10 percent for Alon-C, and 10 percent for P-25. With Span 60, it is 5 percent for tri-calcium phosphate and indeterminable for Cab-O-Sil.

The bulk density tests indicated that, in most cases, bulk density reaches a maximum value at some agent concentration and then decreases with further increase in concentration. Assuming that this maximum occurs at the optimum concentration (see Section IV-C-3) we see, in the cases of both saccharin and Carbowax 6000, optimum concentration is 1 percent for Cab-O-Sil, 5 percent for Alon-C, and 10 percent for P-25. With Span 60, it is 5 percent for Cab-O-Sil, 10 percent for Alon-C, about 25 percent for P-25, and indeterminable for tri-calcium phosphate.

The results of the dynamic angle of repose tests were similar to those of the bulk density tests in that the curves reached a maximum value at some agent concentration and then decreased with further increase in concentration. With saccharin, this maximum angle occurs at a concentration of 1 percent for Cab-O-Sil, Alon-C, and P-25. With Span 60, it occurs at a concentration of 1 percent for Cab-O-Sil and 5 percent for tri-calcium phosphate.

On the basis of the dispersibility tests, we can make the following statements: With saccharin, the optimum concentration is 5 percent for Cab-O-Sil, between 10 and 30 percent for Alon-C, and 30 percent for P-25. With Carbowax 6000, the optimum concentration is 5 percent for Cab-O-Sil, 30 percent for Alon-C, and approximately 30 percent for P-25. With Span 60, optimum concentration is about 10 percent for Cab-O-Sil and 1 percent for tri-calcium phosphate.

The electrostatic charge tests indicated that the most neutral sample in nearly every case is the one having an agent condentration of 1 percent.

By way of a summary of these many tests, we see, first of all, that the optimum concentration is generally smaller for Cab-O-Sil than for the other agents tested; therefore, we must conclude that Cab-O-Sil is the most effective antiagglomerant agent tested. The optimum concentration varies somewhat depending upon the powder property under consideration. For most properties, the optimum Cab-O-Sil concentration is of the order of 1 percent, but for dispersibility it is somewhat higher.

Bulk tensile strength tests conducted on samples of Carbowax 6000 and Span 60 containing 1 percent by weight of Cab-O-Sil indicated that the bulk tensile strengths of the samples containing Cab-O-Sil are less than half those of the unadulterated samples.

4. Mechanism by which Cab-O-Sil Functions

A study of the mechanism by which Cab-O-Sil functions showed (by means of electron micrographs) that the tiny Cab-O-Sil particles form a layer surrounding the host particles (Carbowax 6000 in this case). This layer then acts as a lubricant permitting the host particles to pack together more tightly, thereby increasing bulk density. This layer also serves to decrease bulk tensile strength and shear strength and neutralize the electrostatic charge on the sample.

5. Effects of Surface Active Agents on Powder Properties

The investigation of effects of surface active agents consisted of coating samples of the three base powders with selected representatives of the four main classes of surface active agents (anionic, cationic, non-ionic, and amphoteric) and conducting various tests to determine what changes, if any, occurred.

On the basis of shear strength tests, we can make the following statements: With saccharin, there is no apparent grouping of samples into agent categories. With Carbowax 6000, all samples but one have lower shear strengths than the control, and the three samples having lowest shear strengths were all treated with cationic-type agents. With Span 60, there is a definite grouping of the cationic agents on one side and the amphoteric agents on the other. The samples treated with cationic agents have higher shear strengths and those treated with amphoteric agents have lower shear strengths than the control.

On the basis of dispersibility tests, we found the following to be true: With saccharin, both amphoteric and non-ionic agents have detrimental effects, anionic agents appear to have little or no effect, and cationic agents definitely have a beneficial effect. With Carbowax 6000, the anionic and cationic agents both have detrimental effects, the amphoteric agents and L-45 Silicone have little or no effect, and the non-ionic agents appear to have a beneficial effect. With Span 60, little is to be gained by coating the particles with amphoteric agents, non-ionic agents, or L-45 Silicone. The anionic and cationic agents both have beneficial effects.

The electrostatic charge tests indicated the following: With saccharin, all treated samples were less highly charged than the untreated control. One agent in particular (Alamine 570, a cationic type) significantly reduces the electrostatic charge of saccharin. With Carbowax 6000, several agents of different types significantly reduce electrostatic charge.

In summary, we see that desirable changes in powder properties such as reducing shear strength and producing a more stable aerosol by lowering λ can be accomplished by coating the base powders with the proper surface active agents. This is especially evident in the case of saccharin coated with cationic-type surface active agents. In attempting to explain these phenomena from the chemical standpoint, we find the greatest chance for chemical interaction to be between the cationic agents (which are amines in this case) and saccharin with its active hydrogen.

6. Effects of Adsorbed Vapors on Powder Properties

Effects of adsorbed foreign vapors where investigated by treating samples of the three base powders with four selected vapors (n-butylamine, phenol, acetone, and propionaldehyde) and testing the treated samples to determine what, if any, changes occurred. Samples were tested for shear strength, dispersibility, and electrostatic charge. The adsorbed vapors had the following effects on properties of the three base powders:

1) n-butylamine

   a) Saccharin

      Caused sample to become syrupy, rendering it useless for further tests.

   b) Span 60

      Caused sample to foam up, rendering it useless for further tests.

   c) Carbowax 6000

      Did not react chemically with sample.

      Had little or no effect on dispersibility characteristics.

      Increased number of positively charged particles and decreased number of negatively charged particles.

2) Phenol

a) Saccharin

Did not react chemically with sample.

Reduced shear strength by 25.3 percent.

Had detrimental effect on dispersibility characteristics.

Neutralized electrostatic charge.

b) Span 60

Did not react chemically with sample.

Increased shear strength by 99.9 percent.

Had little or no effect on dispersibility characteristics.

Had little or no effect on electrostatic charge.

c) Carbowax 6000

Did not react chemically with sample.

Increased shear strength by 4.5 percent.

Had little or no effect on dispersibility characteristics.

Had little or no effect on electrostatic charge.

3) Acetone

a) Saccharin

Caused sample to agglomerate, rendering it useless for further tests.

b) Span 60

Caused sample to agglomerate, rendering it useless for further tests.

c) Carbowax 6000

Did not react chemically with sample.

Reduced shear strength by 14.0 percent.

Had little or no effect on dispersibility characteristics.

Changed net charge from slightly positive to slightly negative.

4) Propionaldehyde

a) Saccharin

Caused sample to agglomerate, rendering it useless for further tests.

b) Carbowax 6000

Did not react chemically with sample.
Reduced shear strength by 6.5 percent.
Had little or no effect on dispersibility characteristics.
Had little or no effect on electrostatic charge.

c) Span 60

Did not react chemically with sample.
Increased shear strength by 18.2 percent.
Improved dispersibility characteristics.
Had little or no effect on electrostatic charge.

In summary, it can be said that none of the adsorbed foreign vapors produced any marked improvements in the powder properties investigated.

7. Effects of Removal of Adsorbed Gases and Vapors

Effects of removal of adsorbed gases and vapors were investigated by conducting disc-lifting tests on samples of the three base powders under laboratory conditions and under high vacuum conditions. Results of the tests indicated that for Span 60, the force required to remove the disc from the bed of powder is greater for high vacuum conditions than for laboratory conditions, while the opposite is true for saccharin and Carbowax 6000. This is explained by the fact that the Span 60 sample sublimed under high vacuum conditions, thus increasing the tendency for particles to bond together. In the cases of saccharin and Carbowax 6000, an adsorbed layer of water was probably responsible for causing the disc-lifting force to be higher for laboratory conditions than for high vacuum conditions.

8. Energy Required to Disperse Powders

A theoretical study was conducted to determine the relationship between the bursting pressure in the powder dispersing gun and the actual energy that goes into dispersing the powder sample. The results are presented in graphical form in Figure 73. To calculate the energy required to disperse a powder sample, one must know the mass of the powder used, its actual density, its bulk density, and the diaphragm bursting pressure. Substituting the proper values into Equation (16), one finds the voids volume V_V. The product of V_V and the energy per unit initial volume (obtained from Figure 73) gives the desired information.

An experimental program was conducted to determine the threshold energy required to disperse a 0.20 g sample of Span 60 effectively. On the basis of a series of tests in which decay constant was measured as a function of bursting pressure, it was found that the threshold bursting pressure is 600 psig. Using the procedure described in the previous paragraph, it was found that the threshold energy for this sample is 3.9×10^5 ergs.

9. Properties of Compacted Powders

Two studies were undertaken to investigate properties of compacted powders. These are 1) local bulk density within columns of compacted powders, and 2) dispersibility of compacted plugs of powder. In connection with the first study mentioned above, it was found that, for an uncompressed column of powder, the maximum bulk density is at the bottom. As compressive load is increased, the maximum bulk density shifts to the top. In connection with dispersibility of compacted plugs of powder, it was found that compacted plugs of Carbowax 6000 dispersed with surprisingly little loss of efficiency until bulk densities higher than 0.91 g/cm^3 are reached.

10. Egg Albumin Studies

A study was undertaken to investigate properties of egg albumin. The samples used in this study were samples of unground material having an MMD of 180 microns and samples of ground material having MMD's of 55, 30, 16, and 4.4 microns. Shear strength tests performed on these samples indicated that shear strength at a given compressive load decreases with decreasing particle size. Dispersibility tests indicated that λ decreases while A_o increases with decreasing particle size.

Tests were made to determine how Cab-O-Sil affects various properties of egg albumin. Shear strength tests conducted on samples containing 0, 1, 5, 10, and 100 percent Cab-O-Sil indicated a minimum shear strength at a concentration between 1 and 5 percent. Dispersibility tests indicated that little is to be gained by adding Cab-O-Sil to egg albumin. Electrostatic charge tests indicated that the net charge on egg albumin is negative and that adding Cab-O-Sil to egg albumin causes it to become more highly charged in both + and - directions but does not greatly alter the net charge.

VI. RECOMMENDATIONS FOR FUTURE WORK

We have demonstrated in Section IV-C that it is possible to improve various powder characteristics related to dissemination by adding certain antiagglomerant agents. Agent concentrations investigated were 0, 1, 5, 10, 30, and 100 percent. Indications were that the optimum concentration is generally less than 10 percent. Further work should be done to investigate the 0 to 10 percent region more thoroughly.

Additional work should also be done to correlate optimum antiagglomerant agent concentrations with surface area of the host powder.

All the work related to antiagglomerant agents was done with uncompacted powders. Further work is needed to determine the effects of antiagglomerant agents on powders that are compacted and subsequently disseminated in aerosol form.

We have demonstrated in Section IV-E that it is possible to improve the dispersibility characteristics of some powders by coating the powder particles with certain surface active agents. An outstanding example of this was saccharin coated with cationic-type agents. The agent concentration used in all cases was one percent. There is no reason to believe that this was the optimum concentration. It is quite possible that the optimum concentration is considerably less than one percent. Further work should be done in the area of coating powders with surface active agents and determining optimum concentration.

Further effort is also needed in the general area of compacted powders. One worthwhile study would be to investigate energy of compaction as a function of threshold energy of dispersion.

VII. REFERENCES

1) Hamaker, H. C. The London - van der Waals attraction between spherical particles. Physica 4: 1058-72 (1937).

2) Lifschitz, E. M. The theory of molecular attraction forces between solid bodies. Zhur. Eksptl. i. Teoret. Fiz. 29: 94-110 (1955).

3) Kaiser, R. The agglomeration of zinc oxide powders. PhD Thesis. Massachusetts Institute of Technology (Decem[illegible] 1961).

4) Fowler, H. W. Mixers. 2. Powder mixers. Mfg. Chemist 33: 5-11 (1962).

5) Whitby, K. T. Rapid general purpose centrifuge sedimentation method for measurement of size distribution of small particles. Heating, Piping and Air Conditioning 27, 1: 131-6 (January 1955) and 27, 6: 139-45 (June 1955).

6) Hackh, I. W. D. Hackh's chemical dictionary. 3d ed. Philadelphia, Blakiston, 1944. p. 809.

7) Svedberg, T. and A. Tiselius. Colloid chemistry. 2d ed. rev. N.Y., Chemical Catalog Co., 1928. pp. 148-49.

8) Shaxby, J. H. and J. C. Evans. The variation of pressure with depth in columns of powders. Trans. Faraday Soc. 19: 60-72 (1923).

9) Walker, E. E. The distribution of densities in columns of compressed powder. Trans. Faraday Soc. 19: 83-86 (1923).

10) Athy, L. F. Density, porosity and compaction of sedimentary rocks. Bull. Am. Assoc. Petroleum Geol. 14: 1-24 (1930).

11) Spencer, R. S., G. D. Gilmore and R. M. Wiley. Behavior of granulated polymers under pressure. J. Appl. Phys. 21: 527-31 (1950).

12) U. S. Army. Chemical Corps. Biological Laboratories. Interim Report No. 36. Design, construction, and operation of the aerophilometer, by H. G. Tanner et al (June 26, 1953). [redacted] Declassified authority DA 15 75 dated 15 Sept[illegible] tember 19[illegible]

13) Gillespie, T. and G. O. Langstroth. An instrument for determining the electric charge distribution in aerosols. Can. J. Chem. 30: 1056-68 (1952).

14) General Mills, Inc. Mechanical Division. Report 2148. Fundamental studies of the dispersibility of powdered materials, by J. H. Nash and G. T. Leiter. Contract DA 18-108-405-CML-824. Second quarterly progress report (December 13, 1960) (AD 249, 913).

15) Kunkel, W. B. The static electrification of dust particles on dispersion into a cloud. J. Appl. Phys. 21: 820-32 (1950).

16) McCutcheon, J. W. Detergents and emulsifiers ... up to date 1962. Morristown, N. J., John W. McCutcheon, Inc., 1962.

17) General Mills, Inc. Electronics Group. Report 2234. Investigation of surface phenomena with electron mirror microscopy, by R. C. Menard and W. W. Roepke. Contract AF 33(616)-6178. Eleventh quarterly progress report (October 15, 1961).

18) Fuks, N. A. The mechanics of aerosols (Translation). U. S. Army. Chemical Warfare Laboratories. Special Publication 4-12 (1955). (AD 227, 876).

19) General Mills, Inc. Electronics Group. Report 2183. Fundamental studies of the dispersibility of powdered materials, by J. H. Nash et al. Contract DA-18-108-405-CML-824. Third Quarterly Progress Report (March 31, 1961). (AD 255, 484).

20) ----. Report 2184. Fundamental studies of the dispersibility of powdered materials, by J. H. Nash et al. Contract DA-18-108-405-CML-824. Fourth Quarterly Progress Report (June 30, 1961). (AD 260, 740).

21) Dalla Valle, J. M. Micromeritics, the technology of fine particles. 2d ed. N. Y., Pitman, 1948.

APPENDIX A

DERIVATION OF EQUATION DEPICTING MANNER IN WHICH BULK TENSILE STRENGTH VARIES WITH COLUMN LENGTH

APPENDIX A

DERIVATION OF EQUATION DEPICTING MANNER IN WHICH BULK TENSILE STRENGTH VARIES WITH COLUMN LENGTH

Let us consider a column of compressed powder as illustrated in Figure A-1. Assume that p_h is proportional to p_v and that the latter is uniform across a cross section. Then, $p_h = C_1 p_v$. The frictional force acting on the tube wall is $\tau = \mu p_h$. The equilibrium condition of an element of volume of the column of powder is

$$\pi R^2 \rho g \, dh = \pi R^2 dp_v + 2\pi R \tau \, dh. \tag{A-1}$$

Rewriting Equation (A-1) we obtain

$$\frac{dp_v}{\rho g - \frac{2\mu C_1}{R} p_v} = dh. \tag{A-2}$$

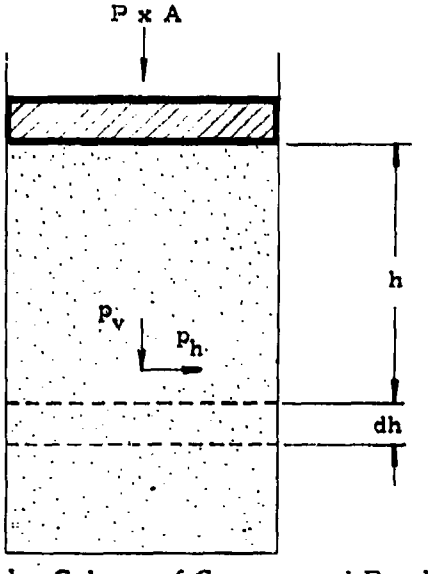

Figure A-1. Column of Compressed Powder

Integrating Equation (A-2), we obtain

$$-\frac{R}{2\mu C_1}\ln\left(\rho g-\frac{2\mu C_1}{R}p_v\right)=h+C_2, \tag{A-3}$$

where C_2 is the integration constant.
At $h = 0$, $p_v = P$, and

$$C_2=-\frac{R}{2\mu C_1}\ln\left(\rho g-\frac{2\mu C_1}{R}P\right). \tag{A-4}$$

Substituting Equation (A-4) into Equation (A-3) and solving for p_v, we obtain a general equation of the form

$$p_v=\frac{\rho g R}{2\mu C_1}-\left(\frac{\rho g R}{2\mu C_1}-P\right)\epsilon^{-\frac{2\mu C_1}{R}h}. \tag{A-5}$$

In the present experimental work, we deal with a special case where $P \gg \rho g R$. If we neglect the term $\frac{\rho g R}{2\mu C_1}$ in Equation (A-5), we have:

$$p_v=P\epsilon^{-\frac{2\mu C_1}{R}h}. \tag{A-6}$$

Let us assume that the bulk tensile strength σ is proportional to the pressure p_v at all values of h. (We know that this assumption is valid at $h = 0$. (see Figure 57). Thus we can write

$$\sigma_o = C_3 P, \tag{A-7}$$

and

$$\sigma = C_3 p_v , \tag{A-8}$$

where C_3 is a constant.

We can now write an expression relating bulk tensile strength to the height of the powder column:

$$\sigma = \sigma_o \epsilon^{-\frac{2\mu C_1}{R} h} . \tag{A-9}$$

APPENDIX B

THEORETICAL ANALYSIS OF OPTIMUM CAB-O-SIL CONCENTRATION

APPENDIX B

THEORETICAL ANALYSIS OF OPTIMUM CAB-O-SIL CONCENTRATION

In this appendix, we calculate how much Cab-O-Sil must be added to a sample of Carbowax 6000 to coat all Carbowax 6000 particles with a layer of Cab-O-Sil particles. Two types of packing are considered--namely, square and hexagonal.

Before such a calculation can be made, it is necessary to have some knowledge of the surface area of the base powder (Carbowax 6000 in this case). By assuming that all particles are spheres and that the size distribution is log normal, the surface area can easily be found.

The fraction of the total number of particles having diameters between d and d + δd is*

$$n(d)\,\delta d = \frac{1}{\sqrt{2\pi}\ln \sigma_g} \exp\left(-\frac{1}{2}\left[\frac{\ln \frac{d}{d_g}}{\ln \sigma_g}\right]^2\right)\delta(\ln d) \qquad \text{(B-1)}$$

The surface area of a single particle of diameter d is πd^2. $n(d)\,\delta d$ can be thought of as the probability of a randomly selected particle having d in the range d to d + δd. The average surface area of all particles can be found from the product of πd^2 and $n(d)\,\delta d$.

$$\overline{\pi d^2} = \frac{\pi}{\sqrt{2\pi}\ln \sigma_g} \int_0^\infty d^2 \exp\left(-\frac{1}{2}\left[\frac{\ln \frac{d}{d_g}}{\ln \sigma_g}\right]^2\right)\delta(\ln d) \qquad \text{(B-2)}$$

*Fuks, N. A. The mechanics of aerosols (Translation). (U. S. Army Chemical Warfare Laboratories. Special Publication 4-12; AD 227, 876).

The total number of particles N in a sample of M grams of a powder of material with density ρ is

$$N = \frac{M}{\frac{\pi \overline{d^3}}{6}\rho} . \tag{B-3}$$

The average volume $\overline{\pi d^3}/6$ can be found by the same process as that for the average surface area. The product of the total number of particles N and the average surface area $\overline{\pi d^2}$ gives the total surface area:

$$S = \frac{M}{\rho}\left[\frac{\frac{\pi}{\sqrt{2\pi}\ln\sigma_g}\int_0^\infty d^2 \exp\left(-\frac{1}{2}\left[\frac{\ln\frac{d}{d_g}}{\ln\sigma_g}\right]^2\right)\delta(\ln d)}{\frac{\pi}{2\pi\ln\sigma_g}\frac{1}{6}\int_0^\infty d^3 \exp\left(-\frac{1}{2}\left[\frac{\ln\frac{d}{d_g}}{\ln\sigma_g}\right]^2\right)\delta(\ln d)}\right] \tag{B-4}$$

While the integrals appear difficult, they can be simplified quite easily. Consider the numerator of Equation (B-4) and perform the following steps:

1) Multiply and divide by d_g^2
2) Replace $\delta(\ln d)$ by its equal $\delta\left(\ln\frac{d}{d_g}\right)$
3) Let $x = \frac{d}{d_g}$
4) Replace x^2 by its equal $e^{2\ln x}$
5) Add and subtract $4\ln^4\sigma_g$ to the exponent. This completes the square and gives

$$e^{2\ln^2\sigma_g}\frac{\pi d_g^2}{\sqrt{2\pi}}\int_0^\infty \exp -\frac{1}{2}\left(\frac{\left[\ln x - 2\ln^2\sigma_g\right]}{\ln^2\sigma_g}\right)\delta(\ln x) \tag{B-5}$$

6) Replace $\delta \ln x$ by its equal $\delta\left(\frac{\ln x - 2\ln^2 \sigma_g}{\ln \sigma_g}\right)$

7) Let $y = \frac{\ln x - 2\ln^2 \sigma_g}{\ln \sigma_g}$

The expression in Step 5) becomes

$$\pi d_g^2 e^{2\ln^2 \sigma_g}\left[\frac{1}{\sqrt{2\pi}}\int_0^\infty e^{-\frac{1}{2}y^2} dy\right].$$

The term enclosed in brackets is equal to 1. Thus, the numerator of Equation (B-4) is

$$\pi d_g^2 e^{2\ln^2 \sigma_g}.$$

By the same process, the denominator is

$$\frac{1}{6}\pi d_g^3 e^{\frac{9}{2}\ln^2 \sigma_g}.$$

The total surface area of M grams of powdered material with density ρ having a geometric mean diameter d_g and a geometric standard deviation σ_g is

$$S = \frac{M}{\frac{1}{6}\rho d_g e^{\frac{5}{2}\ln^2 \sigma_g}}. \qquad \text{(B-5)}$$

If all of the Carbowax 6000 particles are to be covered with Cab-O-Sil particles, the total projected area of the Cab-O-Sil particles will be a fraction of S due to void spaces.

$$s = fS \tag{B-6}$$

where f is the fraction of total area actually covered by Cab-O-Sil.

Consider a single layer of Cab-O-Sil particles covering an area A. For square and hexagonal packing we have

$$f_S = \frac{\pi}{4} \text{ , and} \tag{B-7}$$

$$f_H = \frac{\pi \sqrt{3}}{6} \text{ .} \tag{B-8}$$

If we assume the Cab-O-Sil particles are all equal in size, the projected area also equals $\frac{\pi d^2}{4} N$.

The number of Cab-O-Sil particles is $\frac{m}{\frac{\pi d^3}{6} \rho_a}$, so

$$S = \left(\frac{\pi}{4} d^2\right) \frac{6m}{\pi d^3 \rho_a} = \frac{3}{2} \frac{m}{d\rho_a} \text{ .} \tag{B-9}$$

Equating Equations (B-6) and (B-9), we obtain

$$\frac{3}{2} \frac{m}{d_a \rho_a} = fS = f \frac{M}{\frac{5}{2} \ln^2 \sigma_g \; \frac{1}{6} \rho_a d_g e} \text{ ,} \tag{B-10}$$

and determine that the mass of Cab-O-Sil needed is expressed by

$$m = f \frac{4M}{e^{\frac{5}{2}} \ln^2 \sigma_g} \frac{d_a}{d_g} \frac{\rho_a}{\rho_b},$$

where

M = mass of base powder

ρ_b = density of base powder particles

d_g = geometric mean diameter of base powder particles

σ_g = geometric standard deviation of base powder particl

d_a = diameter of Cab-O-Sil particles

ρ_a = density of Cab-O-Sil particles.

For arbowax 6000, $\rho_b = 1.2$ g/cm^3, $\sigma_b = 2.2$, d_c (count mea eter) = 1. 84 microns. It can be shown that for a log normal distr $d_c = d_g$. For Cab-O-Sil, $\rho_a = 2.3$ g/cm^3 and $d_a = 0.0175$ micron

Let s calculate the amount of Cab-O-Sil required to coat all in 1 g of arbowax 6000. From Equation (B-11) we obtain

$$m = (0.0154) f .$$

For squa e packing, $m = (0.0154) \frac{\pi}{4} = 0.0121$ g; for hexagonal pa $m = (0.01 54) \frac{\pi \sqrt{3}}{6} = 0.0139$ g.

On a ercentage basis, the Cab-O-Sil concentrations are 1.2(for s packing and 1.37 percent for hexagonal packing.

APPENDIX C

DERIVATION OF RELATIONSHIPS TO CALCULATE DISPERSING ENERGY

APPENDIX C

DERIVATION OF RELATIONSHIPS TO CALCULATE DISPERSING ENERGY

Starting with the assumptions that

1) The gas obeys van der Waals' equation, and

2) The expansion is adiabatic,

and considering internal energy as a function of T and V, we have

$$du = \left(\frac{\partial u}{\partial T}\right)_V dT + \left(\frac{\partial u}{\partial V}\right)_T dV. \qquad \text{(C-1)}$$

By definition,

$$C_V = \left(\frac{\partial u}{\partial T}\right)_V, \qquad \text{(C-2)}$$

so

$$du = C_V\, dT + \left(\frac{\partial u}{\partial V}\right)_T dV. \qquad \text{(C-3)}$$

It can be shown that

$$P + \left(\frac{\partial u}{\partial V}\right)_T = T\left(\frac{\partial P}{\partial T}\right)_V \qquad \text{(C-4)}$$

is a general identity for all materials. For a van der Waals' gas

$$P = \frac{RT}{V - b} - \frac{a}{V^2}, \text{ and} \qquad \text{(C-5)}$$

$$\left(\frac{\partial P}{\partial T}\right)_V = \frac{R}{V-b}, \tag{C-6}$$

so

$$\left(\frac{\partial u}{\partial V}\right)_T = T\left(\frac{\partial P}{\partial T}\right)_V - P = T\left(\frac{R}{V-b}\right) - \left(\frac{RT}{V-b} - \frac{a}{V^2}\right) \tag{C-7}$$

$$\left(\frac{\partial u}{\partial V}\right)_T = \frac{a}{V^2}, \tag{C-8}$$

Hence,

$$du = C_V dT + \frac{a}{V^2}\, dV, \tag{C-9}$$

or

$$u_2 - u_1 = \int_{T_1}^{T_2} C_V dT + a\left(\frac{1}{V_1} - \frac{1}{V_2}\right). \tag{C-10}$$

If the process is adiabatic, there is no heat exchange between the system and its surroundings. Hence, by the first law of thermodynamics:

$$u - u_o = -W, \tag{C-11}$$

or the work performed by the gas is

$$W = -\int_{T_1}^{T_2} C_V dT - a\left(\frac{1}{V_1} - \frac{1}{V_2}\right). \tag{C-12}$$

Proeedure

A knowledge of the initial and final temperatures and specific volumes is required in making calculations. The initial pressure and temperature are known from direct measurement at the instant the diaphragm bursts. For purposes of calculation, 22°C was used for T_1. To find the initial specific volume V_1, one must solve the van der Waals' equation

$$V_1 = b + \frac{RT_1}{P_1 + a/V_1^2} . \tag{C-13}$$

To solve this equation, the method of successive approximations is used, with a first approximation being found from the ideal gas law

$$PV = RT . \tag{C-14}$$

With the initial specific volume as well as the initial and final pressures known, the final specific volume can now be found. For an adiabatic process, the following equation holds for a van der Waals' gas:

$$\left(P_1 + \frac{a}{V_1^2}\right)(V_1 - b)^\gamma = \left(P_2 + \frac{a}{V_2^2}\right)(V_2 - b)^\gamma . \tag{C-15}$$

The final pressure P_2 will be one atmosphere. The ratio of specific heats γ can be found from the appropriate tables. Manipulating Equation (C-15) to obtain an expression for V_2, we get

$$V_2 = \left[\frac{\left(P_1 + \frac{a}{V_1^2}\right)(V_1 + b)^\gamma}{P_2 + \frac{a}{V_2^2}}\right]^{\frac{1}{\gamma}} + b . \tag{C-16}$$

Since V_2 is found on both sides of the equation, it is necessary to use the method of successive approximations to solve for V_2. The first approximation is found from the equation

$$P_1 V_1^{\gamma} = P_2 V_2^{\gamma} , \qquad \text{(C-17)}$$

which bears the same relationship to the ideal gas law as Equation (C-15) does to van der Waals' equation.

With P_2 and V_2 known, one can calculate T_2 from the equation of state:

$$T_2 = \frac{1}{R} \left[P_2 + \frac{a}{V_2^2} \right] (V_2 - b) , \qquad \text{(C-18)}$$

All factors are now known, and one can calculate the work per mole from Equation (C-12), which is written in a slightly different form below.

$$W = \int_{T_2}^{T_1} C_V \, dT - a \left(\frac{1}{V_1} - \frac{1}{V_2} \right) . \qquad \text{(C-19)}$$

C_V should be expressed in ergs/mole °K. In order for the last term in Equation (C-19) to have units of ergs/mole, we must multiply "a" by a conversion factor as shown below.

$$a = 1.29 \times 10^6 \frac{\text{cm}^6 \text{ atm}}{\text{mole}^2} \times 1.013 \times 10^6 \frac{\text{erg}}{\text{cm}^3 \text{ atm}}$$

$$= 1.408 \times 10^{12} \frac{\text{erg cm}^3}{\text{mole}^2} .$$

Calculations

The calculation involving the second term in the energy expression (Equation C-19) is straightforward. The integral term is a different matter, however. Referring to National Bureau of Standards Tables[*] it was found that the specific heat C_V for nitrogen departs sharply from constancy over the temperature range being considered. In addition, C_V was found to vary with pressure. A means was devised to take this variation into consideration.

From the National Bureau of Standards Table, five plots of specific heat versus temperature were made, each being valid at and around one of the following pressures: 1 atm, 10 atm, 40 atm, 70 atm, and 100 atm. These plots are shown in Figure C-1. Each of these specific heat curves had to be used in the region of pressures where it was valid. As a result, it was necessary to break up the calculation into several steps and use the appropriate specific heat in each step.

For example, consider the adiabatic expansion when the initial pressure is 136 atm. This is broken up into five intervals as follows:

136 to 85 atm

85 to 55 atm

55 to 25 atm

25 to 5 atm

5 to 1 atm.

This does not mean that the process is considered to be five separate expansions. It is still considered to be a single adiabatic expansion from 136 to 1 atm. The temperatures were calculated at the instant the pressure had decreased to 85, 55, 25, and 5 atm. This breakdown is illustrated by the following expression:

---

* Hilsenrath, J. Tables of Thermal Properties of Gases, Washington, D. C., N. B. S., 1955.

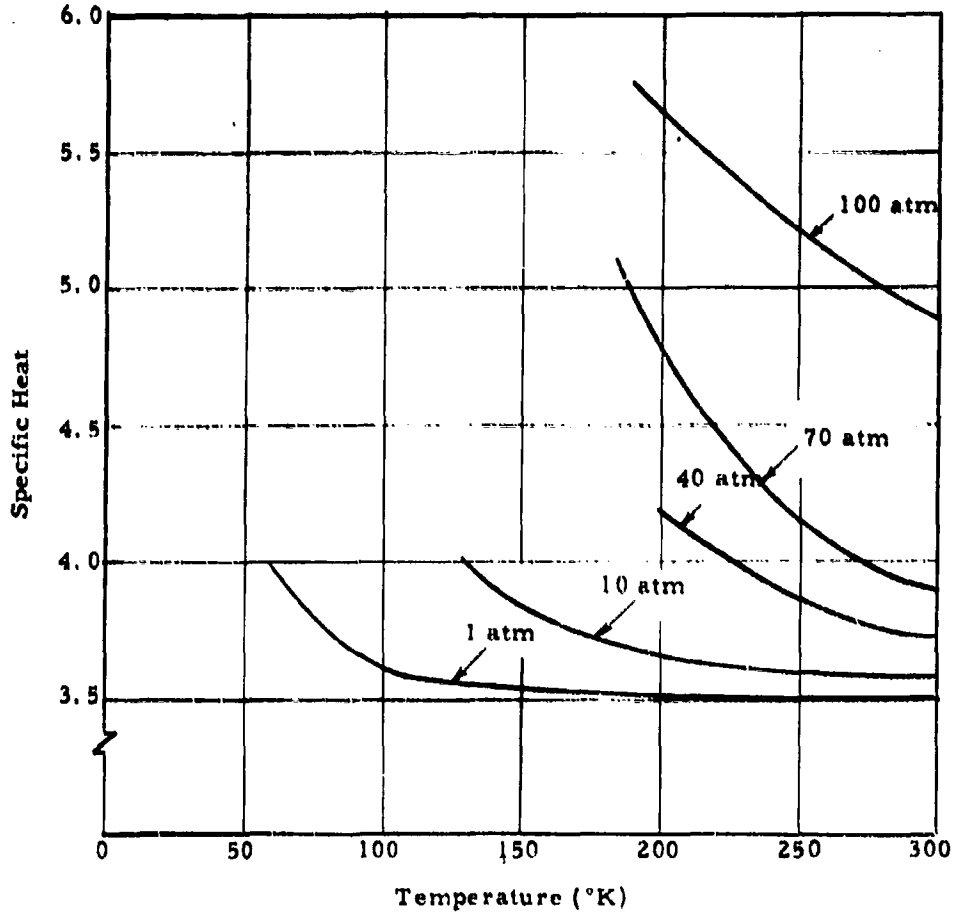

Figure C-1. Specific Heat of Nitrogen as a Function of Temperature

$$\int_{T_1}^{T_2} C_V\, dT = \int_{T_1 = T_{p_1}}^{T_{p_3}} (C_V)_{p_2}\, dT + \int_{T_{p_3}}^{T_{p_5}} (C_V)_{p_4}\, dT + \tag{C-20}$$

$$\int_{T_{p_5}}^{T_{p_7}} (C_V)_{p_6}\, dT + \int_{T_{p_7}}^{T_{p_9}} (C_V)_{p_8}\, dT + \int_{T_{p_9}}^{T_{p_{10}}} (C_V)_{p_{10}}\, dT$$

where

p_1 = 136 atm

p_2 = 100 atm

p_3 = 85 atm

p_4 = 70 atm

p_5 = 55 atm

p_6 = 40 atm

p_7 = 25 atm

p_8 = 10 atm

p_9 = 5 atm

p_{10} = 1 atm.

The integrations are performed by Simpson's Rule, using the C_V versus temperature curves plotted in Figure C-1. The same general method is used for bursting pressures of 102, 62, 34, and 6.8 atm.

After the integral has been evaluated in this manner, the work per mole is calculated from Equation (C-19). The units of ergs per mole are transformed to units of ergs per unit initial volume by multiplying by the reciprocal of the initial specific volume. These values are plotted against pressure in Figure 73, Section IV-H.

APPENDIX D

POTENTIAL REQUIRED TO DEFLECT PARTICLES ONTO SLIDES

APPENDIX D

POTENTIAL REQUIRED TO DEFLECT PARTICLES ONTO SLIDES

Consider a channel made up of two glass slides held parallel by insulating spacers and backed by metal plates as shown in the illustration below.

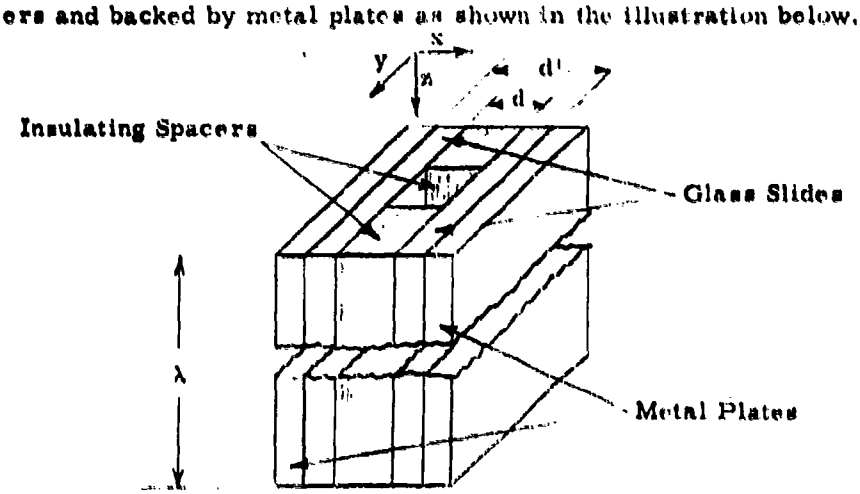

Figure D-1. Cut-Away View of Channel of Electrostatic Charge Analyzer

Assume a charged particle is moving midway between the plates with velocity v in the direction of λ. Then, the time it takes to travel the length of the channel is

$$t = \frac{\lambda}{v} . \qquad \text{(D-1)}$$

If an electric field is applied between the plates, the equations of motion are

$$\dot{v}_z = 0 \tag{D-2}$$

$$\dot{v}_y = 0 \tag{D-3}$$

$$m\dot{v}_x = Eq - 6\pi\eta\, r v_x \tag{D-4}$$

where

$\dot{v}_z$ = acceleration in z direction

$\dot{v}_y$ = acceleration in y direction

$\dot{v}_x$ = acceleration in x direction

m = mass of particle

E = electric field

q = electric charge

η = viscosity of air

r = radius of particle

v_x = velocity in x direction.

In a very short period of time, the particle will reach its terminal velocity in the x direction. Then $\dot{v}_x = 0$ and Equation (D-4) becomes

$$Eq = 6\pi\eta r v_x \tag{D-5}$$

or

$$v_x = \frac{Eq}{6\pi\eta r}. \tag{D-6}$$

If the particle is to be deposited on one of the plates, it must travel a distance d/2 in the x direction before traveling the length of the plates. Therefore

$$v_x t = \frac{Eq}{6\pi\eta r} \frac{\lambda}{v} \approx \frac{d}{2}. \tag{D-7}$$

The required electric field is thus

$$E \approx \frac{d}{2} \frac{v}{\lambda} \frac{6\pi\eta r}{q}. \tag{D-8}$$

For parallel plates, we know

$$D = \frac{V}{d'} \tag{D-9}$$

where V is the potential and d' is the spacing between the plates. Then

$$V \approx \frac{d'dv\ 6\pi\eta r}{2\lambda q}. \tag{D-10}$$

The following values may be substituted into Equation (D-10):

$d = 1.20$ cm

$d' = 1.36$ cm

$\eta = 1.83 \times 10^{-4}$ (cgs units)

$r = R \times 10^{-4}$ (R = radius in microns)

$\lambda = 15.2$ cm

$q = n\,(4.8 \times 10^{-10})$ statcoulombs where n is the number of electric charges on the particle.

Equation (D-10) then reduces to

$$V \approx 38.4 \frac{vR}{n}. \tag{D-11}$$

When Equation (D-11) is expressed in terms of MKS units, we get

$$V \geq 11,500 \frac{vR}{n} . \qquad \text{(D-12)}$$

Assume the largest particles have a radius of 5 microns, carry a single electric charge and travel with an average velocity of 1 mm/sec. Then

$$V \geq 5,750 \text{ volts} . \qquad \text{(D-13)}$$

This is, of course, only an approximation used to find the order of voltage required to insure that all charged particles will strike one of the glass slides before reaching the filter paper. The effect of the presence of the glass slides on the electric field was evaluated and found to be small.

AD ______________ Accession No. ______________

General Mills Electronics Group
FUNDAMENTAL STUDIES OF THE DISPERSIBILITY
OF POWDERED MATERIALS (Final Report)
J. H. Nash, G. G. Leiter, A. P. Johnson,
D. Stender and H. W. Zeller

Report No. 6381, 15 March 63, 249 pp - 88 illus. - 48 tables
Contract No. DA-18-108-405-CML-824
CP-0-405-14890

This is a fundamental study of factors affecting the flow and dispersibility of finely divided organic powders. Most of the investigations pertain to three base powders: saccharin, Carbowax 6000 and Span 60. These powders were chosen to represent crystalline, waxy and gummy types of powders respectively. Late in the program, a fourth powder (egg albumin) was added to the list of powders to be investigated.

The preparation of powders including grinding, deagglomeration, blending, coating with surface active agents, etc., is discussed.

Various tests for measuring physical properties of powders including particle size distribution, shear strength, bulk tensile strength, bulk density, dynamic angle of repose, dispersibility and electrostatic charge are described.

The major studies are discussed, and experimental data are presented in tabular and graphical forms. The major studies are: (1) bulk tensile strength tests, (2) effects of humidity on powder properties, (3) effects of antiagglomerant agents on powder properties, (4) mechanism by which Cab-O-Sil functions, (5) effects of surface active agents on powder properties, (6) effects of adsorbed foreign vapors on powder properties, (7) effects of removal of adsorbed gases and vapors, (8) energy required to disperse a powder sample, (9) properties of compacted powders, and (10) egg albumin studies.

1. Particles-Dispersion
Particles-Adhesion
Powders-Measurement

2. DA-18-108-405-CML-824

(Unclassified)

AD ______________ Accession No. ______________

General Mills Electronics Group
FUNDAMENTAL STUDIES OF THE DISPERSIBILITY
OF POWDERED MATERIALS (Final Report)
J. H. Nash, G. G. Leiter, A. P. Johnson,
D. Stender and H. W. Zeller

Report No. 6381, 15 March 63, 249 pp - 88 illus. - 48 tables
Contract No. DA-18-108-405-CML-824
CP-0-405-14890

This is a fundamental study of factors affecting the flow and dispersibility of finely divided organic powders. Most of the investigations pertain to three base powders: saccharin, Carbowax 6000 and Span 60. These powders were chosen to represent crystalline, waxy and gummy types of powders respectively. Late in the program, a fourth powder (egg albumin) was added to the list of powders to be investigated.

The preparation of powders including grinding, deagglomeration, blending, coating with surface active agents, etc., is discussed.

Various tests for measuring physical properties of powders including particle size distribution, shear strength, bulk tensile strength, bulk density, dynamic angle of repose, dispersibility and electrostatic charge are described.

The major studies are discussed, and experimental data are presented in tabular and graphical forms. The major studies are: (1) bulk tensile strength tests, (2) effects of humidity on powder properties, (3) effects of antiagglomerant agents on powder properties, (4) mechanism by which Cab-O-Sil functions, (5) effects of surface active agents on powder properties, (6) effects of adsorbed foreign vapors on powder properties, (7) effects of removal of adsorbed gases and vapors, (8) energy required to disperse a powder sample, (9) properties of compacted powders, and (10) egg albumin studies.

1. Particles-Dispersion
Particles-Adhesion
Powders-Measurement

2. DA-18-108-405-CML-824

(Unclassified)

AD ______________ Accession No. ______________

General Mills Electronics Group
FUNDAMENTAL STUDIES OF THE DISPERSIBILITY
OF POWDERED MATERIALS (Final Report)
J. H. Nash, G. G. Leiter, A. P. Johnson,
D. Stender and H. W. Zeller

Report No. 6381, 15 March 63, 249 pp - 88 illus. - 48 tables
Contract No. DA-18-108-405-CML-824
CP-0-405-14890

This is a fundamental study of factors affecting the flow and dispersibility of finely divided organic powders. Most of the investigations pertain to three base powders: saccharin, Carbowax 6000 and Span 60. These powders were chosen to represent crystalline, waxy and gummy types of powders respectively. Late in the program, a fourth powder (egg albumin) was added to the list of powders to be investigated.

The preparation of powders including grinding, deagglomeration, blending, coating with surface active agents, etc., is discussed.

Various tests for measuring physical properties of powders including particle size distribution, shear strength, bulk tensile strength, bulk density, dynamic angle of repose, dispersibility and electrostatic charge are described.

The major studies are discussed, and experimental data are presented in tabular and graphical forms. The major studies are: (1) bulk tensile strength tests, (2) effects of humidity on powder properties, (3) effects of antiagglomerant agents on powder properties, (4) mechanism by which Cab-O-Sil functions, (5) effects of surface active agents on powder properties, (6) effects of adsorbed foreign vapors on powder properties, (7) effects of removal of adsorbed gases and vapors, (8) energy required to disperse a powder sample, (9) properties of compacted powders, and (10) egg albumin studies.

1. Particles-Dispersion
Particles-Adhesion
Powders-Measurement

2. DA-18-108-405-CML-824

(Unclassified)

AD ______________ Accession No. ______________

General Mills Electronics Group
FUNDAMENTAL STUDIES OF THE DISPERSIBILITY
OF POWDERED MATERIALS (Final Report)
J. H. Nash, G. G. Leiter, A. P. Johnson,
D. Stender and H. W. Zeller

Report No. 6381, 15 March 63, 249 pp - 88 illus. - 48 tables
Contract No. DA-18-108-405-CML-824
CP-0-405-14890

This is a fundamental study of factors affecting the flow and dispersibility of finely divided organic powders. Most of the investigations pertain to three base powders: saccharin, Carbowax 6000 and Span 60. These powders were chosen to represent crystalline, waxy and gummy types of powders respectively. Late in the program, a fourth powder (egg albumin) was added to the list of powders to be investigated.

The preparation of powders including grinding, deagglomeration, blending, coating with surface active agents, etc., is discussed.

Various tests for measuring physical properties of powders including particle size distribution, shear strength, bulk tensile strength, bulk density, dynamic angle of repose, dispersibility and electrostatic charge are described.

The major studies are discussed, and experimental data are presented in tabular and graphical forms. The major studies are: (1) bulk tensile strength tests, (2) effects of humidity on powder properties, (3) effects of antiagglomerant agents on powder properties, (4) mechanism by which Cab-O-Sil functions, (5) effects of surface active agents on powder properties, (6) effects of adsorbed foreign vapors on powder properties, (7) effects of removal of adsorbed gases and vapors, (8) energy required to disperse a powder sample, (9) properties of compacted powders, and (10) egg albumin studies.

1. Particles-Dispersion
Particles-Adhesion
Powders-Measurement

2. DA-18-108-405-CML-824

(Unclassified)